

**CARACTERIZACIÓN Y MODULACIÓN DE LOS CAMBIOS EN
MÚSCULOS ESQUELÉTICOS DE RATA SECUNDARIOS A LA UREMIA
Y A LA OBESIDAD**

Luz Marina Acevedo Betancourt

TITULO: *Caracterización y modulación de los cambios en músculos esqueléticos de rata secundarios a la uremia y a la obesidad*

AUTOR: *Luz Marina Acevedo Betancourt*

© Edita: UCOPress. 2016
Campus de Rabanales
Ctra. Nacional IV, Km. 396 A
14071 Córdoba

www.uco.es/publicaciones
publicaciones@uco.es

Director: Prof. Dr. José Luis López Rivero
Departamento de Anatomía y Anatomía Patológica Comparadas
Facultad de Veterinaria de Córdoba
Universidad de Córdoba

Co-director: Prof. Dr. Escolástico Aguilera-Tejero
Departamento de Medicina y Cirugía Animal
Facultad de Veterinaria de Córdoba
Universidad de Córdoba

Depósito Legal: CO-1918-2016
Publicado en: Octubre de 2016
Ediciones Don Folio
Córdoba, España

“Hay una fuerza motriz más poderosa que el motor, la electricidad y la energía atómica: La voluntad”

Albert Einstein

A Dios, mi guía en todo momento

A mis padres y a toda mi familia por su apoyo
incondicional

JOSÉ LUIS LÓPEZ RIVERO, Doctor en Veterinaria por la Universidad de Córdoba y Catedrático de Universidad del Departamento de Anatomía y Anatomía Patológica Comparadas de la Universidad de Córdoba,

INFORMA:

Que D^a LUZ MARINA ACEVEDO BETANCOURT, Licenciada en Veterinaria, ha realizado bajo mi dirección en el Departamento de Anatomía y Anatomía Patológica Comparadas de la Universidad de Córdoba, el trabajo titulado: **“Caracterización y Modulación de los Cambios en Músculos Esqueléticos de Rata Secundarios a la Uremia y a la Obesidad”**, el cual reúne, a mi juicio, los méritos suficientes para optar al Grado de Doctora en Veterinaria por la Universidad de Córdoba.

Y para que conste y surta los efectos oportunos, firmo el presente informe en Córdoba a diez de octubre de dos mil dieciséis.



Fdo. José Luis López Rivero

ESCOLÁSTICO AGUILERA TEJERO, Doctor en Veterinaria por la Universidad de Córdoba y Catedrático de Universidad del Departamento de Medicina y Cirugía Animal de la Universidad de Córdoba,

INFORMA:

Que D^a LUZ MARINA ACEVEDO BETANCOURT, Licenciada en Veterinaria, ha realizado bajo mi dirección en el Departamento de Medicina y Cirugía Animal de la Universidad de Córdoba, el trabajo titulado: **“Caracterización y Modulación de los Cambios en Músculos Esqueléticos de Rata Secundarios a la Uremia y a la Obesidad”**, el cual reúne, a mi juicio, los méritos suficientes para optar al Grado de Doctora en Veterinaria por la Universidad de Córdoba.

Y para que conste y surta los efectos oportunos, firmo el presente informe en Córdoba a diez de octubre de dos mil dieciséis.



Fdo. Escolástico Aguilera Tejero



TÍTULO DE LA TESIS: Caracterización y Modulación de los Cambios en Músculos Esqueléticos de Rata Secundarios a la Uremia y a la Obesidad

DOCTORANDO/A: Luz Marina Acevedo Betancourt

INFORME RAZONADO DEL/DE LOS DIRECTOR/ES DE LA TESIS

(se hará mención a la evolución y desarrollo de la tesis, así como a trabajos y publicaciones derivados de la misma).

La doctoranda Luz Marina Acevedo Betancourt ha venido colaborando activamente con nuestro grupo de investigación desde el año 2002 hasta el año 2016. Dicha colaboración se inició como Profesora visitante del Departamento, realizando tareas de investigación en el Laboratorio de Biopatología Muscular. Dicha estancia quedó reflejada en la publicación del artículo científico titulado “New insights into skeletal muscle fiber types in the dog with particular focus towards hybrid myosin phenotypes”, publicado en 2006 en la prestigiosa revista *Cell Tissue and Organs*. En esta etapa, la doctoranda se familiarizó con las técnicas histoquímicas, inmunohistoquímicas y análisis de imagen aplicadas en nuestro Laboratorio al estudio de la diversidad y plasticidad del músculo esquelético de mamíferos.

Durante la etapa de realización de sus trabajos de tesis doctoral, ha disfrutado de una beca otorgada por la Universidad Central de Venezuela para tareas de investigación en nuestra Universidad. La presente tesis doctoral, llevada a cabo bajo nuestra supervisión, se ha desarrollado durante el periodo comprendido entre 2011 y 2016, en el que la doctoranda ha demostrado una gran perseverancia, dedicación e interés por aprender y ejecutar correctamente las tareas de investigación asignadas. De dicha actividad se han producido diferentes publicaciones en revistas científicas y aportaciones en congresos especializados, a nuestro juicio de gran alcance científico en sus respectivas áreas temáticas. A continuación se relaciona la productividad científica generada hasta la fecha por trabajos realizados durante la ejecución de la presente tesis doctoral:

1- Artículos publicados

- 1.1 Guillermo H. Graziotti, Verónica E. Chamizo, Clara Ríos, Luz M. Acevedo, J. M. Rodríguez-Menéndez, C. Victorica and José Luis L. Rivero (2012) Adaptive functional specialisation of architectural design and fibre type characteristics in agonist shoulder flexor muscles of the llama, *Lama glama*. *J Anat* **221**:151-163.
- 1.2 V. Chamizo, L. M. Acevedo, J.-L. L. Rivero (2015) Prevalence and clinical features of exertional rhabdomyolysis in Andalusian horses" *Vet Rec* **177**: 48
- 1.3 Luz M. Acevedo, Alan Peralta-Ramírez, Ignacio López, Verónica E. Chamizo, Carmen Pineda, María E. Rodríguez-Ortiz, Mariano Rodríguez, Escolástico Aguilera-Tejero, and José-Luis L. Rivero (2015) "Slow- and fast-twitch hind limb skeletal muscle phenotypes 12 weeks after 5/6 nephrectomy in Wistar rats of both sexes. *Am*

J Physiol Renal Physiol **309** F638-47

- 1.4 Luz M. Acevedo, Ignacio López, Alan Peralta-Ramírez, Carmen Pineda, Verónica E. Chamizo, Mariano Rodríguez, Escolástico Aguilera-Tejero and José-Luis L. Rivero (2016) High-phosphorus diet maximizes and low dose calcitriol attenuates skeletal muscle changes in long-term uremic rats J Appl Physiol **120**:1059-69
- 1.5 Elisa Diez de Castro, Zafra Rafael, Luz M. Acevedo, José Pérez, Isabel Acosta, José-Luis L. Rivero, and Escolástico Aguilera-Tejero (2016) "Eosinophilic enteritis in horses with motor neuron disease". J Vet Int Med **30**:873-9

2- Artículos enviados

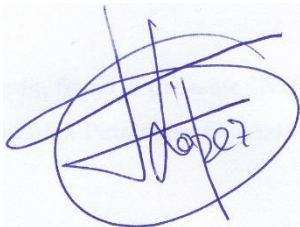
- 2.1 Luz M. Acevedo, Ana Raya, Rafael Ríos, Escolástico Aguilera-Tejero, and José-Luis L. Rivero (2016) Obesity-induced mass reduction and fast phenotype occur with increased oxidative capacity in red and white muscle. Enviado con modificaciones respuesta al arbitraje el 21/09/2016 en la revista *Histochemistry and Cell Biology*.
- 2.2 Luz M. Acevedo, Ana Raya, Escolástico Aguilera-Tejero, and José Luis L. Rivero (2016) Mangiferin protects against adverse skeletal muscle changes and enhances muscle oxidative capacity in obese rats. Para ser reenviado con modificaciones en respuesta al arbitraje en la revista *Plos One*.

3- Abstracts

- 3.1 A. Peralta Ramírez, J.R. Muñoz-Castañeda, M.E. Rodríguez Ortiz, C. Herencia Bellido, C. Pineda Martos, J.M. Martínez Moreno, A. Montes de Oca González, F. Guerrero Pavón, S. Pérez Delgado, L.M. Acevedo, M.E. Peter, S. Steppan, J. Passlick-Deetjen, I. López Villalba, E. Aguilera-Tejero, Y. Almadén Peña (2012) El Magnesio disminuye la Calcificación Vascular en Ratas Urémicas. Presentado en el XLII Congreso Nacional de la Sociedad Española de Nefrología, en Gran Canaria, España*.
- 3.2 Gómez-Laguna J, Cardoso-Toset F, Acevedo L.M, Fernández L., Chamizo V, García-Valverde R, López-Rivero J.L (2014) Myosin heavy chain fibre types and fibre sizes in intensive and free-range finishing Iberian pigs: Interaction with two alternative dietary protein concentration diets. Presentado en el 6th European Symposium of Porcine Health Management, en Sorrento, Italia.
- Por todo lo anterior, se autoriza la presentación de la tesis doctoral.

Córdoba, 10 de Octubre de 2016

Firma del director



Fdo.: José Luis López Rivero

Firma del co-director



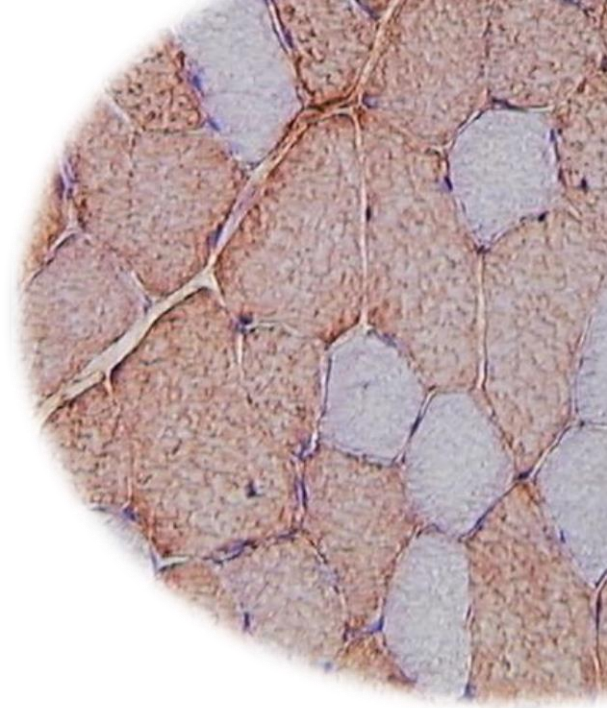
Fdo. Escolástico Aguilera-Tejero

ÍNDICE DE CONTENIDOS

Capítulo 1	
Introducción general	11
Capítulo 2	
Hipótesis y objetivos	19
Chapter 3	
Uremia- and obesity-induced skeletal muscle plasticity: a literature review	23
Chapter 4	
Slow- and fast-twitch hind limb skeletal muscle phenotypes 12 weeks after 5/6 nephrectomy in Wistar rats of both sexes.....	43
Chapter 5	
High-phosphorus diet maximizes and low-dose calcitriol attenuates skeletal muscle changes in long-term uremic rats	65
Chapter 6	
Obesity-induced muscle mass reduction and fast phenotype occur with increased oxidative capacity in red and white rat skeletal muscles	89
Chapter 7	
Mangiferin protects against adverse skeletal muscle changes and enhances muscle oxidative capacity in obese rats	111
Capítulo 8	
Conclusiones	135
Chapter 9	
Resumen – Summary	139
Apéndice	
Abbreviations, <i>Curriculum vitae</i> , Publicaciones, Actividades académicas, Agradecimientos, Financiación	145

CAPÍTULO 1

Introducción general



Introducción

El músculo esquelético es el tejido corporal más abundante y el principal motor metabólico del organismo en vertebrados. Diseñado a base de una admirable diversidad celular y molecular, está dotado de gran capacidad de adaptación frente a numerosos estímulos intrínsecos y extrínsecos. En los años recientes ha existido un interés creciente sobre la asociación entre esta plasticidad del músculo esquelético y determinados problemas de salud que afectan con gran prevalencia a la población mundial. La insuficiencia renal crónica y la obesidad, junto con todas sus comorbilidades asociadas (hiperparatiroidismo secundario y otros desórdenes del metabolismo mineral, resistencia a la insulina, síndrome metabólico y diabetes) constituyen dos de estos problemas con enorme trascendencia para la salud humana, particularmente en vistas de las alarmantes epidemias de muchos de estos trastornos en todo el mundo. Por ello, resulta esencial comprender cómo la disfunción del músculo esquelético contribuye al origen de estos trastornos endocrino-metabólicos, pero también es importante saber cómo estas comorbilidades impactan sobre la estructura y la función del músculo esquelético.

La presente tesis doctoral contiene cuatro estudios de investigación independientes, diseñados de manera complementaria, para satisfacer los siguientes grandes objetivos generales:

Primero. Evaluar el alcance de la plasticidad muscular asociada a la enfermedad renal crónica y a la obesidad.

Segundo. Desarrollar estrategias que sirvan para contrarrestar los efectos adversos de la enfermedad renal crónica y de la obesidad sobre el músculo esquelético.

MÚSCULO ESQUELÉTICO Y SÍNDROME URÉMICO

Pese a existir una gran confusión en la literatura especializada acerca de los cambios en el músculo esquelético de pacientes con insuficiencia renal crónica, es evidente que estos enfermos sufren una constelación de

anomalías estructurales y funcionales en sus músculos esqueléticos, especialmente de las extremidades inferiores, que se describen bajo el término genérico de miopatía urémica (1, 3). Los numerosos estudios realizados sobre esta asociación durante las pasadas cuatro décadas ofrecen resultados contradictorios y, a menudo, presentan importantes limitaciones metodológicas.

La mayoría de estos estudios en humanos han descrito los cambios musculares en pacientes en fases muy avanzadas de la enfermedad renal crónica (19, 23). Por el contrario, los estudios animales que han utilizado el modelo de reducción de 5/6 de la masa renal total, quizás el modelo experimental más usado para inducir uremia, sólo han descrito los cambios musculares que ocurren durante la fase aguda (1-4 semanas) de la insuficiencia renal (11, 31), pero no existen descripciones acerca de los cambios musculares durante el periodo de “estabilización” del fallo renal crónico, esto es, más allá de las 6-8 semanas después de la nefrectomía.

Por otro lado, estos estudios previos no han considerado que el sexo pudiera tener algún efecto sobre los cambios musculares en pacientes urémicos, particularmente teniendo en cuenta los reducidos niveles de hormonas gonadales masculinas, en especial testosterona, de estos pacientes (1). Por ello, y porque la testosterona es un regulador del fenotipo muscular, podemos esperar que la respuesta muscular a la uremia no sea la misma en ambos sexos.

Además, algunos estudios previos han comunicado que esta adaptación varía entre músculos con diferente estructura y función (11). Por ejemplo, los músculos posturales se muestran más resistentes a la hipoxia inducida por uremia que los músculos dinámicos (10). También existen evidencias previas en la literatura especializada que informan que los cambios musculares inducidos por uremia pueden estar relacionados con una inadecuada respuesta celular a la hipoxia (10).

MODULACIÓN DE LA RESPUESTA MUSCULAR A LA UREMIA CRÓNICA

Es bien conocido que los trastornos del metabolismo mineral son comunes en pacientes con enfermedad renal crónica (5). Así, el desarrollo de hiperparatiroidismo secundario es una complicación habitual en estos pacientes (5). Los principales rasgos de este trastorno incluyen una disminución en la producción renal de calcitriol (la forma activa de la vitamina D), retención de fósforo (hiperfosfatemia), hipocalcemia e incremento de los niveles séricos de la hormona paratiroidea (PTH) y del factor de desarrollo fibroblástico 23 (FGF23) (5). También es sabido que el calcitriol y otros análogos de la vitamina D, administrados a dosis bajas y bien controladas, puede ser útil para prevenir la deficiencia de calcitriol en pacientes renales, contrarrestando así el desarrollo de hiperparatiroidismo secundario (36).

Recientemente han emergido evidencias sobre los efectos beneficiosos de la vitamina D sobre el músculo esquelético (12, 25). Tales beneficios incluyen mejoras de la contractibilidad, capacidad oxidativa, miogénesis y angiogénesis muscular. Estas acciones pueden ser, en parte, indirectas, como consecuencia del efecto de la vitamina D sobre la homeostasis del calcio y del fósforo. Pero también por un mecanismo directo mediante la expresión en el músculo esquelético del receptor de la vitamina D (VDR) y de la enzima CYP27B1, que hidroxila la vitamina D₃ a calcitriol.

Aunque algunos estudios escasos de la literatura más inicial habían indicado que el tratamiento con vitamina D puede tener un efecto positivo sobre la función muscular en pacientes con insuficiencia renal crónica (7, 12, 13, 15, 25, 34), los acontecimientos contráctiles, metabólicos y estructurales que sostienen este efecto a nivel celular no han sido explorados en modelos experimentales de uremia.

MÚSCULO ESQUELÉTICO Y OBESIDAD

Diferentes estudios publicados en los últimos 20 años han descrito cambios en la estructura y función del músculo esquelético en distintos modelos humanos y animales de obesidad, pero muchos de estos estudios han proporcionado resultados equívocos e inconsistentes. Por ejemplo, una disminución de la capacidad oxidativa muscular ha sido comunicada frecuentemente en sujetos obesos (8, 35). Sin embargo, otros estudios revelan resultados compatibles con el incremento o con la no modificación de la capacidad oxidativa muscular en estos individuos (17, 18).

Un acontecimiento central en la obesidad es el incremento de lípidos intramusculares, como consecuencia de una disminución en la tasa de β -oxidación lipídica y/o de un incremento de la tasa de transportes de ácidos grasos hasta el músculo esquelético. Pero los incrementos en el contenido mitocondrial y en la tasa de β -oxidación lipídica mitocondrial que han sido comunicados en individuos obesos (17, 18), deberían reflejarse en una disminución del contenido lipídico intracelular. Sin embargo, el acúmulo de lípidos intramusculares obedece a que la tasa de transporte de ácidos grasos hacia la célula muscular es mucho mayor que los incrementos compensatorios en la densidad mitocondrial y en la tasa de β -oxidación mitocondrial de estos ácidos grasos (17).

Por otro lado, algunos estudios han comunicado que los cambios musculares asociados a la obesidad son más evidentes en músculos lentos que en músculos rápidos, probablemente como consecuencia de sus diferentes funciones (9, 17). Así, los músculos rojos (compuestos mayoritariamente de fibras lentas-oxidativas) permanecen tónicamente activos en reposo para proporcionar soporte postural (anti-gravitacional) teniendo una alta dependencia energética de los sustratos sanguíneos circulantes. Por el contrario, los músculos blancos (compuestos mayoritariamente por fibras rápidas-

glucolíticas) están diseñados para desarrollar movimientos rápidos y explosivos, teniendo mayor dependencia energética del glucógeno intramuscular.

La gran variabilidad entre los resultados de los estudios previos probablemente obedece a diferencias en los diseños experimentales y limitaciones metodológicas. En todo caso, aún queda por esclarecerse cómo la obesidad y condiciones colaterales afectan a la masa muscular y a los fenotipos contráctil y metabólico del músculo esquelético.

¿CÓMO CONTRARRESTAR LOS CAMBIOS MUSCULARES ASOCIADOS A LA OBESIDAD?

Los cambios del músculo esquelético inducidos por la obesidad incluyen frecuentemente pérdida de masa muscular, transformación lenta a rápida en los perfiles de los tipos de fibras musculares y una limitada capacidad oxidativa mitocondrial (8, 26, 28). Algunos estudios han mostrado una asociación entre estos cambios a nivel muscular y el riesgo de padecer resistencia a la insulina (16, 21), sugiriendo que la prevención de tales cambios puede ayudar a mejorar la desregulación metabólica inducida por la obesidad (4). Por ejemplo, se ha observado ampliamente que mejorando la función mitocondrial muscular se incrementa la sensibilidad a la insulina y se previene la diabetes de tipo 2 (33).

La inflamación crónica asociada con la obesidad y sobrenutrición, que se caracteriza por un incremento en los niveles de citoquinas pro-inflamatorias como el factor de necrosis tumoral α (TNF α) y la interleuquina 6 (IL-6), ha sido responsabilizada de la atrofia muscular inducida por obesidad, al provocar un balance negativo entre la síntesis y la degradación de proteínas musculares (24). La transformación fibrilar lenta a rápida que también ocurre asociada a la obesidad se ha explicado por infra-regulación de los receptores de peroxisomas PGC1 α y PPAR δ (8), debido a su papel crítico en el control de la composición fibrilar de los músculos (27). También se

conoce que la activación de estos receptores, junto con la proteína quinasa AMP-activada (AMPK), son importantes mecanismos favorecedores de la biogénesis mitocondrial.

En los años recientes, además de reducir el consumo calórico de la dieta e incrementar los niveles de ejercicio físico, se han considerado diferentes farmacóforos con propiedades anti-oxidantes y anti-inflamatorias entre las estrategias de lucha contra la obesidad. En este contexto, los estudios realizados sobre la mangiferina, un glucósido natural de la xantona presente en gran proporción en la planta del mango (*Mangiferina indica L.*), han sugerido que esta sustancia puede ser de gran ayuda para contrarrestar los problemas metabólicos relacionados con la obesidad (6, 30). Entre las múltiples actividades biológicas beneficiosas de la mangiferina se incluyen sus potentes efectos anti-inflamatorios (32), anti-oxidantes (29) y anti-diabéticos (22). Los mecanismos fisiológicos que sustentan estas acciones incluyen la inhibición de citoquinas pro-inflamatorias como TNF α e IL-6, y la activación de los receptores PPAR δ , PGC1 α y AMPK. Además, estudios recientes también han demostrado que la mangiferina sobre-regula las proteínas claves de la bioenergética mitocondrial (20). En conjunto, estas acciones de la mangiferina mejoran la utilización de carbohidratos en el metabolismo oxidativo, incrementando la sensibilidad a la insulina y disminuyendo la lipogénesis (6).

Ciertos estudios han alumbrado que la suplementación de la dieta con mangiferina tiene efectos beneficiosos sobre algunos aspectos de la función muscular en individuos obesos. Por ejemplo, se ha descrito una mejora en el catabolismo lipídico en el músculo esquelético de animales obesos, a través de una sobre-regulación de genes involucrados en la β -oxidación de ácidos grasos a nivel muscular, tras la administración de mangiferina (14). Esta sustancia también induce un cambio en el cociente respiratorio muscular desde lípidos hacia la utilización de carbohidratos mediante un incremento de la

Capítulo 1

oxidación de glucosa y de piruvato (2). Pero los efectos a nivel celular de la mangiferina sobre la masa muscular y sobre los fenotipos contráctiles y metabólicos del músculo esquelético no han sido investigados en modelos experimentales de obesidad.

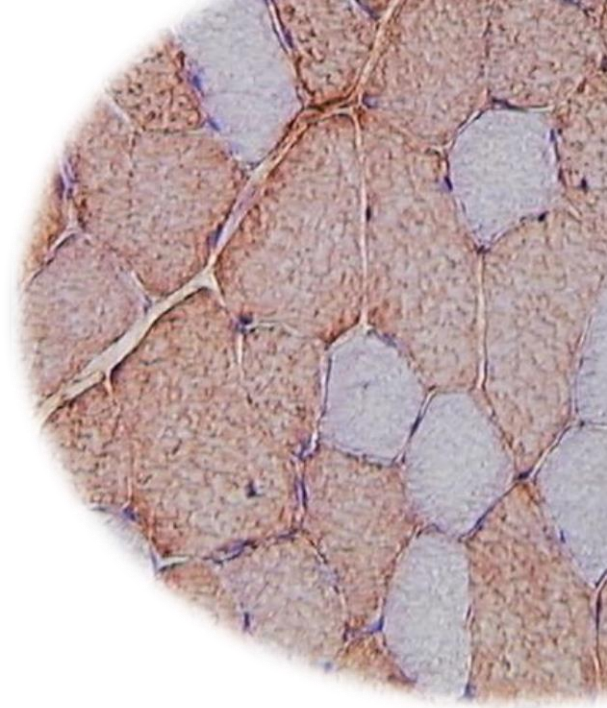
BIBLIOGRAFÍA

1. **Adams GR, and Vaziri ND.** Skeletal muscle dysfunction in chronic renal failure: effects of exercise. *Am J Physiol Renal Physiol* 290: F753-761, 2006.
2. **Apontes P, et al.** Mangiferin stimulates carbohydrate oxidation and protects against metabolic disorders induced by high-fat diets. *Diabetes* 63: 3626-3636, 2014.
3. **Arimura Y, and Hirakata H.** Uremic myopathy. *Ryōkibetsu shōkōgun shirizu* 72-75, 1997.
4. **Atlantis E, et al.** Inverse associations between muscle mass, strength, and the metabolic syndrome. *Metabol Clin Exp* 58: 1013-1022, 2009.
5. **Bardin T.** Musculoskeletal manifestations of chronic renal failure. *Curr Op Rheumatol* 15: 48-54, 2003.
6. **Benard O, and Chi Y.** Medicinal properties of mangiferin, structural features, derivative synthesis, pharmacokinetics and biological activities. *Mini Rev Med Chem* 15: 582-594, 2015.
7. **Bertoli M, et al.** Uremic myopathy and calcitriol therapy in CAPD patients. *ASAI Trans* 37: M397-M398, 1991.
8. **Couturier A, et al.** Correction: Carnitine supplementation to obese Zucker rats prevents obesity-induced type I to type II muscle fiber transition and favors an oxidative phenotype of skeletal muscle. *Nutr Metabol* 11: 16, 2014.
9. **Chabowski A, et al.** Fatty acid transport and FAT/CD36 are increased in red but not in white skeletal muscle of ZDF rats. *Am J Physiol Endocrinol Metab* 291: E675-682, 2006.
10. **Flisinski M, et al.** Decreased hypoxia-inducible factor-1alpha in gastrocnemius muscle in rats with chronic kidney disease. *Kidney Blood Press Res* 35: 608-618, 2012.
11. **Flisinski M, et al.** Morphometric analysis of muscle fibre types in rat locomotor and postural skeletal muscles in different stages of chronic kidney disease. *J Physiol Pharmacol* 65: 567-576, 2014.
12. **Girgis CM, et al.** The roles of vitamin D in skeletal muscle: form, function, and metabolism. *Endocr Rev* 34: 33-83, 2013.
13. **Gomez-Fernandez P, et al.** [Chronic kidney insufficiency and respiratory muscle function. Changes induced by treatment with 1,25(OH)2D3]. *Med Clin* 94: 204-207, 1990.
14. **Guo F, et al.** Beneficial effects of mangiferin on hyperlipidemia in high-fat-fed hamsters. *Mol Nutr Food Res* 55: 1809-1818, 2011.
15. **Henderson RG, et al.** Effects of 1,25-dihydroxycholecalciferol on calcium absorption, muscle weakness, and bone disease in chronic renal failure. *Lancet* 1: 379-384, 1974.
16. **Hickey MS, et al.** Skeletal muscle fiber composition is related to adiposity and in vitro glucose transport rate in humans. *Am J Physiol* 268: E453-457, 1995.
17. **Holloway GP, et al.** Regulation of skeletal muscle mitochondrial fatty acid metabolism in lean and obese individuals. *Am J Clin Nutr* 89: 455S-462S, 2009.
18. **Lally JS, et al.** Subcellular lipid droplet distribution in red and white muscles in the obese Zucker rat. *Diabetologia* 55: 479-488, 2012.
19. **Lewis MI, et al.** Metabolic and morphometric profile of muscle fibers in chronic hemodialysis patients. *J Appl Physiol* 112: 72-78, 2012.
20. **Lim J, et al.** Dual mode action of mangiferin in mouse liver under high fat diet. *PLoS One* 9: e90137, 2014.
21. **Martins AR, et al.** Mechanisms underlying skeletal muscle insulin resistance induced by fatty acids: importance of the mitochondrial function. *Lipids Health Dis* 11: 30, 2012.
22. **Miura T, et al.** Antidiabetic activity of a xanthone compound, mangiferin. *Phytomed Int J Phytother Phytopharmacol* 8: 85-87, 2001.
23. **Molsted S, et al.** Myosin heavy-chain isoform distribution, fibre-type composition and fibre size in skeletal muscle of patients on haemodialysis. *Scand J Urol Nephrol* 41: 539-545, 2007.
24. **Perry BD, et al.** Muscle atrophy in patients with Type 2 Diabetes

- Mellitus: roles of inflammatory pathways, physical activity and exercise. *Exerc Immunol Rev* 22: 94-109, 2016.
25. **Pojednic RM, and Ceglia L.** The emerging biomolecular role of vitamin D in skeletal muscle. *Exerc Sport Sci Rev* 42: 76-81, 2014.
 26. **Pompeani N, et al.** Skeletal muscle atrophy in sedentary Zucker obese rats is not caused by calpain-mediated muscle damage or lipid peroxidation induced by oxidative stress. *J Negat Results Biomed* 13: 19, 2014.
 27. **Rasbach KA, et al.** PGC-1alpha regulates a HIF2alpha-dependent switch in skeletal muscle fiber types. *Proc Nat Acad Sci USA* 107: 21866-21871, 2010.
 28. **Ringseis R, et al.** Supplementing obese Zucker rats with niacin induces the transition of glycolytic to oxidative skeletal muscle fibers. *J Nutr* 143: 125-131, 2013.
 29. **Sellamuthu PS, et al.** Protective nature of mangiferin on oxidative stress and antioxidant status in tissues of streptozotocin-induced diabetic rats. *ISRN Pharmacol* 2013: 750109, 2013.
 30. **Shah KA, et al.** Mangifera indica (mango). *Pharmacog Rev* 4: 42-48, 2010.
 31. **Taes YEC, et al.** Effect of dietary creatine on skeletal muscle myosin heavy chain isoform expression in an animal model of uremia. *Nephron Exp Nephrol* 96: e103-e110, 2004.
 32. **Tsubaki M, et al.** Mangiferin suppresses CIA by suppressing the expression of TNF-alpha, IL-6, IL-1beta, and RANKL through inhibiting the activation of NF-kappaB and ERK1/2. *Am J Trans Res* 7: 1371-1381, 2015.
 33. **Valero T.** Mitochondrial biogenesis: pharmacological approaches. *Cur Pharm Design* 20: 5507-5509, 2014.
 34. **Wanic-Kossowska M, et al.** Does calcitriol therapy improve muscle function in uremic patients. *Perit Dial Int* 16 Suppl 1: S305-308, 1996.
 35. **Wessels B, et al.** Pioglitazone treatment restores in vivo muscle oxidative capacity in a rat model of diabetes. *Diabetes Obes Metab* 17: 52-60, 2015.
 36. **Wuthrich RP, et al.** The role of calcimimetics in the treatment of hyperparathyroidism. *Eur J Clin Invest* 37: 915-922, 2007.

CAPÍTULO 2

Hipótesis y objetivos



Objetivos

Partiendo de los antecedentes bibliográficos sobre la relación entre músculo esquelético, insuficiencia renal crónica y obesidad sintetizados en el capítulo de Introducción, los cuáles serán expuestos con mayor extensión en un próximo capítulo sobre Revisión bibliográfica, la presente tesis doctoral está fundamentada en las siguientes hipótesis y objetivos concretos.

HIPÓTESIS

Hipótesis Estudio 1

1. Los cambios en las características contráctiles, metabólicas y morfológicas de las fibras musculares esqueléticas inducidos por la insuficiencia renal crónica durante la fase de “estabilización” (8-12 semanas) deben ser diferentes a los que se han descrito previamente en la literatura especializada durante la fase aguda (1-6 semanas) de este proceso.
2. Esta plasticidad muscular debe ser más pronunciada en el músculo tibial craneal, un músculo típico de contracción rápida y prácticamente inactivo en reposo, que en el músculo sóleo, un músculo característico de contracción lenta y activo de manera tónica en reposo para proporcionar soporte postural anti-gravitatorio.
3. El sexo debe tener una interacción significativa en la respuesta del músculo esquelético a la uremia prolongada durante 12 semanas, esperándose cambios musculares más acusados en machos que en hembras.
4. Por último, los cambios musculares secundarios a la uremia deben estar asociados con una alteración de la respuesta a la hipoxia a nivel celular.

Hipótesis Estudio 2

1. La alimentación de ratas urémicas con dietas altas en fósforo debe intensificar la severidad de los cambios musculares inducidos por uremia.
2. Por el contrario, el tratamiento de ratas urémicas con dosis bajas de calcitriol debe atenuar estos cambios,

revertiendo las características de los tipos de fibras musculares de estos animales hacia los perfiles basales de músculos controles.

Hipótesis Estudio 3

1. La atrofia muscular y la transformación tipo-fibrilar lenta a rápida inducidas por la obesidad ocurren en paralelo con un incremento generalizado de la capacidad oxidativa mitocondrial del músculo esquelético.
2. Además, esta plasticidad muscular secundaria a la obesidad debe ser más pronunciada en músculos rojos, con gran dependencia energética de sustratos sanguíneos circulantes, que en músculos blancos, con mayor dependencia metabólica del glucógeno intramuscular.

Hipótesis Estudio 4

1. El consumo crónico de mangiferina debe contrarrestar la atrofia muscular y la transformación tipo-fibrilar lenta a rápida que ocurren frecuentemente en músculos esqueléticos de ratas secundarias a la obesidad. También debe favorecer la capacidad oxidativa mitocondrial del músculo esquelético.
2. La prevención de los cambios musculares secundarios a la obesidad puede ser una estrategia de utilidad práctica para mejorar las alteraciones metabólicas asociadas a la obesidad, tales como resistencia a la insulina y diabetes de tipo 2.

OBJETIVOS

Objetivos Estudio 1

1. Determinar el impacto de 12 semanas de nefrectomía subtotal de 5/6 sobre los rasgos fenotípicos (composición fibrilar, tamaño, perfil metabólico, capilarización y densidad nuclear) de los tipos de fibras de los músculos sóleo (lento) y tibial craneal (rápido)

Capítulo 2

- de ratas Wistar de ambos sexos.
2. Probar si el sexo interactúa sobre los efectos de este modelo de uremia experimental en las características de los tipos de fibras de estos dos músculos.
 3. Establecer si los cambios musculares inducidos por uremia son secundarios a una inadecuada respuesta celular a la hipoxia, investigando la expresión a nivel de proteína del factor inducible de hipoxia 1α en estos dos músculos con funciones opuestas.

Objetivo Estudio 2

Analizar los efectos de una dieta alta en fósforo y del tratamiento con dosis bajas de calcitriol sobre los cambios en las proporciones y en los rasgos metabólicos y estructurales de los tipos de fibras de músculos esqueléticos con perfiles lento y rápido en ratas con

uremia prolongada (12 semanas).

Objetivo Estudio 3

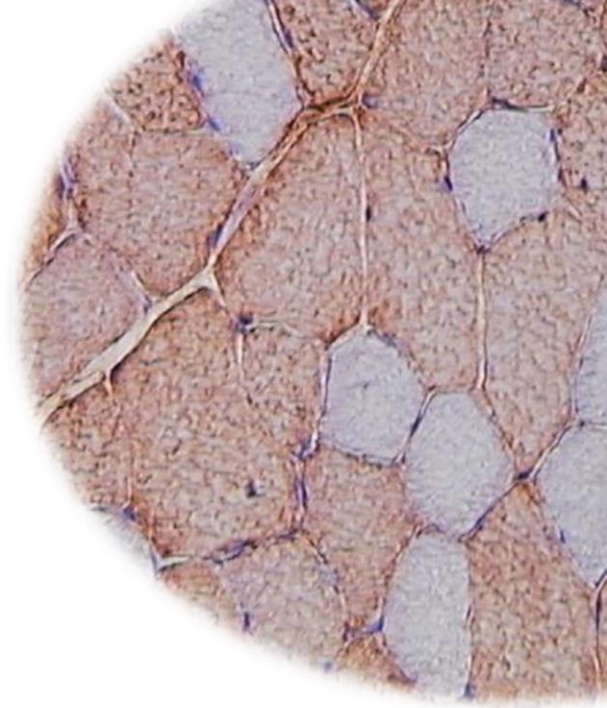
Clarificar los efectos de la obesidad sobre la masa muscular y sobre las características contráctiles, metabólicas y estructurales de los tipos de fibras de músculos esqueléticos con diferentes perfiles funcionales y energéticos, prestando atención especial a la capacidad oxidativa mitocondrial.

Objetivo Estudio 4

Examinar los efectos de la suplementación crónica de la dieta con dosis bajas de mangiferina sobre el tamaño, la composición y la capacidad oxidativa de los tipos de fibras de músculos esqueléticos con diferente estructura y función de ratas obesas.

CHAPTER 3

Uremia- and obesity-induced skeletal muscle plasticity: a literature review



Literature review

Luz M. Acevedo,^{1,3} Escolástico Aguilera–Tejero,²
and José–Luis L. Rivero¹

¹*Laboratory of Muscular Biopathology, Department of
Comparative Anatomy and Pathological Anatomy,
Faculty of Veterinary Sciences, University of Cordoba,
Cordoba, Spain*

²*Department of Animal Medicine and Surgery, University
of Cordoba, Spain*

³*Departamento de Ciencias Biomédicas, Facultad de
Ciencias Veterinarias, Universidad Central de Venezuela,
Maracay, Venezuela*

ABSTRACT

Skeletal muscle is the most abundant tissue and the main metabolic engine in the body of vertebrates. Designed by means of an admirable cellular and molecular diversity, it is endowed with great resilience against numerous intrinsic and extrinsic stimuli. In recent years, there has been a growing interest on the association between this plasticity of skeletal muscle and certain health problems affecting the world population with high prevalence. Chronic renal failure and obesity, with all its associated comorbidities (secondary hyperparathyroidism and other disorders of mineral metabolism, insulin resistance, metabolic syndrome and diabetes) are two of these problems with enormous significance for human health, particularly in view the alarming epidemics of many of these disorders worldwide. Therefore, it is essential to understand how the skeletal muscle dysfunction contributes to the origin of these endocrine-metabolic disorders, but it is also important to know how these comorbidities impact on the structure and function of skeletal muscle. This literature review aims to assess the plasticity of skeletal muscle associated with chronic renal disease and obesity. But it also includes monitoring the useful strategies to counteract the adverse effects of these conditions on skeletal muscle.

Key words: Skeletal muscle; muscle fiber types; chronic renal disease; secondary hyperparathyroidism; obesity; metabolic syndrome; anti-oxidant substances.

INTRODUCTION

Skeletal muscle, the most abundant tissue and the major metabolic engine in the body of vertebrates, is heavily impacted by chronic renal failure (CRF) (2) and obesity (21).

Patients with CRF suffer skeletal muscle structure and function abnormalities termed uremic myopathy (6, 96). However, there is great confusion in the nature and magnitude of these effects. In addition, patients with CRF

have disorders of mineral metabolism. Secondary hyperparathyroidism (HPT) develops early in CRF (91). Main features of secondary HPT in CRF include decreased production of calcitriol by the kidneys, hyperphosphatemia, hypocalcemia and increased levels of serum parathyroid hormone (PTH), and fibroblastic growth factor 23 (91).

On the other hand, obesity provides a model to examine how systematic metabolic and endocrine disturbances influence skeletal muscle structure and function. Muscle atrophy and a switch toward a faster contractile phenotype are well-documented changes in skeletal muscle of obese subjects (80). In addition to a reduced caloric intake and increased level of exercise, some natural pharmacophores are being used to counteract adverse effects of obesity. In this context, *Mangiferin indica L.*, has been used in ayurvedic medicine for centuries and may have a potential as a novel parent compound for treating obesity-related metabolic conditions (12, 97, 102, 111).

The general aim of this study was to analyze muscle plasticity associated with chronic renal failure and obesity, and propose strategies to counteract the adverse effects of these conditions on skeletal muscle structure and function.

SKELETAL MUSCLE PHENOTYPES

Muscle fiber types

Mammalian skeletal muscle comprises different fiber types, whose identity is first established during embryonic development by intrinsic myogenic control mechanisms and is later modulated by neuronal and hormonal factors (92). Mammalian adult limb skeletal muscles are composed of four major myosin heavy-chain isoform termed: slow or β /MHC and three fast IIA-, IIX and IIB-MHCs. They are expressed in type I, IIA, IIX, and IIB fibers, respectively (93). In addition to these pure fiber-

types, containing a single MHC, hybrid fibres coexpressing two or even more MHCs are also found under normal conditions (101). The distribution of different fiber types varies in a muscle-specific and species-specific manner (43). Muscle fiber composition varied markedly in the rat hind limb musculature. The muscle with the highest proportion of type I fibers is the red soleus muscle, with 84 % of these fibers, while the fast tibialis cranialis muscle show a low percentage of type I and high percentage of fast fiber-types (IIA, IIX and IIB) (20).

Muscle fiber cross-sectional size is estimated through the cross-sectional area (CSA) and the lesser fiber diameter (LFD), defined as the lesser diameter across the muscle fiber. The average CSA of muscle fibers in several muscles of the rat vary significantly in the rank order IIB >IIX >IIA >I (20).

On the other hand, to analyse metabolic profile of skeletal muscle fiber types studies of oxidative and glycolytic enzymes in muscle by quantitative histochemical reactions are required. Two of the most useful histochemical reactions used are succinate dehydrogenase (SDH), an oxidative enzyme (24), and glycerol-3-phosphate-dehydrogenase (GPDH), an enzyme used as an indirect marker for glycolytic potential of myofibers. These enzyme activities are assayed by quantitative histochemical methods previously adjusted and validated in rat skeletal muscle (88). Histochemical studies of oxidative enzymes in rat skeletal muscle reported that the mean SDH activity in the slow fibers is higher than in fast fibers (107). Conversely, GPDH activity is higher in fast than in slow fibers (88).

Other muscle variable interesting to evaluate in muscle plasticity studies is the vascular supply. It is readily apparent on routine stains such as periodic acid-Schiff (PAS), especially after α -amylase digestion. Medium-size arterioles and veins run between the fascicles, while within the fascicles there is a capillary

network in close relation to individual fibers (24). The capillarity is an important determinant of peripheral gas and substrate exchange. The size of capillary bed should match to the needs of muscle fibers (49). Another morphological parameter important to study is the size of the myonuclear domain. It shows a relation between the quantity of the genetic machinery and the protein requirement of the fiber (89). A study of single fibers showed that there are differences of myonucleus densities among fiber types. In adult rats, slow muscle fibers show significantly greater number of myonucleus/mm² than fast muscle fibers (107).

Muscle phenotype

Specialized fiber types are present in skeletal muscles from all mammalian species. Body size has a major role in determining the functional demands on skeletal muscles. Muscles from small mammals like mice consist predominantly of IIX and IIB fibers, whereas muscles from large mammals like humans are mainly composed of type I and IIA fibers (92). Slow muscles generate ATP mainly by oxidative mitochondrial processes. They contract more slowly, generate less mechanical power and spend less ATP. Moreover, they maintain contractile activity in absence of fatigue. By contrast, fast muscles depend largely on glycolytic process to generate ATP. They contract more quickly, produce high mechanical power but spend more ATP (92).

Skeletal muscle of female and male rats shows different fiber-type composition. Studies have confirmed gender differences in body mass, muscle mass, fiber size and number of muscle fibers in rats (69). There is evidence that CRF reduces levels of gonadal hormones, particularly testosterone, due to a dysfunction of the hypothalamic–pituitary–gonadal axis (reviewed in Ref. 2). Eason *et al.*, (27) demonstrated that the adult mouse masseter is a sexually dimorphic muscle and that maintenance of its contractile phenotype is dependent on

testosterone. Males have greater amounts of cells that contain type IIb MHC, and females have greater amounts of cells that contain type IIa MHC. This maintenance of sexual dimorphism is, at least partly, testosterone-dependent because castration results in an increase of the type IIa MHC in males (27). Drzymala-Celichowska *et al.*, (23) also reported differences in MHC isoform content in red and white rat skeletal muscles. Welle *et al.*, (113) showed differences in the expression of genes related with sex differences in human skeletal muscles.

Muscle plasticity

Mammalian skeletal muscles have remarkable plasticity in response to different physiological and pathological stimuli (92). Immunohistochemical and *in situ* hybridization analyses of MHC isoforms are still considered as the best approaches for muscle fiber typing at the protein and transcript levels, respectively (92). In rat muscles, they show the existence of a spectrum of fiber-types according to the so-called ‘nearest-neighbour’ scheme for MHC combinations, where hybrid fibers bridge the gaps between pure fibers: I ↔ I+IIA ↔ IIA ↔ IIAX ↔ IIX ↔ IIXB ↔ IIB (88). Due to the slow protein turnover of myosin, hybrid fibers with mixed MHC content are very frequent in muscles undergoing fiber-type transformation, and they provide insight regarding the nature (direction) of MHC switching (92). A slow-to-fast switch in the direction I→IIA→IIX→IIB occurs in muscles unloaded by decreased neuromuscular activity, as well as in denervated muscles, whereas a fast-to-slow transformation in the opposite direction IIB→IIX→IIA→I is seen in muscles overloaded, by increased neuromuscular activity, as well as by hypothyroidism (92). Available evidence from several physiological studies indicates that fiber-type transformation involves coordinated changes in all muscle cell compartments, including components of energy metabolism and contractile machinery (92). However, as

these two muscle cell properties are controlled by distinct signaling pathways, dissociation between metabolic and contractile adaptive response can occur (92).

There are several mechanisms controlling coordinated regulation of fast and slow gene programs. For example, AMP-activated protein kinase (AMPK) is a major regulator of muscle energy metabolism acting as a fuel and energy status sensor. AMPK activation or inhibition can also affect MHC gene expression and fiber type profile. In rat skeletal muscle, AMPK protein levels are highest in the soleus (slow) muscle and lowest in the white gastrocnemius (fast) muscle. AMPK is activated in response to exercise and muscle contraction via the increased AMP concentration secondary to ATP consumption in both rodents and humans (92). The peroxisome proliferator-activated receptors (PPAR), are members of the nuclear receptor superfamily that bind DNA as heterodimers with retinoid X receptors. The constitutively active PPAR δ , the more abundant isoform in skeletal muscle, leads to a more oxidative fiber type profile with increased mitochondrial DNA, upregulation of some slow contractile protein genes, and increased resistance to fatigue (92). PGC-1 α is a principal factor regulating muscle fibre type determination, is expressed more in oxidative than in glycolytic muscles (62), and it is a regulatory molecule of mitochondrial biogenesis (110).

SKELETAL MUSCLE AND CHRONIC RENAL FAILURE

Muscle changes and uremia

Several studies over the past 40 yr have described the adaptive changes in skeletal muscle performance parameters in response to uremic stimulus both in human patients with CRF (5, 15, 16, 22, 26, 29, 55, 60, 70, 90) and in animal models of uremia (3, 9, 13, 32, 33, 96, 104). These studies have reported changes at both the fiber-type (e.g., fiber-type proportion, cross-sectional size,

metabolic enzyme activities, capillarity and/or nuclei) and the whole muscle (e.g., muscle metabolism derived from either biochemistry of key enzymes or nuclear magnetic resonance spectroscopy) levels. A major problem with most of these studies is that they provide contradictory findings. For example, muscle fiber atrophy is generally cited in reviews on the effects of uremia on skeletal muscles (2, 30, 36). However, studies performed on skeletal muscles of human patients with CRF revealed results ranging from uniform atrophy (90) to generalized hypertrophy of all muscle fiber types (60). Several limitations to some of these studies have been discussed in recent reports (33, 60). They include small sample size, suboptimal control subjects (e.g., healthy athletes) or absence of controls, use of classical histochemical techniques with low analytic precision and high subjectivity, heterogeneous acquisition and handling of muscle sample specimens for optimal analysis, diversity of skeletal muscle studied (including non-limb muscles), overestimation of results without statistical significance, and misunderstanding of phenotypic changes reported in skeletal muscle fibers.

Comparisons between human and animal studies on the impact of CRF on skeletal muscle are complicated by the different stages of the renal failure. Human studies have described almost unanimously the changes in skeletal muscle in renal patients with several years of hemodialysis or during the period of progression to the end-stage renal failure (5, 15, 16, 22, 26, 29, 55, 60, 70, 90). Conversely, studies using the 5/6 reduction in total renal mass (Nx), the most widely used animal model to induce uremia (47), have described the changes of skeletal muscles within the acute stage (the first 48 h after the surgery) and/or the period of improvement resulting from functional hypertrophy, i.e., 3–4 wk after surgery (3, 13, 32, 33, 104). However, there is no information about the nature and magnitude of these changes during the period when the CRF is ‘stabilized’, i.e., beyond the 6th–

8th week after surgery (47). Considering the slow protein turnover of myosin and other contractile and metabolic proteins of mammalian skeletal muscle cells, requiring usually a minimum between 4 and 8 wk (see Ref. 92 for a recent review), it seems highly improbable to obtain significant changes in muscle fiber-types (i.e., fiber-type switching) in the short period of time (4 wk or even less) that has been studied in animal models of uremia.

Previous studies in short-term animal models of uremia have noted a different impact on skeletal muscles with different functional competences (31–33). For example, the fiber atrophy of fast-twitch fibers and capillary rarefaction that occur in rats in early stages (4 wk) of CRF was noted to be more severe in limb (gastrocnemius) than in trunk (longissimus thoracis) muscles (31, 32), being attributed to a different fiber-type-dependent resistance to hypoxia of these two muscles (31). However, a modest difference in fiber-type distribution was noted between these muscles (33). From the available literature, it seems that postural as opposed to locomotor muscles might be more resistant to hypoxia and fiber atrophy secondary to uremia. The mechanism involves increased expression of inducible nitric oxide synthase, which is interpreted as a protective factor against hypoxia through hypoxia inducible factor 1 α (HIF-1 α) stabilization (31). This transcription factor is a key regulator for the induction of genes that facilitate adaptation of cells from normoxia to hypoxia (51). Under normal conditions, higher HIF-1 α expression plays an active role in skeletal muscle plasticity, leading to fiber-type transitions in the fast direction, fiber hypertrophy, oxidative-to-glycolytic energy metabolism transition and neovascularisation (65, 82). However, under hypoxic-conditions (renal anemia), the reduced expression of HIF-1 α which has been found in locomotor muscles of rats 4 wk after Nx (31) does not support this role in muscle plasticity.

In rat hind limb, the most superficial muscles, which are composed predominantly of fast-glycolytic fibers, such as the tibialis cranialis muscle (98% in its white region), are only recruited at high intensity-physical activity, being normally inactive at rest (20). In contrast, the deep muscles composed predominantly of slow-oxidative fibers, such as the soleus muscle (84%), are primarily active at rest providing postural (antigravitatory) support (20). Based upon their dramatic differences in both resting muscle activity and fiber-type composition, the comparative evaluation of muscle fiber-type characteristics between these two hind limb muscles in uremic rats could lead to a broader understanding of

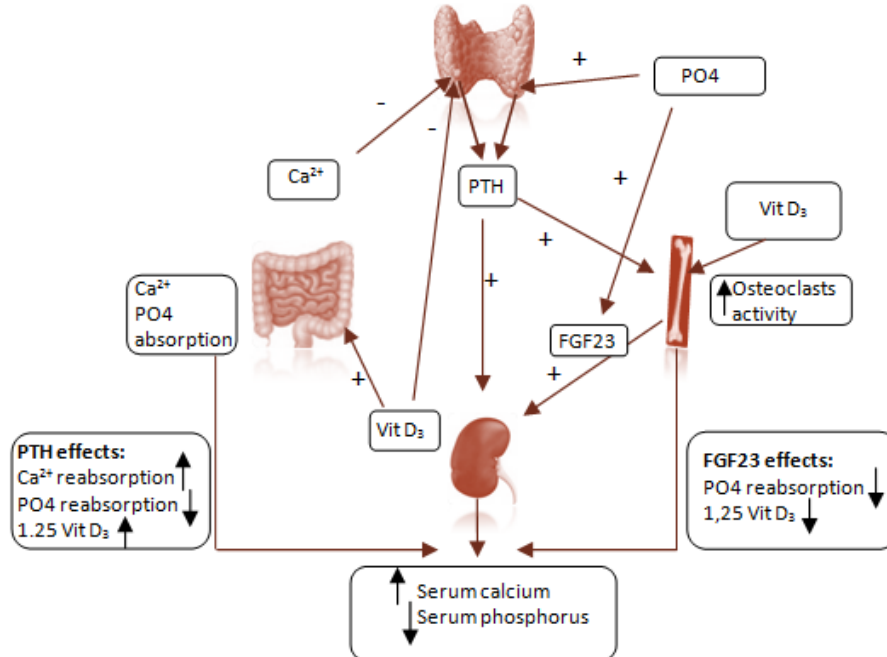
the role that muscle function plays in the changes of skeletal muscle in patients with chronic renal failure.

Mineral metabolism disorders and renal failure

The homeostasis of calcium and phosphorus is the result of complex relations between calcemia, phosphatemia, and different hormones and factors working synergistically to keep a normal balance of these minerals (91) (Fig. 3.1).

Mineral metabolism alteration begins early with progressing of chronic kidney disease. It is characterized by increment of serum PTH levels, low serum levels of activated vitamin D and alteration of calcium and

▼ **Fig. 3.1** Illustration of normal calcium and phosphorus homeostasis. PTH, parathyroid hormone; Ca^{2+} : Calcium; PO_4 : Phosphate; FGF23, fibroblast growth factor 23; 1,25 VitD_3 : 1,25 Vitamin D_3 . (Adapted from Ref. 91).



showed, in a cross-sectional study of human patients, that FGF23 levels increase at early CRF stages whereas PTH levels increase at more advanced CKD stages. FGF23 is an excellent marker of disease severity and outcomes, particularly in CRF (94).

Vitamin D and skeletal muscle

Vitamin D is an essential factor in the regulation of calcium and phosphorus balance (91) and mineral bone metabolism (42) and affects numerous other cell types (19). It is regarded traditionally as a regulator of bone metabolism (83). Vitamin D₃ is synthesized in the skin from 7-dehydrocholesterol upon exposure to UV irradiation and it can be taken in the diet. Bound to a vitamin D binding protein, vitamin D₃ is transported to the liver where it is hydroxylated to 25-hydroxyvitamin D₃ (25OHD₃), the major circulating form of vitamin D and biomarker of vitamin D status. 25OHD₃ is further hydroxylated at position 1 by the enzyme CYP27B1 to form 1,25-hydroxyvitamin D₃ [1,25(OH)₂D₃], the most active form of vitamin D, which is then transported to target tissues (19, 83). The vitamin D hydroxylases have an important role in providing a tightly regulated supply of 1, 25 (OH)₂D₃ (18).

The actions of vitamin D on skeletal muscle may, in part, be indirect by way of vitamin D's effect on calcium and phosphate homeostasis, possibly via mechanisms mediated by intestinal absorption (83). Its main action is to enhance the availability of calcium and phosphorus for new bone formation (91). Vitamin D and its receptor are important for normal skeletal muscle development and in optimizing muscle strength and performance (14). Vitamin D plays a role in the preservation of muscle size and strength in hemodialysis patients (40). Vitamin D deficiency in animal models results in negative effects on muscle fiber structure and calcium/phosphorus handling, suggesting an integral role of vitamin D in skeletal muscle function (45).

The biologically active 1,25 (OH)₂ D₃ binds to the vitamin D receptor (VDR), a classic steroid receptor that principally acts as a nuclear transcription factor. However, non-nuclear receptor mediating non-genomic actions also has been described (83). Vitamin D regulates gene expression and modulates ligand-dependent uptake of 25-hydroxyvitamin D₃ in primary myofibers. Muscle is a direct target of vitamin D with an autoregulatory vitamin D-endocrine system in primary myotubes and the 1,25(OH)₂D₃-modulated uptake of 25OH in wild type myofibers. (38).

In vitro studies have been performed to investigate the effect of vitamin D₃ (1 α , 25-hydroxyvitamin D₃) on the proliferating, differentiating and differentiated phases of C2C12 myoblast, a mouse skeletal muscle cell line. The authors found that vitamin D₃ plays an important role in cell proliferation and differentiation in C2C12. They showed by western blot analysis that vitamin D₃ treatment enhanced fast myosin heavy chain expression in the differentiated C2C12 cells (75). In order to understand the mechanism of the effect of the vitamin D₃ previously described, Tanaka *et al.*, (105) designed a study to determine the role of signals transmitted through the VDR during differentiation of myoblast cell lines. Their results suggested that myoblast require signals transmitted through VDR for differentiation into myocytes and emphasized the importance of VDR expression in skeletal muscles for maintaining muscle volume in the elderly. Two mechanisms by which vitamin D may act in skeletal muscle have been proposed. VDR acts as a nuclear receptor which mediates the so-called genomic effects or via nonnuclear receptor mediating nongenomic actions.

In consideration that low vitamin D status, reduced renal function, and low dietary intake of calcium can result in mild secondary HPT, which may be associated with low muscle mass and reduced muscle strength in elderly populations, Genaro *et al.*, (37) performed a study to investigate whether low vitamin D, high PTH, or both,

are associated with sarcopenia. They found that vitamin D deficiency, associated with secondary HPT, increased the risk of sarcopenia in elderly women.

Vitamin D may play a significant role in Ca^{2+} uptake by the mitochondria which in turn are involved in the orchestration of cellular metabolic homeostasis (99). Consistent relationships exist between vitamin D status and muscle function. Vitamin D supplementation has beneficial effects on muscle strength, balance, and gait in diverse settings including adolescents, the elderly, and patients with CRF (42).

SKELETAL MUSCLE AND OBESITY

Muscle changes in obesity

Several obesity experimental studies have used Zucker fatty rat like an animal model of genetic obesity and related conditions such as insulin resistance, diabetes and metabolic syndrome (1, 17, 25, 34, 48, 59, 81, 84-86, 114). Obesity in this animal is inherited as an autosomal recessive trait. Zucker fatty rats were generated by a cross between the Merk stock M and Sherman rats. Animals are homozygous for the *fa/fa* gen. Lipid proportions in Zucker fatty are 50 % to body weight (reviewed in Ref. 8). Diverse studies have reported changes in morphological parameters in skeletal muscle of the obese Zucker rat (OZR). Peterson *et al.*, (81) showed that OZR has lower skeletal muscle size than the lean Zucker rat (LZR). A decrease in the number of satellite cells could be a factor that contributes to the reduced mass observed in control muscles of OZR. In addition, Pompeani *et al.*, (84), confirmed that OZR skeletal muscles are atrophic in skeletal muscle weight and in size determined by measurement of mean fiber area compared with counterpart control animals. By contrast, Ringseis *et al.*, (86) did not report differences in skeletal fiber size of obese and lean Zucker rats.

Muscular changes in obesity include fiber transition

from type I to type II, with decreased fiber type I and increased fiber type II in OZR (17, 86). Similarly, a study with a high fat-diet model of obesity also reported decreased proportion of type I and increased of type I/IIA hybrid fibers in the soleus muscle (21). Studies in a spontaneous diabetic animal model, called non-obese diabetic goto-kakisaki rats, showed an altered fiber type distribution in red and white muscles with decrease of the percentage of type IIA in soleus and type I and IIA in plantaris muscle, and increase of type IIB. These findings have been related with an impairment in insulin sensitive and glucose metabolism (115). Several studies in obese and metabolic syndrome patients have reported low percentages of type I and high proportion of type II fibers (46, 52, 103, 106). Albers *et al.*, (7) reported that diabetic and obese patients have an increase in the relative number of type IIX compared with lean subjects.

In vitro studies tested the hypothesis that all facets of skeletal muscle fatty acid metabolism are upregulated in skeletal muscles of OZR, and that the increased triacylglycerol concentration is attributable to an inability to upregulate fatty acid oxidation sufficiently to cope with a large influx of protein-mediated fatty acid transport. The results suggest that the increased intramuscular accumulation of lipids is attributable to an increased rate of fatty acid transport that exceeds the currently increased capacity for mitochondrial fatty acid oxidation and more of these fatty acids that have entered the muscle are esterified (48). Furthermore, Malenfant *et al.*, (67) reported disturbances of the intramyocellular lipid distribution with an increased localization of fat stores away from the sarcolemma. This lipid distribution could impact on the ability of the cell for lipid oxidation.

A study of lipid metabolism in skeletal muscle of insulin resistant rodent model showed that oxidative capacity is increased (109). By contrast, SDH activities did not show significant differences in whole soleus muscle in OZR compared with LZR, even though they

found a decrease of SDH activities in diabetic OZR (1). These findings are opposite of the results reported in other studies with a decrease of SDH activity in rectus femoris muscle of obese versus lean Zucker rats reported by Ringseis *et al.*, (86), and a decrease of mitochondrial volume density in OZR (67). In addition, Wessels *et al.*, (114) found lower muscle oxidative capacity in diabetic OZR compared with lean rats, but it was not attributable to impairments of mitochondrial respiratory capacity or a lower mitochondrial content.

Patients with type 2 diabetes showed metabolic alterations in skeletal muscle as consequence of both changes in fiber composition and in fiber-specific metabolism (74). In another study on patients with type 2 diabetes a decrease of oxidative capacity in the vastus lateralis muscle due to reduction in slow oxidative fibers was noted. Moreover, Simoneau *et al.*, (98) found a decrease of mitochondrial volume density in obese patients. However, both oxidative and glycolytic enzymes activities were significantly increased in fast glycolytic and fast oxidative glycolytic fibers. In summary, there is ample controversy in the specialized literature regarding the specific effects of obesity on skeletal muscle metabolism.

Muscle changes and metabolic dysregulation

Obesity is a strong risk factor for the development of insulin resistance. Earlier research in human reported that reduced skeletal muscle of fiber type I population in obese non-insulin-dependent diabetes mellitus patients may be one component of a multifactorial process involved in the development of insulin resistance (46). Metabolic alteration within muscle include defects in skeletal muscle lipid metabolism such as increased accumulation of intramuscular lipid (48, 56). It can be as a biomarker of peripheral insulin resistance in OZR (54).

Insulin resistance, which represents an impaired ability of insulin to exert its effects on glucose and lipid

homeostasis, is a key metabolic defect associated with obesity and type 2 diabetes (57, 109). The findings suggest that mitochondrial fatty acid oxidative capacity is increased in skeletal muscle from insulin-resistant rodents, in which β -hydroxyacyl CoA dehydrogenase, medium chain acyl-CoA dehydrogenase, and citrate synthase enzyme activities were increased. These results are potentially a compensatory response to elevated fatty acid substrate availability (109). Koves *et al.*, (57) agree that obesity, diabetes and high-fat feeding are conditions that increase the rate of β -oxidation in skeletal muscle, but there is a relation from skeletal muscle insulin resistance to lipid-induced mitochondrial stress that could be responsible of impaired mitochondrial function. In a review, Martin *et al.*, proposed that mitochondrial dysfunction in elevated free fatty acid levels plays a central role in the pathogenesis of insulin resistance (68). The association between skeletal muscle insulin resistance in obesity and mitochondrial dysfunction suggests that insulin resistance arises due to an imbalance of cellular bioenergetics.

PROTECTION AGAINST ADVERSE OBESITY-INDUCED MUSCLE CHANGES

Mechanisms involved

Obesity is associated with an inflammatory chronic state (8). The increased protein degradation in the skeletal muscle of the OZR may be due to increased activity of the ubiquitin-dependent proteolytic system (11). In addition, recent research reported that systemic inflammation promotes muscle atrophy via decreased muscle protein synthesis and increased ubiquitin-proteasome, lysosomal proteasome and caspase 3 mediated protein degradation (80).

In a study to examine fiber type distribution and PGC-1 α levels in soleus muscle in obesity and diabetes-obesity, using Zucker rats, Adachi *et al.*, (1) reported lower

percentage of type IIA fibers in diabetic OZR than in non-diabetic OZR and LZR. Furthermore, the mRNA expression levels of PGC-1 α were decreased in the soleus muscle of diabetic OZR compared with the other two groups. In addition, the changes observed in muscle fiber types in obese rats can be explained by down-regulation of the mRNA and protein levels of PPAR δ and PGC-1 α , which are critical regulators of muscle fiber transformation (17). On the other hand, Kove *et al.*, (56) showed a link between PGC-1 α and efficient mitochondrial oxidation of fatty acid. Their findings suggest that increased PGC-1 α activity and/or enhanced mitochondrial efficiency may protect against lipid induced insulin resistance.

To protect against the skeletal muscle changes observed in obesity, Ringseis *et al.*, 2013 designed an experimental study with OZR fed with niacin supplement. The results showed an increase of type I fibers and mRNA levels of genes encoding regulators of muscle fiber composition, mitochondrial biogenesis, angiogenesis, and genes involved in fatty acid catabolism and oxidative phosphorylation.

Mangiferin as an anti-obesity agent

Different pharmacophores are being used against the deleterious effects of obesity and related comorbidities on human health, mangiferin being one of them (10, 12, 17, 50, 58, 61, 66, 95, 102, 108, 111, 112). *Mangifera indica L.*, has been used in ayurvedic medicine for centuries, because several beneficial properties have been attributed to different components of the mango tree. The chemical components studied are C-glucosyl-xanthone or mangiferin, mangiferonic acid, hydroxymangiferin, polyphenols and carotenes (97). The literature has reported different pharmacological activities such as antioxidant, anti-inflammatory, antidiabetic, and lipolytic among others (4, 12, 39, 71, 73, 77, 95, 97, 112).

Mangiferin, as an anti-obesity agent, decreases plasma

free fatty acid (FFA) levels through promoting FFA uptake and oxidation, inhibits FFA and triglycerides accumulation by regulating the key enzymes expression in liver through the activation of the AMPK pathway. It increases AMPK phosphorylation and its downstream proteins involved in fatty acid translocase and carnitine palmitoyltransferase 1 (73). Similarly, using X-3, a derivate of mangiferin, in *db/db* mice, Han *et al.*, (44) showed a decrease of hyperglycemia and obesity. In addition, in vitro studies revealed that X-3 increased glucose uptake and AMPK activity in 3T3-L1 cells (44).

On the other hand, experiments in vivo and in vitro showed that mangiferin protected against high-fat diet, gain, increased aerobic mitochondrial capacity and thermogenesis, and improved glucose and insulin profile. These beneficial effects of mangiferin were due to increased carbohydrate utilization in oxidative metabolism through of the activation of pyruvate dehydrogenase complex (10). Another experimental study showed the hypolipidemic effect of mangiferin by upregulation mRNA expression of PPAR α , fatty acid translocase, carnitine palmitoyltransferase 1 in liver and muscle, and lipoprotein lipase in muscle (41)

A recent report describes the molecular mechanism of the beneficial effects of mangiferin on obesity and related endocrine and metabolic disorders, indicating that mangiferin upregulates proteins pivotal for mitochondrial bioenergetics and downregulates proteins controlling de novo lipogenesis (61). In addition, another study found that mangiferin reduced reactive oxygen intermediate and inhibited lipogenesis through inhibition of sterol regulatory binding protein activation (66). Moreover, anti-oxidant effects of mangiferin are related to inhibition of apoptotic pathways, showing a protective effect on renal tissue of streptozotocin- induced type 1 diabetic rats (77).

Several studies support the antidiabetic effects of mangiferin by different cellular and molecular

mechanisms. One mechanism proposed to explain the hypoglycaemic activity of *Mangifera indica* could be due to an intestinal reduction of the absorption of glucose (4). Recently, a report found that mangiferin increased glucose uptake in parallel with increased phosphorylation of AMPK in 3T3-L1 cells (95). This was confirmed in a study by Wang *et al.*, (112), who found that mangiferin improved the glucose utilization and insulin sensitivity through up-regulation of the AMPK phosphorylation. Furthermore, antidiabetic effect of mangiferin resulted by increasing GLUT 4 expression and translocation in muscle cells. These effects are probably mediated through two independent pathways that are related to AMPK and PPAR δ .

Moreover, mangiferin showed significant antihyperlipidemic and antiatherogenic activities as evidenced by significant decrease in plasma total cholesterol, triglycerides, low-density lipoprotein cholesterol levels coupled together with elevation of high-density lipoprotein cholesterol level and diminution of atherogenic index in streptozotocin-induced-diabetic rats. In addition, the chronic administration of mangiferin (10 and 20 mg/kg, i.p.) for 14 days markedly improved oral glucose tolerance in glucose-loaded normal rats, suggesting a potent antihyperglycemic activity (71). Finally, a recent review emphasizes the medicinal properties of mangiferin improving metabolic disorders. For example, enhancement of carbohydrate utilization in oxidative metabolism, and increased insulin sensitivity in animal models of obesity and insulin resistance (12).

A few studies provided evidence that mangiferin has beneficial effects on various aspects of muscle function in obese animals. For example, mangiferin supplementation enhanced lipid catabolism in skeletal muscle of these animals by upregulating genes involved in muscle fatty acid β -oxidation (41). This substance also induced a shift in muscle respiratory quotient from lipid toward pyruvate oxidation (10). However, cellular effects of mangiferin on

skeletal muscle mass, and contractile and metabolic phenotypes have not been explored in experimental models of obesity.

FINAL REMARKS AND CONCLUSIONS

Skeletal muscle is the most abundant tissue and the major metabolic engine in the body of vertebrates. This tissue is severely impacted by diseases that cause systemic alterations such as CRF, obesity and related comorbidities. Over the past four decades several investigations in human and animal models have been carried out to know the adaptive changes of skeletal muscle in response to the uremic environment. These studies not only report contradictory findings, but they have serious methodological limitations. Over the past recent years different strategies have been implemented to ameliorate the adverse effects caused by uremia. Among these, low doses of vitamin D seems to play beneficial effects in skeletal muscle abnormalities and the development of secondary HPT associated with CRF.

In a similar context, recent studies on obesity show inconsistent findings regarding skeletal muscle changes associated with this pathological condition and their associated comorbidities. For example, they report changes from decreased to increased oxidative capacity, being more pronounced in slow than in fast muscles. Diverse strategies have been proposed to counteract the adverse effects of obesity and related conditions on peripheral skeletal muscles. Thus, researchers have studied different pharmacophores with anti-oxidant, anti-inflammatory and antidiabetic properties from the perspective of therapeutic substances against the obesity and related conditions. In this context, evidences show that mangiferin, a major glucoside of xanthone in the mango plant *Mangifera indica L.*, has multiple biological activities, including beneficial action on skeletal muscles.

In conclusion, from the available literature it seems clear that skeletal muscle is heavily impacted by

Literature review

systematic conditions such as uremia and obesity. Overall, the results of these studies are inconsistent and require further attention with new methodological approaches. Also, the search of dietary supplements such

as vitamin D and mangiferin can result useful to counteract adverse effects of uremia and obesity on contractile and metabolic features of skeletal muscles.

REFERENCES

1. **Adachi T, et al.** Fibre type distribution and gene expression levels of both succinate dehydrogenase and peroxisome proliferator-activated receptor-gamma coactivator-1 α of fibres in the soleus muscle of Zucker diabetic fatty rats. *Exp Physiol* 92: 449-455, 2007.
2. **Adams GR, and Vaziri ND.** Skeletal muscle dysfunction in chronic renal failure: effects of exercise. *Am J Physiol Renal Physiol* 290: F753-761, 2006.
3. **Adams GR, et al.** Voluntary exercise during chronic renal failure in rats. *Med Sci Sports Exerc* 37: 557-562, 2005.
4. **Aderibigbe AO, et al.** Antihyperglycaemic effect of *Mangifera indica* in rat. *Phytother Res* 13: 504-507, 1999.
5. **Ahonen RE.** Light microscopic study of striated muscle in uremia. *Acta Neuropathol* 49: 51-55, 1980.
6. **Al-Hayk K, and Bertorini TE.** Neuromuscular complications in uremics: A review. *Neurologist* 13: 188-196, 2007.
7. **Albers PH, et al.** Human muscle fiber type-specific insulin signaling: impact of obesity and type 2 diabetes. *Diabetes* 64: 485-497, 2015.
8. **Alexandre A, and Miguel M.** Zucker rats as an experimental model for the study of various diseases. *Endocrinol Nutr* 55: 217-222, 2008.
9. **Amann K, et al.** Rats with moderate renal failure show capillary deficit in heart but not skeletal muscle. *Am J Kidney Dis* 30: 382-388, 1997.
10. **Apontes P, et al.** Mangiferin stimulates carbohydrate oxidation and protects against metabolic disorders induced by high-fat diets. *Diabetes* 63: 3626-3636, 2014.
11. **Argiles JM, et al.** Mechanism for the increased skeletal muscle protein degradation in the obese Zucker rat. *J Nutr Biochem* 10: 244-248, 1999.
12. **Benard O, and Chi Y.** Medicinal properties of mangiferin, structural features, derivative synthesis, pharmacokinetics and biological activities. *Mini Rev Med Chem* 15: 582-594, 2015.
13. **Bundschu HD, et al.** Myopathy in experimental uremia. *Res Exp Med* 165: 205-212, 1975.
14. **Ceglia L.** Vitamin D and its role in skeletal muscle. *Curr Opin Clin Nutr Metab Care* 12: 628-633, 2009.
15. **Clyne N, et al.** Effects of renal failure on skeletal muscle. *Nephron* 63: 395-399, 1993.
16. **Conjard A, et al.** Effects of chronic renal failure on enzymes of energy metabolism in individual human muscle fibers. *J Am Soc Nephrol* 6: 68-74, 1995.
17. **Couturier A, et al.** Carnitine supplementation to obese Zucker rats prevents obesity-induced type II to type I muscle fiber transition and favors an oxidative phenotype of skeletal muscle. *Nutr Metab* 10: 1743-7075, 2013.
18. **Christakos S, et al.** Vitamin D: metabolism. *Endocrinol Metab Clin North Am* 39: 243-253, 2010.
19. **Christakos S, et al.** Vitamin D: beyond bone. *Ann N Y Acad Sci* 17, 2013.
20. **Delp MD, and Duan C.** Composition and size of type I, IIA, IID/X, and IIB fibers and citrate synthase activity of rat muscle. *J Appl Physiol* 80: 261-270, 1996.
21. **Denies MS, et al.** Diet-induced obesity alters skeletal muscle fiber types of male but not female mice. *Physiol Rep* 2: 1, 2014.
22. **Diesel W, et al.** Morphologic features of the myopathy associated with chronic renal failure. *Am J Kidney Dis* 22: 677-684, 1993.
23. **Drzymala-Celichowska H, et al.** The content of myosin heavy chains in hindlimb muscles of female and male rats. *J Physiol Pharmacol* 63: 187-193, 2012.
24. **Dubowitz V, et al.** Normal Muscle. In: *Muscle Biopsy: A Practical Approach* edited by Dubowitz V, et al. Edinburg, UK: Saunders Elsevier, Elsevier Ltd., 2013, p. 28-54.
25. **Durham HA, and Truett GE.** Development of insulin resistance and hyperphagia in Zucker fatty rats. *Am J Physiol Regul Integr Comp Physiol* 290: 13, 2006.
26. **Durozard D, et al.** 31P NMR

Literature review

- spectroscopy investigation of muscle metabolism in hemodialysis patients. *Kidney Int* 43: 885-892, 1993.
27. **Eason JM, et al.** Sexually dimorphic expression of myosin heavy chains in the adult mouse masseter. *J Appl Physiol* 89: 251-258, 2000.
28. **Edwards RM.** Disorders of phosphate metabolism in chronic renal disease. *Curr Opin Pharmacol* 2: 171-176, 2002.
29. **Fahal L, and Bell GM.** Uraemic myopathy: Fact or fiction. *Int J Artif Organs* 21: 185-187, 1998.
30. **Fanzani A, et al.** Molecular and cellular mechanisms of skeletal muscle atrophy: an update. *J Cachex Sarcop Muscle* 3: 163-179, 2012.
31. **Flisiński M, et al.** Decreased hypoxia-inducible factor-1 α in gastrocnemius muscle in rats with chronic kidney disease. *Kidney Blood Pres Res* 35: 608-618, 2012.
32. **Flisinski M, et al.** Influence of different stages of experimental chronic kidney disease on rats locomotor and postural skeletal muscles microcirculation. *Ren Fail* 30: 443-451, 2008.
33. **Flisinski M, et al.** Morphometric analysis of muscle fibre types in rat locomotor and postural skeletal muscles in different stages of chronic kidney disease. *J Physiol Pharmacol* 65: 567-576, 2014.
34. **Frisbee JC, et al.** Distinct temporal phases of microvascular rarefaction in skeletal muscle of obese Zucker rats. *Am J Physiol Heart Circ Physiol* 307: 10, 2014.
35. **Garber AJ.** Effects of parathyroid hormone on skeletal muscle protein and amino acid metabolism in the rat. *J Clin Invest* 71: 1806-1821, 1983.
36. **Garibotto G.** Muscle amino acid metabolism and the control of muscle protein turnover in patients with chronic renal failure. *Nutrition* 15: 145-155, 1999.
37. **Genaro Pde S, et al.** Dietary protein intake in elderly women: association with muscle and bone mass. *Nutr Clin Pract* 30: 283-289, 2015.
38. **Girgis CM, et al.** The vitamin D receptor (VDR) is expressed in skeletal muscle of male mice and modulates 25-hydroxyvitamin D (25OHD) uptake in myofibers. *Endocrinology* 155: 3227-3237, 2014.
39. **Giron MD, et al.** Salacia oblonga extract increases glucose transporter 4-mediated glucose uptake in L6 rat myotubes: role of mangiferin. *Clin Nutr* 28: 565-574, 2009.
40. **Gordon PL, et al.** Relationship between vitamin D and muscle size and strength in patients on hemodialysis. *J Ren Nutr* 17: 397-407, 2007.
41. **Guo F, et al.** Beneficial effects of mangiferin on hyperlipidemia in high-fat-fed hamsters. *Mol Nutr Food Res* 55: 1809-1818, 2011.
42. **Halfon M, et al.** Vitamin D: a review on its effects on muscle strength, the risk of fall, and frailty. *Biomed Res Int* 953241: 27, 2015.
43. **Hamalainen N, and Pette D.** Patterns of myosin isoforms in mammalian skeletal muscle fibres. *Microsc Res Tech* 30: 381-389, 1995.
44. **Han J, et al.** X-3, a mangiferin derivative, stimulates AMP-activated protein kinase and reduces hyperglycemia and obesity in db/db mice. *Mol Cell Endocrinol* 405: 63-73, 2015.
45. **Hazell TJ, et al.** Vitamin D: an overview of its role in skeletal muscle physiology in children and adolescents. *Nutr Rev* 70: 520-533, 2012.
46. **Hickey MS, et al.** Skeletal muscle fiber composition is related to adiposity and in vitro glucose transport rate in humans. *Am J Physiol* 268: E453-457, 1995.
47. **Holecek M.** Muscle wasting in animal models of severe illness. *Int J Exp Pathol* 93: 157-171, 2012.
48. **Holloway GP, et al.** In obese rat muscle transport of palmitate is increased and is channeled to triacylglycerol storage despite an increase in mitochondrial palmitate oxidation. *Am J Physiol Endocrinol Metab* 296: 13, 2009.
49. **Hoppeler, H, and Kayar, SR.** Capillarity and Oxidative Capacity of Muscles. *Physiology* 3: 113-116, 1988.
50. **Huang TH, et al.** Salacia oblonga root improves postprandial

- hyperlipidemia and hepatic steatosis in Zucker diabetic fatty rats: activation of PPAR-alpha. *Toxicol Appl Pharmacol* 210: 225-235, 2006.
51. **Ke Q, and Costa M.** Hypoxia-inducible factor-1 (HIF-1). *Mol Pharmacol* 70: 1469-1480, 2006.
52. **Kern PA, et al.** Effect of weight loss on muscle fiber type, fiber size, capillarity, and succinate dehydrogenase activity in humans. *J Clin Endocrinol Metab* 84: 4185-4190, 1999.
53. **Kestenbaum B, and Belozeroff V.** Mineral metabolism disturbances in patients with chronic kidney disease. *Eur J Clin Invest* 37: 607-622, 2007.
54. **Korach-Andre M, et al.** Age and muscle-type modulated role of intramyocellular lipids in the progression of insulin resistance in nondiabetic Zucker rats. *Metabolism* 54: 522-528, 2005.
55. **Kouidi E, et al.** The effects of exercise training on muscle atrophy in haemodialysis patients. *Nephrol Dial Transpl* 13: 685-699, 1998.
56. **Koves TR, et al.** Peroxisome proliferator-activated receptor-gamma co-activator 1 alpha-mediated metabolic remodeling of skeletal myocytes mimics exercise training and reverses lipid-induced mitochondrial inefficiency. *J Biol Chem* 280: 33588-33598, 2005.
57. **Koves TR, et al.** Mitochondrial overload and incomplete fatty acid oxidation contribute to skeletal muscle insulin resistance. *Cell Metab* 7: 45-56, 2008.
58. **Kumar BD, et al.** Effect of Mangiferin and Mahanimbine on Glucose Utilization in 3T3-L1 cells. *Pharmacogn Mag* 9: 72-75, 2013.
59. **Lally JS, et al.** Subcellular lipid droplet distribution in red and white muscles in the obese Zucker rat. *Diabetologia* 55: 479-488, 2012.
60. **Lewis MI, et al.** Metabolic and morphometric profile of muscle fibers in chronic hemodialysis patients. *J Appl Physiol* 112: 72-78, 2012.
61. **Lim J, et al.** Dual mode action of mangiferin in mouse liver under high fat diet. *PLoS One* 9: 2014.
62. **Lin J, et al.** Transcriptional co-activator PGC-1 alpha drives the formation of slow-twitch muscle fibres. *Nature* 418: 797-801, 2002.
63. **López JR, et al.** Altered Ca²⁺ homeostasis in human uremic skeletal muscle: Possible involvement of cADPR in elevation of intracellular resting [Ca²⁺]. *Nephron Physiol* 100: p51-p60, 2005.
64. **Lorenzo Sellares V, and Torregrosa V.** [Changes in mineral metabolism in stage 3, 4, and 5 chronic kidney disease (not on dialysis)]. *Nefrologia* 3: 67-78, 2008.
65. **Lunde IG, et al.** Hypoxia inducible factor 1 links fast-patterned muscle activity and fast muscle phenotype in rats. *J Physiol* 589: 1443-1454, 2011.
66. **Mahali SK, et al.** Advanced glycation end products induce lipogenesis: regulation by natural xanthone through inhibition of ERK and NF-kappaB. *J Cell Physiol* 229: 1972-1980, 2014.
67. **Malenfant P, et al.** Fat content in individual muscle fibers of lean and obese subjects. *Int J Obes Relat Metab Disord* 25: 1316-1321, 2001.
68. **Martins AR, et al.** Mechanisms underlying skeletal muscle insulin resistance induced by fatty acids: importance of the mitochondrial function. *Lipids Health Dis* 11: 11-30, 2012.
69. **Mierzejewska-Krzyzowska B, et al.** Gender differences in morphometric properties of muscle fibres measured on cross-sections of rat hindlimb muscles. *Anat Histol Embryol* 41: 122-129, 2012.
70. **Molsted S, et al.** Myosin heavy-chain isoform distribution, fibre-type composition and fibre size in skeletal muscle of patients on haemodialysis. *Scand J Urol Nephrol* 41: 539-545, 2007.
71. **Muruganandan S, et al.** Effect of mangiferin on hyperglycemia and atherogenicity in streptozotocin diabetic rats. *J Ethnopharmacol* 97: 497-501, 2005.
72. **Negri AL.** [Fibroblast growth factor 23 (FGF 23): a new fosfaturic hormone?]. *Nefrologia*. 2003 Nov-Dec;23(6):478-81.
73. **Niu Y, et al.** Mangiferin decreases plasma free fatty acids through

Literature review

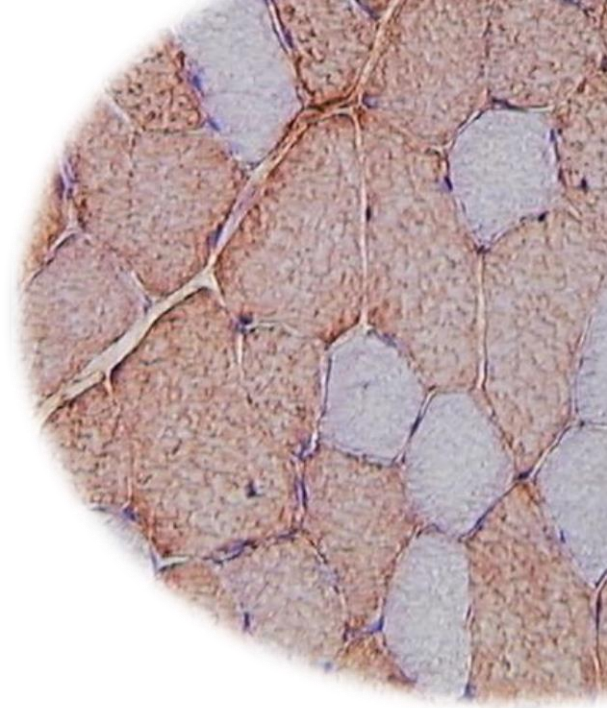
- promoting its catabolism in liver by activation of AMPK. *PLoS One* 7: 23, 2012.
74. **Oberbach A, et al.** Altered fiber distribution and fiber-specific glycolytic and oxidative enzyme activity in skeletal muscle of patients with type 2 diabetes. *Diabetes Care* 29: 895-900, 2006.
75. **Okuno H, et al.** 1alpha,25-dihydroxyvitamin D(3) enhances fast-myosin heavy chain expression in differentiated C2C12 myoblasts. *Cell Biol Int* 36: 441-447, 2012.
76. **Olauson H, and Larsson TE.** FGF23 and Klotho in chronic kidney disease. *Curr Opin Nephrol Hypertens* 22: 397-404, 2013.
77. **Pal PB, et al.** Mangiferin attenuates diabetic nephropathy by inhibiting oxidative stress mediated signaling cascade, TNFalpha related and mitochondrial dependent apoptotic pathways in streptozotocin-induced diabetic rats. *PLoS One* 9: 2014.
78. **Passeri E, et al.** Vitamin D, parathyroid hormone and muscle impairment in myotonic dystrophies. *J Neurol Sci* 331: 132-135, 2013.
79. **Pavik I, et al.** Secreted Klotho and FGF23 in chronic kidney disease Stage 1 to 5: a sequence suggested from a cross-sectional study. *Nephrol Dial Transplant* 28: 352-359, 2013.
80. **Perry BD, et al.** Muscle atrophy in patients with Type 2 Diabetes Mellitus: roles of inflammatory pathways, physical activity and exercise. *Exerc Immunol Rev* 22: 94-109, 2016.
81. **Peterson JM, et al.** Satellite cell proliferation is reduced in muscles of obese Zucker rats but restored with loading. *Am J Physiol Cell Physiol* 295: 28, 2008.
82. **Pisani DF, and Dechesne CA.** Skeletal muscle HIF-1alpha expression is dependent on muscle fiber type. *J Gen Physiol* 126: 173-178, 2005.
83. **Pojednic RM, and Ceglia L.** The emerging biomolecular role of vitamin D in skeletal muscle. *Exerc Sport Sci Rev* 42: 76-81, 2014.
84. **Pompeani N, et al.** Skeletal muscle atrophy in sedentary Zucker obese rats is not caused by calpain-mediated muscle damage or lipid peroxidation induced by oxidative stress. *J Negat Results Biomed* 13: 014-0019, 2014.
85. **Reeds PJ, et al.** Tissue and whole-body protein synthesis in immature Zucker rats and their relationship to protein deposition. *Biochem J* 204: 393-398, 1982.
86. **Ringseis R, et al.** Supplementing obese Zucker rats with niacin induces the transition of glycolytic to oxidative skeletal muscle fibers. *J Nutr* 143: 125-131, 2013.
87. **Ritter CS, and Slatopolsky E.** Phosphate Toxicity in CKD: The Killer among Us. *Clin J Am Soc Nephrol* 11: 1088-1100, 2016.
88. **Rivero JL, et al.** Interrelationships of myofibrillar ATPase activity and metabolic properties of myosin heavy chain-based fibre types in rat skeletal muscle. *Histochem Cell Biol* 111: 277-287, 1999.
89. **Roy RR, et al.** Modulation of myonuclear number in functionally overloaded and exercised rat plantaris fibers. *J Appl Physiol* 87: 634-642, 1999.
90. **Sakkas GK, et al.** Atrophy of non-locomotor muscle in patients with end-stage renal failure. *Nephrol Dial Transplant* 18: 2074-2081, 2003.
91. **Saliba W, and El-Haddad B.** Secondary hyperparathyroidism: pathophysiology and treatment. *J Am Board Fam Med* 22: 574-581, 2009.
92. **Schiaffino S, and Reggiani C.** Fiber types in mammalian skeletal muscles. *Physiol Rev* 91: 1447-1531, 2011.
93. **Schiaffino S, and Reggiani C.** Myosin isoforms in mammalian skeletal muscle. *J Appl Physiol* 77: 493-501, 1985.
94. **Schnedl C, et al.** FGF23 in Acute and Chronic Illness. *Dis Markers* 358086: 28, 2015.
95. **Sellamuthu PS, et al.** Beneficial effects of mangiferin isolated from *Salacia chinensis* on biochemical and hematological parameters in rats with streptozotocin-induced diabetes. *Pak J Pharm Sci* 27: 161-167, 2014.
96. **Serratrice G, et al.** Neuropathies, myopathies and neuromyopathies in chronic uremic patients.

Chapter 3

- Neuropathies, myopathies et neuromyopathies chez des urémiques chroniques* 75: 1835-1838, 1967.
97. **Shah KA, et al.** *Mangifera indica* (mango). *Pharmacogn Rev* 4: 42-48, 2010.
98. **Simoneau JA, and Kelley DE.** Altered glycolytic and oxidative capacities of skeletal muscle contribute to insulin resistance in NIDDM. *J Appl Physiol* 83: 166-171, 1985.
99. **Sinha A, et al.** Improving the vitamin D status of vitamin D deficient adults is associated with improved mitochondrial oxidative function in skeletal muscle. *J Clin Endocrinol Metab* 98: 2012-3592, 2013.
100. **Smogorzewski M, et al.** Chronic renal failure, parathyroid hormone and fatty acids oxidation in skeletal muscle. *Kidney Int* 33: 555-560, 1988.
101. **Staron RS, and Pette D.** The continuum of pure and hybrid myosin heavy chain-based fibre types in rat skeletal muscle. *Histochemistry* 100: 149-153, 1993.
102. **Stohs SJ, and Ray S.** Anti-diabetic and Anti-hyperlipidemic Effects and Safety of *Salacia reticulata* and Related Species. *Phytother Res* 29: 986-995, 2015.
103. **Stuart CA, et al.** Slow-twitch fiber proportion in skeletal muscle correlates with insulin responsiveness. *J Clin Endocrinol Metab* 98: 2027-2036, 2013.
104. **Taes YEC, et al.** Effect of dietary creatine on skeletal muscle myosin heavy chain isoform expression in an animal model of uremia. *Nephron Exp Nephrol* 96: e103-e110, 2004.
105. **Tanaka M, et al.** Vitamin D receptor gene silencing effects on differentiation of myogenic cell lines. *Muscle Nerve* 49: 700-708, 2014.
106. **Tanner CJ, et al.** Muscle fiber type is associated with obesity and weight loss. *Am J Physiol Endocrinol Metab* 282: E1191-1196, 2002.
107. **Tseng BS, et al.** Cytoplasm-to-myonucleus ratios and succinate dehydrogenase activities in adult rat slow and fast muscle fibers. *Cell Tissue Res* 275: 39-49, 1994.
108. **Tsutsumi R, et al.** Sudachitin, a polymethoxylated flavone, improves glucose and lipid metabolism by increasing mitochondrial biogenesis in skeletal muscle. *Nutr Metab* 11: 1743-7075, 2014.
109. **Turner N, et al.** Excess lipid availability increases mitochondrial fatty acid oxidative capacity in muscle: evidence against a role for reduced fatty acid oxidation in lipid-induced insulin resistance in rodents. *Diabetes* 56: 2085-2092, 2007.
110. **Valero T.** Mitochondrial biogenesis: pharmacological approaches. *Curr Pharm Des* 20: 5507-5509, 2014.
111. **Vyas A, et al.** Perspectives on medicinal properties of mangiferin. *Mini Rev Med Chem* 12: 412-425, 2012.
112. **Wang F, et al.** Mangiferin and its aglycone, norathyriol, improve glucose metabolism by activation of AMP-activated protein kinase. *Pharm Biol* 52: 68-73, 2014.
113. **Welle S, et al.** Sex-related differences in gene expression in human skeletal muscle. *PLoS One* 3: e1385, 2008.
114. **Wessels B, et al.** Pioglitazone treatment restores in vivo muscle oxidative capacity in a rat model of diabetes. *Diabetes Obes Metab* 17: 52-60, 2015.
115. **Yasuda K, et al.** Abnormality in fibre type distribution of soleus and plantaris muscles in non-obese diabetic Goto-Kakizaki rats. *Clin Exp Pharmacol Physiol* 29: 1001-1008, 2002.

CHAPTER 4

Slow- and fast-twitch hind limb skeletal muscle phenotypes 12 weeks after 5/6 nephrectomy in Wistar rats of both sexes



Muscle fiber-types in long-term uremic rats of both sexes

Luz M. Acevedo,^{1,4} Alan Peralta-Ramírez,^{2,5} Ignacio López,² Verónica E. Chamizo,¹ Carmen Pineda,² Maria E. Rodríguez-Ortiz,⁶ Mariano Rodríguez,³ Escolástico Aguilera-Tejero,^{2*} and José-Luis L. Rivero^{1*}

¹*Laboratory of Muscular Biopathology, Department of Comparative Anatomy and Pathological Anatomy, Faculty of Veterinary Sciences, University of Cordoba, Cordoba, Spain*

²*Department of Animal Medicine and Surgery, University of Cordoba, Spain*

³*Unidad de Investigación y Servicio de Nefrología (Red in Ren), Instituto Sanitario de Investigación Biomédica de Córdoba (IMIBIC), Reina Sofía University Hospital, University of Cordoba, Spain*

⁴*Departamento de Ciencias Biomédicas, Facultad de Ciencias Veterinarias, Universidad Central de Venezuela, Maracay, Venezuela*

⁵*Escuela de Medicina Veterinaria, Universidad Nacional Autónoma de Nicaragua, León, Nicaragua*

⁶*Laboratory of Nephrology, IIS-Fundación Jiménez Díaz (Red in Ren), Madrid, Spain*

*E. Aguilera-Tejero and J.-L. L. Rivero contributed equally to this study

Am J Physiol Renal Physiol 209:F638-F647, 2015

ABSTRACT

This study describes fiber-type adaptations in hind-limb muscles, the interaction of the sex and the role of hypoxia on this response in 12 wk 5/6 nephrectomized rats (*Nx*). Contractile, metabolic and morphological features of muscle fiber-types were assessed in the slow-twitch *soleus* and the fast-twitch *tibialis cranialis* muscles of *Nx* rats, and compared with sham-operated controls. Rats of both sexes were considered in both groups. A slow-to-fast fiber-type transformation occurred in the *tibialis cranialis* of *Nx* rats, particularly in males. This adaptation was accomplished by impaired oxidative capacity and capillarity, increased glycolytic capacity and no changes in size and nuclear density of muscle fiber-types. An oxidative-to-glycolytic metabolic transformation was also found in the *soleus* muscle of *Nx* rats. However, a modest fast-to-slow fiber-type transformation, fiber hypertrophy and nuclear proliferation were observed in *soleus* muscle fibers of male, but not of female, *Nx* rats. Serum testosterone levels decreased by 50% in male but not in female *Nx* rats. Hypoxia-inducible factor-1 α protein level decreased by 42% in the *tibialis cranialis* muscle of male *Nx* rats. These data demonstrate that 12 wk of *Nx* induces a muscle-specific adaptive response in which myofibers do not change (or enlarge minimally) in size and nuclear density, but acquire markedly different contractile and metabolic characteristics, which are accompanied by capillary rarefaction. Muscle function and sex play relevant roles in these adaptations.

Key words: chronic renal failure, uremia, myosin heavy chain, muscle plasticity, gonadal hormones, hypoxia-inducible factor-1 α .

INTRODUCTION

Skeletal muscle, the most abundant tissue in the body of vertebrates, is heavily impacted by chronic renal failure (CRF) (2). Patients with CRF suffer a constellation of

abnormalities in skeletal muscle structure and function, mainly affecting to limb muscles, which are described under the general term of uremic myopathy (5). Several studies over the past 40 yr have described the adaptive changes in skeletal muscle in response to uremic stimulus, both in human patients with CRF (e.g., 4, 9, 12, 23, 26) and in animal models of uremia (3, 6, 8, 16, 17, 35), but many of these studies provide contradictory findings. For example, uremic muscle fiber atrophy is considered as a common feature (2, 14), however, studies performed on skeletal muscles of human patients with CRF reveal results ranging from uniform atrophy (32) to generalized hypertrophy of all muscle fiber types (23). Several limitations to some of these studies have been discussed in recent reports (17, 23). They include small sample sizes, lack of appropriate controls (e.g., healthy athletes), methodological deficiencies for optimal analysis of muscle fibers, diversity of skeletal muscle studied (including non-limb muscles), overestimation and/or misunderstanding of phenotypic changes reported in skeletal muscle fibers.

Comparisons between human and animal studies on the impact of CRF on skeletal muscle are complicated by the different stages of the renal failure. Most human studies have described the changes in skeletal muscle in renal patients with several years of hemodialysis or during the period of progression to the end-stage renal failure (4, 9, 12, 23, 26). Studies using the 5/6 reduction in total renal mass (*Nx*), the most widely used animal model to induce uremia (20), have described, however, acute changes of skeletal muscles, ranging from 2 days to 3–4 weeks (3, 8, 16, 17, 35). Thus, there is no information regarding muscle changes during the period when the CRF is ‘stabilized’, i.e., beyond the 6th–8th week after surgery (20). In addition, neither human nor animal studies have taken into account the effect of the sex on the skeletal muscle changes in response to CRF. There is evidence that CRF reduces levels of male gonadal

hormones, particularly testosterone (reviewed in Ref. 2). Given the potent anabolic action of testosterone on skeletal muscle (36) and its demonstrated role in the maintenance of skeletal muscle fiber-type expression (13, 18), a different impact of CRF between sexes could be expected.

Furthermore, previous studies in short-term animal models of uremia have reported a different impact on skeletal muscles with different functional competences (15-17). For example, the fiber atrophy of fast-twitch fibers and capillary rarefaction that occur in rats in early stages (4 wk) of CRF was noted to be more severe in limb (*gastrocnemius*) than in trunk (*longissimus thoracis*) muscles (15-17). From the available literature, it seems that postural as opposed to locomotor muscles might be more resistant to hypoxia and fiber atrophy secondary to uremia, through an increased expression of inducible nitric oxide synthase, which is interpreted as a protective factor against hypoxia through hypoxia inducible factor 1 α (HIF-1 α) stabilization (15). This transcription factor is a key regulator for the induction of genes that facilitate adaptation of cells from normoxia to hypoxia (reviewed in Ref. 21). Under normal conditions, higher HIF-1 α expression plays an active role in skeletal muscle plasticity, leading to fiber-type transitions in the fast direction, fiber hypertrophy, oxidative-to-glycolytic energy metabolism transition and neovascularisation (25, 29). However, under hypoxic-conditions (renal anemia), the reduced expression of HIF-1 α which has been found in locomotor muscles of rats 4 wk after Nx (15) does not support this role in muscle plasticity.

We hypothesized that, during its 'stable' phase (~8-12 wk), CRF should induce changes in contractile, metabolic, and morphological features of individual skeletal muscle fibers different to those previously described in more acute stages of the CRF (1-6 wk). Additionally, this muscle plasticity should be more pronounced in the mostly inactive at rest fast-twitch

tibialis cranialis muscle than in the tonically active slow-twitch *soleus* muscle providing postural (antigravitatory) support. The authors also expected that sex would have a significant interaction on the skeletal muscle response to long-term (12 wk) Nx with males showing more pronounced changes than females. Furthermore, we hypothesized that muscle changes secondary to uremia are associated to an aberrant response to hypoxia at the cellular level. Therefore, the present investigation was primarily aimed at determining the impact of 12 wk of Nx on the phenotypic features (fiber-type composition, size, oxidative and glycolytic capabilities, capillarity and nuclear density) of muscle fiber types of slow (*soleus*)- and fast (*tibialis cranialis*)-twitch rat hind limb muscles. A second objective was to test whether sex interacted with the effects of this Nx model on the fiber-type characteristics of these two muscles. To find out if uremia-induced muscle changes are secondary to an inadequate response to hypoxia at the cellular level, we also investigated the expression of HIF-1 α protein content in these two functionally different muscles.

MATERIALS AND METHODS

Experimental design and procedures

Ethics. All experimental protocols were reviewed and approved by the Ethics Committee for Animal Research of the University of Cordoba (Cordoba, Spain). They followed the guidelines laid down by the Higher Council of Scientific Research of Spain following the normal procedures directing animal welfare (Real Decreto 223/88, BOE of 18 of March) and adhered to the recommendations included in the Guide for Care and Use of Laboratory Animals (US Department of Health and Human Services, NIH) and European laws and regulations on protection of animals, under the advice of specialized personnel.

Animals. Twenty-seven adult (3.5-4 mo old) Wistar

rats of both sexes (13 females and 14 males) with body weight of 257 ± 54 g (mean \pm SD) at the beginning of the experiment were used. Animals were provided by the Central Service of Experimental Animals of the University of Cordoba, Cordoba (Spain). They were individually housed in standard vivarium cages in a temperature- and humidity-controlled environment, with a 12:12-h light-dark cycle and given *ad libitum* access to standard rat diet (Altromin Spezialfutter GmbH, Germany; values per 100 g: energy 351.8 kcal 1100 kJ⁻¹, protein content 18%, lysine 1.74%, methionine 1.0%, cysteine 0.31%, tryptophan 0.20%, fat 5%, ash 4.5%, sodium 0.24%, calcium 0.6%, phosphorus 0.6%) and tap water.

Design and surgical procedures. Before the experiment began, all rats were maintained for 2 wk on the standard diet. Afterwards, rats were randomly allocated to two different groups with balanced sexes: sham operated control (*So*; $n=10$, 4 females and 6 males) and 5/6 nephrectomy (*Nx*, $n=17$ rats, 9 females and 8 males). The *Nx* was carried out following a two-step procedure that reduces the original renal mass by five-sixths as previously described (24). Briefly, in the first step, 2/3 of the left kidney was removed under general anaesthesia (Sevofluorane, Abbott, Madrid, Spain; intraperitoneal injection). After 1 week of recovery, in the second step and also under general anaesthesia, the right kidney was removed. The control *So* rats were sham operated with the same protocol and total duration of the surgery, except both kidneys were maintained intact. After the second surgery, the mineral content of the diet was changed to 0.9% phosphorus in the *Nx* group. Both food intake and body weight of individual rats were assessed weekly.

Muscle sampling and tissue preparation. After 12 wk, rats from both groups were sacrificed by aortic puncture and exsanguination under deep general anaesthesia (sodium thiopental 50 mg kg⁻¹, Pentotal®, Abbot,

Illinois, USA; intraperitoneal injection). Bilateral *soleus* (*soleus*) and *tibialis cranialis* (*tibialis cranialis*) muscles were dissected and individual muscles were wet weighted. These muscles were selected as two representative muscles of a typical slow-twitch muscle (*soleus*, composed primarily of slow-twitch muscle fibers) and a characteristic fast-twitch muscle (*tibialis cranialis*, composed primarily of fast-twitch muscle fibers in its white region), respectively (10). Also because these two hind limb muscles are opposite regarding their resting functional activities. While the *tibialis cranialis* muscle is only recruited at high-intensity physical activity, being normally inactive at rest, the *soleus* muscle is primarily active at rest providing postural (antigravitatory) support (10). Upon collection, tissue blocks from the muscle belly were mounted on cork blocks with the use of OCT embedding medium (Tissue-Tek II, Miles Laboratories, Naperville, IL, USA) and oriented so that myofibers could be cut transversely (11). Specimens were systematically frozen by immersion in isopentane (30 s), kept at the freezing point in liquid nitrogen, and stored at -80 °C until analyzed (11). Muscle samples were routinely frozen between 2 and 4 min after removal, because it has been demonstrated that the interval between removal and freezing has a significant (negative) effect on skeletal muscle fiber size (22). All muscle sampling and muscle preparation procedures were always carried out by the same investigator, experienced in skeletal muscle biopsy studies, taking care to standardize both the location and the freezing of the sample.

Laboratory analyses

Blood biochemistry. Blood samples were obtained from the abdominal aorta in heparinised syringes at the time of death. Plasma was separated by centrifugation and stored at -80 °C until assayed. Plasma creatinine and blood urea nitrogen were measured by spectrophotometry

(BioSystems, Barcelona, Spain) as previously described (24), and used as indicators of renal function. Plasma testosterone levels were determined using a commercial available ELISA kit for the quantitative determination of testosterone in serum or plasma of rats and mice (Demeditec Diagnostics, Kiel, Germany), according to the manufacturer's instruction. The sensitivity of the ELISA reported by the manufacturer is 0.066 ng/ml. The intra-assay variation is less than 11%, and the inter-assay variation less than 11% in serum samples.

Myosin heavy chain immunohistochemistry. Muscle samples were serially sectioned (10- μ m-thick) in a cryostat (Frigocut, Reichert Jung, Nubloch, Germany) at -20 °C and used for immunohistochemistry.

Immunohistochemistry was performed with five monoclonal antibodies specific against myosin heavy chain isoforms (Table 4.1; Fig. 4.1A). The specificity of these antibodies for myosin heavy chains in rat skeletal muscle has previously been reported (19, 33). The immunoperoxidase staining protocol with avidin-biotin complex protocol was used as previously described (30).

Quantitative enzyme histochemistry. Additional serial sections were used for quantitative enzyme histochemistry. The activities of the enzymes succinate dehydrogenase (SDH, EC 1.3.4.1), used as an oxidative marker, and glycerol-3-phosphate-dehydrogenase (GPDH), used as an indirect marker for glycolytic potential of myofibers, were determined on 10- μ m- and 14- μ m-thick sections, respectively, by using quantitative histochemical methods previously adjusted and validated in rat skeletal muscle (30). However, it is not known whether the GPDH histochemical method used in the present study stains for activity of the cytosolic NAD-dependent GPDH (EC 1.1.1.8) or the mitochondrial FAD-dependent GPDH (EC 1.1.99.5). Neither GPDH is directly involved in the glycolytic pathway; however, both are directly involved in the transfer of NADH from glycolysis in the cytosol into FADH₂ in the mitochondria

of skeletal muscles. Furthermore, GPDH histochemical activity correlates with the activities of other glycolytic enzymes (28).

Capillary and nuclei histology. Additional 14- μ m-thick serial sections were incubated in a 2.2% solution of α -amylase and then stained according to a standardized periodic-acid-Schiff technique by using a 1% solution of acid (1). These sections were used to visualize capillaries (Fig. 4.1B). Additional 10- μ m-thick sections were stained with haematoxylin and eosin and used to visualize total nuclei within or around each individual muscle fiber (Fig. 4.1B).

Image analysis and morphometry

Sections were examined in a blind fashion by the same investigator (L.M.A.), who had experience of the normal appearance of mammalian skeletal muscle fibers. All serial sections for immunohistochemistry, enzyme histochemistry and histology were visualized and digitized as previously described (1). A region containing between 150 and 250 fibers was selected for further analyses. In the *tibialis cranialis* muscle, this area was selected from the core of the white (superficial) portion of the muscle, since it contains a higher number of fast-twitch muscle fibers (98%) than the red (deep) portion (93%) of the muscle (10). Images were saved as digitized frames at 256 gray levels. The gray levels were converted to optical density units by using a calibrated set of optical density filters. The digitized images of the fibers in the two histochemical reactions (SDH and GPDH) within the selected region were traced manually and analyzed for the fiber cross-sectional area (area) and the average optical density for each histochemical reaction of individual muscle fibers. The average fiber optical density for each histochemical reaction was determined as the average optical density for all pixels within the traced fiber from three sections incubated with substrate minus the average optical density for all pixels of the same fiber from other

Table 4.1 Specificity of monoclonal antibodies (MAbs) against rat skeletal myosin heavy chain (MHC) isoforms, and immunohistochemical characterization of muscle fiber types

MAbs*	Specificity [‡]	MHC-based muscle fiber types [†]						
		I (1)	I+IIA (2)	IIA (3)	IIAX (4)	IIX (5)	IIXB (6)	IIB (7)
BA-D5	I	+	+	–	–	–	–	–
SC-71	IIa	–	+	+	+	–	–	–
BF-35	I, IIa, IIb	+	+	+	+	–	+/-	+
S5-8H2	I, IIX, IIb	+	+	–	+	+	+	+
BF-F3	IIb	–	–	–	–	+	+/-	+

* Sources of all MAbs were DMS, Braunschweig, Germany except the MAb S5-8H2 (Biocytex Biotechnology, Marseille, France). [‡] According to (33) except the MAb S5-8H2 (19). [†] According to (30) except for the MAb S5-8H2 (19). +, – and +/-, positive, negative and intermediate immunohistochemical staining, respectively, for that specific muscle fiber with that specific MAb. The number of each fiber type (1–7) corresponds to those showed in **Fig. 4.1**

two sections incubated without substrate (30). Because a number of factors can influence the reliability of histochemical enzyme activity determinations, we checked the variability on three consecutive sections for both SDH and GPDH histochemical reactions by repeated measurements of the same individual fibers. Only coefficients of variation for triplicate measurements of optical densities below 5% were accepted in the present study; this demonstrated the high analytical precision that can be achieved for the measurement of fiber optical density on enzyme histochemical sections.

The number of capillaries and nuclei around each individual muscle fiber in the selected area of the sample was also obtained from the α -amylase-periodic-acid-Schiff and haematoxylin and eosin staining techniques, respectively (1). They were expressed as absolute number of capillaries or nuclei in contact with each muscle fiber.

The fibers in the selected area were classified according to their myosin heavy chain content by means of visual examination of immunostainings of the five serial sections stained with the battery of anti-myosin heavy chain monoclonal antibodies (**Table 4.1; Fig. 4.1A**). The reactivity of each individual muscle fiber in

these five consecutive sections was judged as positive, intermediate or negative by comparing the intensity of the reaction of neighbouring fibers. Seven fiber types were categorized, four of them as pure fibers expressing a unique myosin heavy chain isoform (i.e., type I, IIA, IIX and IIB), and other three as hybrid phenotypes co-expressing two different myosin heavy chain isoforms (type I+IIA, IIAX and IIXB).

The relative frequency of different muscle fiber types in the selected region was used to numerically express the fiber type composition of each muscle sample. The area, SDH and GPDH optical densities, and absolute numbers of capillaries and nuclei of the same muscle fibers were averaged according to fiber-type and used for statistical analyses. The SDH-to-GPDH ratio of individual muscle fibers was also determined and used as an indicator of the relative oxidative vs glycolytic metabolic capacities of individual muscle fibers. For minor fibre types (I+IIA and IIA in the *soleus* muscle, and I, I+IIA and IIAX in the *tibialis cranialis* muscle), there were so few fibres in most muscle samples that a statistically reliable determination of their area, SDH, GPDH, capillarity and nuclear density was impossible. In consequence, muscle fibre-types

► **Fig. 4.1** Serial frozen sections of *tibialis cranialis* muscle from a representative normal female sham operated rat (*So*) and other 5/6 nephrectomized female rat (*Nx*) stained for immunohistochemistry (*Panel A*) and enzyme histochemistry and histology (*Panel B*). *A*: Sections were reacted with monoclonal antibodies against specific myosin heavy chain (MHC) isoforms: BA-D5 (anti MHC-I), SC-71 (anti MHC-IIa), BF-35 (anti MHCs-I, -IIa and -IIb), S5-8H2 (anti MHCs-I, -IIx and -IIb) and BF-F3 (anti MHC-IIb). *B*: Additional serial sections were stained for quantitative enzyme histochemistry of succinate dehydrogenase (SDH) and glycerol-3-phosphate dehydrogenase (GPDH) activities, and for histology of α -amylase periodic acid Schiff (PAS) for visualizing capillaries and haematoxylin and eosin (H&E) for visualizing nuclei. The seven MHC-based muscle fiber types are labelled in all serial sections; four of them were pure fibers expressing a unique MHC isoform (i.e., fibers '1', '3', '5' and '7' which correspond with type I, IIA, IIX and IIB fibers, respectively), and other three were hybrid phenotypes coexpressing two different MHC isoforms [i.e., MHCs-I and -IIa (type I+IIA, fiber labelled '2'), MHCs-IIa and -IIx (type IIAX, not shown) and MHCs-IIx and -IIb (type IIXB, fiber labelled '6'). Note in the muscle from the *Nx* rat (bottom rows in both panels), the lower number of fibers expressing MHCs either I, IIa or IIx, the abundance of fibers expressing MHC-IIb, the larger size of all muscle fibers, the lower SDH staining, the higher GPDH staining and the lower muscle fiber capillarity and nuclei, compared with the *So* animal (upper rows of both panels). Bar, 150 μ m.

showing, on average, a fibre percentage below 5% were excluded from these analyses.

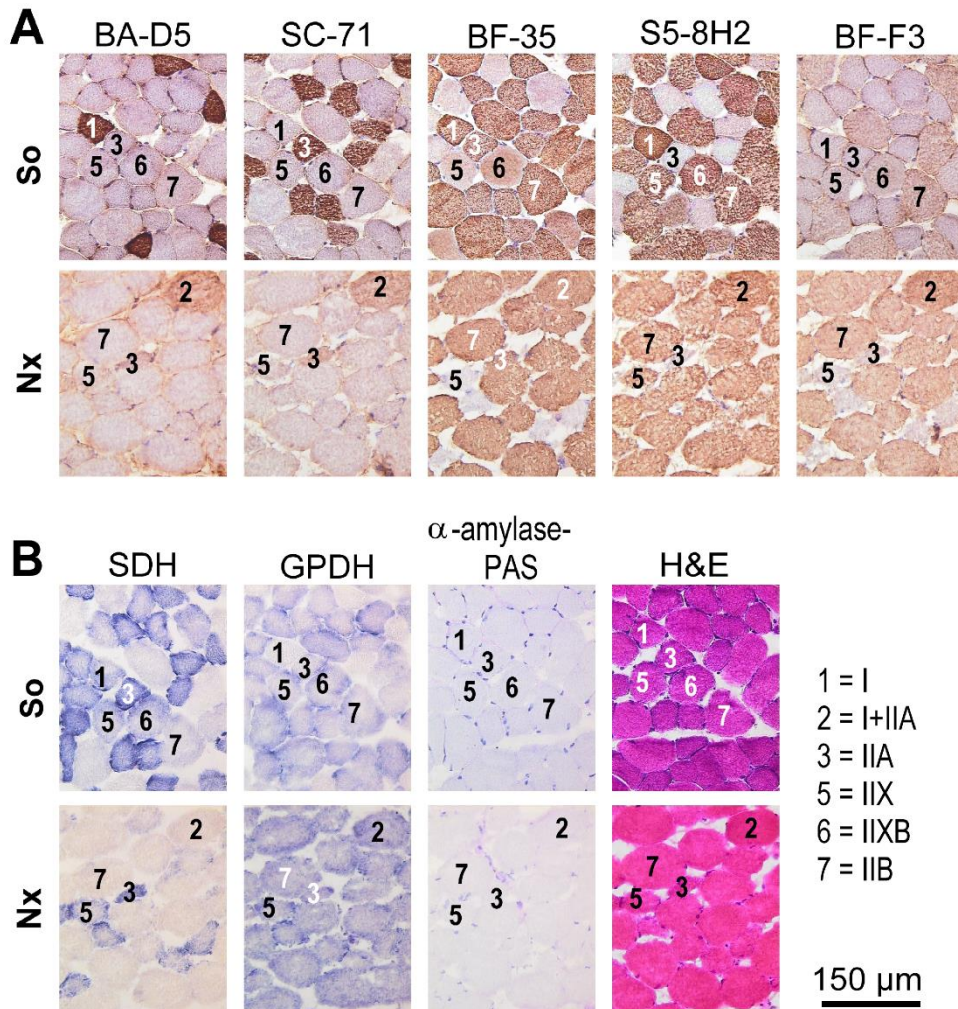
Western blot analysis of HIF-1 α protein

Muscle tissue was homogenized and protein was isolated following the protocol described by Schreiber et al. (34). Protein concentration was assessed by Bradford method (7). Fifty μ g of nuclear protein were electrophoresed in a 12% polyacrilamide gel (Bio-Rad, Hercules, CA) and electrophoretically transferred (Transfer Systems, Bio-Rad) from the gels onto nitrocellulose membranes (Pall Corporation, Pensacola, FL). The following steps were performed with gentle shaking. Membranes were incubated in TTBS-L solution (20 mM Tris-HCl pH 6.6, 0.2% Tween 20, 150 mM NaCl, and 5% nonfat dry milk) at room temperature for 1 h to avoid non-specific binding. Membranes were incubated overnight at 4°C with a 1:700 dilution of an anti-HIF-1 α antibody (Abcam, Cambridge, UK). TFIIB (1:1000, Danvers, MA) was used as a housekeeping protein. Membranes were washed with TTBS buffer and

immunolabeled using a peroxidase-conjugated secondary antibody (Santa Cruz Biotechnologies, Santa Cruz, CA). Finally, western blots were developed using ECL Plus Western Blotting Detection System (GE Healthcare, Piscataway, NJ). Protein levels were quantified using ImageJ software (National Institutes of Health, Bethesda, MD).

Statistical analyses

All statistics and charts were run on Statistica 7.0 for Windows (StatSoft I, Statistica, Data software System, www.statsoft.com). Muscle sample was the unit of analysis for the present dataset. A total of 108 muscle samples (27 animals x two muscles –*soleus* and *tibialis cranialis*– x two sides –left and right) were available for statistical analysis. Sample size and the power of a contrast of hypothesis were estimated by power analysis and interval. Accepting an α -risk of 0.05 and a β -risk of 0.2 in a two-sided test, a minimum of 8 samples/group were considered necessary to recognize as statistically significant a minimum difference of 1.75 SD units



between any pair of groups assuming that 4 groups exists (2 sexes x 2 treatments –So and Nx), as well as a common deviation of 20% of the mean value, and anticipating a drop-out rate of 0%. Normality of muscle variables was tested using a Kolmogorov–Smirnov test and data are

expressed as means \pm SE, except in **Table 4.2** (means \pm SD). Two-factorial analysis of variance (ANOVA) was used to test for sex, Nx and sex–Nx interaction effects. When a significant effect was observed for sex–Nx interaction ($p < 0.05$), the Fisher LSD *post hoc* test was

Muscle fiber-types in long-term uremic rats of both sexes

Table 4.2 Renal function, food intake, live weight of subjects, muscle weights and muscle somatic index (MSI)

	Females		Males		p values		
	So (n=4)	Nx (n=9)	So (n=6)	Nx (n=8)	Sex	Nx	S-Nx
Creatinine, mg dl ⁻¹	0.75±0.14	1.24±0.42**	0.67±0.06	1.01±0.10*	0.1	<0.001	0.5
Blood urea nitrogen, mg dl ⁻¹	43.8±11.6	66.2±16.9**	43.9±4.4	81.8±10.0***	0.1	<0.001	0.1
Food intake, g d ⁻¹	14± 3	14±3	20± 3	20± 3	<0.01	0.9	0.8
Energy intake, kcal d ⁻¹	50± 9	50±9	70±12	72±20	<0.01	0.9	0.8
Body weight, g	251±11	240±9	440±19	415±29*	<0.001	0.03	0.4
Weight gain, g	38± 9	38±7	118±20	126±18	<0.001	0.5	0.5
M. soleus	(n=8)	(n=18)	(n=12)	(n=16)			
Weight, mg	127±17	119±14	172±26	190±30**	<0.001	0.5	0.05
MSI, arbitrary units	0.51±0.06	0.49±0.05	0.39±0.06	0.46±0.06**	<0.001	0.1	0.03
M. tibialis cranialis	(n=8)	(n=18)	(n=12)	(n=16)			
Weight, mg	712±39	655±47	1021±93	1055±93	<0.001	0.6	0.04
MSI, arbitrary units	2.85±0.11	2.73±0.18	2.32±0.18	2.55±0.24**	<0.001	0.3	<0.01

Values are means±SD; n=number of samples; So=sham operated rats; Nx=5/6 nephrectomy rats. Two-way ANOVA was used to test for sex and Nx effects; p values denote main effect results for sex, Nx, and sex-Nx interactions (S-Nx). *** p<0.001, ** p<0.01, * p<0.05 compared with So

used to locate specific significant differences between pairwise groups.

RESULTS

Renal function, food intake, body weight, muscle mass and muscle-somatic index. The decrease in renal function induced by Nx was reflected in plasma creatinine and blood urea nitrogen concentrations that were 62% and 66% higher, respectively, in Nx than in So rats (**Table 4.2**). Sex had a strong influence on food intake, body weight, wet muscle weight and muscle-somatic index (wet muscle weight referred to body weight), with males having higher values than females (**Table 4.2**). Total food

and energy intakes were similar in Nx and So rats. After 12 wk, Nx rats reduced the body weight by 12%, compared with So. Both wet weights and muscle somatic indexes of *soleus* and *tibialis cranialis* muscles were similar in So and Nx rats. However, *tibialis cranialis* muscle weight and both *soleus* and *tibialis cranialis* muscle somatic indexes increased in male but not in female Nx rats, compared with So subjects.

Muscle fiber-type composition. The muscle fibers of both *soleus* and *tibialis cranialis* muscles were classified based on their immunoreactions to antibodies against specific myosin heavy chains (**Table 4.1**; **Fig. 4.1A**), and the proportions of seven fiber types (I, I+IIA, IIA, IIAX,

Table 4.3 Muscle fiber–type composition, %

Fiber–type	Females		Males		p values		
	So (n=8)	Nx (n=18)	So (n=12)	Nx (n=16)	Sex	Nx	S–Nx
M. soleus							
I	100.0±0.0	96.8±0.8	94.4±1.9	97.4±0.7*	0.03	0.9	<0.01
I+IIA	0.0±0.0	0.5±0.3	0.9±0.3	2.3±0.7*	<0.01	0.06	0.3
IIA	0.0±0.0	2.7±0.8	4.7±2.0	0.3±0.2**	0.3	0.4	<0.01
M. tibialis cranialis							
I	2.4±0.9	1.6±0.6	3.7±1.4	1.1±0.4*	0.6	0.06	0.3
I+IIA	0.2±0.1	2.3±1.0	2.6±1.2	1.7±0.6	0.4	0.5	0.1
IIA	20.5±5.4	10.8±2.2	17.8±3.9	13.4±2.6	1.0	0.04	0.4
IIAX	4.3±2.7	5.3±1.2	7.1±1.6	2.7±0.9*	0.9	0.2	0.07
IIX	27.5±4.2	17.8±1.9*	23.1±2.3	17.0±2.2*	0.3	<0.01	0.5
IIXB	22.8±4.3	36.6±3.0**	21.9±2.8	24.7±3.1	0.07	0.01	0.1
IIB	22.3±7.2	25.6±2.1	23.8±4.1	39.4±3.4**	0.04	0.02	0.1

Values are means±SE; n=number of samples; So=sham operated rats; Nx=5/6 nephrectomy rats. Two–way ANOVA was used to test for sex and Nx effects; p values denote main effect results for sex, Nx, and sex–Nx interactions (S–Nx). *** p<0.001, ** p<0.01, * p<0.05 compared with So.

IIX, IIXB and IIB) were determined for both *So* and *Nx* rats. All these seven fiber–types were identified in the *tibialis cranialis* muscle, but only three fiber–types (I, I+IIA and IIA) were found in the *soleus* muscle. Sex and *Nx* had an effect on *soleus* and *tibialis cranialis* muscle fiber–type distribution (**Table 4.3**). In the *soleus* muscle of male rats but not in female ones, *Nx* increased type I fibers by 3% and type I+IIA fibers by 150 %, and decreased IIA fibers by 94%, compared with *So* rats. After 12 wk of *Nx*, the *tibialis cranialis* muscle fiber–type composition changed significantly compared with *So* rats, particularly in male rats. In *Nx* rats, there were decreased proportions of type IIA (37%) and IIX (30%) fibers, and increased frequencies of type IIXB (39%) and IIB (36%) fibers, compared with *So* subjects. Significant interactions between sex and *Nx* also indicated that in the *tibialis cranialis* of male rats, but not of females, *Nx* decreased

the percentage of type I fibers (70%) and increased the proportion of type IIB fibers (66%), compared with *So* controls.

Muscle fiber size. The mean area of individual muscle fiber types was estimated for *So* and *Nx* rats (**Table 4.4**). Sex did not have any effect on the size of *soleus* type I fibers, but had an effect on size of all *tibialis cranialis* muscle fiber types, with males having larger fibers (35% on average) than females. *Nx* did not have any effect on size of individual muscle fiber types of both *soleus* and *tibialis cranialis* muscles ($p>0.05$). However, when all fiber types were analyzed together, *Nx* increased fiber area in the *tibialis cranialis* muscle (12%), compared with *So* rats (see **Fig. 4.1**). Furthermore, a significant interaction between sex and *Nx* on fiber size of *soleus* type I fibers demonstrated that these fibers increased by 31% in area in male rats, but not in females, compared

Muscle fiber-types in long-term uremic rats of both sexes

Table 4.4 Muscle fiber-type cross-sectional area, μm^2

Fiber-type	Females		Males		p values		
	So (n=8)	Nx (n=18)	So (n=12)	Nx (n=16)	Sex	Nx	S- Nx
M. soleus							
I	3783±263	3251±171	3190±174	4192±252**	0.4	0.3	0.001
M. tibialis cranialis							
IIA	1213± 78	1259± 91	1611± 56	1679± 96	<0.001	0.6	0.9
IIX	1632± 92	1762±120	2250± 90	2075±107	<0.001	0.8	0.2
IIXB	2202± 91	2529±118	3252±226	3129± 90	<0.001	0.5	0.1
IIB	3566±164	3968±181	4810±332	5190±147	<0.001	0.08	0.9
All fibers	2172±239	2545±125	3012±257	3479±103	<0.001	0.02	0.8

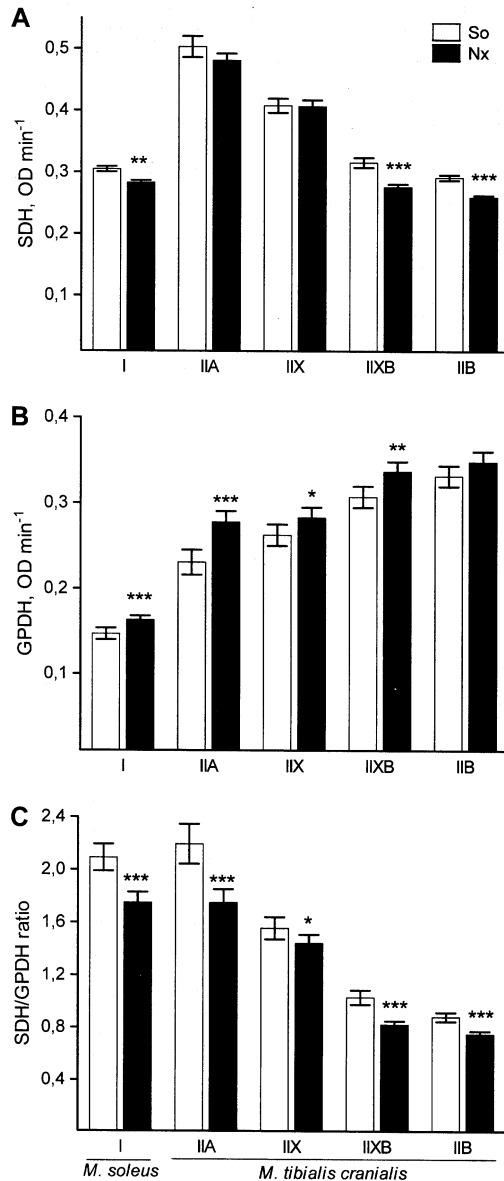
Values are means±SE; n=number of samples; So=sham operated rats; Nx=5/6 nephrectomy rats. Two-way ANOVA was used to test for sex and Nx effects; p values denote main effect results for sex, Nx, and sex-Nx interactions (S-Nx). *** p<0.001, ** p<0.01, * p<0.05 compared with So. For clarity, muscle fiber-types with a percentage below 5% are excluded from this analysis

with *So* controls.

Muscle fiber-type SDH and GPDH activities. Both *soleus* and *tibialis cranialis* muscle oxidative and glycolytic capacities were assessed by measuring the rate of SDH and GPDH activities, respectively, within individual muscle fiber types (Fig. 4.1B). As sex did not have any significant interaction with *Nx* ($p>0.05$) on these metabolic activities, results are depicted in Fig. 4.2 as pooled means of both sexes. The mean SDH activities from individual type I fibers in the *soleus* and from type IIXB and IIB muscle fibers in the *tibialis cranialis* of *Nx* rats were found to be lower by 7%, 12% and 10%, respectively, compared to those of *So* subjects (Fig. 4.2A). The mean SDH of all muscle fiber-types of *Nx* rats decreased by 10% in the *soleus* and by 21% in the *tibialis cranialis* ($p<0.0001$ in both), compared with *So* rats. Twelve weeks of *Nx* increased the mean GPDH activities of type I fibers in the *soleus* (9%), and of type IIA (22%), IIX (8%) and IIXB (10%) muscle fibers in the *tibialis*

cranialis, compared with *So* rats (Fig. 4.2B). The overall mean GPDH activity of all muscle fiber-types of *Nx* rats increased by 12% in the *soleus* ($p<0.0001$) and by 15% in the *tibialis cranialis* muscle ($p<0.001$), compared with *So* animals. The mean SDH-to-GPDH enzyme ratios from individual type I fibers in the *soleus* and from type IIA, IIX, IIXB and IIB muscle fibers in the *tibialis cranialis* of *Nx* rats were found to be lower by 17%, 20%, 8%, 20% and 15%, respectively, compared to those of *So* subjects (Fig. 4.2C). In relation to all fiber-types, the SDH-to-GPDH enzyme ratios decreased by 19% in the *soleus* and by 32% in the *tibialis cranialis* ($p<0.0001$ in both), compared with *So* rats.

Muscle fiber-type capillarity. The mean number of capillaries in contact with individual muscle fiber types differed significantly between sexes, with males showing more muscle fiber capillaries than females (Table 4.5). The absolute mean number of capillaries contacting type IIA, IIX and IIXB fibers in the *tibialis cranialis* muscle of



◀ **Fig. 4.2** Mean succinate dehydrogenase (SDH; A), glycerol-3-phosphate-dehydrogenase (GPDH; B), and SDH-to-GPDH enzyme activity ratio (C) from individual fiber types in *soleus* (type I fibers) and *tibialis cranialis* (IIA, IIX, IIXB and IIB fiber-types) muscles of sham operated rats (open bars, So; $n=20$ samples) and 5/6 nephrectomy rats (closed bars, Nx; $n=34$ samples). For clarity, muscle fiber types with a percentage below 5% are excluded from this analysis. Values are means \pm SE; asterisks denote significantly different from So group: *** $p < 0.001$, ** $p < 0.01$, * $p < 0.05$.

Nx rats were found to be lower by 12%, 13% and 12%, compared with those of So rats.

Muscle fiber-type nuclear density. Muscle fiber nuclei were measured in both So and Nx rats (representative fiber types with small densely-stained nuclei in a subsarcolemmal position are shown in Fig. 4.1B). The fixed effect of sex on the mean number of nuclei within or around individual muscle fiber types was significant, with males having higher absolute numbers of nuclei than females (Table 4.6). Nx did not have any significant effect on the absolute number of nuclei of individual muscle fiber types in both *soleus* and *tibialis cranialis* muscles. However, the number of nuclei of *soleus* type I fibers was 27% higher in male, but not in female, Nx rats, compared with So rats.

Testosterone measurements. Plasma testosterone levels were 3.2 times higher in males than in females ($p < 0.001$; Fig. 4.3A). After 12 wk, Nx reduced plasma testosterone levels by 50% in male rats ($p = 0.003$), but not in female rats ($p > 0.05$), compared with So rats. Within the male group, the level of testosterone was negatively correlated with the proportion of type IIB fibers in the *tibialis cranialis* muscle (Fig. 4.3B) and positively correlated with the percentage of type IIA fibers in the *soleus* muscle ($r = 0.73$, $p = 0.003$). Also in male rats, the

Muscle fiber-types in long-term uremic rats of both sexes

Table 4.5 Mean number of capillaries per fiber, capillaries fiber⁻¹

Fiber-type	Females		Males		p values		
	So (n=8)	Nx (n=18)	So (n=12)	Nx (n=16)	Sex	Nx	S-Nx
M. soleus							
I	6.50±0.45	6.60±0.18	7.38±0.54	7.75±0.36	0.01	0.5	0.7
M. tibialis cranialis							
IIA	4.01±0.38	3.77±0.12	4.71±0.26	4.06±0.12*	0.02	0.03	0.3
IIIX	4.21±0.37	3.67±0.10*	4.84±0.30	4.39±0.16	<0.01	0.01	0.7
IIIXB	4.74±0.35	3.94±0.16*	4.79±0.24	4.48±0.17	0.2	0.01	0.3
IIIB	4.83±0.36	4.51±0.18	5.61±0.36	5.24±0.15	<0.01	0.2	0.9
All fibers	4.41±0.30	3.94±0.11	4.93±0.24	4.67±0.13	<0.01	0.05	0.6

Values are means±SE; n=number of samples; So=sham operated rats; Nx=5/6 nephrectomy rats. Two-way ANOVA was used to test for sex and Nx effects; p values denote main effect results for sex, Nx, and sex-Nx interactions (S-Nx). *** p<0.001, ** p<0.01, * p<0.05 compared with So. For clarity, muscle fiber-types with a percentage below 5% are excluded from this analysis

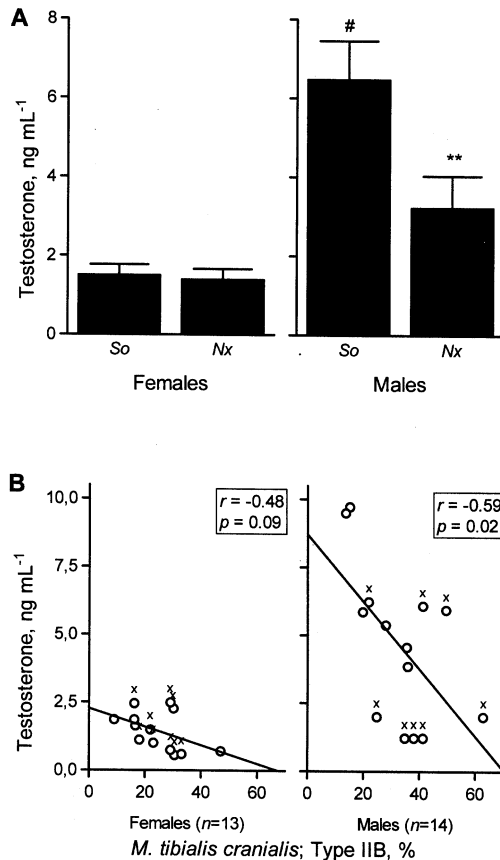
Table 4.6 Mean number of nuclei per fiber, nuclei fib⁻¹

Fiber type	Females		Males		p values		
	So (n=8)	Nx (n=18)	So (n=12)	Nx (n=16)	Sex	Nx	S-Nx
M. soleus							
I	6.11±0.57	5.09±0.21	5.09±0.33	6.44±0.45*	0.7	0.7	<0.01
M. tibialis cranialis							
IIA	4.08±0.34	3.91±0.24	4.99±0.29	4.40±0.24	0.02	0.2	0.5
IIIX	4.04±0.27	3.96±0.20	4.87±0.26	4.35±0.28	0.03	0.3	0.4
IIIXB	4.16±0.31	3.92±0.17	4.64±0.22	4.16±0.14	0.07	0.08	0.5
IIIB	4.29±0.28	4.12±0.19	4.78±0.27	4.37±0.16	0.1	0.2	0.6
All fibers	4.12±0.24	3.96±0.18	4.80±0.23	4.39±0.17	0.01	0.2	0.5

Values are means±SE; n=number of samples; So=sham operated rats; Nx=5/6 nephrectomy rats. Two-way ANOVA was used to test for sex and Nx effects; p values denote main effect results for sex, Nx, and sex-Nx interactions (S-Nx). *** p<0.001, ** p<0.01, * p<0.05 compared with So. For clarity, muscle fiber-types with a percentage below 5% are excluded from this analysis

level of testosterone was negatively correlated with both the mean area ($r=-0.56$, $p=0.038$) and the mean number

of nuclei ($r=-0.68$, $p=0.008$) in *soleus* muscle fibers. Within the female group, no significant correlations



▲ **Fig. 4.3** (A) Plasma testosterone levels of sham-operated (*So*) and 5/6 nephrectomy (*Nx*) rats of both sexes; values are means \pm SE; # $p < 0.001$ compared with females; ** $p < 0.01$ compared with male *So* rats. (B) Correlation between plasma testosterone levels and percentage of type IIB fibers from the *M. tibialis cranialis* of both sexes; r = correlation coefficient; 'x' denotes 5/6 nephrectomized rats.

between testosterone and fiber-type characteristics were noted.

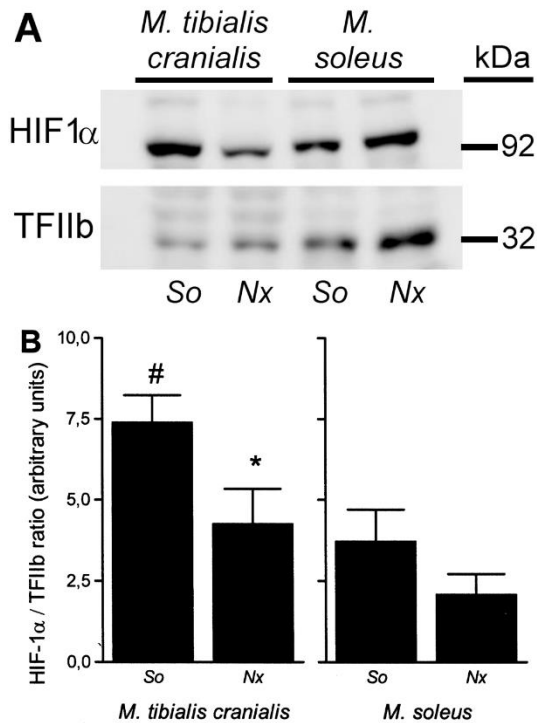
HIF-1 α protein expression. We compared HIF-1 α expression between a sub-set of *So* and *Nx* male rats. The analysis was performed on nuclear extracts from both *tibialis cranialis* and *soleus* muscles, and the HIF-1 α protein levels were investigated by Western blotting (**Fig. 4.4A**). Analysis of the relative band densities of HIF-1 α protein in *So* rats indicated about 100% more HIF-1 α protein content in *tibialis cranialis* than in *soleus* muscles (**Fig. 4.4B**). The effects of *Nx* on HIF-1 α protein levels were different in the two muscles, HIF-1 α decreased by 42% in the *tibialis cranialis* ($p = 0.029$) but was unchanged in the *soleus* ($p > 0.23$), as compared with *So* rats.

DISCUSSION

To our knowledge the present is the first study to address the impact of long-term (12 wk) 5/6 nephrectomy (*Nx*) on skeletal muscle phenotype in an animal model of uremia. The data obtained indicate that: 1) 12 wk of *Nx* results in hind limb muscle phenotypes that are different from those of the control *So* rats; 2) this long-term response to *Nx* was not homogeneous in slow- and fast-twitch hind limb muscles with different functions and fiber-type characteristics; 3) sex seems to play a pivotal role in the magnitude of these effects, which were more accentuated in males than in females; and 4) an inadequate response to hypoxia seems to be involved in uremia-induced muscle changes.

In agreement with present results in the *tibialis cranialis* muscle, evidence of slow-to-fast fiber-type transitions has been reported in fast-twitch hind limb muscles of rats 4 wk after *Nx* (35). Also in agreement with present results in the *soleus* muscle, a fast-to-slow fiber-type switching has already been reported in trunk (postural rather than locomotor) muscles of 4 wk *Nx* rats (17).

In both muscles, but particularly in the *soleus*, fiber-type transformations in responses to 12 wk *Nx* were more



▲ **Fig. 4.4** Comparison of HIF-1 α expression in *M. tibialis cranialis* and *M. soleus* of sham-operated (*So*) and 5/6 nephrectomized (*Nx*) male rats. (A) A representative protein analysis by Western blotting on skeletal muscle nuclear protein extracts. HIF-1 α was detected as a specific 92-kDa band, and a 32-kDa TFIIb band is shown as an even-lane evenly band. Note the higher difference between the densities of the two bands in the *M. tibialis* of the *So* rat compared with both the *M. soleus* of the same *So* rat and the *M. tibialis* of the *Nx* rat. (B) Histograms showing mean \pm SE HIF-1 α /TFIIb ratios of the *M. tibialis cranialis* and *M. soleus* of *So* and *Nx* male rats ($n=6$ rats per group). # $p=0.01$ compared with *M. soleus*; * $p<0.05$ compared with *So* rats.

pronounced in males than in females. This finding is compatible with the reduced levels of testosterone

reported in male *Nx* rats in the present study, probably reflecting the broader role that testosterone plays in the maintenance of skeletal muscle phenotype, compared with estrogens and progestins (36). It has been proposed that, in the male, testosterone acts directly on the muscle fiber by binding to androgen receptors within the cytosol (13), and that this receptor/ligand complex is transported into the nucleus to stimulate tissue-specific transcription factors (27). The current results suggest that this cellular mechanism seems to be muscle-specific. Thus, in the slow-twitch *soleus* muscle, this binding would repress transcription of the myosin heavy chain I gene and result in a decrease in the expression of myosin heavy chain I, as shown in the present study in male *So* rats (see Table 4.3). After 12 wk of *Nx*, these inhibitory transcriptional factors would be diminished, and susceptible fibers would begin expressing the myosin heavy chain I at the expense of the myosin heavy chain IIa. As a result, the fibers would undergo phenotypic transformation by switching from type IIA toward type I fibers in this postural muscle. In agreement with this contention, castration resulted in a fast-to-slow expression of myosin heavy chains in the adult mouse masseter, but ovariectomy has no effect on the fiber type composition in females (13). In the fast-twitch *tibialis cranialis* muscle, however, high levels of testosterone would repress transcription of the myosin heavy chain IIb and stimulate myosin heavy chain IIx expression, as shown in the fast-twitch *M. gastrocnemius* of orchietomized rats (18). The decrease of testosterone levels seem in males after 12 wk of *Nx* is compatible with the higher increase in the number of type IIB fibers at the expense of type IIX fibers in male than in female *Nx* rats. The additive influence of testosterone on fiber types is also substantiated by the significant correlation between these parameters within the male group, but not in females (Fig. 4.3B).

Previous data connected HIF-1 α causally to changes in muscle phenotype, since elevating the level of HIF-1 α

in adult rats *in vivo*, without altering the pattern of muscle activity, triggered a fast phenotype programme encompassing myosin heavy chain fiber type, metabolic enzymes and fiber size (25). However, the muscle changes observed in the present study after 12 wk of *Nx* were associated with either decreased (in the *tibialis cranialis* muscle) or unaltered (in the *soleus*) expression of HIF-1 α protein content (Fig. 4.4B). These discrepancies might indicate: (1st) an altered response to hypoxia at the muscle fiber level in the course of the uremic myopathy and (2nd) that changes seen in fiber-type composition, oxidative and glycolytic enzymes, and fiber size in *Nx* animals were not induced by high levels of HIF-1 α . The higher expression of HIF-1 α protein seen in the present study in the fast versus the slow muscle is in agreement with previous results in rat control muscles (15, 25, 29), and confirms that HIF-1 α may play a role in maintaining normal properties in fast muscles (25). The reduced expression of HIF-1 α protein found in our study in the fast *tibialis cranialis* muscle, but not in the slow *soleus* muscle from *Nx* rats, are not new findings (15), indicating that postural muscles seem to be more resistant to hypoxia and muscle changes secondary to uremia than locomotor muscles. This difference has been related to an increased expression of inducible nitric oxide synthase postural muscles (with abundant oxidative fibers) as opposed to locomotor muscles (primarily composed of glycolytic fibers) (15).

In the present study, the size of individual muscle fiber-types resulted unaffected by 12 wk of *Nx* in both muscles. However, a modest (12%) increase in area of pooled muscle fibers was observed in the *tibialis cranialis* muscle of *Nx* rats, as well as a consistent (31%) hypertrophy of type I fibers in the *soleus* of male *Nx* rats. In accordance with the present results, no significant changes were reported neither in the area of muscle fibers of a non-limb (*psaos*) muscle of 8 wk *Nx* rats (6) nor in the diameter of muscle fiber types of locomotor and

postural muscles of male rats 4 wk after *Nx* (17). A tendency, that did not reach statistical significance, for a decreased size of IIB fibers was noted in the latter study (17). Uniform atrophy of all muscle fiber types was reported, however, in locomotor and respiratory muscles of uremic rats 3 wk after *Nx* (8). Together, these findings indicate that impaired muscle fiber size seems to occur in the early stages of *Nx*. However, muscle fiber size is normalized or even increased in hind limb muscles during the period of ‘stabilization’ of the renal failure, i.e., 12 wk after the surgery.

The significant interaction between sex and *Nx* on the size of type I fibers in the *soleus* muscle seen in the present study does not agree with the notion that decreased levels of testosterone reported in subjects with CRF should lead to a reduction of muscle mass (2). Since a similar sexual effect on muscle fiber size could not be detected in the *tibialis cranialis* muscle of the same *Nx* rats, the sexual dimorphism noted on the hypertrophic response to long-term *Nx* in the *soleus* muscle could be explained in terms of both functional differences between the two muscles and physical overloading differences between the two sexes. Thus, the higher body weight of male rats compared with females (46% at the start and 75% at the end of the experiment), could explain the fiber hypertrophy noted in the postural (antigravitatory) *soleus* muscle of male *Nx* rats.

Twelve wk of *Nx* reduced significantly the relative oxidative vs glycolytic metabolic capabilities of principal muscle fiber types in both slow- and fast-twitch hind limb muscles of rats of both sexes. Impaired oxidative capacity of skeletal muscles has been documented in uremic rats during the acute phase of renal failure (3). This decreased activity of muscle mitochondrial oxidative enzyme is the likely biochemical basis of the impaired exercise capacity of CRF subjects. In accordance with the present results, Durozard et al. (12), using nuclear magnetic resonance spectroscopy, reported that, in

maintenance hemodialysis patients, the impaired energy production via oxidative metabolism is compensated by an increase in anaerobic capacity. Higher HIF-1 α expression has been implicated in the oxidative-to-glycolytic energy metabolism transition which occurs in skeletal muscles under hypoxia-free conditions, (25, 29). However, under hypoxic-conditions, the reduced expression of HIF-1 α which has been found in locomotor muscles of rats 4 (15) and 12 (present results) wk after *Nx* does not support this metabolic conversion.

Taken together, the present data indicate that 12 wk of *Nx* could lead to impaired capillarity in the *tibialis cranialis* muscle, but not in the *soleus* muscle. Capillary deficit in rat skeletal muscles was also present in early stages (4 wk) of *Nx* (16). In agreement with the present study, the impaired capillarity was more evident in locomotor (*gastrocnemius*) than in postural (*longissimus thoracis*) muscles (16), and it was associated with a decreased expression of HIF-1 α protein in the locomotor muscle (15). These findings confirm again that slow muscles as opposed to fast muscles are more resistant to the hypoxia-induced disturbances of uremic rats. The diminished expression of HIF-1 α protein in fast muscles of uremic rats has been explained by severe HIF-1 α breakdown secondary to high reactive oxygen species generation and low level of inducible nitric oxide synthase in glycolytic fibers (15). Since HIF-1 α triggers a coordinated response of angiogenesis (21), a reduced protein level of this factor in locomotor muscles (15; present results) could be responsible for impaired muscle angiogenesis of uremic animals.

In this study, 12 wk of *Nx* did not affect the absolute number of nuclei in the *tibialis cranialis* muscle of uremic rats. In accordance with the present data, a change of sarcolemmal nuclei per fiber area could not be detected in the rat *quadriceps femoris* muscle after 2–4 wk of *Nx* (8). As myonuclear domain size is related with both protein synthesis and protein turnover rates of muscle fiber types

(31), a maintained absolute number of nuclei, as noted in the present study in the *tibialis cranialis* muscle, does not support evidence of an altered synthesis and/or breakdown of proteins in fast-twitch muscles of rats 12 wk after *Nx*. However, the increased number of nuclei observed in the present study in the *soleus* type I fibers of male *Nx* rats suggests an increased synthesis of proteins which is compatible with the increased size noted in these fibers.

A weakness of this study was the lack of objective data on physical activity of the animals, since a diminished physical activity of *Nx* vs *So* rats could be a contributing factor explaining some obtained differences in muscle fiber-type characteristics between the two groups. Nevertheless, by subjective evaluation, daily physical activity seemed to be similar in both groups.

Conclusion

In conclusion, the present study provides evidence that the adaptive response of uremic rat skeletal muscle during the phase of ‘stable’ CRF (12 wk after surgery) takes the form of remodelling without atrophy or with discrete hypertrophy, where muscle fibers do not change (or enlarge modestly) in size and nuclear density, but acquire markedly different contractile and metabolic characteristics, which are accompanied by impaired capillarity. It is noteworthy that this malleability is muscle-specific and sex-dependent. While in the entirely inactive at rest *tibialis cranialis* muscle, 12 wk of 5/6 nephrectomy resulted in slow-to-fast fiber transformation, oxidative-to-glycolytic enzymatic conversion and reduced capillary density, in the tonically active slow-twitch *soleus* muscle, which provides postural support at rest, the same uremic stimuli induced a diminished oxidative-to-glycolytic enzyme ratio which was accomplished by discrete fast-to-slow fiber transformation, fiber hypertrophy and nuclear proliferation. Changes in both muscles were more

pronounced in male than in female uremic rats, showing evidence that low levels of testosterone reported in male but not in female *Nx* rats also seems to play a role in the skeletal muscle response to sustained uremia. The diminished protein level of HIF-1 α seen in the fast muscle of *Nx* rats supports impaired angiogenesis, but does not support muscle changes in fiber types, metabolic enzymes and fiber size seen in these animals, suggesting an altered response to hypoxia of uremic animals.

GRANTS

The work reported here was supported by a Spanish Government Grant from the Instituto de Salud Carlos III (PI14/00467 and PI00386) with co-financing from European Funds. L.M.A., V.E.Ch. and J.L.L.R. were supported by grants of the PAI Group CTS-179 and Project P10-AGR-5963, Junta de Andalucía, Spain.

DISCLOSURES

None of the authors of this paper has a financial or personal relationship with other people or organisation that could inappropriately influence or bias the content of the paper.

AUTHOR CONTRIBUTIONS

L.M.A., I.L., M.R., E.A.-T., and J.-L.L.R. conception and design of research. L.M.A., V.E.Ch., and J.-L.L.R. revised the literature. L.M.A., A.P.-R., I.L. and C.P. performed experiments and surgery. L.M.A., V.E.Ch., C.P., M.E.R.-O. and J.-L.L.R. performed laboratory analyses. L.M.A., I.L., M.R., E.A.-T., M.E.R.-O. and J.-L.L.R. analyzed data and interpreted results. L.M.A., A.P.-R., V.E.Ch., M.E.R.-O. and J.-L.L.R. prepared tables and figures. L.M.A., E.A.-T., and J.-L.L.R. drafted manuscript. All authors edited and revised critically the manuscript and approved its final version.

REFERENCES

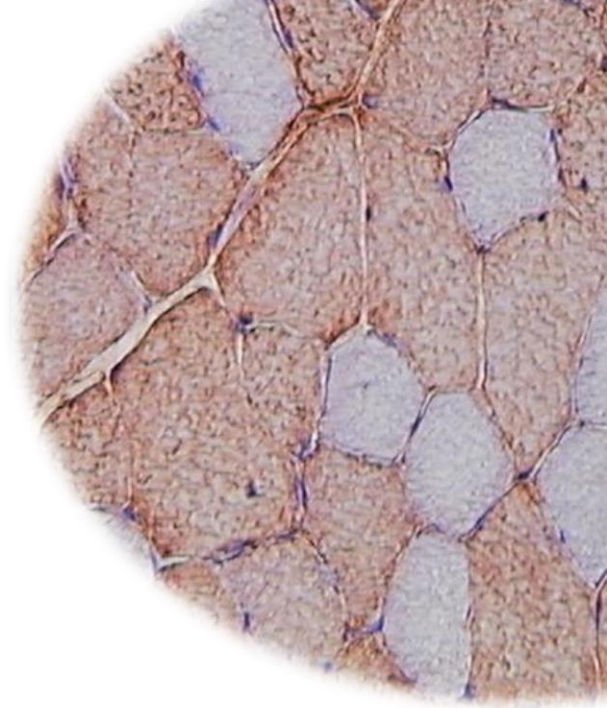
1. **Acevedo LM, and Rivero JL.** New insights into skeletal muscle fibre types in the dog with particular focus towards hybrid myosin phenotypes. *Cell Tiss Res* 323: 283-303, 2006.
2. **Adams GR, and Vaziri ND.** Skeletal muscle dysfunction in chronic renal failure: effects of exercise. *Am J Physiol Ren Physiol* 290: F753-761, 2006.
3. **Adams GR, Zhan CD, Haddad F, and Vaziri ND.** Voluntary exercise during chronic renal failure in rats. *Med Sci Sports Exer* 37: 557-562, 2005.
4. **Ahonen RE.** Light microscopic study of striated muscle in uremia. *Acta Neuropathol* 49: 51-55, 1980.
5. **Al-Hayk K, and Bertorini TE.** Neuromuscular complications in uremics: A review. *Neurol* 13: 188-196, 2007.
6. **Amann K, Neimeier KA, Schwarz U, Tornig J, Matthias S, Orth SR, Mall G, and Ritz E.** Rats with moderate renal failure show capillary deficit in heart but not skeletal muscle. *Am J Kid Dis* 30: 382-388, 1997.
7. **Bradford MM.** A rapid and sensitive method for the quantitation of microgram quantities of protein utilizing the principle of protein-dye binding. *Anal Biochem* 72: 248-254, 1976.
8. **Bundschu HD, Pfeilsticker D, Matthews C, and Ritz E.** Myopathy in experimental uremia. *Res Exp Med* 165: 205-212, 1975.
9. **Conjard A, Ferrier B, Martin M, Caillette A, Carrier H, and Baverel G.** Effects of chronic renal failure on enzymes of energy metabolism in individual human muscle fibers. *J Am Soc Nephrol* 6: 68-74, 1995.
10. **Delp MD, and Duan C.** Composition and size of type I, IIA, IID/X, and IIB fibers and citrate synthase activity of rat muscle. *J Appl Physiol* 80: 261-270, 1996.
11. **Dubowitz V, and Sewry CA.** The procedure of muscle biopsy. In: *Muscle Biopsy: A Practical Approach* edited by Dubowitz V, and Swery CA. Edinburg, UK: Saunders Elseviers, Elsevier Ltd., 2007, p. 3-20.
12. **Durozard D, Pimmel P, Baretto S, Caillette A, Labeeuw M, Baverel G, and Zech P.** 31P NMR spectroscopy investigation of muscle metabolism in hemodialysis patients. *Kid Int* 43: 885-892, 1993.
13. **Eason JM, Schwartz GA, Pavlath GK, and English AW.** Sexually dimorphic expression of myosin heavy chains in the adult mouse masseter. *J Appl Physiol* 89: 251-258, 2000.
14. **Fanzani A, Conraads VM, Penna F, and Martinet W.** Molecular and cellular mechanisms of skeletal muscle atrophy: an update. *J Cachex Sarcop Mus* 3: 163-179, 2012.
15. **Flisinski M, Brymora A, Bartlomieczyk I, Wisniewska E, Golda R, Stefanska A, Paczek L, and Manitius J.** Decreased hypoxia-inducible factor-1alpha in gastrocnemius muscle in rats with chronic kidney disease. *Kid Blood Pres Res* 35: 608-618, 2012.
16. **Flisinski M, Brymora A, Elminowska-Wenda G, Bogucka J, Walasik K, Stefanska A, Odrowaz-Sypniewska G, and Manitius J.** Influence of different stages of experimental chronic kidney disease on rats locomotor and postural skeletal muscles microcirculation. *Ren Fail* 30: 443-451, 2008.
17. **Flisinski M, Brymora A, Elminowska-Wenda G, Bogucka J, Walasik K, Stefanska A, Strozecki P, and Manitius J.** Morphometric analysis of muscle fibre types in rat locomotor and postural skeletal muscles in different stages of chronic kidney disease. *J Physiol Pharmacol* 65: 567-576, 2014.
18. **Frese S, Velders M, Schleipen B, Schanzer W, Bloch W, and Diel P.** Myosin heavy chain expression pattern as a marker for anabolic potency: desoxymethyltestosterone (madol), norandrostenedione and testosterone repress MHC-IIb expression and stimulate MHC-IIId/x expression in orchietomized rat gastrocnemius muscle. *Arch Toxicol* 85: 635-643, 2011.
19. **Graziotti GH, Rios CM, and Rivero JL.** Evidence for three fast myosin

Chapter 4

- heavy chain isoforms in type II skeletal muscle fibers in the adult llama (*Lama glama*). *J Histochem Cytochem* 49: 1033-1044, 2001.
20. **Holecek M.** Muscle wasting in animal models of severe illness. *Int J Exp Pathol* 93: 157-171, 2012.
21. **Ke Q, and Costa M.** Hypoxia-inducible factor-1 (HIF-1). *Mol Pharmacol* 70: 1469-1480, 2006.
22. **Larsson L, and Skogsberg C.** Effects of the interval between removal and freezing of muscle biopsies on muscle fiber size. *J Neurol Sci* 85: 27-38, 1988.
23. **Lewis MI, Fournier M, Wang H, Storer TW, Casaburi R, Cohen AH, and Kopple JD.** Metabolic and morphometric profile of muscle fibers in chronic hemodialysis patients. *J Appl Physiol* 112: 72-78, 2012.
24. **Lopez I, Mendoza FJ, Guerrero F, Almaden Y, Henley C, Aguilera-Tejero E, and Rodriguez M.** The calcimimetic AMG 641 accelerates regression of extraosseous calcification in uremic rats. *Am J Physiol Ren Physiol* 296: F1376-1385, 2009.
25. **Lunde IG, Anton SL, Bruusgaard JC, Rana ZA, Ellefsen S, and Gundersen K.** Hypoxia inducible factor 1 links fast-patterned muscle activity and fast muscle phenotype in rats. *J Physiol* 589: 1443-1454, 2011.
26. **Molsted S, Eidemak I, Sorensen HT, Kristensen JH, Harrison A, and Andersen JL.** Myosin heavy-chain isoform distribution, fibre-type composition and fibre size in skeletal muscle of patients on haemodialysis. *Scand J Urol Nephrol* 41: 539-545, 2007.
27. **Perry JE, Grossmann ME, and Tindall DJ.** Androgen regulation of gene expression. *Prost Suppl* 6: 79-81, 1996.
28. **Peter JB, Barnard RJ, Edgerton VR, Gillespie CA, and Stempel KE.** Metabolic profiles of three fiber types of skeletal muscle in guinea pigs and rabbits. *Biochem* 11: 2627-2633, 1972.
29. **Pisani DF, and Dechesne CA.** Skeletal muscle HIF-1 α expression is dependent on muscle fiber type. *The Journal of general physiology* 126: 173-178, 2005.
30. **Rivero JL, Talmadge RJ, and Edgerton VR.** Interrelationships of myofibrillar ATPase activity and metabolic properties of myosin heavy chain-based fibre types in rat skeletal muscle. *Histochem Cell Biol* 111: 277-287, 1999.
31. **Roy RR, Monke SR, Allen DL, and Edgerton VR.** Modulation of myonuclear number in functionally overloaded and exercised rat plantaris fibers. *J Appl Physiol* 87: 634-642, 1999.
32. **Sakkas GK, Ball D, Mercer TH, Sargeant AJ, Tolfrey K, and Naish PF.** Atrophy of non-locomotor muscle in patients with end-stage renal failure. *Nephrol Dial Transplant* 18: 2074-2081, 2003.
33. **Schiaffino S, Gorza L, Sartore S, Saggini L, Ausoni S, Vianello M, Gundersen K, and Lomo T.** Three myosin heavy chain isoforms in type 2 skeletal muscle fibres. *J Mus Res Cell Motil* 10: 197-205, 1989.
34. **Schreiber E, Matthias P, Muller MM, and Schaffner W.** Rapid detection of octamer binding proteins with 'mini-extracts', prepared from a small number of cells. *Nucl Ac Res* 17: 6419, 1989.
35. **Taes YEC, Speeckaert M, Bauwens E, De Buyzere MR, Libbrecht J, Lameire NH, and Delanghe JR.** Effect of dietary creatine on skeletal muscle myosin heavy chain isoform expression in an animal model of uremia. *Neph Exp Nephrol* 96: e103-e110, 2004.
36. **Welle S, Tawil R, and Thornton CA.** Sex-related differences in gene expression in human skeletal muscle. *PloS one* 3: e1385, 2008.

CHAPTER 5

High-phosphorus diet maximizes and low-dose calcitriol attenuates skeletal muscle changes in long-term uremic rats



Effect of hyperphosphatemia and calcitriol on skeletal muscle in uremia

Luz M. Acevedo,^{1,4} Ignacio López,² Alan Peralta-Ramírez,^{2,5} Carmen Pineda,² Verónica E. Chamizo,¹ Mariano Rodríguez,³ Escolástico Aguilera-Tejero,^{2*} and José-Luis L. Rivero^{1*}

¹*Laboratory of Muscular Biopathology, Department of Comparative Anatomy and Pathological Anatomy, Faculty of Veterinary Sciences, University of Cordoba, Cordoba, Spain*

²*Department of Animal Medicine and Surgery, University of Cordoba, Spain*

³*Unidad de Investigación y Servicio de Nefrología (Ren in Ren), Instituto Sanitario de Investigación Biomédica de Córdoba (IMIBIC), Reina Sofía University Hospital, University of Cordoba, Spain*

⁴*Departamento de Ciencias Biomédicas, Facultad de Ciencias Veterinarias, Universidad Central de Venezuela, Maracay, Venezuela*

⁵*Escuela de Medicina Veterinaria, Universidad Nacional Autónoma de Nicaragua, León, Nicaragua*

*E. Aguilera-Tejero and J.-L. L. Rivero contributed equally to this study

J Appl Physiol 120:1059-1069, 2016

ABSTRACT

Although disorders of mineral metabolism and skeletal muscle are common in chronic kidney disease (CKD), their potential relationship remains unexplored. Elevations in plasma phosphate, parathyroid hormone and fibroblastic growth factor 23 together with decreased calcitriol levels are common features of CKD. High phosphate intake is a major contributor to progression of CKD. This study was primarily aimed to determine the influence of high phosphate intake on muscle and to investigate whether calcitriol supplementation counteracts negative skeletal muscle changes associated with long-term uremia. Proportions, and metabolic and morphological features of myosin-based muscle fiber-types were assessed in the slow-twitch soleus and the fast-twitch tibialis cranialis muscles of uremic rats (5/6 nephrectomy, Nx) and compared with sham-operated (So) controls. Three groups of Nx rats received either a standard diet (0.6% phosphorus, Nx-Sd), or a high-phosphorus diet (0.9% phosphorus, Nx-Pho), or a high-phosphorus diet plus calcitriol (10 ng/kg 3 d/wk ip, Nx-Pho+Cal) for 12 wk. Two groups of So rats received either a standard diet or a high-phosphorus diet (So-Pho) over the same period. A multivariate analysis encompassing all fiber-type characteristics indicated that Nx-Pho+Cal rats displayed skeletal muscle phenotypes intermediate between Nx-Pho and So-Pho rats, and that uremia-induced skeletal muscle changes were of greater magnitude in Nx-Pho than in Nx-Sd rats. In uremic rats, treatment with calcitriol preserved fiber-type composition, cross-sectional size, myonuclear domain size, oxidative capacity and capillarity of muscle fibers. These data demonstrate that high phosphorus diet potentiates and low dose calcitriol attenuates adverse skeletal muscle changes in long-term uremic rats.

NEW AND NOTEWORTHY

This study investigates the impact of dietary

phosphate and calcitriol treatment on phenotypic characteristics of slow- and fast-twitch hind limb skeletal muscles in uremia. A multivariate analysis encompassing all fiber-type characteristics indicated that a diet with high phosphate content induced skeletal muscle changes of greater magnitude compared with a standard diet. Treatment with calcitriol preserved fiber-type composition, cross-sectional size, myonuclear domain size, oxidative capacity and capillarity of muscle fibers.

Key words: chronic renal failure, active vitamin D, phosphorus, secondary hyperparathyroidism, muscle fiber type

INTRODUCTION

Disorders of mineral metabolism are common in patients with chronic kidney disease (CKD) (7). Secondary hyperparathyroidism (HPT) develops early in CKD and is present virtually in all patients with end-stage renal disease (7, 15, 46). Main features of secondary HPT in CKD include decreased production of calcitriol (1 α ,25 dihydroxyvitamin D₃, the active form of vitamin D) by the kidneys, retention of phosphorus (hyperphosphatemia), low serum calcium (hypocalcemia) and increased levels of serum parathyroid hormone (PTH) and fibroblastic growth factor 23 (FGF23) (7, 15, 46). Secondary HPT is a progressive disease associated with systemic complications, including renal osteodystrophy, soft tissue and vascular calcifications, and adverse cardiovascular outcomes (55). It is well known that calcitriol and other vitamin D analogues reduce serum PTH levels at the expense of a concomitant increase in phosphate and calcium intestinal absorption (46, 55). It is also known that calcitriol increases the risk of adynamic bone disease in patients with advanced CKD (35) and induces aortic calcifications in rats with secondary HPT (29). However, vitamin D analogues are widely used in early CKD to prevent calcitriol deficiency, an important factor in the development of secondary HPT (55).

Skeletal muscle is heavily impacted by CKD, suffering from a constellation of structural and functional abnormalities referred to as uremic myopathy (3). Changes in skeletal muscle performance parameters have been extensively described over the past 40 years in both CKD patients (e.g., 5, 11, 13, 14, 16, 34, 45) and animal models of uremia (4, 9, 18, 19, 38, 52) but the reported findings are not uniform. A recent study by the authors' group provided evidence that skeletal muscle cells change their proportions and metabolic and structural features 12 wk after 5/6 nephrectomy (Nx), a widely used animal model of uremia (1). This malleability was muscle-specific, being of greater magnitude in the fast-twitch (normally inactive at rest) tibialis cranialis (TC) muscle than in the slow-twitch (primarily active at rest providing postural support) soleus (SOL) muscle. Although the precise mechanism underlying these changes remains unclear, it seems to be multifactorial and complex (see Ref. 3 for review).

There is now emerging evidence that vitamin D exerts a range of beneficial effects in skeletal muscle (23, 41). They include improvements of muscle contractibility and myosin heavy chain expression (37), mitochondrial oxidative phosphorylation (49), muscle cell differentiation and myogenesis (21), angiogenesis (22) and muscle growth (10, 24, 47). These actions may, in part, be indirect by way of vitamin D's effect on calcium and phosphorus homeostasis, but also by a direct mechanism via the expression in skeletal muscle of both vitamin D receptor (VDR) and the enzyme CYP27B1 (1- α -hydroxylase), which hydroxylates 25-hydroxyvitamin D₃ to calcitriol (41). These data provide clear support for the concept that skeletal muscle is a target organ of vitamin D action.

Although collectively a few studies from the earliest literature provide evidence that treatment with vitamin D may have a positive effect on various aspects of muscle function in patients with advanced CKD (8, 25, 28, 54),

contractile, metabolic and structural events underlying this effect at the cellular level have not been explored in experimental models of uremia. Moreover, methodological limitations of these studies (discussed in Ref. 26), make it difficult to draw firm conclusions or to generalize these results.

We hypothesized that feeding uremic rats with high phosphorus diets would increase the severity of muscle changes and that treatment of uremic rats with low-dose calcitriol would attenuate muscle changes by reverting muscle fiber-type characteristics toward those of control skeletal muscle phenotypes. Thus, the main purpose of this study was to analyze the effect of high-phosphorus diet and low-dose calcitriol on frequency, metabolic and structural changes of skeletal muscle fiber-types in long-term uremic rats.

MATERIALS AND METHODS

Experimental Design and Procedures

Ethics. All experimental protocols were reviewed and approved by the Ethics Committee for Animal Research of the University of Cordoba (Cordoba, Spain). They followed the guidelines laid down by the Higher Council of Scientific Research of Spain following the normal procedures directing animal welfare (Real Decreto 223/88, BOE of 18 of March) and adhered to the recommendations included in the Guide for Care and Use of Laboratory Animals (US Department of Health and Human Services, NIH) and European laws and regulations on protection of animals, under the advice of specialized personnel.

Animals. Sixty adult (3.5–4 mo old) Wistar rats of both sexes (30 females and 30 males) with body weight of 249 ± 52 g (mean \pm SD) at the beginning of the experiment were used. Animals were provided by the Central Service of Experimental Animals of the University of Cordoba, Cordoba (Spain). They were

individually housed in standard vivarium cages in a temperature- and humidity-controlled environment, with a 12:12-h light-dark cycle and given *ad libitum* access to standard rat diet (Altromin Spezialfutter GmbH, Germany; values per 100 g: energy 351.8 kcal 1100 kJ⁻¹, protein content 18%, lysine 1.74%, methionine 1.0%, cysteine 0.31%, tryptophan 0.20%, fat 5%, ash 4.5%, sodium 0.24%, calcium 0.6%, phosphorus 0.6%) and tap water.

Design and surgical procedures. Before the experiment began, all rats were maintained for 2 wk on the standard diet. Afterwards, rats were randomly allocated to the following groups with balanced sexes: sham operated control (So; n=24) and 5/6 nephrectomy (Nx, n=36 rats). The Nx was carried out following a two-step procedure that reduces the original renal mass by five-sixths as previously described (1). The control So rats were sham operated with the same protocol and total duration of the surgery, except both kidneys were maintained intact. After the second surgery, So rats were randomly allocated to the following two groups of 12 individuals each with balanced sexes: So-Sd and So-Pho. Rats in the So-Sd group were maintained for 12 wk on the standard diet, whereas animals in the So-Pho group received a high-phosphate diet (0.9% phosphorus) over the same experimental period. After surgery, Nx rats were randomly allocated to the following three groups of 12 rats each with balanced sexes: Nx-Sd, Nx-Pho and Nx-Pho+Cal. Rats in the Nx-Sd group were maintained for 12 wk on the standard diet, animals in the Nx-Pho group received a high-phosphate (0.9% phosphorus) diet and rats in the Nx-Pho+Cal were supplemented with a high-phosphate diet (0.9% phosphorus) and calcitriol (10 ng kg⁻¹, Calcijex, Abbot, Madrid, Spain; 3 d wk⁻¹, ip). Both food intake and body weight of individual rats were assessed weekly.

Muscle sampling and tissue preparation. After 12 wk, rats from both groups were sacrificed by aortic puncture

and exsanguination under deep general anaesthesia (sodium thiopental 50 mg kg⁻¹, Pentotal®, Abbot, Illinois, USA; ip). Soleus (SOL) and tibialis cranialis (TC) muscles were dissected and individual muscles were wet weighted. These muscles were selected as two representative muscles of a typical slow-twitch muscle (SOL, composed primarily of slow-twitch muscle fibers) and a characteristic fast-twitch muscle (TC, composed primarily of fast-twitch muscle fibers in its white region), respectively (12). Also because these two hind limb muscles are opposite regarding their resting functional activities (see Ref. 12). Upon collection, tissue blocks from the muscle belly were mounted on cork blocks with the use of OCT embedding medium (Tissue-Tek II, Miles Laboratories, Naperville, IL, USA) and oriented so that myofibers could be cut transversely. Specimens were systematically frozen by immersion in isopentane (30 s), kept at the freezing point in liquid nitrogen, and stored at -80 °C until analyzed. Muscle samples were routinely frozen between 2 and 4 min after removal, because it has been demonstrated that the interval between removal and freezing has a significant (negative) effect on skeletal muscle fiber size (33). All muscle sampling and muscle preparation procedures were always carried out by the same investigator, experienced in skeletal muscle biopsy studies, taking care to standardize both the location and the freezing of the sample.

Laboratory Analyses

Blood biochemistry. Blood samples were obtained from the abdominal aorta in heparinized syringes at the time of the death. Measurements of ionized calcium levels were analyzed immediately using a Ciba-Corning 634 ISE Ca²⁺/pH Analyzer (Ciba-Corning, Essex, UK). Afterward, plasma was separated by centrifugation and stored at -80 °C until assayed. Plasma creatinine, blood urea nitrogen, and phosphorus levels were measured by spectrophotometry (Biosystems, Barcelona, Spain).

► **Fig. 5.1** Serial frozen sections of *tibialis cranialis* muscle from a representative sham operated rat (So) stained for immunohistochemistry (A-E) and enzyme histochemistry and histology (F-I). A-E: Sections were reacted with monoclonal antibodies against specific myosin heavy chain (MHC) isoforms: BA-D5 (A, anti MHC-I), SC-71 (B, anti MHC-IIa), BF-35 (C, anti MHCs-I, -IIa and -IIb), S5-8H2 (D, anti MHCs-I, -IIx and -IIb) and BF-F3 (E, anti MHC-IIb). F-I: Additional serial sections were stained for quantitative enzyme histochemistry of succinate dehydrogenase (F, SDH) and glycerol-3-phosphate dehydrogenase (G, GPDH) activities, and for histology of α -amylase periodic acid Schiff (H, PAS) for visualizing capillaries and haematoxylin and eosin (I, H&E) for visualizing nuclei. The seven MHC-based muscle fiber types are labelled in all serial sections; four of them were pure fibers expressing a unique MHC isoform (i.e., fibers '1', '3', '5' and '7' which correspond with type I, IIA, IIX and IIB fibers, respectively), and other three were hybrid phenotypes coexpressing two different MHC isoforms [i.e., MHCs-I and -IIa (type I+IIA, not shown), MHCs-IIa and -IIx (type IIAX, not shown) and MHCs-IIx and -IIb (type IIXB, fiber labelled '6'). Bar, 150 μ m.

ELISA tests were used to quantify plasma FGF23 (Kainos Laboratories, Tokyo, Japan) and PTH (Rat Bioactive Intact PTH ELISA kit, Immunotopics Inc, San Clemente, CA, USA).

Myosin heavy chain (MHC) immunohistochemistry.

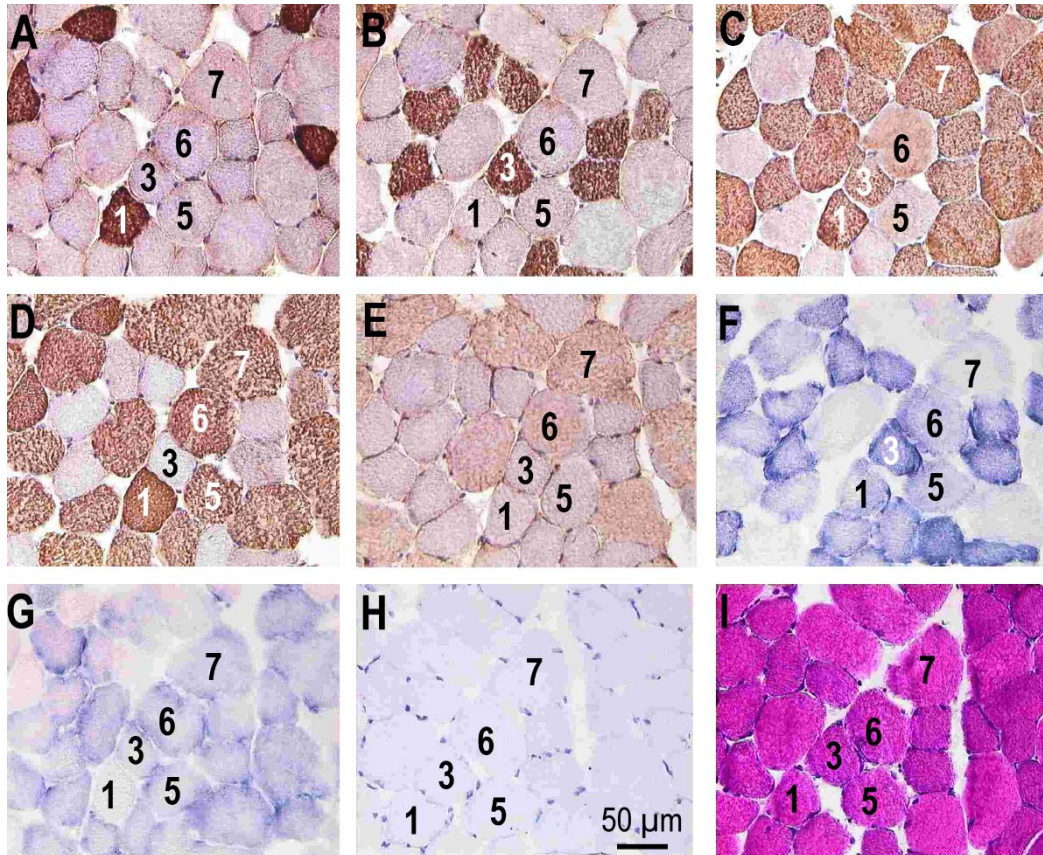
Muscle samples were serially sectioned (10- μ m-thick) in a cryostat (Frigocut, Reichert Jung, Nubloch, Germany) at -20 °C and used for immunohistochemistry.

Immunohistochemistry was performed with five monoclonal antibodies (MAbs) specific against MHC isoforms: BA-D5 (DMS, Braunschweig, Germany; anti-MHC-I; **Fig. 5.1A**), SC-71 (DMS; anti-MHC-IIa; **Fig. 5.1B**), BF-35 (DMS; anti-MHCs-I plus -IIa and -IIb; **Fig. 5.1C**), S5-8H2 (Biocytex Biotechnology, Marseille, France; anti-MHCs-I plus -IIx and -IIb; **Fig. 5.1D**), and BF-F3 (DMS; anti-MHC-IIb; **Fig. 5.1E**). The specificity of these MAbs for MHCs in rat skeletal muscle has previously been reported (1, 27, 48). The immunoperoxidase staining protocol with avidin-biotin complex (ABC) protocol was used as previously described (43).

Quantitative enzyme histochemistry. Additional serial sections were used for quantitative enzyme histochemistry. The activities of the enzymes succinate

dehydrogenase (SDH, EC 1.3.4.1; **Fig. 5.1F**), used as an oxidative marker, and glycerol-3-phosphate-dehydrogenase (GPDH; **Fig. 5.1G**), used as an indirect marker for glycolytic potential of myofibers, were determined on 10- μ m- and 14- μ m-thick sections, respectively, by using quantitative histochemical methods previously adjusted and validated in rat skeletal muscle (43). However, it is not known whether the GPDH histochemical method used in the present study stains for activity of the cytosolic NAD-dependent GPDH (EC 1.1.1.8) or the mitochondrial FAD-dependent GPDH (EC 1.1.99.5). Neither GPDH is directly involved in the glycolytic pathway; however, both are directly involved in the transfer of NADH from glycolysis in the cytosol into FADH₂ in the mitochondria of skeletal muscles. Furthermore, GPDH histochemical activity correlates with the activities of other glycolytic enzymes (40).

Nuclei and capillary histology. Additional 10- μ m-thick sections were stained with haematoxylin and eosin (H&E; **Fig. 5.1I**) and used to visualize total nuclei within or around each individual muscle fiber. Additional 14- μ m-thick serial sections were incubated in a 2.2% solution of α -amylase and then stained according to a standardized periodic-acid-Schiff (PAS; **Fig. 5.1H**)



technique by using a 1% solution of acid (2). These sections were used to visualize capillaries.

Image analysis and morphometry. Sections were examined in a blind fashion by the same investigator (L.M.A.), who had experience of the normal appearance of mammalian skeletal muscle fibers. All serial sections for immunohistochemistry, enzyme histochemistry and histology were visualized and digitized as previously described (2). A region containing between 150 and 250

fibers was selected for further analyses. In the TC muscle, this area was selected from the core of the white (superficial) portion of the muscle, since it contains a higher number of fast-twitch muscle fibers (98%) than the red (deep) portion (93%) of the muscle (12). Images were saved as digitized frames at 256 gray levels. The gray levels were converted to optical density (OD) units by using a calibrated set of OD filters. The digitized images of the fibers in the two histochemical reactions

(SDH and GPDH) within the selected region were traced manually and analyzed for the fiber cross-sectional area (CSA) and the average OD for each histochemical reaction of individual muscle fibers. The average fiber OD for each histochemical reaction was determined as the average OD for all pixels within the traced fiber from three sections incubated with substrate minus the average OD for all pixels of the same fiber from other two sections incubated without substrate (43). Because a number of factors can influence the reliability of histochemical enzyme activity determinations, we checked the variability on three consecutive sections for both SDH and GPDH histochemical reactions by repeated measurements of the same individual fibers. Only coefficients of variation for triplicate measurements of ODs below 5% were accepted in the present study; this demonstrated the high analytical precision that can be achieved for the measurement of fiber OD on enzyme histochemical sections.

The number of nuclei and capillaries around each individual muscle fiber in the selected area of the sample was also obtained from the haematoxylin and eosin staining and α -amylase-PAS techniques, respectively (2). They were expressed in absolute terms as number of nuclei or capillaries in contact with each muscle fiber.

The fibers in the selected area were classified according to their MHC content by means of visual examination of immunostainings of the five serial sections stained with the battery of anti-MHC MAbs as previously described (1). The reactivity of each individual muscle fiber in these five consecutive sections was judged as positive or negative by comparing the intensity of the reaction of neighbouring fibers. Seven fiber types were categorized, four of them as pure fibers expressing a unique MHC isoform (i.e., type I, IIA, IIX and IIB), and other three as hybrid phenotypes co-expressing two different MHC isoforms (type I+IIA, IIAX and IIXB).

The relative frequency of different muscle fiber types

in the selected region was used to numerically express the fiber type composition of each muscle sample. The CSA of the same fibers were averaged according to fiber type. Individual SDH and GPDH ODs and absolute numbers of nuclei and capillaries of muscle fibers were averaged according to the MHC muscle fiber-type and used for statistical analyses. The SDH-to-GPDH ratio of individual muscle fibers was used as an indicator of the relative oxidative vs glycolytic metabolic capacities of individual muscle fibers. For minor fibre types (I+IIA and IIA in the SOL muscle, and I, I+IIA and IIAX in the TC muscle), there were so few fibres in most muscle samples that a statistically reliable determination of their CSA, nuclei, SDH, GPDH, and capillarity was impossible. In consequence, muscle fibre-types showing, on average, a fibre percentage below 5% were excluded from these analyses.

Statistical analyses

All statistics and charts were run on Statistica 7.0 for Windows (StatSoft I, Statistica, Data software System, www.statsoft.com). Muscle sample was the unit of analysis for the present dataset. A total of 120 muscle samples (60 animals x two muscles –SOL and TC) were available for statistical analysis. Sample size and the power of a contrast of hypothesis were estimated by power analysis and interval estimation of the statistical software employed. Accepting an α -risk of 0.05 and a β -risk of 0.2 in a two-sided test, a minimum of 12 subjects/group were considered necessary to recognize as statistically significant a minimum difference of 1.5 SD units between any pair of groups assuming that 5 groups exists, as well as a common deviation of 20% of the mean value, and anticipating a drop-out rate of 0%. Normality of muscle variables was tested using a Kolmogorov-Smirnov test and data were expressed as means \pm SE. One-way analysis of variance (ANOVA) was used to test for differences between groups. When either a significant

($P < 0.05$) or a marginal ($0.05 < P < 0.1$) effect was observed, the Fisher LSD *post hoc* test was used to locate specific significant differences between pairwise groups.

Overall differences among experimental groups were estimated by squared Mahalanobis coefficients provided by multivariate discriminant analyses of the two hind-limb muscles. This distance takes into account all muscle fiber-type variables summarising the overall phenotype of each individual muscle sample, allowing its classification into one of the five groups. These coefficients served to compare the overall muscle characteristics of group pairs in order to establish their homologies and differences regarding the control skeletal muscle phenotype.

RESULTS

Plasma biochemistry. As expected, all Nx groups had higher plasma creatinine and urea levels than So groups ($P < 0.001$) and no significant differences were found between Nx groups (**Table 5.1**). Plasma phosphorus concentration was higher in the groups fed high-phosphorus diet (Pho subgroups), and hyperphosphatemia was more severe in the Nx-Pho and Nx-Pho+Cal rats (**Table 5.1**). The plasma ionized calcium level only was reduced in Nx-Pho rats, when compared with the So-Sd group. Both nephrectomy and feeding high-phosphorus diet resulted in increases in FGF23 that were not significant; however, the combination Nx-Pho produced a highly significant increase in FGF23 that was potentiated by treatment with calcitriol (**Table 5.1**). Plasma PTH behaved similar to FGF23 with the exception that treatment with calcitriol reduced PTH concentrations (**Table 5.1**).

Food intake, body weight, muscle weight and muscle-somatic index. Food and energy intakes and body weight gain throughout the experiment (12 wk) were similar in the five experimental groups ($P > 0.05$; **Table 5.1**). Thus, final body weights were similar in all groups ($P > 0.05$).

Wet weight and muscle-somatic index (MSI, wet muscle weight referred to body weight) of the TC muscle did not vary between groups ($P > 0.05$; **Table 5.1**). However, wet weight and MSI of the SOL muscle were higher in Nx-Pho+Cal rats than in the remaining groups ($P = 0.05$ and $P < 0.01$, respectively).

Fiber-type composition. Seven fiber-types were identified in the TC muscle, but only three fiber-types were found in the SOL muscle. SOL and TC muscle fiber-type distributions are shown in **Table 5.2**. The five experimental groups were comparable regarding their SOL muscle fiber-type compositions ($P > 0.05$). There were, however, statistically significant differences in TC muscle fiber-type distribution between the five groups ($P < 0.05$ – $P < 0.01$). In this muscle, Nx induced a slow-to-fast fiber-type switching in the direction I→IIA→IIX→IIB, compared with the two So groups. However, the amplitude of this change was not homogeneous in the three Nx groups of rats. Nx-Sd decreased types I and IIA fibers by 56% ($P = 0.05$) and 41% ($P < 0.05$), respectively, and increased type IIB fibers by 54% ($P < 0.05$), compared with So-Sd rats. Nx-Pho decreased type IIX fibers by 50% ($P < 0.001$) and increased type IIB fibers by 78% ($P < 0.01$), compared with So-Pho subjects. And Nx-Pho+Cal did not vary significantly this muscle fiber type-composition, compared with So-Pho rats ($P > 0.05$). The three Nx groups were comparable regarding their TC muscle fiber-type composition, but a tendency for Nx-Pho+Cal rats having a lower percentage of type IIB fibers than Nx-Pho subjects was noted ($P = 0.067$). So-Pho increased the percentage of hybrid IIXB fibers in the TC muscle by 74% ($P < 0.01$), compared with So-Sd animals.

Muscle fiber CSA. The five experimental groups were comparable concerning their muscle fiber CSAs of both muscle types. This was noted both at the individual muscle fiber-type level (**Table 5.3**) and when all muscle fibers were analyzed together without fiber-type

Effect of hyperphosphatemia and calcitriol on skeletal muscle in uremia

Table 5.1 Blood biochemistry, food intake, body weight, muscle weights and muscle somatic index (MSI) of subjects

	So-Sd	So-Pho	Nx-Sd	Nx-Pho	Nx-Pho+Cal	P value
[Creatinine] mg dL ⁻¹	0.70±0.02 a	0.70±0.05 a	1.02±0.06 b	1.30±0.05 b	1.10±0.09 b	P=0.001
[Urea] mg dL ⁻¹	50.2±1.8 a	39.5±2.5 a	72.5±5.9 b	80.4±12.1 b	68.2±18.4 b	P=0.000
[Bicarbonate] mmol L ⁻¹	24.7±2.3	24.3±0.3	29.2±1.1	31.1±4.2	30.4±3.5	NS
[P] mg dl ⁻¹	3.34±0.16 a	4.96±0.23 bc	4.40±0.59 ab	6.30±0.70 cd	6.63±0.75 d	P=0.001
[Ca ⁺⁺] mmol L ⁻¹	1.23±0.02 b	1.23±0.01 ab	1.22±0.01 ab	1.16±0.05 a	1.22±0.02 ab	P<0.1
[FGF23] pg mL ⁻¹	67.7 ±7.8 a	165±11 a	106±38 a	705±198 b	1825±401 c	P=0.000
[PTH] pg mL ⁻¹	20.8±1.2 a	102.6±41.9 a	115.8±50.1 a	1815±660 b	1186±488 b	P=0.01
Food intake, g d ⁻¹	20.0±1.4	14.3±1.2	18.7±1.0	15.7±0.8	17.0±3.5	NS
Energy intake, kcal d ⁻¹	70.3±4.8	50.2±4.1	65.8±3.4	55.1±2.7	59.8±12.3	NS
Initial body weight, g	270±27	265±23	246±21	238±14	249±23	NS
Final body weight, g	345±41	347±44	323±39	308±37	339±44	NS
Weight gain, g	75±14	82±22	77±17	80±21	90±22	NS
M. soleus						
Weight, mg	143±9 a	157±9 ab	136±8 a	143±12 a	177±14 b	P=0.05
MSI, mg g ⁻¹	0.43±0.02 a	0.47±0.02 a	0.43±0.02 a	0.44±.01 a	0.53±0.01 b	P<0.01
M. tibialis cranialis						
Weight, mg	893±49	840±51	821±59	802±51	890±73	NS
MSI, mg g ⁻¹	2.65±0.08	2.51±0.10	2.58±0.09	2.56±0.05	2.65±0.04	NS

Values are means±SE, n= 12; So-Sd=sham-operated standard diet; So-Pho=sham-operated high-phosphorus diet; Nx-Sd=5/6 nephrectomy standard diet; Nx-Pho=5/6 nephrectomy and high-phosphorus diet; Nx-Pho+Cal=5/6 nephrectomy high-phosphorus diet plus calcitriol. One-way ANOVA was used to test for differences between groups; P values denote significance of differences between groups, NS=not significant. Within a row, means with different letters differ significantly (P<0.05, at least)

specification (**Fig. 5.2A**). Nevertheless, the mean CSA of type IIX fibres in the TC muscle of Nx-Pho rats was found to be lower by 21% (P<0.05) and 27% (P<0.01) compared with those found in So-Pho and Nx-Pho+Cal groups, respectively (**Table 5.3**). Furthermore, a no-significant tendency for Nx-Pho+Cal rats having greater muscle fibers in the SOL muscle than So-Sd subjects was observed (20%, P=0.058). This difference could underlies

the higher weight and MSI of the SOL muscle noted in the Nx-Pho+Cal group in comparison with the remaining groups (**Table 5.1**).

Muscle fiber nuclear density. The mean number of nuclei associated with individual muscle fibers changed significantly between groups, but the direction of the changes was divergent in the two hind-limb muscles (**Table 5.3; Fig. 5.2B**). In the SOL muscle, the muscle

Table 5.2 Muscle fiber-type composition, %

Fiber-type	So-Sd	So-Pho	Nx-Sd	Nx-Pho	Nx-Pho+Cal	<i>P</i> values
M. soleus						
I	96.0±2.0	98.4±0.8	97.9±0.7	97.2±0.8	96.8±1.0	NS
I+IIA	0.3±0.2	0.6±0.3	1.6±0.6	1.7±0.7	0.8±0.3	NS
IIA	3.7±2.0	1.0±0.8	0.5±0.3	1.1±0.6	2.4±1.1	NS
M. tibialis cranialis						
I	4.1±1.4 b	2.0±0.6 ab	1.8±0.9 a	1.0±0.3 a	1.3±0.4 a	<i>P</i> <0.1
I+IIA	2.3±1.2	0.5±0.3	0.3±0.2	2.5±1.04	2.4±0.7	NS
IIA	22.7±2.8 b	15.6±3.4 ab	13.3±2.4 a	9.1±2.5 a	13.4±1.2 a	<i>P</i> <0.05
IIAX	7.4±2.1	4.1±1.3	3.8±1.5	4.7±1.4	4.5±1.4	NS
IIX	21.7±2.8 bc	26.7±3.2 c	18.4±2.1 ab	13.3±2.2 a	17.1±2.7 ab	<i>P</i> <0.05
IIXB	16.9±2.5 a	29.4±2.5 b	24.3±3.7 ab	31.7±3.9 b	33.3±3.3 b	<i>P</i> <0.01
IIB	25.0±4.9 a	21.7±4.5 a	38.5±4.7 b	38.6±2.5 b	28.2±2.2 ab	<i>P</i> <0.01

See **Table 5.1**'s legend for keys

fiber nuclear densities of Nx-Pho+Cal were found to be higher by 26% (*P*<0.05) and 36% (*P*<0.01), compared with those of So-Pho and Nx-Sd groups, respectively. In the TC muscle, however, Nx-Sd decreased the mean number of nuclei of all muscle fiber-types by 17% on average (*P*<0.01), compared with So-Sd. Nx-Pho and Nx-Pho+Cal did not change myofiber nuclear density in this muscle, compared with So-Pho subjects. However, Nx-Pho decreased this density by 17% (*P*<0.01), compared with So-Sd rats. The mean number of nuclei of type IIB fibers in the TC muscle of Nx-Pho+Cal rats was found to be higher by 18% (*P*<0.05), compared with those of Nx-Sd and Nx-Pho groups. The two control groups (So-Sd and So-Pho) were comparable regarding their muscle fiber nuclear densities in the two muscle types (*P*>0.05).

Muscle fiber SDH-to-GPDH enzyme ratio. The SDH-to-GPDH histochemical enzyme ratios, used as an index of the relative contribution of oxidative vs glycolytic pathways for energy provision within single

muscle cells, are depicted in **Table 5.4** (expressed at the single fiber-type level) and **Fig. 5.2C** (pooled for all muscle fiber-types). The mean SDH-to-GPDH ratios of muscle fibers in SOL and TC muscles of the three groups of Nx rats were found to be lower compared with those of the two So groups (*P*<0.05–*P*=0.000), but the magnitude of these changes differed between the three Nx groups. Thus, whereas Nx-Sd and Nx-Pho+Cal decreased SDH-to-GPDH ratios of muscle fibers in a range from 13% (*P*<0.05) to 26% (*P*<0.001), compared with their respective control groups (So-Sd and So-Pho), Nx-Pho decreased these ratios in a range between 22% (*P*<0.01) and 37% (*P*=0.000). As a consequence, the Nx-Sd and Nx-Pho+Cal groups were comparable regarding their muscle fiber SDH-to-GPDH ratios of both SOL and TC muscles (*P*>0.05). However, these ratios were lower in Nx-Pho rats compared with both Nx-Sd and Nx-Pho+Cal (*P*<0.05–*P*<0.001). The two control groups (So-Sd and So-Pho) also were comparable concerning their muscle fiber SDH-to-GPDH enzyme ratios.

Effect of hyperphosphatemia and calcitriol on skeletal muscle in uremia

Table 5.3 Muscle fiber size and nuclei per fiber

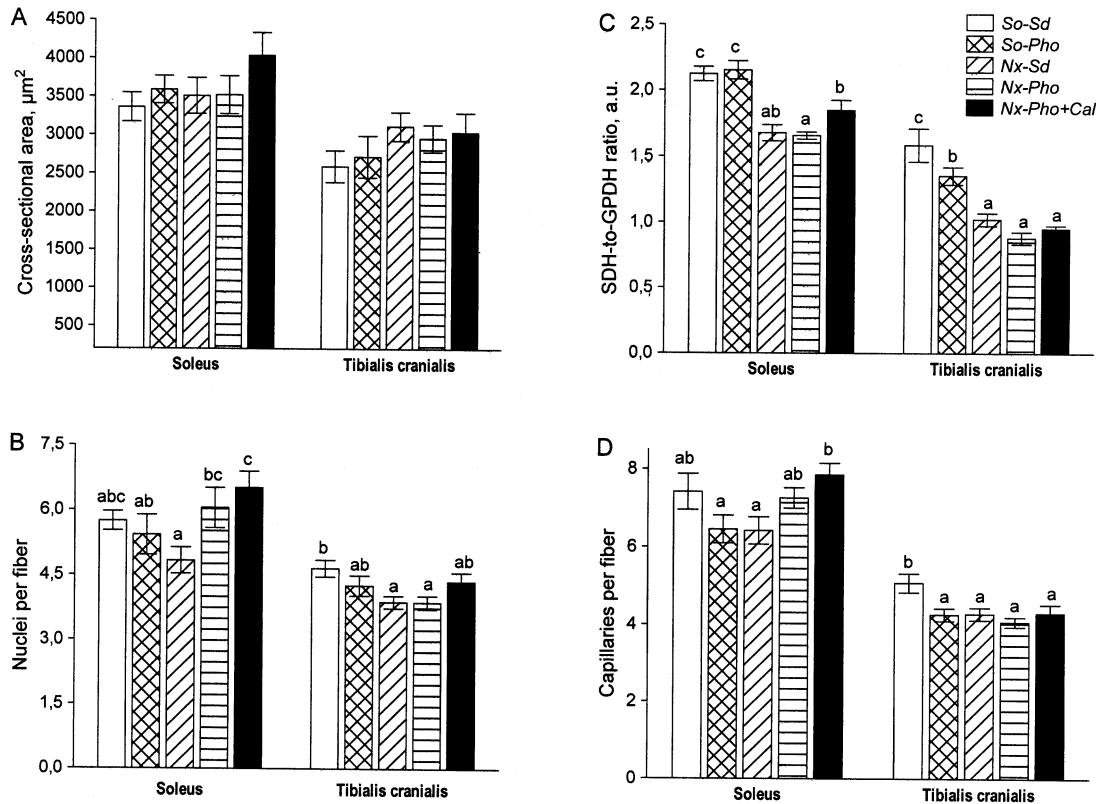
Fiber-type	So-Sd	So-Pho	Nx-Sd	Nx-Pho	Nx-Pho+Cal	P values
Muscle fiber-type cross-sectional area, μm^2						
M. soleus						
I	3378±205	3596±189	3516±247	3538±257	4069±317	NS
M. tibialis cranialis						
IIA	1442±58	1388±112	1306±67	1596±165	1543±138	NS
IIX	2231±208 ab	2278±203 b	2098±138 ab	1797±124 a	2462±151 b	$P<0.1$
IIXB	2392±170	2872±304	2803±121	2623±126	2766±196	NS
IIB	3601±294	4321±425	4568±205	4260±208	4372±376	NS
Muscle fiber-type number of nuclei per fiber, nuclei fiber ⁻¹						
M. soleus						
I	5.78±0.24abc	5.42±0.48 ab	4.82±0.32 a	6.01±0.53 bc	6.56±0.40 c	$P<0.05$
M. tibialis cranialis						
IIA	4.68±0.27 b	4.36±0.35 ab	3.81±0.18 a	4.08±0.18 ab	4.31±0.37 ab	$P<0.1$
IIX	4.69±0.27 b	4.33±0.23 ab	3.88±0.23 a	3.92±0.24 a	4.17±0.23 ab	$P<0.1$
IIXB	4.58±0.22 b	4.19±0.25 ab	3.80±0.17 a	3.78±0.19 a	4.28±0.17 ab	$P<0.05$
IIB	4.63±0.20 b	4.40±0.30 ab	3.87±0.13 a	3.85±0.17 a	4.55±0.22 b	$P<0.05$

See **Table 5.1**'s legend for keys. For clarity, muscle fiber-types with a percentage below 5% are excluded from this analysis

Muscle fiber capillarity. The mean number of capillaries contacting muscle fibers differed significantly between groups, but the nature of these differences was not homogeneous in the two muscle types (**Table 5.4; Fig. 5.2D**). In the SOL muscle, Nx-Pho+Cal increased muscle fiber capillarization by 22% compared with both So-Pho ($P<0.05$) and Nx-Sd ($P<0.01$). In the TC muscle, however, the three Nx groups were comparable concerning their muscle fiber capillarity ($P>0.05$). Nx-Sd decreased TC muscle fiber capillaries ~15% ($P<0.01$), compared with So-Sd rats. Both Nx-Pho and Nx-Pho+Cal groups were comparable with So-Pho animals regarding their mean number of capillaries supplying TC muscle fibers, but they decreased this number by 15%–20% ($P<0.05$ – $P<0.001$), compared with So-Sd subjects.

So-Pho also decreased the number of capillaries surrounding TC muscle fibers by 16% ($P<0.01$), compared with So-Sd rats.

Multivariate analysis. To summarize quantitatively the degree of similarity or discrepancy between skeletal muscle phenotypes of the five experimental groups, a discriminant analysis was conducted with data available for each muscle. The following variables were included in the discriminant model: muscle weight, MSI, fiber-type percentage, mean CSA, nuclear density, SDH-to-GPDH enzyme ratio, and capillarity of muscle fibers. Data were restricted to type I fibers in the SOL muscle and to type IIA, IIX, IIXB and IIB fibers in the TC. With these parameters, 46/60 (77%) and 57/60 (95%) observations (muscle samples) of the SOL and TC muscle,



▲ **Fig. 5.2** Cross-sectional area (A), number of nuclei per fiber (B), succinate dehydrogenase (SDH)–to–glycerol–3–phosphate dehydrogenase (GPDH) enzyme ratio (C), and number of capillaries per fiber (D) of all muscle fibers (without fiber–type specification) of soleus and tibialis cranialis muscles of the five experimental groups (So–Sd=sham–operated standard diet, So–Pho=sham–operated high phosphorus diet, Nx–Sd=5/6 nephrectomy standard diet, Nx–Pho=5/6 nephrectomy high phosphorus diet, Nx–Pho+Cal=5/6 nephrectomy high phosphorus diet plus calcitriol). Values are means \pm SE; a.u.=arbitrary units; means with different letters are statistically different ($P<0.05$, at least)

respectively, were correctly discriminated in their respective experimental groups. The Mahalanobis distances between group pairs and their significances are

depicted in **Fig. 5.3**. These coefficients highlight the similarities or differences of the overall phenotypic features of each muscle between groups. The two control

Effect of hyperphosphatemia and calcitriol on skeletal muscle in uremia

Table 5.4 Muscle fiber-type metabolic profile and capillarity

Fiber-type	So-Sd	So-Pho	Nx-Sd	NxPho	Nx-Pho+Cal	<i>P</i> values
Succinate dehydrogenase-to-glycerol-3-phosphate dehydrogenase ratio, arbitrary units						
M. soleus						
I	2.11±0.05 c	2.13±0.07 c	1.69±0.07 ab	1.67±0.03 a	1.86±0.08 b	<i>P</i> =0.000
M. tibialis cranialis						
IIA	2.15±0.10 c	2.25±0.07 c	1.79±0.10 b	1.41±0.05 a	1.75±0.07 b	<i>P</i> =0.000
IIIX	1.40±0.08 b	1.49±0.10 b	1.37±0.05 b	1.15±0.08 a	1.44±0.05 b	<i>P</i> <0.05
IIIXB	1.16±0.06 b	1.07±0.06 b	0.86±0.02 a	0.75±0.07 a	0.81±0.02 a	<i>P</i> <0.001
IIIB	0.92±0.04 c	0.93±0.03 c	0.78±0.02 b	0.61±0.02 a	0.75±0.02 b	<i>P</i> =0.000
Muscle fiber-type number of capillaries per fiber, capillaries fib ⁻¹						
M. soleus						
I	7.42±0.49ab	6.46±0.38 a	6.42±0.37 a	7.29±0.28ab	7.87±0.32 b	<i>P</i> <0.05
M. tibialis cranialis						
IIA	4.75±0.28 b	4.02±0.26 a	3.80±0.15 a	3.80±0.12 a	3.98±0.16 a	<i>P</i> <0.01
IIIX	5.27±0.27 b	4.05±0.19 a	4.10±0.17 a	3.90±0.22 a	4.01±0.20 a	<i>P</i> <0.001
IIIXB	5.21±0.25 b	4.17±0.17 a	4.14±0.23 a	4.05±0.13 a	4.20±0.25 a	<i>P</i> <0.01
IIIB	5.65±0.36 b	4.77±0.27 a	4.86±0.23 a	4.55±0.15 a	4.76±0.28 a	<i>P</i> =0.05

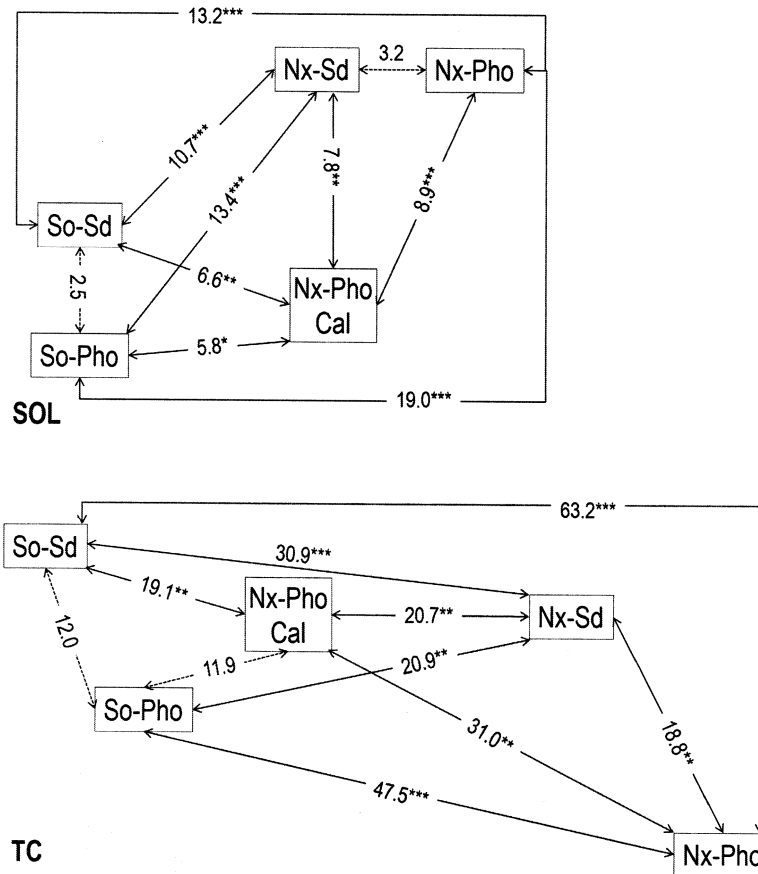
See **Table 5.1**'s legend for keys. For clarity, muscle fiber-types with a percentage below 5% are excluded from this analysis

groups (So-Sd and So-Pho) were comparable regarding their SOL and TC muscle phenotypes (*P*>0.05). Ample differences were noted, however, between the three Nx groups, particularly in the TC muscle. The Nx-Sd and Nx-Pho groups were comparable concerning their SOL phenotypes (*P*>0.05), but not regarding their TC muscle phenotypes (18.8, *P*<0.01). Nx-Sd rats showed lower distances than Nx-Pho subjects both in the SOL (10.7 vs 19.0, *P*<0.001 in both) and in the TC muscle (30.9 vs 46.5, *P*<0.001), compared with their respective So-Sd and So-Pho control groups. The distance between Nx-Pho+Cal and So-Pho groups was reduced in the SOL muscle (5.8, *P*<0.05) and both groups were comparable

regarding their TC muscle phenotypes (11.9, *P*>0.05). Thus, muscle characteristics of Nx-Pho+Cal rats were intermediate, but closer to those of the control So-Pho group than those of the Nx-Pho group, particularly in the TC muscle.

DISCUSSION

The present investigation is to our knowledge the first study to address the impact of high phosphate diet and calcitriol treatment on phenotypic characteristics of slow- and fast-twitch hind limb skeletal muscles in experimental uremia. The main findings were that, after 12 wk of Nx, 1) a diet with high phosphorus content



▲ **Fig. 5.3** Squared Mahalanobis distances between the five experimental groups (So-Sd=sham-operated standard diet, So-Pho=sham-operated high phosphorus diet, Nx-Sd=5/6 nephrectomy standard diet, Nx-Pho=5/6 nephrectomy high phosphorus diet, Nx-Pho+Cal=5/6 nephrectomy high phosphorus diet plus calcitriol) derivate by multivariate discriminant analysis on all fiber-type characteristics (fiber composition, size, metabolic profile, capillarity and nuclear density) of soleus (SOL, upper) and tibialis cranialis (TC, bottom) muscles. Asterisks denote significance of distances between groups: * $P < 0.05$, ** $P < 0.01$, *** $P < 0.001$

induced skeletal muscle changes of greater magnitude compared with a standard diet with lower phosphorus content, and 2) low-dose calcitriol resulted in muscle

phenotypes that were intermediate between Nx and So rats. Consequently, the authors' initial hypotheses were borne out.

The current data confirm that 12 wk of Nx induced skeletal muscle changes which were highly muscle-specific (1). In the entirely inactive at rest fast-twitch TC muscle, these changes were extensive and included slow-to-fast fiber type transformation, oxidative-to-glycolytic enzymatic conversion and impaired capillarity. In the primarily active at rest (providing antigravity support) slow-twitch SOL muscle, however, these changes were reduced to decreased oxidative-to-glycolytic enzymatic ratios, as well as to moderate increments in nuclear densities and capillary of myofibers. The significance and potential factors triggering these changes were discussed in a previous study by the authors' group (see Ref. 1).

Although similar in nature, skeletal muscle changes in uremic rats were found to be of greater magnitude in animals receiving a high-phosphorus diet than those fed with a standard diet. In quantitative terms, this was supported by the longer distances between Nx and So groups provided by the multivariate analysis in rats with a high phosphorus diet compared with rats receiving a standard diet (**Fig. 5.3**), as well as by the lower SDH-to-GPDH enzymatic ratios noted in Nx-Pho vs Nx-Sd groups (**Table 5.4**). Taken together, these data provide clear evidence that, in addition to its well-recognized role as a contributing factor of secondary HPT, vascular calcification, myocardial dysfunction and increased mortality (7), high phosphorus diet also seems to be an important factor maximizing the adverse effects of sustained uremia on skeletal muscle. The mechanisms underlying this additional effect are not clear. A direct effect of hyperphosphatemia on muscle is unlikely. However, feeding high phosphate diet resulted in changes in other parameters that may influence skeletal muscle. The parameter whose changes best correlated with the muscle alterations induced by high phosphorus diet was PTH. Moreover, treatment with calcitriol, in addition to attenuate the changes induced by uremia and high phosphorus diet (as discussed below), also decreased

PTH. Our data are in agreement with previous studies in which PTH has been reported to enhance muscle proteolysis, impair muscle bioenergetics and impair oxidation of long-chain fatty acids in chronic renal failure (50). Other studies have also suggested that high serum PTH levels may indicate a muscle impairment (20, 39, 42). It is therefore possible that direct effects of PTH on skeletal muscle may account in part for the muscle impairment observed in chronic uremic rats fed with a high-phosphorus diet. PTH is known to influence bicarbonate homeostasis, and metabolic alkalosis is a feature of hyperparathyroidism (31). In our rats a non-significant trend towards alkalosis was detected in the groups with higher PTH concentrations. It is likely that since the higher PTHs were observed in groups with renal failure the alkalotic trend may have been counteracted by the acidosis typically found in uremic individuals.

A remarkable finding of the present study was provided by the multivariate analysis performed, which using different markers of contractile, metabolic and morphological features of individual muscle fiber-types, clearly indicated that slow- and fast-twitch skeletal muscle phenotypes of Nx-Pho+Cal rats were different from those of Nx-Pho subjects, but they were closer to those of So-Pho rats, particularly in the TC muscle (**Fig. 5.3**). This result, together with the high percentage of correctly classified observations obtained in this analysis, provides solid evidence of the impact of calcitriol treatment on maintenance of skeletal muscle phenotypes in long-term uremic rats fed with a high-phosphate diet.

In agreement with present results in the tibialis cranialis muscle, evidence of slow-to-fast fiber-type transitions in the course of uremic myopathy has been reported in fast-twitch hind limb muscles of both humans and rats (36, 52). This adaptation has been related to multiple potential causes: neural deficit, carnitine deficiency, decreased physical activity, increased proinflammatory cytokines and different catabolic factors.

Also in agreement with present results in the soleus muscle, a fast-to-slow fiber-type switching has already been reported in trunk (postural rather than locomotor) muscles of 4 wk Nx rats (19). However, in disagreement with the present data, findings compatible with a fast-to-slow fiber-type transition have also been reported in the fast-twitch vastus lateralis muscle of human patients with CRF, being interpreted to be compensatory for the overall decrease in oxidative capacity (32, 34).

The results of the present study suggest that long-term uremic rats who received a high phosphorus diet plus low-dose active vitamin D treatment preserved their fiber-type composition, attenuated their uremia-induced oxidative-to-glycolytic metabolic conversion and showed a trend for increased size, nuclear density and capillarity of specific muscle fiber-types, compared to uremic rats with the same high-phosphorus diet not receiving calcitriol. These findings were not unexpected since vitamin D plays essential roles in regulating skeletal muscle function, metabolism and structure (23, 41). A few studies from the earliest literature provided evidence that vitamin D treatment seems to improve muscle function in CKD patients (8, 25, 28, 54). More recently, treatment with vitamin D was associated with greater muscle growth in patients on hemodialysis (26). Recent data indicate that adequate supplementation of calcitriol has beneficial effects on skeletal muscle that include improvements in myosin heavy chain expression (37), mitochondrial oxidative phosphorylation (49), fiber size through activation of protein synthesis (10, 24, 47, 51), myogenesis (22), and angiogenesis (21). These studies, that collectively lend support to our observations, suggest that vitamin D *per se* have multiple effects in skeletal muscle, playing a role in cellular and molecular processes involved in muscle contraction, metabolism, anabolism and structure, with far reaching effects on health and welfare.

In the present study, both muscle mass and the size of

individual muscle fiber types were unaffected by 12 wk of Nx in both muscles. However, a significant decrease (21%) in the mean area of type IIX muscle fibers was observed in the tibialis cranialis muscle of Nx rats feed with a high phosphorus diet. In accordance with the present results, no significant changes were reported in the size of muscle fiber types of 8 wk (6) and 4 wk (19) Nx rats. A tendency, which did not reach statistical significance, for a decreased size of IIB fibers was noted in the latter study (19). Also in agreements with the present results, in the Cy/+ rat model of progressive uremia, muscle mass resulted unaffected at 35 wk of age (38). However, these rats showed uniform atrophy of all muscle fiber types compared with their nonaffected littermates (38). Together, these findings suggest that impaired muscle fiber size seems to occur during the period of progression to the end-stage renal failure. However, muscle fiber is normalized or minimally decreased during the early stages of renal failure and/or when the renal failure is “stabilized” (30).

Evidence of slow-to-fast fiber-type transition was observed in the TC muscle of uremic rats that did not receive exogenous calcitriol, but not in uremic rats receiving calcitriol. This result suggests that vitamin D treatment counteracts the fiber-type switching in the direction I→IIA→IIX→IIB reported in fast-twitch hind limb muscles in the course of uremic myopathy (1, 5, 36, 52). In a small uncontrolled study, it was reported an increase in the percentage of type IIA fibers accompanied by a reduction of type IIB fibers in muscle biopsies from elderly women treated with calcitriol and calcium for 3–6 mo (51). Two other randomized controlled studies, found that vitamin D supplementation in older women, significantly increased the percentage of fast-twitch muscle fibers over a 2-yr period (47), but not after a 4–mo period (10). A tendency, that did not reach statistical significance ($P=0.067$), for a decreased proportion of type IIB fibers was also noted in the present study in the TC

muscle of Nx rats treated with calcitriol, compared with Nx rats not treated with calcitriol (see **Table 5.2**). Together, these data seem to indicate that calcitriol promotes a fiber-type switching in the direction from IIB toward IIA fibers, e.g., in the opposite direction that usually occurs in uremia (1).

Evidence for increased muscle mass and muscle fiber size in uremic rats treated with calcitriol was also observed in the present study. It is unlike that this effect could be attributed to improvement of kidney function because serum creatinine levels were only slightly decreased by calcitriol administration. Interestingly, this was accomplished by increments in the number of nuclei associated with individual muscle fibers, which is related with both protein synthesis and protein turnover rates (44). A retrospective cross-sectional study, also reported that treatment with active vitamin D was associated with greater muscle size and strength in patients on hemodialysis, suggesting a role of calcitriol in the preservation of muscle mass in this population (26). Support in the role of vitamin D in muscle growth stems from human studies reporting increased muscle fiber size associated with vitamin D supplementation (10, 47, 51). This relationship is corroborated by studies *in vitro*, by which myotubes are increased in diameter after treatment with calcitriol, potentially through an inhibitory effect of calcitriol on myostatin, a negative regulator of muscle mass (24). Recent studies clearly indicate that an adequate concentration of calcitriol might have an anabolic effect on differentiate skeletal muscle that enhances the expression of myosin heavy chain (37), and that skeletal muscle may indeed require VDR-mediated signaling for successful myoblast differentiation into myocytes, since silencing VDR the expression of myosin heavy chain and other contractile proteins is significantly decreased (53).

Our data also demonstrates that calcitriol treatment attenuates the oxidative-to-glycolytic metabolic conversion that occurs in muscle fibers of uremic rats

with a high-phosphorus diet. This effect resulted from a small reduction in SDH activity rather than from a great increment in GPDH activity in uremic rats treated with calcitriol in the present study (result not shown). To our knowledge this is the first description of the effect of vitamin D on skeletal muscle metabolism in uremic subjects. In vitamin D-deficient individuals, the therapy with the vitamin D analogue 1 α -hydroxycholecalciferol increased significantly the activities of muscle oxidative enzymes (51) and post-exercise muscle mitochondrial oxidative phosphorylation, as assessed by NMR spectrophotometry (49). The precise basis for this effect is unclear, but several evidences support the notion that intracellular Ca²⁺ may be an important signaling molecule in the energy metabolism interplay of the cytosol with the mitochondria, and that vitamin D may therefore play a relevant role in Ca²⁺ uptake by the mitochondria which in turn are involved in the orchestration of cellular metabolic homeostasis (discussed in Ref. 49).

The present study also provides evidence that supplementation of calcitriol to uremic rats improved the number of capillaries contacting muscle fibers in the postural SOL muscle but not in the fast-twitch TC muscle. Recent data show that postural skeletal muscles, with abundant oxidative fibers and increased expression of inducible nitric oxide synthase and hypoxia inducible factor 1 α , seems to be more resistant to hypoxia-induced disturbances of uremia than locomotor muscles, explaining observed differences between muscles in capillary rarefaction (1, 17). To our knowledge there is a lack of studies addressing the impact of calcitriol treatment on capillarity of uremic muscles. However, a recent study show solid evidence that the addition of calcitriol to cultured skeletal muscle cells promotes not only myogenesis, but also neo-vascularization by increasing the expression of key angiogenic growth factors and decreasing angiogenic inhibitors (21).

Strengths of this study include the long duration (12

wk) of the Nx model used to induce uremia, which allows the characterization of skeletal muscle phenotypes during the period of ‘stable’ renal failure. The low dose of calcitriol used effectively attenuated skeletal muscle changes in uremic rats, minimizing the risk of other adverse systemic effects of high dose of calcitriol in patients with advanced CKD such as adynamic bone disease (35) and vascular calcifications (29). The sample size used was sufficient to detect small effects on muscle fiber-type characteristics. It is noteworthy that this study identified not only components of the contractile machinery (i.e., MHC-based fiber-types) as sensitive markers of changes in skeletal muscle in response to different treatments, but also components of muscle mass (cross-sectional size), muscle protein turnover (nuclear density), energy metabolism (oxidative-glycolytic balance) and capillarity on a fiber-to-fiber basis by using histochemical methods with high analytical precision. As a consequence, the multivariate analysis performed allowed quantitative comparisons between groups according to their overall skeletal muscle phenotypes based upon the analysis of diverse markers of contractile, metabolic and morphological properties of their constituent fiber-types.

A weakness of this study was the lack of objective data on physical activity of the animals, since a diminished physical activity of Nx vs So rats could be a contributing factor explaining some obtained differences in muscle fiber-type characteristics between the two groups. Nevertheless, by subjective evaluation, daily physical activity seemed to be similar in both groups.

Conclusion

The study provided evidence that hyperphosphatemia maximized skeletal muscle changes in 12 wk uremic rats, including a consistent slow-to-fast fiber-type transformation, selective atrophy, diminished myonuclear domain size, impaired oxidative-to-glycolytic enzyme

ratio and capillary rarefaction of muscle fibers. Our results also demonstrated that low dose of calcitriol (10 ng kg⁻¹, 3 d wk⁻¹, ip) attenuated significantly adverse skeletal muscle changes in uremic rats receiving a diet with high phosphorus content for 12 wk. This action, which was more profound in the fast-twitch TC muscle than in the slow-twitch SOL muscle, included preservation of muscle fiber-type composition, discrete hypertrophy, enlarged myonuclear domain size, enhanced oxidative-to-glycolytic metabolic balance and neo-vascularization of muscle fibers.

GRANTS

The work reported here was supported by a Spanish Government Grant from the Instituto de Salud Carlos III (PI14/00467) (PI 14/00386) with co-financing from European Funds. L.M.A., V.E.Ch. and J.L.L.R. were supported by grants of the PAI Group CTS-179 and Project P10-AGR-5963, Junta de Andalucía, Spain.

DISCLOSURES

None of the authors of this paper has a financial or personal relationship with other people or organisation that could inappropriately influence or bias the content of the paper.

AUTHOR CONTRIBUTIONS

L.M.A., I.L., M.R., E.A.-T., and J.-L.L.R. conception and design of research. L.M.A., V.E.Ch., and J.-L.L.R. revised the literature. L.M.A., A.P.-R., C.P. and I.L. performed experiments and surgery. L.M.A., V.E.Ch., C. P. and J.-L.L.R. performed analyses. L.M.A., I.L., M.R., E.A.-T., and J.-L.L.R. analyzed data and interpreted results. L.M.A., A.P.-R., V.E.Ch. and J.-L.L.R. prepared tables and figures. L.M.A., E.A.-T., and J.-L.L.R. drafted manuscript. All authors edited and revised critically the manuscript and approved its final version.

REFERENCES

1. **Acevedo LM, Peralta-Ramirez A, Lopez I, Chamizo VE, Pineda C, Rodriguez-Ortiz ME, Rodriguez M, Aguilera-Tejero E, and Rivero JL.** Slow- and fast-twitch hindlimb skeletal muscle phenotypes 12 wk after (5/6) nephrectomy in Wistar rats of both sexes. *Am J Physiol Ren Physiol* 309: F638-647, 2015.
2. **Acevedo LM, and Rivero JL.** New insights into skeletal muscle fibre types in the dog with particular focus towards hybrid myosin phenotypes. *Cell Tis Res* 323: 283-303, 2006.
3. **Adams GR, and Vaziri ND.** Skeletal muscle dysfunction in chronic renal failure: effects of exercise. *Am J Physiol Ren Physiol* 290: F753-761, 2006.
4. **Adams GR, Zhan CD, Haddad F, and Vaziri ND.** Voluntary exercise during chronic renal failure in rats. *Med Sci Sports Exer* 37: 557-562, 2005.
5. **Ahonen RE.** Light microscopic study of striated muscle in uremia. *Acta Neuropathol* 49: 51-55, 1980.
6. **Amann K, Neimeier KA, Schwarz U, Tornig J, Matthias S, Orth SR, Mall G, and Ritz E.** Rats with moderate renal failure show capillary deficit in heart but not skeletal muscle. *Am J Kid Dis* 30: 382-388, 1997.
7. **Bardin T.** Musculoskeletal manifestations of chronic renal failure. *Cur Opin Rheumatol* 15: 48-54, 2003.
8. **Bertoli M, Luisetto G, Arcuti V, and Urso M.** Uremic myopathy and calcitriol therapy in CAPD patients. *ASAIO Transactions* 37: M397-M398, 1991.
9. **Bundschu HD, Pfeilsticker D, Matthews C, and Ritz E.** Myopathy in experimental uremia. *Res Exp Med* 165: 205-212, 1975.
10. **Ceglia L, Niramitmahapanya S, da Silva Morais M, Rivas DA, Harris SS, Bischoff-Ferrari H, Fielding RA, and Dawson-Hughes B.** A randomized study on the effect of vitamin D(3) supplementation on skeletal muscle morphology and vitamin D receptor concentration in older women. *J Clin Endocrinol Metabol* 98: E1927-1935, 2013.
11. **Conjard A, Ferrier B, Martin M, Caillette A, Carrier H, and Baverel G.** Effects of chronic renal failure on enzymes of energy metabolism in individual human muscle fibers. *J Am Soc Nephrol* 6: 68-74, 1995.
12. **Delp MD, and Duan C.** Composition and size of type I, IIA, IID/X, and IIB fibers and citrate synthase activity of rat muscle. *J Appl Physiol* 80: 261-270, 1996.
13. **Diesel W, Emms M, Knight BK, Noakes TD, Swanepoel CR, van Zyl Smit R, Kaschula RO, and Sinclair-Smith CC.** Morphologic features of the myopathy associated with chronic renal failure. *Am J Kid Dis* 22: 677-684, 1993.
14. **Durozard D, Pimmel P, Baretto S, Caillette A, Labeeuw M, Baverel G, and Zech P.** ³¹P NMR spectroscopy investigation of muscle metabolism in hemodialysis patients. *Kid Internat* 43: 885-892, 1993.
15. **Edwards RM.** Disorders of phosphate metabolism in chronic renal disease. *Cur Opin Pharmacol* 2: 171-176, 2002.
16. **Fahal IH, Bell GM, Bone JM, and Edwards RH.** Physiological abnormalities of skeletal muscle in dialysis patients. *Nephrol Dial Transplant* 12: 119-127, 1997.
17. **Flisinski M, Brymora A, Bartlomiejczyk I, Wisniewska E, Golda R, Stefanska A, Paczek L, and Manitius J.** Decreased hypoxia-inducible factor-1alpha in gastrocnemius muscle in rats with chronic kidney disease. *Kid Blood Pres Res* 35: 608-618, 2012.
18. **Flisinski M, Brymora A, Elminowska-Wenda G, Bogucka J, Walasik K, Stefanska A, Odrowaz-Sypniewska G, and Manitius J.** Influence of different stages of experimental chronic kidney disease on rats locomotor and postural skeletal muscles microcirculation. *Ren Fail* 30: 443-451, 2008.
19. **Flisinski M, Brymora A, Elminowska-Wenda G, Bogucka J, Walasik K, Stefanska A, Strozecki P, and Manitius J.** Morphometric analysis of muscle fibre types in rat locomotor and postural skeletal

- muscles in different stages of chronic kidney disease. *J Physiol Pharmacol* 65: 567-576, 2014.
20. **Garber AJ.** Effects of parathyroid hormone on skeletal muscle protein and amino acid metabolism in the rat. *J Clin Invest* 71: 1806-1821, 1983.
 21. **Garcia LA, Ferrini MG, Norris KC, and Artaza JN.** 1,25(OH)(2)vitamin D(3) enhances myogenic differentiation by modulating the expression of key angiogenic growth factors and angiogenic inhibitors in C(2)C(12) skeletal muscle cells. *J Ster Biochem Mol Biol* 133: 1-11, 2013.
 22. **Garcia LA, King KK, Ferrini MG, Norris KC, and Artaza JN.** 1,25(OH)2vitamin D3 stimulates myogenic differentiation by inhibiting cell proliferation and modulating the expression of promyogenic growth factors and myostatin in C2C12 skeletal muscle cells. *Endocrinology* 152: 2976-2986, 2011.
 23. **Girgis CM, Clifton-Bligh RJ, Hamrick MW, Holick MF, and Gunton JE.** The roles of vitamin D in skeletal muscle: form, function, and metabolism. *Endocrine Rev* 34: 33-83, 2013.
 24. **Girgis CM, Clifton-Bligh RJ, Mokbel N, Cheng K, and Gunton JE.** Vitamin D signaling regulates proliferation, differentiation, and myotube size in C2C12 skeletal muscle cells. *Endocrinology* 155: 347-357, 2014.
 25. **Gomez-Fernandez P, Sanchez Agudo L, and Calatrava JM.** [Chronic kidney insufficiency and respiratory muscle function. Changes induced by treatment with 1,25(OH)2D3]. *Med Clin* 94: 204-207, 1990.
 26. **Gordon PL, Sakkas GK, Doyle JW, Shubert T, and Johansen KL.** Relationship between vitamin D and muscle size and strength in patients on hemodialysis. *J Ren Nutr* 17: 397-407, 2007.
 27. **Graziotti GH, Rios CM, and Rivero JL.** Evidence for three fast myosin heavy chain isoforms in type II skeletal muscle fibers in the adult llama (*Lama glama*). *J Histochem Cytochem* 49: 1033-1044, 2001.
 28. **Henderson RG, Russell RG, Ledingham JG, Smith R, Oliver DO, Walton RJ, Small DG, Preston C, and Warner GT.** Effects of 1,25-dihydroxycholecalciferol on calcium absorption, muscle weakness, and bone disease in chronic renal failure. *Lancet* 1: 379-384, 1974.
 29. **Henley C, Colloton M, Cattley RC, Shatzen E, Towler DA, Lacey D, and Martin D.** 1,25-Dihydroxyvitamin D3 but not cinacalcet HCl (Sensipar/Mimpara) treatment mediates aortic calcification in a rat model of secondary hyperparathyroidism. *Nephrol Dial Transplantation* 20: 1370-1377, 2005.
 30. **Holecek M.** Muscle wasting in animal models of severe illness. *Int J Exp Pathol* 93: 157-171, 2012.
 31. **Hulter HN, Toto RD, Ilnicki LP, Halloran B, and Sebastian A.** Metabolic alkalosis in models of primary and secondary hyperparathyroid states. *Am J Physiol Ren Physiol* 245: F450-461, 1983.
 32. **Kouidi E, Albani M, Natsis K, Megalopoulos A, Gigis P, Guiba-Tziampiri O, Tourkantonis A, and Deligiannis A.** The effects of exercise training on muscle atrophy in haemodialysis patients. *Nephrol Dial Transplant* 13: 685-699, 1998.
 33. **Larsson L, and Skogsberg C.** Effects of the interval between removal and freezing of muscle biopsies on muscle fiber size. *J Neurol Sci* 85: 27-38, 1988.
 34. **Lewis MI, Fournier M, Wang H, Storer TW, Casaburi R, Cohen AH, and Kopple JD.** Metabolic and morphometric profile of muscle fibers in chronic hemodialysis patients. *J Appl Physiol* 112: 72-78, 2012.
 35. **Malluche HH, Mawad H, and Koszewski NJ.** Update on vitamin D and its newer analogues: actions and rationale for treatment in chronic renal failure. *Kid Int* 62: 367-374, 2002.
 36. **Molsted S, Eidemak I, Sorensen HT, Kristensen JH, Harrison A, and Andersen JL.** Myosin heavy-

- chain isoform distribution, fibre-type composition and fibre size in skeletal muscle of patients on haemodialysis. *Scand J Urol Nephrol* 41: 539-545, 2007.
37. **Okuno H, Kishimoto KN, Hatori M, and Itoi E.** 1alpha,25-dihydroxyvitamin D(3) enhances fast-myosin heavy chain expression in differentiated C2C12 myoblasts. *Cell Biol Inte* 36: 441-447, 2012.
38. **Organ JM, Srisuwananukorn A, Price P, Joll JE, Biro KC, Rupert JE, Chen NX, Avin KG, Moe SM, and Allen MR.** Reduced skeletal muscle function is associated with decreased fiber cross-sectional area in the Cy/+ rat model of progressive kidney disease. *Nephrol Dial Transplant* 0:1-8, 2015.
39. **Passeri E, Bugiardini E, Sansone VA, Valaperta R, Costa E, Ambrosi B, Meola G, and Corbetta S.** Vitamin D, parathyroid hormone and muscle impairment in myotonic dystrophies. *J Neurol Sci* 331: 132-135, 2013.
40. **Peter JB, Barnard RJ, Edgerton VR, Gillespie CA, and Stempel KE.** Metabolic profiles of three fiber types of skeletal muscle in guinea pigs and rabbits. *Biochem* 11: 2627-2633, 1972.
41. **Pojednic RM, and Ceglia L.** The emerging biomolecular role of vitamin D in skeletal muscle. *Exer Sport Sci Rev* 42: 76-81, 2014.
42. **Ritz E, Boland R, and Kreusser W.** Effects of vitamin D and parathyroid hormone on muscle: potential role in uremic myopathy. *Am J Clin Nutr* 33: 1522-1529, 1980.
43. **Rivero JL, Talmadge RJ, and Edgerton VR.** Interrelationships of myofibrillar ATPase activity and metabolic properties of myosin heavy chain-based fibre types in rat skeletal muscle. *Histochem Cell Biol* 111: 277-287, 1999.
44. **Roy RR, Monke SR, Allen DL, and Edgerton VR.** Modulation of myonuclear number in functionally overloaded and exercised rat plantaris fibers. *J Appl Physiol* 87: 634-642, 1999.
45. **Sakkas GK, Ball D, Mercer TH, Sargeant AJ, Tolfrey K, and Naish PF.** Atrophy of non-locomotor muscle in patients with end-stage renal failure. *Nephrol Dial Transplant* 18: 2074-2081, 2003.
46. **Saliba W, and El-Haddad B.** Secondary hyperparathyroidism: pathophysiology and treatment. *J Am Board Fam Med* 22: 574-581, 2009.
47. **Sato Y, Iwamoto J, Kanoko T, and Satoh K.** Low-dose vitamin D prevents muscular atrophy and reduces falls and hip fractures in women after stroke: a randomized controlled trial. *Cerebrovasc Dis* 20: 187-192, 2005.
48. **Schiaffino S, Gorza L, Sartore S, Saggin L, Ausoni S, Vianello M, Gundersen K, and Lomo T.** Three myosin heavy chain isoforms in type 2 skeletal muscle fibres. *J Mus Res Cell Motil* 10: 197-205, 1989.
49. **Sinha A, Hollingsworth KG, Ball S, and Cheetham T.** Improving the vitamin D status of vitamin D deficient adults is associated with improved mitochondrial oxidative function in skeletal muscle. *J Clin Endocrinol Metabol* 98: E509-513, 2013.
50. **Smogorzewski M, Piskorska G, Borum PR, and Massry SG.** Chronic renal failure, parathyroid hormone and fatty acids oxidation in skeletal muscle. *Kid Int* 33: 555-560, 1988.
51. **Sorensen OH, Lund B, Saltin B, Andersen RB, Hjorth L, Melsen F, and Mosekilde L.** Myopathy in bone loss of ageing: improvement by treatment with 1 alpha-hydroxycholecalciferol and calcium. *Clin Sci* 56: 157-161, 1979.
52. **Taes YEC, Speeckaert M, Bauwens E, De Buyzere MR, Libbrecht J, Lameire NH, and Delanghe JR.** Effect of dietary creatine on skeletal muscle myosin heavy chain isoform expression in an animal model of uremia. *Neph Exp Nephrol* 96: e103-e110, 2004.
53. **Tanaka M, Kishimoto KN, Okuno H, Saito H, and Itoi E.** Vitamin D receptor gene silencing effects on differentiation of myogenic cell lines. *Muscle Nerve* 49: 700-708, 2014.
54. **Wanic-Kossowska M, Grzegorzewska A, Plotast H, and**

Chapter 5

Bombicki K. Does calcitriol therapy improve muscle function in uremic patients. *Perit Dial Int* 16 Suppl 1:

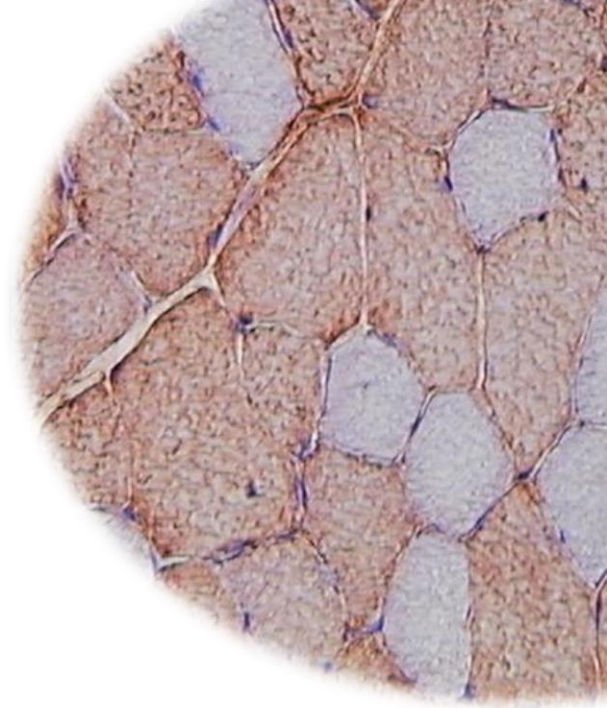
S305-308, 1996.

55. **Wuthrich RP, Martin D, and Bilezikian JP.** The role of

calcimimetics in the treatment of hyperparathyroidism. *Europ J Clin Invest* 37: 915-922, 2007.

CHAPTER 6

Obesity-induced muscle mass reduction and fast phenotype occur with increased oxidative capacity in red and white rat skeletal muscles



Skeletal muscle changes in obesity

Luz M. Acevedo^{1,3}, Ana I. Raya², Rafael Ríos²,
Escolástico Aguilera–Tejero^{2,+}, and José–Luis L.
Rivero^{1,*,+}

¹Laboratory of Muscular Biopathology, Department of
Comparative Anatomy and Pathological Anatomy,
University of Cordoba, 14014 Cordoba, Spain

²Department of Animal Medicine and Surgery, University
of Cordoba, 14014 Cordoba, Spain and Instituto
Maimonides de Investigación Biomédica de Cordoba
(IMIBIC), Hospital Universitario Reina Sofia, University
of Cordoba, Cordoba, Spain

³Departamento de Ciencias Biomédicas, Universidad
Central de Venezuela, Maracay, Venezuela

⁺These authors contributed equally to this work

Histochem Cell Biol (under revision), 2016

ABSTRACT

A clear picture of skeletal muscle adaptations to obesity and related comorbidities remains elusive. This study describes fibre-type adaptations (size, proportions and oxidative capacity) in hind limb muscles in an animal model of genetic obesity. Lesser diameter, fibre composition, and histochemical succinic dehydrogenase activity (an oxidative marker) of muscle fibre types were assessed in red (soleus) and white (tibialis cranialis) muscles of obese Zucker rats, and compared with age- (16 weeks) and sex-matched (females) lean Zucker rats (n=20/group). Muscle mass and lesser fibre diameter were lower in both muscles of obese compared with lean animals, even though body weights were increased in the obese cohort. A faster fibre-type phenotype also occurred in red and white muscles of obese subjects, compared with lean rats. These adaptations were accompanied by a generalized increment in oxidative capacity of all fibre-types in the two muscles. These data demonstrate that obesity induces a muscle-unspecific inhibition of muscle growth in which muscle fibres retain a reduced fibre size and show a faster and more oxidative phenotype. It was noteworthy that these adaptations were of comparable nature and extent in red and white muscles, indicating that the influence of obesity on muscle phenotype is unspecific in regards to muscle structure and function.

Keywords Muscle fiber type, muscle mass, muscle oxidative capacity, obesity, metabolic syndrome

INTRODUCTION

A growing interest in the association between changes in skeletal muscle and obesity has emerged in recent years, particularly in the face of the impending world-wide diabetes and metabolic syndrome epidemics (Petersen et al. 2007; Zimmet et al. 2001). It is essential to understand how skeletal muscle dysfunction contributes to obesity and related conditions, but it is also important to know how these comorbidities affect the muscles themselves.

From this perspective, obesity provides a model to examine how systematic metabolic and endocrine disturbances influence skeletal muscle structure and function (Denies et al. 2014).

There is now ample evidence showing that skeletal muscle is heavily impacted by obesity and other associated conditions like metabolic syndrome, insulin resistance and diabetes. Several studies over the past 20 years have described different abnormalities in skeletal muscle structure and function in human and animal models of obesity, but many of these studies provide inconsistent findings. For example, muscle atrophy is considered a hallmark of obesity and associated conditions (Argiles et al. 1999; Paturi et al. 2010; Perry et al. 2016; Peterson et al. 2008; Pompeani et al. 2014; Reeds et al. 1982), but several studies have shown that skeletal muscle mass is either unaltered (Adachi et al. 2007; Denies et al. 2014; Malenfant et al. 2001; Yasuda et al. 2006; Ringseis et al. 2013; Yasuda et al. 2002) or increased (Shortreed et al. 2009; Turpin et al. 2009) in obese subjects. Furthermore, the obesity-induced slow-to-fast muscle fibre-type transformation has been related with a change of the muscle's metabolic phenotype. An impaired mitochondrial oxidative enzyme capacity (Couturier et al. 2014; Ringseis et al. 2013; Wessels et al. 2015) and microvascular rarefaction (Frisbee et al. 2014) have been reported in muscle from obese people and animals. However, other studies in patients with Type 2 diabetes and obese rats reveal results compatible with either unaltered (Adachi et al. 2007; Couturier et al. 2014; Yasuda et al. 2006; Yasuda et al. 2002) or increased (Holloway et al. 2009a; Holloway et al. 2009b; Lally et al. 2012; Oberbach et al. 2006; Turner et al. 2007) mitochondrial density and oxidative enzyme activities in skeletal muscles.

A central event in obesity and related conditions is an increased intramuscular lipid accumulation (Korach-Andre et al. 2005; Lally et al. 2012; Malenfant et al.

2001), that results from a decreased rate of fatty acid oxidation (Kelley et al. 2002) and/or an increased rate of fatty acid transport into skeletal muscle (Chabowski et al. 2006; Holloway et al. 2009a; Holloway et al. 2009b). On the other hand, the increase in mitochondrial content and mitochondrial fatty acid oxidation reported in obese animals (Holloway et al. 2009a; Holloway et al. 2009b; Lally et al. 2012), should lead to increased capacity for fatty acid oxidation. However, intramuscular lipid accumulation occurs at much greater rate than the compensatory increase in both mitochondrial density and the rate of mitochondrial fatty acid oxidation (Holloway et al. 2009a).

It is also noteworthy that these changes in muscle oxidative capacity seem to occur only in red, not white, muscles of obese animals (Chabowski et al. 2006; Holloway et al. 2009a; Lally et al. 2012). The lower malleability in white versus red muscles in obese subjects has been related to differences in physiological roles between these two muscle profiles (Chabowski et al. 2006; Holloway et al. 2009a). Red muscles (composed primarily of slow-oxidative fibres) are tonically active at rest to provide continued postural (antigravitatory) support and have high energetic dependence on blood borne substrates. By contrast, white muscles (composed primarily of fast-glycolytic fibres) are designed to develop rapid and explosive bursts of movements that rely heavily on intramuscular glycogen, rather than on blood borne substrates (Delp and Duan 1996).

Obesity- and diabetes-induced changes in fibre types towards fast phenotype has been explained by downregulation of peroxisome proliferator activated receptors (PPAR), such as PPAR γ and coactivator-1 α PGC1 α (Couturier et al. 2014). These receptors are critical regulators of fibre-type composition and mitochondrial biogenesis (Ehrenborg and Krook 2009; Rasbach et al. 2010). These receptors are typically higher expressed in slow-oxidative type I muscle fibres than in

fast-glycolytic type II muscle fibres (Evans et al. 2004).

Taken together, data in the literature do not support the notion that mitochondrial oxidative capacity is reduced in muscles of obese and diabetic rodent models compared to lean models, as previously documented (Ringseis et al. 2013; Wessels et al. 2015).

The variability in results from previous studies likely stem from differences in experimental designs and methodological limitations. In any case, a solid picture of how obesity and related conditions affect muscle mass, and contractile and metabolic phenotypes of skeletal muscles remains to be established. In the current study, we were interested in clarify how obesity affects skeletal muscle mass and muscle fibre types, with particular focus on muscle oxidative capacity. Our hypothesis was that obesity-induced muscle mass reduction and fast phenotype occur in parallel with increased mitochondrial oxidative capacity. These obesity-induced muscle features should be accompanied by compatible changes in protein levels of PPAR γ and PGC1 α receptors. In addition, we hypothesized that muscle changes should be more pronounced in the red soleus muscle than in the white tibialis cranialis muscle. As an experimental model we used obese Zucker rats, a well-established genetic model of obesity, insulin resistance and metabolic syndrome (Bray 1977). Lean Zucker rats served as non-obese controls.

MATERIALS AND METHODS

Ethics

All experimental protocols were reviewed and approved by the Ethics Committee for Animal Research of the University of Cordoba (Cordoba, Spain). They followed the guidelines laid down by the Higher Council of Scientific Research of Spain following the normal procedures directing animal welfare (Real Decreto 223/88, BOE of 18 of March) and adhered to the

recommendations included in the Guide for Care and Use of Laboratory Animals (US Department of Health and Human Services, NIH) and European laws and regulations on protection of animals, under the advice of specialized personnel.

Animals

Two strains of rats were used in this study: Zucker rats with the obese (*fa/fa*) phenotype ($n=20$) and Zucker rats with the lean (*Fa/Fa* or *Fa/fa*) phenotype ($n=20$). All rats were females and aged 4 months when they were euthanized. Since previous studies have demonstrated that sex plays a relevant role on skeletal muscle plasticity (Acevedo et al. 2015; Denies et al. 2014), rats of the same sex were used. Female rats were selected because the broader role that testosterone plays in the maintenance of skeletal muscle phenotype compared with estrogens and progestins (Welle et al. 2008). Animals (Harlan Laboratories Models, Barcelona, Spain) were individually housed in standard vivarium cages in a temperature- and humidity-controlled environment, with a 12:12-h light-dark cycle and given *ad libitum* access to standard rat diet (Altromin Spezialfutter GmbH, Germany; values per 100 g: energy 351.8 kcal 1100 kJ⁻¹, protein content 18%, lysine 1.74%, methionine 1.0%, cysteine 0.31%, tryptophan 0.20%, fat 5%, ash 4.5%, sodium 0.24%, calcium 0.6%, phosphorus 0.6%) and tap water. Food intake was recorded daily and the animals were weighed at the end of the experiment.

Blood biochemistry

Rats from both strains were sacrificed by aortic puncture and exsanguination under deep general anaesthesia (sodium thiopental 50 mg kg⁻¹, Pentotal®, Abbot, Illinois, USA; ip). Blood samples were obtained from the abdominal aorta in heparinized syringes at the time of the euthanasia. Plasma separated by centrifugation was used for measurements of glucose, cholesterol and

triglycerides levels by spectrophotometry (Biosystems, Barcelona, Spain), insulin and leptin concentrations by radioimmunoassay (Millipore, St. Charles, MO, USA), and fibroblastic growth factor 21 by ELISA (Millipore, St. Charles, MO, USA).

Muscle sampling and tissue preparation

Soleus and tibialis cranialis muscles were dissected and individual muscles were wet weighted. These muscles were selected as two representative muscles of a typical red muscle (soleus, composed primarily of slow-twitch muscle fibres) and a characteristic white muscle (tibialis cranialis, composed primarily of fast-twitch muscle fibres in its white region), respectively (Delp and Duan 1996). Also because these two hind limb muscles are opposite regarding their resting functional activities and energetic dependence on blood borne substrates (Delp and Duan 1996).

Upon collection, tissue blocks from the muscle belly were mounted on cork blocks with the use of OCT embedding medium (Tissue-Tek II, Miles Laboratories, Naperville, IL, USA) and oriented so that myofibres could be cut transversely. Specimens were systematically frozen by immersion in isopentane (30 seconds), kept at the freezing point in liquid nitrogen, and stored at -80 °C until analysed. Muscle samples were routinely frozen between 2 and 4 minutes after removal, because it has been demonstrated that the interval between removal and freezing has a significant (negative) effect on skeletal muscle fibre size (Larsson and Skogsberg 1988). In addition, a portion of muscle samples was immediately quenched in liquid nitrogen and used for muscle biochemical analysis. All muscle sampling and muscle preparation procedures were always carried out by the same investigator, experienced in skeletal muscle biopsy studies, taking care to standardize both the location and the freezing of the sample.

Myosin heavy chain (MHC) immunohistochemistry

Muscle samples were serially sectioned (10- μ m-thick) in a cryostat (Frigocut, Reichert Jung, Nubloch, Germany) at -20 °C and used for immunohistochemistry. Immunohistochemistry was performed with five monoclonal antibodies specific against MHC isoforms: BA-D5 (DMS, Braunschweig, Germany; anti-MHC-I), SC-71 (DMS; anti-MHC-IIa), BF-35 (DMS; anti-MHCs-I plus -IIa and -IIb), S5-8H2 (Biocytex Biotechnology, Marseille, France; anti-MHCs-I plus -IIx and -IIb), and BF-F3 (DMS; anti-MHC-IIb). The specificity of these monoclonal antibodies for MHCs in rat skeletal muscle has previously been reported (Acevedo et al. 2015; Schiaffino et al. 1989; Acevedo et al. 2016). The immunoperoxidase staining protocol with avidin-biotin complex (ABC) protocol was used as previously described (Rivero et al. 1999).

Quantitative enzyme histochemistry

Additional serial sections were used for quantitative enzyme histochemistry. The activity of the enzyme succinate dehydrogenase (SDH, EC 1.3.4.1), used as an oxidative marker, was determined on 10- μ m-thick sections, by using quantitative histochemical methods previously adjusted and validated in rat skeletal muscle (Rivero et al. 1999).

Image analysis and morphometry

Sections were examined in a blind fashion by the same investigator (L.M.A.), who had experience of the normal appearance of mammalian skeletal muscle fibres. All serial sections for immunohistochemistry and enzyme histochemistry were visualized and digitized as previously described (Acevedo and Rivero 2006). A region containing between 450 and 650 fibres was selected for further analyses. In the tibialis cranialis muscle, this area was selected from the core of the white (superficial) portion of the muscle, since it contains a

higher number of fast-twitch muscle fibres (98%) than the red (deep) portion (93%) of the muscle (Delp and Duan 1996). Images were saved as digitized frames at 256 grey levels. The grey levels were converted to optical density (OD) units by using a calibrated set of OD filters. The digitized images of the fibres in the histochemical reaction (SDH) within the selected region were traced manually and analysed for the lesser fibre diameter and the average OD for each individual muscle fibre. The average fibre OD for each histochemical reaction was determined as the average OD for all pixels within the traced fibre from three sections incubated with substrate minus the average OD for all pixels of the same fibre from other two sections incubated without substrate (Rivero et al. 1999). Because a number of factors can influence the reliability of histochemical enzyme activity determinations, we checked the variability on three consecutive sections for the SDH histochemical reaction by repeated measurements of the same individual fibres. Only coefficients of variation for triplicate measurements of ODs below 5% were accepted in the present study; this demonstrated the high analytical precision that can be achieved for the measurement of fibre OD on enzyme histochemical sections.

The fibres in the selected area were classified according to their MHC content by means of visual examination of immunostainings of the five serial sections stained with the battery of anti-MHC monoclonal antibodies as previously described (Acevedo et al. 2016; Acevedo et al. 2015). The reactivity of each individual muscle fibre in these five consecutive sections was judged as positive or negative by comparing the intensity of the reaction of neighbouring fibres. Seven fibre types were categorized, four of them as pure fibres expressing a unique MHC isoform (i.e., type I, IIA, IIX and IIB), and other three as hybrid phenotypes co-expressing two different MHC isoforms (type I+IIA, IIX and IIXB).

The relative frequency of different muscle fibre types in the selected region was used to numerically express the fibre type composition of each muscle sample. The lesser fibre diameter of the same fibres was averaged according to fibre type. Individual SDH ODs of muscle fibres were averaged according to the MHC muscle fibre–type and used for statistical analyses. For minor fibre types (I+IIA in the soleus muscle, and I, I+IIA and IIAX in the tibialis cranialis muscle), there were so few fibres in most muscle samples that a statistically reliable determination of their lesser diameter and SDH activities was impossible. In consequence, muscle fibre–types showing, on average, a fibre percentage below 5% were excluded from these analyses. A polymorphism index for obese and lean animals was calculated in each muscle by dividing the number of hybrid fibres expressing more than one MHC isoform by the total number of fibres in the muscle sample (Caiozzo et al. 2003).

Prediction of muscle shortening velocity

In an attempt to provide a functional assessment of the variation of myosin-based muscle fibre distribution on muscle's shortening speed, we used the following equation to predict the maximal shortening velocity (V_{\max} Muscle) of soleus and tibialis cranialis muscles (Caiozzo et al. 2003), according to the mathematical model proposed by A. V. Hill (Hill 1938):

$$V_{\max} \text{ Muscle} = \sum [\%_{ft} \times V_{\max ft}] / 100$$

where $\%_{ft}$ is the proportion of each fibre type in Muscle, and $V_{\max ft}$ is the maximal shortening velocity for a given fibre type (fibre length s^{-1}). Values from Bottinelli et al. (Bottinelli et al. 1991) were used for $V_{\max ft}$, and $V_{\max ft}$ of hybrid fibres were averaged between V_{\max} of their respective pure fibre-types.

Muscle biochemical analysis

The activity of the enzyme citrate synthase (CS, EC 4.1.3.7), a mitochondrial enzyme and marker of muscle oxidative potential, was measured from whole homogenates by using the fluorometric technique described elsewhere (Serrano et al. 2000). The activity of this enzyme was calculated in units of $\mu\text{mol NADH}$ converted per minute per gram of freeze-dried muscle.

Protein extraction and Western blot analysis.

Proteins were isolated from muscle tissue by using a lysis buffer containing HEPES (10 mmol/l), KCl (10 mmol/l), EDTA (0.1 mmol/l), EGTA (0.1 mmol/l), DTT (1 mmol/l), PMSF (0.5 mmol/l), protease inhibitor cocktail (70 $\mu\text{g/ml}$), and I-Gepal CA-630 (0.6%), pH 7.9 (Sigma Aldrich, St. Louis, MO). The suspension was centrifuged, and the supernatant (cytosolic extract) was stored. Nuclear extracts were obtained by incubating the pellet separated from the cytosolic extract in a lysis buffer containing HEPES (20 mmol/l), NaCl (0.4 mmol/l), EDTA (1 mmol/l), EGTA (1 mmol/l), dithiothreitol (1 mmol/l), PMSF (1 mmol/l), and protease inhibitor cocktail (46 mg/ml) at pH 7.9. Protein concentration was determined by Bradford method (Bio-Rad Laboratories, Munich, Germany). For Western Blot analysis, 50 μg of protein were electrophoresed on a 10% SDS-polyacrilamide gel (Invitrogen, Carlsbad, CA) and electrophoretically transferred (Transfer Systems, BioRad, Hercules, CA) from the gels onto nitrocellulose membranes (Invitrogen). The following steps were performed with gentle shaking. Membranes were incubated in TTBS-L solution [20 mM Tris-HCl (pH 6.6), 0.2% Tween 20, 150 mM NaCl] (Sigma Aldrich), and 5% nonfat dry milk (Bio-Rad) at room temperature for 2,5 hours to avoid nonspecific binding. Membranes were then washed with TTBS buffer (the same composition as TTBS-L without nonfat dry milk) and then incubated overnight at 4°C with a rabbit polyclonal anti-PGC-1 α

Skeletal muscle changes in obesity

Table 6.1 Plasma biochemistry of subjects

Variable	Lean	Obese	<i>P</i> value
Plasma glucose, mg dl ⁻¹	98.1 ± 8.1	181.5 ± 34.3	<0.001
Insulin, ng ml ⁻¹	2.2 ± 1.3	9.6 ± 2.8	0.005
Tryglycerides, mg dl ⁻¹	51.4 ± 12.1	635.4 ± 325.4	<0.001
Total colessterol, mg dl ⁻¹	61.6 ± 6.6	108.6 ± 18.9	0.004
Leptin, ng ml ⁻¹	4.9 ± 3.8	46.4 ± 19.3	<0.001
Fibroblastic growth factor 21, pg ml ⁻¹	397 ± 230	16,506 ± 12,140	<0.001

Values are means ± SD, n = 20 rats/group. Student's unpaired *t*-test was used to test for differences between groups and expressed as *P* values

Table 6.2 Body and muscle weights and muscle somatic index (MSI) of subjects

Variable	Lean	Obese	<i>P</i> value
Food intake, g d ⁻¹	14.8± 1.1	27.3± 0.8	0.03
Body weight, g	262.9± 42.6	505.4± 14.7	<0.001
M. soleus weight, mg	156.8± 19.0	137.5± 18.8	0.003
M. soleus MSI, mg g ⁻¹	0.6± 0.1	0.3± 0.0	<0.001
M. tibialis weight, mg	645.7± 86.3	550.1± 56.3	<0.001
M. tibialis MSI, mg g ⁻¹	2.5± 0.3	1.1± 0.1	<0.001

Values are means ± SD, n = 20 rats/group. Student's unpaired *t*-test was used to test for differences between groups and expressed as *P* values

antibody (1:500; AB3242, Millipore) or rabbit polyclonal anti-PPAR γ antibody (1:500; ab191407, Abcam). The membranes were then washed with TTBS buffer and immunolabeled using a peroxidase-conjugated secondary antibody (1:5000; Santa Cruz Biotechnology Inc). Finally, they were revealed on autoradiographic film using ECL Plus Western Blotting Detection System (GE Healthcare, Piscataway, NJ). Beta-Actin was used as housekeeping protein to ensure equal loading of the gels. Protein levels were quantified using ImageJ software (National Institutes of Health, Bethesda, MD).

Statistical analyses

All statistics and charts were run on Statistica 7.0 for

Windows (StatSoft I, Statistica, Data software System, www.statsoft.com). Muscle sample was the unit of analysis for the present dataset. A total of 80 muscle samples (40 animals x two muscles –soleus and tibialis cranialis) were available for statistical analysis. Sample size and the power of a contrast of hypothesis were estimated by power analysis and interval estimation of the statistical software employed. Accepting an α -risk of 0.05 and a β -risk of 0.2 in a one-sided test, 20 subjects/group were considered necessary to recognize as statistically significant a difference greater than or equal to 0.05 OD units for SDH histochemical activity. The common standard deviation (SD) was assumed to be 0.06 and it was anticipated a drop-out rate of -5%. Normality

Table 6.3 Mean lesser muscle fibre-type diameter, μm

Muscle	Fibre type	Lean	Obese	<i>P</i> values
M. soleus	I	63.9 \pm 10.1	50.7 \pm 4.0	<0.001
	IIA	53.1 \pm 10.4	44.8 \pm 5.5	0.004
	All fibre-types	62.9 \pm 9.9	50.0 \pm 4.1	<0.001
M. tibialis cranialis	IIA	39.5 \pm 8.4	32.1 \pm 3.7	0.001
	IIIX	46.0 \pm 8.5	36.8 \pm 4.9	<0.001
	IIIXB	50.0 \pm 9.5	35.1 \pm 4.6	<0.001
	IIIB	57.0 \pm 9.1	41.6 \pm 4.5	<0.001
	All fibre-types	48.4 \pm 8.3	34.6 \pm 4.0	<0.001

Values are means \pm SD, $n = 20$ rats/group. Student's unpaired *t*-test was used to test for differences between groups and expressed as *P* values. For clarity, muscle fibre-types with a percentage below 5% (see **Table 6.4**) are excluded from this analysis

of muscle variables was tested using a Kolmogorov–Smirnov test and data were expressed as means \pm SD. Two-tailed Student's unpaired *t*-test was used to test for differences between lean and obese rats, accepting a significant difference at $P < 0.05$.

RESULTS

Blood biochemistry

The obese Zucker phenotype was characterized by hyperglycemia, hyperinsulinemia, dyslipidemia and an increase in plasma adipokines when compared to lean controls (**Table 6.1**). Plasma glucose and insulin levels were two- and four-fold higher, respectively, in obese vs lean rats (**Table 6.1**). Significant increases in plasma concentrations of triglycerides, cholesterol, leptin and fibroblastic growth factor 21 were also observed in the obese cohort (**Table 6.1**).

Body and muscle weights

As expected, obese rats ate approximately twice as much and their body weight duplicated that of the lean

rats (**Table 6.2**). However, obese rats displayed significantly decreased skeletal muscle weights (soleus, 12%; tibialis, 15%) and muscle somatic indexes (soleus, 50%; tibialis, 56%) compared to lean rats (**Table 6.2**).

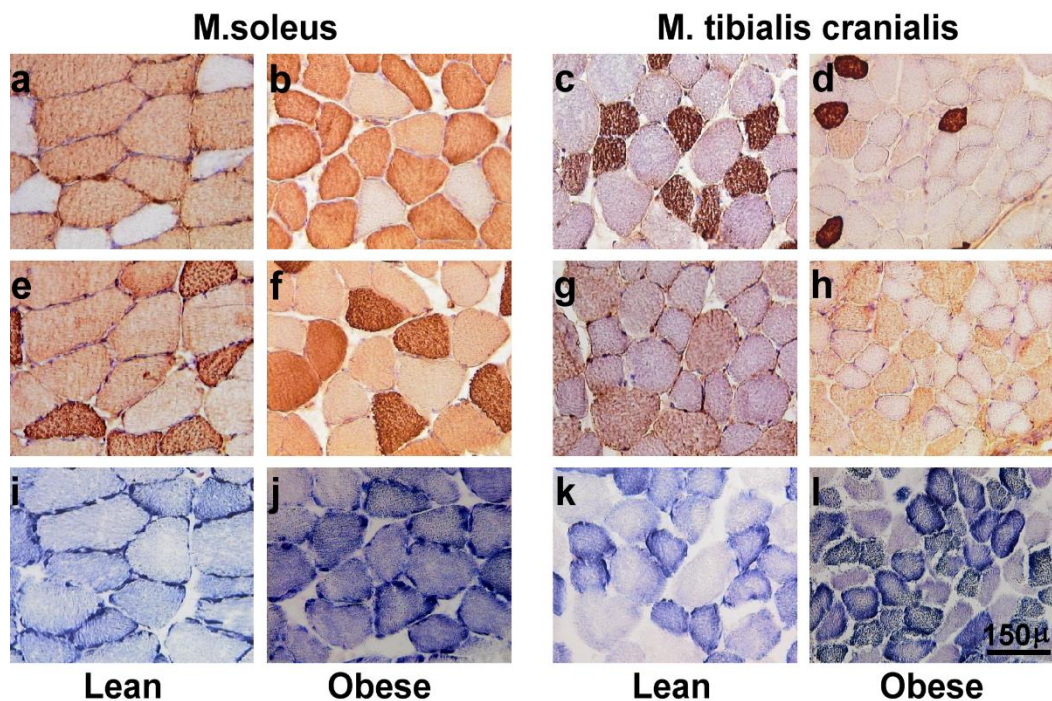
Muscle fibre size

The mean lesser diameter of muscle fibre types was estimated from obese and lean Zucker rats (**Table 6.3**). The lower muscle weights observed in the obese rats (**Table 6.2**) corresponded with a 21% and a 29% smaller mean lesser fibre diameters in soleus and tibialis cranialis muscles, respectively ($P < 0.001$ in both muscles), compared with lean controls (**Table 6.3; Fig. 6.1**). Obesity-induced muscle mass reduction affected all soleus and tibialis cranialis muscle fibre types. Soleus muscle fibres were larger than tibialis cranialis muscle fibres (**Table 6.3, Fig. 6.1**).

Muscle fibre-type composition

The muscle fibres of both soleus and tibialis cranialis muscles were classified based on their immunoreactions to antibodies against specific myosin heavy chain

Skeletal muscle changes in obesity



▲ **Fig. 6.1** Illustration of fibre-types in soleus and tibialis cranialis muscles of obese versus lean Zucker rats. Serial transverse sections of the soleus (left) and tibialis cranialis (right) muscles of representative lean (**a, e, i, c, g, and k**) and obese (**b, f, j, d, h and l**) Zucker rats stained for immunohistochemistry against specific anti-myosin heavy chain (MHC) monoclonal antibodies and succinic dehydrogenase (SDH) histochemistry. **a-h**: Sections were reacted with monoclonal antibodies against specific MHC isoforms: BA-D5 (**a-d**, anti MHC-I), SC-71 (**e-f**, anti MHC-IIa), and BF-F3 (**g-h**, anti MHC-IIb). **i-l**: Additional serial sections were stained for quantitative enzyme histochemistry of SDH activity. Note in the muscles from the Zucker obese rats, the smaller size of muscle fibres, the lower number of fibres expressing MHC-I, the abundance of fibres expressing either MHC-IIa (M. soleus) or MHC-IIb (M. tibialis cranialis), and the higher SDH staining, compared with the muscles from the Zucker lean rats.

isoforms. The proportions of seven fibre types (I, I+IIA, IIA, IIAX, IIX, IIXB, and IIB) were determined for both obese and lean rats. All these seven fibre types were

identified in the tibialis cranialis muscle, but only three fibre types (I, I+IIA, and IIA) were found in the soleus muscle.

Table 6.4 Muscle fibre-type composition, %

Muscle	Fibre type	Lean	Obese	<i>P</i> values
M. soleus	I	89.6± 7.6	83.1± 7.2	0.009
	I+IIA	1.5± 2.9	3.6± 3.3	0.03
	IIA	8.9± 5.9	13.3± 6.2	0.02
M. tibialis cranialis	I	4.7± 1.5	3.1± 2.8	0.03
	I+IIA	1.7± 0.4	0.9± 1.1	0.003
	IIA	27.9± 8.9	21.6± 8.1	0.02
	IIAX	4.0± 1.7	2.1± 2.3	0.007
	IIX	24.7± 8.5	18.6± 7.4	0.02
	IIXB	10.4± 12.0	18.5± 7.6	0.01
	IIB	26.6± 11.9	35.2± 14.0	0.03
Hybrid fibres	16.1± 11.7	20.3± 8.6	0.20	

Values are means ± SD, n = 20 rats/group. Student's unpaired *t*-test was used to test for differences between groups and expressed as *P* values

Obesity had a significant effect on soleus and tibialis cranialis muscle fibre-type distribution (**Table 6.4**). In the soleus muscle of Zucker rats with the obese phenotype, the slow-twitch type I fibre fraction was reduced by 7%, whereas the hybrid type I+IIA and the fast-twitch type IIA fibre fractions were increased by 140% and 49%, respectively, compared to the lean phenotype (**Fig. 6.1a-b** and **6.1e-f**). In the tibialis cranialis muscle of obese rats, proportions of type I (34%), I+IIA (47%), IIA (23%), IIAX (50%), and IIX (25%) fibres were decreased, and frequencies of type IIXB (78%) and IIB (32%) fibres were increased, when compared with lean controls (**Fig. 6.1c-d** and **6.1g-h**). The total relative number of hybrid fibres in the tibialis cranialis muscle did not differ significantly between obese and lean rats.

Prediction of whole muscle shortening velocity

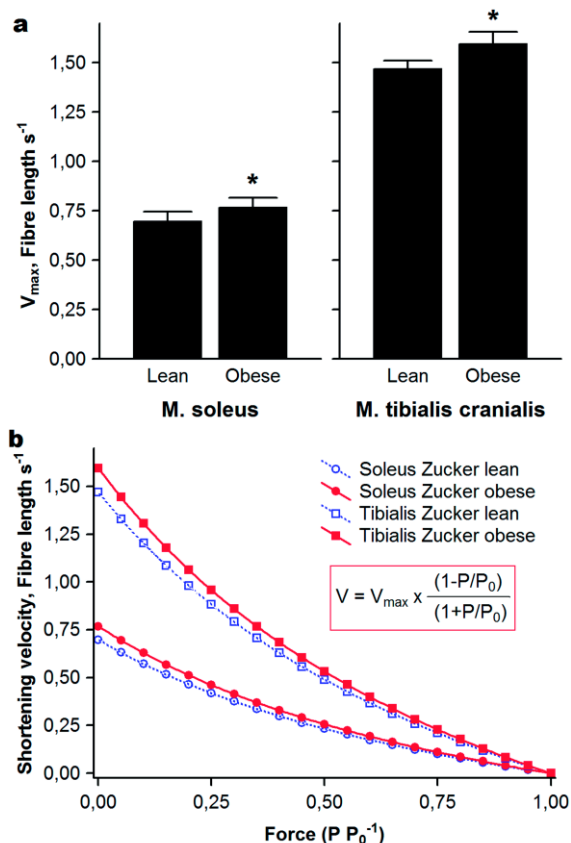
The effects of obesity on the force-velocity relationship of soleus and tibialis cranialis muscles were

estimated according to the Hill's equation using relative proportions of myosin-based muscle fibre types in the two muscles of lean and obese Zucker rats. The predicted maximal shortening velocities of soleus and tibialis muscles of lean rats were 0.70 ± 0.05 and 1.47 ± 0.04 fibre lengths s^{-1} , respectively. As illustrated in **Fig. 6.2**, a shift toward a faster phenotype was observed in the two muscles of obese rats: soleus, 0.77 ± 0.05 fibre length s^{-1} ; tibialis, 1.60 ± 0.06 fibre length s^{-1} ($P < 0.001$ in both muscles, Student's unpaired *t* test).

Muscle fibre-type succinic dehydrogenase (SDH) activity

Soleus and tibialis cranialis muscle oxidative capacities were assessed by measuring the rate of histochemical SDH activity within individual muscle fibre types in obese versus lean Zucker rats (**Table 6.5**). The overall mean SDH activity of all muscle fibre types of obese rats increased by 15% in the soleus and by 18%

Skeletal muscle changes in obesity



◀ **Fig. 6.2** Prediction of the effects of obesity on maximal shortening velocity (V_{max}) and the force-velocity relationship of soleus and tibialis muscles in obese versus lean Zucker rats. **a:** Predicted V_{max} of soleus and tibialis cranialis muscles of lean and obese Zucker rats. Values are means \pm SD ($n=20$ rats/group); * $P<0.001$ compared with lean rats, Student's unpaired t test. **b:** Force-velocity curves in soleus and tibialis cranialis muscles were determined according to the Hill-type mathematical model (*inset*), (Jakubiec-Puka et al. 1999) and compared between lean (blue dashed lines) and obese (red solid lines) Zucker rats. The proportion of each myosin-based muscle fibre type contributes to the whole muscle force-velocity relationship. (Caiozzo et al. 2003) Data are expressed as means of 20 rats per group. V , shortening velocity; V_{max} , maximal shortening velocity; P , isometric tension; P_0 , maximal isometric tension.

in the tibialis cranialis ($P<0.001$ in both), compared with the lean animals (Table 6.4, Fig. 6.1i-1). The obesity-induced improvement of muscle oxidative capacity involved all soleus and tibialis cranialis muscle fibre types, with soleus muscle fibres being less oxidative than tibialis cranialis muscle fibres (Table 6.5, Fig. 6.1i-1).

Whole muscle citrate synthase (CS) activity

The effects of obesity on muscle oxidative capacity

were also examined by biochemical analysis of CS activity of whole soleus and tibialis cranialis muscle homogenates. In agreement with quantitative SDH activity in individual muscle fiber types, whole CS activity of obese rats increased by 16% in the soleus muscle (22.3 ± 2.0 vs. 19.2 ± 2.1 $\mu\text{mol}/\text{min}/\text{g}$, $P<0.001$) and by 8% in the tibialis cranialis muscle (24.3 ± 2.0 vs. 22.6 ± 2.8 $\mu\text{mol}/\text{min}/\text{g}$, $P=0.03$), compared with the lean animals (Fig. 6.3).

Protein levels of PPAR γ and PGC1 α receptors

The protein levels of the two critical regulators of muscle fibre transformation and mitochondrial biogenesis (PPAR γ and PGC1 α) in soleus and tibialis cranialis muscles did not differ significantly between lean and obese rats ($P>0.05$; Fig. 6.4). However, the relative protein levels of PPAR γ was 70% lower in soleus and 60% lower in tibialis cranialis in the obese group than in

Table 6.5 Muscle fibre-type succinic dehydrogenase activity, OD min⁻¹

Muscle	Fibre type	Lean	Obese	<i>P</i> values
M. soleus	I	0.38± 0.04	0.44± 0.04	<0.001
	IIA	0.45± 0.04	0.49± 0.06	0.02
	All fibre-types	0.39± 0.04	0.45± 0.04	<0.001
M. tibialis cranialis	IIA	0.58± 0.06	0.62± 0.05	0.05
	IIIX	0.48± 0.10	0.57± 0.04	0.001
	IIIXB	0.43± 0.03	0.46± 0.02	0.001
	IIIB	0.31± 0.03	0.36± 0.02	<0.001
	All fibre-types	0.44± 0.06	0.52± 0.05	<0.001

Values are means ± SD, n = 20 rats/group. Student's unpaired *t*-test was used to test for differences between groups and expressed as *P* values. For clarity, muscle fibre-types with a percentage below 5% (see **Table 6.4**) are excluded from this analysis

the lean control group, but these differences did not reach the required level of significance (*P* = 0.06 and *P* = 0.07, respectively; **Fig. 6.4a**). The relative protein content of PGC1 α in the red soleus muscle was 55% higher in the obese group than in the lean control group but this effect was not significant (*P* = 0.08; **Fig. 6.4b**).

DISCUSSION

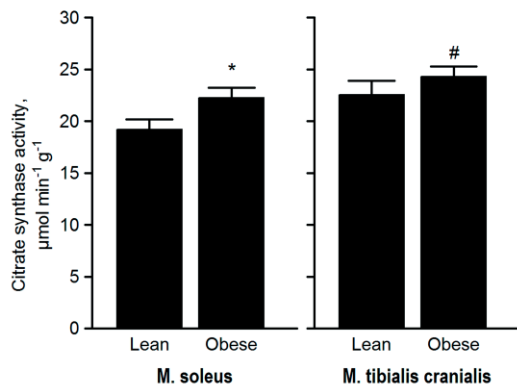
The results of the present study show that: 1) slow- and fast-twitch hind limb skeletal muscle phenotypes are clearly different in obese versus lean adult Zucker rats; and 2) obesity-induced muscle growth inhibition and faster fiber-type phenotype are compatible with an increased oxidative capacity in all muscle fibre types of both muscles.

The obese Zucker rat is a well-established model of obesity and Type 2 diabetes, exhibiting the characteristic biochemical features of these conditions, including hyperinsulinemia, hyperglycemia, and hyperlipidemia, in addition to insulin resistance, as confirmed in this and other studies (Durham and Truett 2006; Pompeani et al. 2014). The obese Zucker (*fa/fa*) rat becomes obese due to

increased food intake secondary to a genetic leptin receptor deficiency that results in lack of satiety response (Bray 1977).

A reduced skeletal muscle mass is a well-documented consequence of obesity in Zucker rats (Argiles et al. 1999; Paturi et al. 2010; Peterson et al. 2008; Pompeani et al. 2014; Reeds et al. 1982). This has been confirmed in the current study, with a significant reduction in the muscle weights of obese versus lean Zucker rats. This was accompanied by decreased diameter of all muscle fibre types in slow and fast muscles. This diminished skeletal muscle mass was observed despite significantly increased body weights which should theoretically induce compensatory hypertrophy to bear the increased body mass, particularly in the tonically active at rest soleus muscle that provides postural (antigravitatory) support. Previous data suggest that metabolic syndrome, insulin resistance and other related comorbidities may impair satellite cell proliferation (Peterson et al. 2008) and the ability to undergo load-induced hypertrophic adaptation (Paturi et al. 2010) in the soleus muscle of obese Zucker rats. Inflammatory pathways in muscle, initiated by

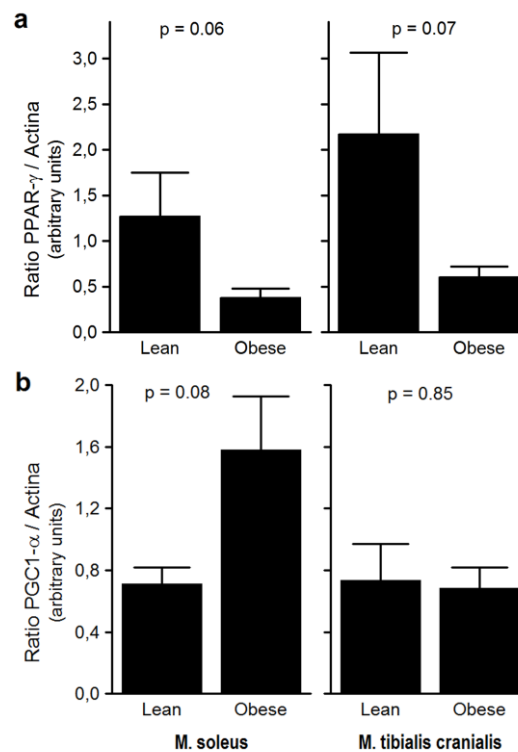
Skeletal muscle changes in obesity



▲ **Fig. 6.3** Citrate synthase activity of soleus and tibialis cranialis muscles in obese versus lean female Zucker rats. Values are means±SD (n=20 rats/group); * P<0.001 and #P=0.03 compared with lean rats, Student's unpaired *t* test.

obesity and prolonged over-nutrition, also promote muscle atrophy via decreased synthesis and increased degradation of muscle contractile proteins (Perry et al. 2016). Furthermore, because the obese Zucker rat seems to be significantly less active than the lean Zucker rat (Bray 1977), diminished physical activity might also adversely affects muscle mass in obese subjects (Perry et al. 2016). Nonetheless, and despite the lack of objective data on physical activity of the animals used in the present study, we consider unlikely that this difference could be a relevant contributor to differences observed in muscle mass adaptations. This contention is supported by the fact that similar adaptations were observed in both the practically inactive at rest tibialis muscle and the tonically active at rest soleus muscle.

In agreement with present results, obesity also resulted in a decreased number of type I muscle fibres and an increased number of type II fibres in previous studies



▲ **Fig. 6.4** Relative protein level of PPAR γ (a) and PGC1 α (b) receptors in soleus and tibialis cranialis muscles in obese versus lean Zucker rats. Bars represent means \pm SD (n=7 rats/group); p denotes P values between groups, Student's unpaired *t* test.

with Zucker rats (Couturier et al. 2014; Ringseis et al. 2013). Our results also indicate that, within type II fibres of the tibialis cranialis muscle, obesity results in high percentages of low-oxidative, fastest type IIXB and IIB fibres and low proportions of high-oxidative, slowest type IIA, IIAX and IIX fibres. This variation in myosin fibre

type composition increased by ~10% the predicted maximal shortening velocity of both soleus and tibialis muscles in obese versus lean rats. The fibre-type composition observed in the present study in the obese rats is in agreement with previous studies reporting that, in addition to a decreased type I-to-type II fibre ratio (Denies et al. 2014; Yasuda et al. 2006), patients and animal models with diabetes and/or obesity have a high percentage of low-oxidative type II fibres (particularly type IIB), and a low percentage of high-oxidative type II fibres (particularly type IIA) in fast-twitch skeletal muscles (Abou Mrad et al. 1992; Malenfant et al. 2001; Nyholm et al. 1997; Oberbach et al. 2006). Our data are also consistent with the inverse correlation reported between type I fibre proportions and obesity in previous studies (Denies et al. 2014; Oberbach et al. 2006).

Adult skeletal muscles are featured by many hybrid fibres expressing more than one myosin isoform. In this study, fibre-to-fibre analysis showed that long-term obesity leads to increase the proportion of hybrid fibres in the soleus muscles, but does not alter the overall proportion of these fibres in the tibialis cranialis muscle. These findings support the notion that hybrid fibres represent fibres in a transitional state between pure fibre-types (Acevedo and Rivero 2006; Staron and Pette 1993).

The mechanism underlying differences in muscle fibre proportions in obese subjects remains an unresolved issue. Obesity- and diabetes-induced decrease of the type I-to-type II fibre ratio has been explained by down-regulation of PGC1 α and PPAR receptors (Koves et al. 2008; Li et al. 2007), but the mRNA levels of these critical regulators of muscle fibre transformation in control skeletal muscle of obese versus lean Zucker rats were unchanged in previous studies (Couturier et al. 2014; Adachi et al. 2007; Ringseis et al. 2013). In the present study, protein levels of PPAR γ and PGC1 α were also unchanged in obese versus lean Zucker rats. However, a non-significant tendency for a reduction in

PPAR γ levels was noted in red and white muscles of obese rats compared with lean Zucker rats (Fig. 6.4a). This finding is in agreement with the lower type I-to-type II fiber-type ratio observed in obese subjects, since PPAR receptors show higher expression in oxidative type I muscle fibres than in glycolytic type II muscle fibres (Evans et al. 2004). Several studies have demonstrated functional associations, including changes in glucose uptake and insulin sensitivity and responsiveness, between muscle fibre-type composition and obesity, leading to significant impairments in these metabolic processes (Nyholm et al. 1997; Stuart et al. 2013; Yasuda et al. 2006). Some authors have also suggested the possibility that differences in physical activity, rather than obesity and related conditions *per se*, might be responsible for the altered fibre-type composition observed in skeletal muscles of the genetically obese (*ob/ob*) mouse (Kemp et al. 2009; Warmington et al. 2000). However, as explained above, it is unlikely that the altered fibre types observed in the present study resulted from differences in activity levels between the two strains of Zucker rats, since changes of similar nature occurred in the two functionally different muscles.

A key result of the present study was that the histochemical SDH activity of individual muscle fibres was increased in all fibre types of both soleus and tibialis muscles in obese versus lean Zucker rats. This histochemical finding was supported by an increase of CS activity (Fig. 6.3) and a non-significant tendency for an increment in protein levels of the PGC1 α receptor (Fig. 6.4b) in whole muscle homogenates from obese rats (Fig. 6.3). These findings indicate that obesity favors an oxidative muscle phenotype despite a significant faster fibre-type phenotype in obese versus lean subjects. This observation is in disagreement with previous studies reporting that obese Zucker rats have a decreased proportion of type I muscle fibres and a non-significant tendency for decreased mitochondrial enzyme activity,

indicating that muscle oxidative capacity is impaired in obesity and related conditions (Ringseis et al. 2013; Couturier et al. 2014). It is important to take into account that in these studies (Ringseis et al. 2013; Couturier et al. 2014), muscle oxidative capacity was not investigated in specific muscle fibre-types like in the present study.

Results obtained in other genetic models of obesity, which have compared obese versus lean subjects, have shown, however, no differences in muscle fibre SDH histochemical activity (Adachi et al. 2007; Yasuda et al. 2006; Yasuda et al. 2002), and relative mRNA levels of genes encoding this enzyme (Couturier et al. 2014), suggesting that rat models of genetic obesity are not associated with mitochondrial dysfunction in skeletal muscle. However, in agreement with present results, comparisons of obese and lean Zucker rat muscles also revealed increased muscle oxidative enzyme activities (e.g., citrate synthase and β -hydroxyacyl-coenzyme A dehydrogenase) and mitochondrial content in obese animals, particularly in red muscles, with abundant slow-oxidative fibre-types (Franch et al. 2002; Holloway et al. 2009a; Holloway et al. 2009b; Lally et al. 2012; Turner et al. 2007). In addition, an increased histochemical SDH activity was reported in muscle fibre types of patients with Type 2 diabetes, and it was interpreted as a muscle's compensatory mechanism in responses to the altered glucose metabolism (Oberbach et al. 2006). An increased fatty acid uptake and altered fatty acid metabolism, together with an elevated level of acyl-CoA binding protein, have also been reported in insulin-resistance muscles of the obese Zucker rat (Franch et al. 2002; Turcotte et al. 2001). A relative increase in mitochondrial content and a more oxidative muscle phenotype have also been reported in non-genetic models of obesity (e.g., high-fat and diet-induced obesity) (de Wilde et al. 2008; Shortreed et al. 2009; Trajcevski et al. 2013; Turner et al. 2007). Together, these findings suggest that high lipid availability does not lead to intramuscular lipid

accumulation and insulin resistance in obese rodents by decreasing muscle mitochondrial fatty acid oxidative capacity. Conversely, the current study supports that insulin resistance can be present without reductions in muscle mitochondrial content and that obesity increases muscle mitochondrial content and fatty acid oxidation (Garcia-Roves et al. 2007; Holloway et al. 2009a; Holloway et al. 2009b; Lally et al. 2012; Turner et al. 2007; Franch et al. 2002; Turcotte et al. 2001). The increased intramuscular accumulation of lipids observed in obese animals (Lally et al. 2012), has been attributed to an increased rate of fatty acid transport that exceeds the concurrently increased capacity for mitochondrial fatty acid oxidation (Holloway et al. 2009a; Turcotte et al. 2001).

A novel observation in our study is the increased mitochondrial oxidative capacity observed in muscle fibres of the white tibialis cranialis muscle of obese Zucker rats, compared with the lean phenotype. Previous studies in this model of obesity have reported a lack of any significant change in acyl-CoA binding protein, mitochondrial content, oxidative enzyme activities and transport of fatty acids into muscle cells in white muscles, composed of abundant fast-glycolytic fibre types (Chabowski et al. 2006; Holloway et al. 2009a; Franch et al. 2002). Similarly, enhanced oxidative capacity was noted in the soleus, but not tibialis cranialis muscles of diet-induced obese mice (Shortreed et al. 2009). It has been argued that white muscles might be less susceptible than red muscles to alterations in the substrate-endocrine environment (Chabowski et al. 2006), probably because they accumulate less fatty acids (Lally et al. 2012; Benton et al. 2006; Megeney et al. 1993), and exhibit lower rate of insulin-stimulated glucose transport (Megeney et al. 1993). These observations have been related to the physiological role of fast-twitch muscle, which is to develop rapid, explosive bursts of movements that rely heavily on intramuscular glycogen, rather than on blood

borne substrates (Chabowski et al. 2006; Holloway et al. 2009a). However, previous studies have associated intramyocellular lipid accumulation and insulin resistance in white muscles of obese Zucker rats (Korach-Andre et al. 2005; Lally et al. 2012), substantiating that these muscles also play a role during the onset of insulin resistance. Also in agreement with present results, whole muscle mitochondrial DNA was significantly increased in white muscle of obese Zucker rats (Lally et al. 2012).

In conclusion, the present study provides consistent evidence that the adaptive response of rat skeletal muscle to obesity takes the form of generalized inhibition of muscle fibre growth and a significant change toward a faster fibre-type phenotype. These changes occurred with a switch towards a more oxidative phenotype, indicative of an increased mitochondrial content of skeletal muscles. It is noteworthy that obesity-induced muscle adaptations were unspecific in regards to muscle structure and

function.

CONFLICTS OF INTERESTS

None of the authors of this paper has a financial or personal relationship with other people or organisation that could inappropriately influence or bias the content of the paper. In consequence, the author(s) declare no competing financial interests.

ACKNOWLEDGEMENTS

The work reported here was supported by a Spanish Government Grant from the Instituto de Salud Carlos III (PI14/00467) with co-financing from European Funds. L.M.A., and J.L.L.R. were supported by grants of the PAI Group CTS-179 and Project P10-AGR-5963, Junta de Andalucía, Spain.

Skeletal muscle changes in obesity

REFERENCES

- Abou Mrad J, Yakubu F, Lin D, Peters JC, Atkinson JB, Hill JO (1992) Skeletal muscle composition in dietary obesity-susceptible and dietary obesity-resistant rats. *Am J Physiol* 262:R684-688
- Acevedo LM, Lopez I, Peralta-Ramirez A, Pineda C, Chamizo VE, Rodriguez M, Aguilera-Tejero E, Rivero JL (2016) High-phosphorus diet maximizes and low-dose calcitriol attenuates skeletal muscle changes in long-term uremic rats. *J Appl Physiol* 120:1059-1069
- Acevedo LM, Peralta-Ramirez A, Lopez I, Chamizo VE, Pineda C, Rodriguez-Ortiz ME, Rodriguez M, Aguilera-Tejero E, Rivero JL (2015) Slow- and fast-twitch hindlimb skeletal muscle phenotypes 12 wk after (5/6) nephrectomy in Wistar rats of both sexes. *Am J Physiol Ren P* 309:F638-647
- Acevedo LM, Rivero JL (2006) New insights into skeletal muscle fibre types in the dog with particular focus towards hybrid myosin phenotypes. *Cell Tis Res* 323:283-303
- Adachi T, Kikuchi N, Yasuda K, Anahara R, Gu N, Matsunaga T, Yamamura T, Mori C, Tsujimoto G, Tsuda K, Ishihara A (2007) Fibre type distribution and gene expression levels of both succinate dehydrogenase and peroxisome proliferator-activated receptor-gamma coactivator-1 α of mice in the soleus muscle of Zucker diabetic fatty rats. *Exp Physiol* 92:449-455
- Argiles JM, Busquets S, Alvarez B, Lopez-Soriano FJ (1999) Mechanism for the increased skeletal muscle protein degradation in the obese Zucker rat. *J Nutr Biochem* 10:244-248
- Benton CR, Han XX, Febbraio M, Graham TE, Bonen A (2006) Inverse relationship between PGC-1 α protein expression and triacylglycerol accumulation in rodent skeletal muscle. *J Appl Physiol* 100:377-383
- Bottinelli R, Schiaffino S, Reggiani C (1991) Force-velocity relations and myosin heavy chain isoform compositions of skinned fibres from rat skeletal muscle. *J Physiol* 437:655-672
- Bray GA (1977) The Zucker-fatty rat: a review. *Fed Proc* 36:148-153
- Caiozzo VJ, Baker MJ, Huang K, Chou H, Wu YZ, Baldwin KM (2003) Single-fiber myosin heavy chain polymorphism: how many patterns and what proportions? *Am J Physiol Reg Int Comp Physiol* 285:R570-580
- Couturier A, Ringseis R, Mooren FC, Kruger K, Most E, Eder K (2014) Correction: Carnitine supplementation to obese Zucker rats prevents obesity-induced type I to type II muscle fiber transition and favors an oxidative phenotype of skeletal muscle. *Nutr Metabol* 11:16
- Chabowski A, Chatham JC, Tandon NN, Calles-Escandon J, Glatz JF, Luiken JJ, Bonen A (2006) Fatty acid transport and FAT/CD36 are increased in red but not in white skeletal muscle of ZDF rats. *Am J Physiol Endocrinol Metabol* 291:E675-682
- de Wilde J, Mohren R, van den Berg S, Boekschooten M, Dijk KW, de Groot P, Muller M, Mariman E, Smit E (2008) Short-term high fat-feeding results in morphological and metabolic adaptations in the skeletal muscle of C57BL/6J mice. *Physiol Genom* 32:360-369
- Delp MD, Duan C (1996) Composition and size of type I, IIA, IID/X, and IIB fibers and citrate synthase activity of rat muscle. *J Appl Physiol* 80:261-270
- Denies MS, Johnson J, Maliphol AB, Bruno M, Kim A, Rizvi A, Rustici K, Medler S (2014) Diet-induced obesity alters skeletal muscle fiber types of male but not female mice. *Physiol Rep* 2:e00204
- Durham HA, Truett GE (2006) Development of insulin resistance and hyperphagia in Zucker fatty rats. *Am J Physiol RegInt Comp Physiol* 290:R652-658
- Ehrenborg E, Krook A (2009) Regulation of skeletal muscle physiology and metabolism by peroxisome proliferator-activated receptor delta. *Pharmacol Rev* 61:373-393
- Evans RM, Barish GD, Wang YX (2004) PPARs and the complex journey to obesity. *Nature Med* 10:355-361

Chapter 6

- Franch J, Knudsen J, Ellis BA, Pedersen PK, Cooney GJ, Jensen J (2002) Acyl-CoA binding protein expression is fiber type- specific and elevated in muscles from the obese insulin-resistant Zucker rat. *Diabetes* 51:449-454
- Frisbee JC, Goodwill AG, Frisbee SJ, Butcher JT, Brock RW, Olfert IM, DeVallance ER, Chantler PD (2014) Distinct temporal phases of microvascular rarefaction in skeletal muscle of obese Zucker rats. *Am J Physiol Heart Circ Physiol* 307:H1714-1728
- Garcia-Roves P, Huss JM, Han DH, Hancock CR, Iglesias-Gutierrez E, Chen M, Holloszy JO (2007) Raising plasma fatty acid concentration induces increased biogenesis of mitochondria in skeletal muscle. *Proc Nat Acad Sci USA* 104:10709-10713
- Hill AV (1938) The heat of shortening and the dynamic constants of muscle. *Proc R Soc Lond B Biol Sci* 126:136-195
- Holloway GP, Benton CR, Mullen KL, Yoshida Y, Snook LA, Han XX, Glatz JF, Luiken JJ, Lally J, Dyck DJ, Bonen A (2009a) In obese rat muscle transport of palmitate is increased and is channeled to triacylglycerol storage despite an increase in mitochondrial palmitate oxidation. *Am J Physiol Endocrinol Metabol* 296:E738-747
- Holloway GP, Bonen A, Spriet LL (2009b) Regulation of skeletal muscle mitochondrial fatty acid metabolism in lean and obese individuals. *Am J Clin Nutr* 89:455S-462S
- Jakubiec-Puka A, Ciechomska I, Mackiewicz U, Langford J, Chomontowska H (1999) Effect of thyroid hormone on the myosin heavy chain isoforms in slow and fast muscles of the rat. *Acta Biochim Pol* 46:823-835
- Kelley DE, He J, Menshikova EV, Ritov VB (2002) Dysfunction of mitochondria in human skeletal muscle in type 2 diabetes. *Diabetes* 51:2944-2950
- Kemp JG, Blazev R, Stephenson DG, Stephenson GM (2009) Morphological and biochemical alterations of skeletal muscles from the genetically obese (ob/ob) mouse. *Int J Obes* 33:831-841
- Korach-Andre M, Gounarides J, Deacon R, Beil M, Sun D, Gao J, Laurent D (2005) Age and muscle-type modulated role of intramyocellular lipids in the progression of insulin resistance in nondiabetic Zucker rats. *Metabol Clin Exp* 54:522-528
- Koves TR, Ussher JR, Noland RC, Slentz D, Mosedale M, Ilkayeva O, Bain J, Stevens R, Dyck JR, Newgard CB, Lopaschuk GD, Muoio DM (2008) Mitochondrial overload and incomplete fatty acid oxidation contribute to skeletal muscle insulin resistance. *Cell Metabol* 7 :45-56
- Lally JS, Snook LA, Han XX, Chabowski A, Bonen A, Holloway GP (2012) Subcellular lipid droplet distribution in red and white muscles in the obese Zucker rat. *Diabetol* 55:479-488
- Larsson L, Skogsberg C (1988) Effects of the interval between removal and freezing of muscle biopsies on muscle fibre size. *J Neurol Sci* 85:27-38
- Li D, Kang Q, Wang DM (2007) Constitutive coactivator of peroxisome proliferator-activated receptor (PPARgamma), a novel coactivator of PPARgamma that promotes adipogenesis. *Mol Endocrinol* 21:2320-2333
- Malenfant P, Joannis DR, Theriault R, Goodpaster BH, Kelley DE, Simoneau JA (2001) Fat content in individual muscle fibers of lean and obese subjects. *Int J Obes Rel Metabol Dis* 25:1316-1321
- Megency LA, Neuffer PD, Dohm GL, Tan MH, Blewett CA, Elder GC, Bonen A (1993) Effects of muscle activity and fiber composition on glucose transport and GLUT-4. *Am J Physiol* 264:E583-593
- Nyholm B, Qu Z, Kaal A, Pedersen SB, Gravholt CH, Andersen JL, Saltin B, Schmitz O (1997) Evidence of an increased number of type IIb muscle fibers in insulin-resistant first-degree relatives of patients with NIDDM. *Diabetes* 46:1822-1828
- Oberbach A, Bossenz Y, Lehmann S, Niebauer J, Adams V, Paschke R,

Skeletal muscle changes in obesity

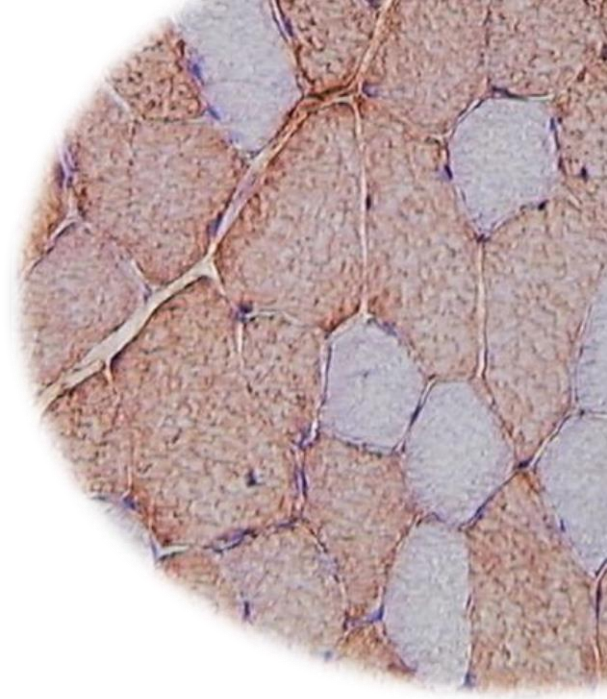
- Schon MR, Bluhner M, Punkt K (2006) Altered fiber distribution and fiber-specific glycolytic and oxidative enzyme activity in skeletal muscle of patients with type 2 diabetes. *Diabetes Care* 29:895-900
- Paturi S, Gutta AK, Kakarla SK, Katta A, Arnold EC, Wu M, Rice KM, Blough ER (2010) Impaired overload-induced hypertrophy in obese Zucker rat slow-twitch skeletal muscle. *J Appl Physiol* 108:7-13
- Perry BD, Caldwell MK, Brennan-Speranza TC, Sbaraglia M, Jerums G, Garnham A, Wong C, Levinger P, Asrar UI Haq M, Hare DL, Price SR, Levinger I (2016) Muscle atrophy in patients with Type 2 Diabetes Mellitus: roles of inflammatory pathways, physical activity and exercise. *Exerc Immunol Rev* 22:94-109
- Petersen KF, Dufour S, Savage DB, Bilz S, Solomon G, Yonemitsu S, Cline GW, Befroy D, Zeman L, Kahn BB, Papademetris X, Rothman DL, Shulman GI (2007) The role of skeletal muscle insulin resistance in the pathogenesis of the metabolic syndrome. *Proc Nat Acad Sci USA* 104:12587-12594
- Peterson JM, Bryner RW, Alway SE (2008) Satellite cell proliferation is reduced in muscles of obese Zucker rats but restored with loading. *Am J Physiol Cell Physiol* 295:C521-528
- Pompeani N, Rybalka E, Latchman H, Murphy RM, Croft K, Hayes A (2014) Skeletal muscle atrophy in sedentary Zucker obese rats is not caused by calpain-mediated muscle damage or lipid peroxidation induced by oxidative stress. *J Neg Res Biomed* 13:19
- Rasbach KA, Gupta RK, Ruas JL, Wu J, Naseri E, Estall JL, Spiegelman BM (2010) PGC-1 α regulates a HIF2 α -dependent switch in skeletal muscle fiber types. *Proc Nat Acad Sci USA* 107:21866-21871
- Reeds PJ, Haggarty P, Wahle KW, Fletcher JM (1982) Tissue and whole-body protein synthesis in immature Zucker rats and their relationship to protein deposition. *Biochem J* 204:393-398
- Ringseis R, Rosenbaum S, Gessner DK, Herges L, Kubens JF, Mooren FC, Krüger K, Eder K (2013) Supplementing obese Zucker rats with niacin induces the transition of glycolytic to oxidative skeletal muscle fibers. *J Nutr* 143:125-131
- Rivero JL, Talmadge RJ, Edgerton VR (1999) Interrelationships of myofibrillar ATPase activity and metabolic properties of myosin heavy chain-based fibre types in rat skeletal muscle. *Histochem Cell Biol* 111:277-287
- Schiaffino S, Gorza L, Sartore S, Saggin L, Ausoni S, Vianello M, Gundersen K, Lomo T (1989) Three myosin heavy chain isoforms in type 2 skeletal muscle fibres. *J Musc Res Cell Motil* 10:197-205
- Serrano AL, Quiroz-Rothe E, Rivero JL (2000) Early and long-term changes of equine skeletal muscle in response to endurance training and detraining. *Pflug Archiv Eur J Physiol* 441:263-274
- Shortreed KE, Krause MP, Huang JH, Dhanani D, Moradi J, Ceddia RB, Hawke TJ (2009) Muscle-specific adaptations, impaired oxidative capacity and maintenance of contractile function characterize diet-induced obese mouse skeletal muscle. *PLoS One* 4:e7293
- Staron RS, Pette D (1993) The continuum of pure and hybrid myosin heavy chain-based fibre types in rat skeletal muscle. *Histochemistry* 100:149-153
- Stuart CA, McCurry MP, Marino A, South MA, Howell ME, Layne AS, Ramsey MW, Stone MH (2013) Slow-twitch fiber proportion in skeletal muscle correlates with insulin responsiveness. *J Clin Endocrinol Metabol* 98:2027-2036
- Trajcevski KE, O'Neill HM, Wang DC, Thomas MM, Al-Sajee D, Steinberg GR, Ceddia RB, Hawke TJ (2013) Enhanced lipid oxidation and maintenance of muscle insulin sensitivity despite glucose intolerance in a diet-induced obesity mouse model. *PLoS One* 8:e71747
- Turcotte LP, Swenberger JR, Zavitz Tucker M, Yee AJ (2001) Increased fatty acid uptake and altered fatty acid metabolism in insulin-resistant

Chapter 6

- muscle of obese Zucker rats. *Diabetes* 50:1389-1396
- Turner N, Bruce CR, Beale SM, Hoehn KL, So T, Rolph MS, Cooney GJ (2007) Excess lipid availability increases mitochondrial fatty acid oxidative capacity in muscle: evidence against a role for reduced fatty acid oxidation in lipid-induced insulin resistance in rodents. *Diabetes* 56:2085-2092
- Turpin SM, Ryall JG, Southgate R, Darby I, Hevener AL, Febbraio MA, Kemp BE, Lynch GS, Watt MJ (2009) Examination of 'lipotoxicity' in skeletal muscle of high-fat fed and ob/ob mice. *J Physiol* 587:1593-1605
- Warmington SA, Tolan R, McBennett S (2000) Functional and histological characteristics of skeletal muscle and the effects of leptin in the genetically obese (ob/ob) mouse. *Int J Obes Rel Metabol Dis* 24:1040-1050
- Welle S, Tawil R, Thornton CA (2008) Sex-related differences in gene expression in human skeletal muscle. *PLoS One* 3:e1385
- Wessels B, Ciapaite J, van den Broek NM, Houten SM, Nicolay K, Prompers JJ (2015) Pioglitazone treatment restores in vivo muscle oxidative capacity in a rat model of diabetes. *Diab Obes Metabol* 17:52-60
- Yasuda K, Adachi T, Kikuchi N, Tsujimoto G, Aoki N, Ishihara A (2006) Effects of running exercise on fibre-type distribution of soleus and plantaris muscles in diabetic Otsuka Long-Evans Tokushima fatty rats. *Diab Obes Metabol* 8:311-321
- Yasuda K, Nishikawa W, Isanaka N, Nakamura E, Seino Y, Tsuda K, Ishihara A (2002) Abnormality in fibre type distribution of soleus and plantaris muscles in non-obese diabetic Goto-Kazizaki rats. *Clin Exp Pharmacol Physiol* 29:1001-1008
- Zimmet P, Alberti KG, Shaw J (2001) Global and societal implications of the diabetes epidemic. *Nature* 414:782-787

CHAPTER 7

Mangiferin protects against adverse skeletal muscle changes and enhances muscle oxidative capacity in obese rats



Protective effects of mangiferin on skeletal muscle of obese rats

Luz M. Acevedo,^{1,3} Ana I. Raya,² Escolástico
Aguilera-Tejero,² and José-Luis L. Rivero¹

¹Laboratory of Muscular Biopathology, Department of
Comparative Anatomy and Pathological Anatomy,
University of Cordoba, Cordoba, Spain

²Department of Animal Medicine and Surgery, University
of Cordoba, Spain

³Departamento de Ciencias Biomédicas, Universidad
Central de Venezuela, Maracay, Venezuela

PloS One (under revisión), 2016

ABSTRACT

Obesity-related skeletal muscle changes include muscle atrophy, slow-to-fast fiber-type transformation, and impaired mitochondrial oxidative capacity. These changes relate with increased risk of insulin resistance. Mangiferin, the major component of the plant *Mangifera indica*, is a well-known anti-inflammatory, anti-diabetic, and antihyperlipidemic agent. This study tested the hypothesis that mangiferin treatment counteracts obesity-induced fiber atrophy and slow-to-fast fiber transition, and favors an oxidative phenotype in skeletal muscle of obese rats. Obese Zucker rats were fed gelatin pellets with (15 mg/kg BW/day) or without (placebo group) mangiferin for 8 weeks. Lean Zucker rats received the same gelatin pellets without mangiferin and served as non-obese and non-diabetic controls. Lesser diameter, fiber composition, and histochemical succinic dehydrogenase activity (an oxidative marker) of myosin-based fiber-types were assessed in soleus and tibialis cranialis muscles. A multivariate discriminant analysis encompassing all fiber-type features indicated that obese rats treated with mangiferin displayed skeletal muscle phenotypes significantly different compared with both lean and obese control rats. Mangiferin significantly preserved skeletal muscle mass, fiber cross-sectional size, and fiber-type composition, and enhanced muscle fiber oxidative capacity. These data demonstrate that mangiferin attenuated adverse skeletal muscle changes in obese rats, opening a novel application of mangiferin to improve obesity-induced metabolic dysregulation.

INTRODUCTION

Studies over the past 20 years have described changes in skeletal muscle in human and animal models of both genetic and diet-induced obesity. Muscle atrophy and a switch toward a faster contractile phenotype are well-documented changes in skeletal muscle of obese subjects [1-4]. In addition, an impaired mitochondrial oxidative

enzyme capacity has been reported in muscle from obese people and animals [5,6]. However, other studies in patients with Type 2 diabetes and rats with genetic obesity revealed increased mitochondrial density and oxidative enzyme activities in skeletal muscles [7-9]. In addition, studies showed a link between obesity-associated skeletal muscle changes (i.e., decreased muscle mass, slow-to-fast fiber transformation, and impaired mitochondrial function), and the risk of insulin resistance [10-13], suggesting that the prevention of these skeletal muscle changes might improve obesity-induced metabolic dysregulation [14]. For example, it has been widely observed that improving mitochondrial function also improves insulin sensitivity and prevents type 2 diabetes [15].

Chronic inflammation associated with obesity and over-nutrition, characterized by increased levels of inflammatory cytokines such as tumor necrosis factor α (TNF α) and interleukin 6 (IL-6), has been implicated in obesity-induced muscle atrophy via an imbalance in contractile protein synthesis and degradation [3]. Obesity- and diabetes-induced slow-to-fast muscle fiber type transformation has been explained by downregulation of peroxisome proliferator-activated receptors, such as PGC1 α and PPAR δ [16], which are critical regulators of fiber-type composition [17]. These receptors are typically higher expressed in slow-oxidative type I muscle fibers than in fast-glycolytic type II muscle fibers [18]. It is also known that the activation of the PPAR δ -PGC1 α axis, together with AMP-activated protein kinase (AMPK), are critical regulators of mitochondrial biogenesis [15,17].

Preliminary work done on mangiferin, a major glucoside of xanthone in the mango plant *Mangifera indica* L., suggests a potential for this pharmacophore as a novel parent compound for treating obesity-related metabolic conditions [19-22]. Evidences show that mangiferin has multiple beneficial biological activities, including potent anti-inflammatory [23-25], anti-oxidant

[23,26], and anti-diabetic effects [27-33]. Mechanistic links underlying these actions include inhibition of pro-inflammatory cytokines such as TNF α and IL-6 [23-25], activation of PPAR δ and PGC1 α receptors [23,34], activation of AMPK [35-38], increments of glucose transporters in adipose and muscle cells [39], and activation of pyruvate dehydrogenase complex [40]. In addition, recent unbiased proteomics studies reveal that mangiferin upregulates proteins pivotal for mitochondrial bioenergetics and downregulates proteins controlling de novo lipogenesis in liver [23,41]. Together, these actions of mangiferin lead to enhancement of carbohydrate utilization in oxidative metabolism, increasing insulin sensitivity and decreasing lipogenesis [22].

A few studies provided evidence that supplementation with mangiferin has beneficial effects on various aspects of muscle function in obese animals. For example, mangiferin supplementation enhanced lipid catabolism in skeletal muscle of these animals by upregulating genes involved in muscle fatty acid β -oxidation [27]. This substance also induced a shift in muscle respiratory quotient from lipid toward carbohydrate utilization through increased glucose and pyruvate oxidation [40], and by increasing glucose transporters expression and translocation in muscle cells [39]. However, cellular effects of mangiferin on skeletal muscle mass, and contractile and metabolic phenotypes have not been explored in experimental models of obesity.

Based on previous observations supporting mechanistic links of anti-inflammatory, anti-oxidant and anti-diabetic effects of mangiferin, we hypothesized that chronic intake of this pharmacophore should counteract obesity-induced muscle atrophy and slow-to-fast fiber-type switch, as well as to maximize oxidative mitochondrial capacity in skeletal muscle. Thus, the main purpose of this study was to analyze the effect of long-term low-dose mangiferin on size, frequency, and oxidative capacity of skeletal muscle fiber types in obese

rats. As an experimental model, we used obese Zucker rats, a well-established model of genetic obesity, insulin resistance, and metabolic syndrome, which were treated with gelatin pellets containing mangiferin (15 mg/kg BW/day) or without mangiferin (placebo) for 8 weeks. Lean Zucker rats served as non-obese and non-diabetic controls. Two muscles with opposite structure and functional significance, the red soleus and the white tibialis cranialis, were examined.

RESULTS

Mangiferin improved plasma cholesterol fractions, FGF21 levels, and hyperglycemic response in obese rats

The effect of mangiferin treatment on plasma metabolites was examined by comparing plasma variables of obese Zucker rats treated with (15 mg/kg BW/day) and without (placebo group) mangiferin, before and after 8 weeks (**Table 7.1**). Mangiferin significantly decreased plasma levels of total cholesterol, LDL cholesterol, and FGF21 levels, and significantly increased serum concentration of HDL cholesterol, but had no effect on serum glucose, triglycerides, insulin, and leptin levels, compared with the placebo group. Despite no effect on final plasma glucose concentration, mangiferin treatment for 8 weeks significantly attenuated hyperglycemic response in a standardized glucose tolerance test compared with the placebo group (**Fig. 7.1**).

Mangiferin ameliorated body weight gain, and protected against obesity-induced muscle atrophy

Daily feed intake was slightly greater in the obese placebo group (mean \pm SD, 26.6 \pm 1.3 g/d) than in the obese mangiferin group (24.4 \pm 1.0 g/d; $P = 0.04$). Similarly, daily body weight gain was significantly greater in the obese placebo group (4.56 \pm 0.24 g/d) than in the obese mangiferin group (4.27 \pm 0.33 g/d; $P = 0.03$).

Table 7.1 Mangiferin effects on plasma metabolites in genetic-obese rats

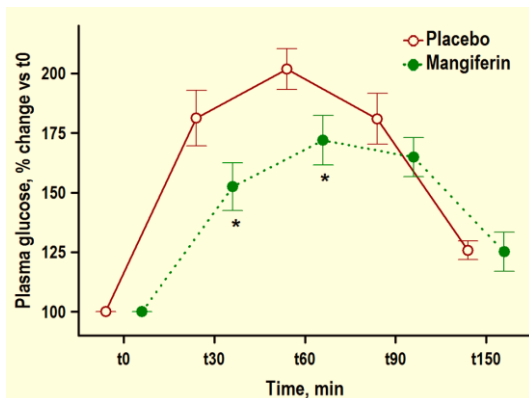
	Obese Placebo		Obese Mangiferin	
	Pre-treatment (wk 0)	Post-treatment (wk 8)	Pre-treatment (wk 0)	Post-treatment (wk 8)
Glucose, mg/dl	164± 32	183± 31	167± 12	189± 21
Cholesterol, mg/dl	96± 10	112± 8 *	90± 11	104± 10 * †
Chol LDL, mg/dl	4.2± 1.2	10.2± 3.2 *	3.2± 2.6	6.9± 3.8 * †
Chol HDL, mg/dl	41.4± 3.7	42.3± 2.5	42.6± 4.5	46.0± 3.3 * †
Triglycerides, mg/dl	440± 106	695± 226 *	471± 136	864± 268*
Adiponectin, µg/ml	8.0± 1.6	5.1± 3.5 *	7.2± 1.6	6.5± 1.8
Insulin, ng/ml	1.5± 0.7	10.6± 6.9 *	1.3± 0.4	9.9± 4.0 *
Leptin, ng/ml	9.9± 5.0	50.8± 9.6 *	11.3± 4.9	60.7± 13.1 *
FGF21, pg/ml	911± 635	18053± 1009 *	3258± 2958	9735± 1803 †

Values are means ± SD, n = 10 rats/group. Bonferroni unpaired t-test was used to test for differences before and after treatment and between Placebo and Mangiferin groups: * P < 0.05 compared with pre-treatment within the same group; † P < 0.05 compared with Placebo group within the same time of treatment

Obese rats treated with mangiferin experienced substantial weight gain reduction compared with the obese placebo group over the 8-week experimental period (Fig. 7.2). Thus, final body weights significantly differed in the three groups (Table 7.2). Obese rats treated with mangiferin for 8 weeks significantly increased their body

weights by 82% compared with lean control rats (P = 0.00), but decreased their body weights by 5% compared with obese control rats (P < 0.01).

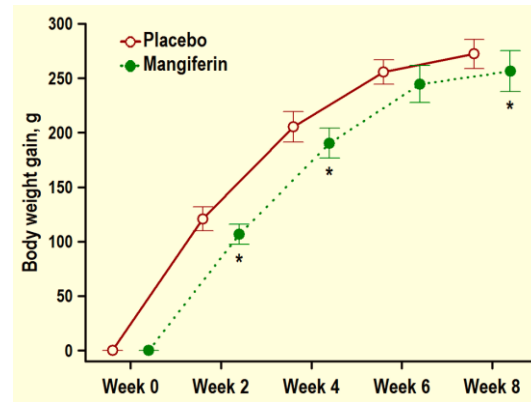
Despite increased final body weights, wet weights and muscle somatic indexes (MSI; wet muscle weight referred to body weight) of soleus and tibialis cranialis muscles



◀ **Fig. 7.1 Mangiferin attenuates hyperglycemic response in obese rats after glucose oral administration.** Zucker rats with the obese (*fa/fa*) phenotype (2 months old) were treated with placebo or mangiferin (15 mg/kg BW/day) for 8 weeks (n = 10 rats/group), and plasma glucose was monitored every 30 minutes after oral glucose administration (2 g/kg BW). Graph shows means ± SD plasma glucose change vs basal levels over time. * P < 0.05 indicates significant differences between Placebo and Mangiferin groups obtained by unpaired Student's *t* test.

Protective effects of mangiferin on skeletal muscle of obese rats

► **Fig. 7.2 Mangiferin mitigates overweight in obese rats.** Zucker rats with the obese (*fa/fa*) phenotype (2 months old) were treated with placebo or with mangiferin (15 mg/kg BW/days) for 8 weeks (n = 10 rats/group), and body weight was monitored every two weeks. Graph shows means \pm SD body weight gain over time. * P < 0.05 indicates significant differences between Placebo and Mangiferin groups obtained by unpaired Student's *t* test.



significantly decreased in obese vs lean control rats (**Table 7.2**). M. tibialis wet weight was also significantly lower in the obese mangiferin group than in the lean control group, and it did not differ significantly in mangiferin vs placebo obese rats. However, soleus wet weight and MSIs of both muscles were significantly greater in the obese mangiferin group than in the obese control group.

Mangiferin preserved muscle fiber cross-sectional size in obese rats

Mean lesser diameters of main myosin-based muscle fiber types were estimated in soleus and tibialis cranialis

muscles, and compared in the three experimental groups (**Table 7.3**; **Fig. 7.3**). Soleus muscle fibers were larger than tibialis cranialis muscle fibers. The lower muscle weights observed in the obese control rats (**Table 7.2**), corresponded with smaller mean lesser diameters in all soleus and tibialis muscle fiber types (21% and 29% on average, respectively) compared with lean control rats. Mean lesser diameters of soleus and tibialis muscle fiber types were found to be significantly greater (18% and

Table 7.2 Mangiferin effects on final body, and muscle weights and muscle somatic index (MSI) of subjects

Variable	Lean	Obese Control	Obese Mangiferin	P value
Body weight, g	262.9 \pm 42.6 a	505.4 \pm 14.7 c	479.6 \pm 17.6 b	<0.001
M. soleus weight, mg	156.8 \pm 19.0 b	137.5 \pm 18.8 a	148.5 \pm 14.8 b	<0.01
M. soleus MSI, mg/g	0.60 \pm 0.06 c	0.27 \pm 0.04 a	0.31 \pm 0.04 b	0.00
M. tibialis weight, mg	645.8 \pm 86.3 b	550.1 \pm 56.3 a	581.8 \pm 58.5 a	<0.001
M. tibialis MSI, mg/g	2.48 \pm 0.29 b	1.09 \pm 0.11 a	1.22 \pm 0.14 b	0.00

Values are means \pm SD, n = 20 rats/group. One-way ANOVA (*P* values denote significance of differences between groups) and Fisher least significant difference post hoc were used to test for differences between pairwise groups; within a row, means with different letters differ significantly (*P* < 0.05, at least)

Table 7.3 Mangiferin effects on lesser fiber diameter (μm) in genetic-obese rats

Fiber-Type	Lean	Obese Control	Obese Mangiferin	P value
M. soleus				
I	63.9 \pm 10.1 b	50.7 \pm 4.0 a	60.6 \pm 4.4 b	0.00
IIA	53.1 \pm 10.4 b	44.8 \pm 5.5 a	52.2 \pm 6.1 b	<0.001
All fiber-types	62.9 \pm 9.9 b	50.0 \pm 4.1 a	58.9 \pm 4.7 b	<0.001
M. tibialis cranialis				
IIA	39.5 \pm 8.4 b	32.1 \pm 3.7 a	39.1 \pm 4.9 b	<0.001
IIX	46.0 \pm 8.5 b	36.8 \pm 4.9 a	44.2 \pm 7.3 b	<0.001
IIXB	50.0 \pm 9.5 c	35.1 \pm 4.6 a	42.5 \pm 7.4 b	0.00
IIB	57.0 \pm 9.1 b	41.6 \pm 4.5 a	43.1 \pm 8.0 a	0.00
All fiber types	48.4 \pm 8.3 c	34.6 \pm 4.0 a	41.7 \pm 6.3 b	0.00

Values are means \pm SD, n = 20 rats/group. One-way ANOVA (*P* values denote significance of differences between groups) and Fisher least significant difference post hoc were used to test for differences between pairwise groups; within a row, means with different letters differ significantly ($P < 0.05$, at least). For clarity, muscle fiber-types with a percentage below 5% (see **Table 7.4**) are excluded from this analysis

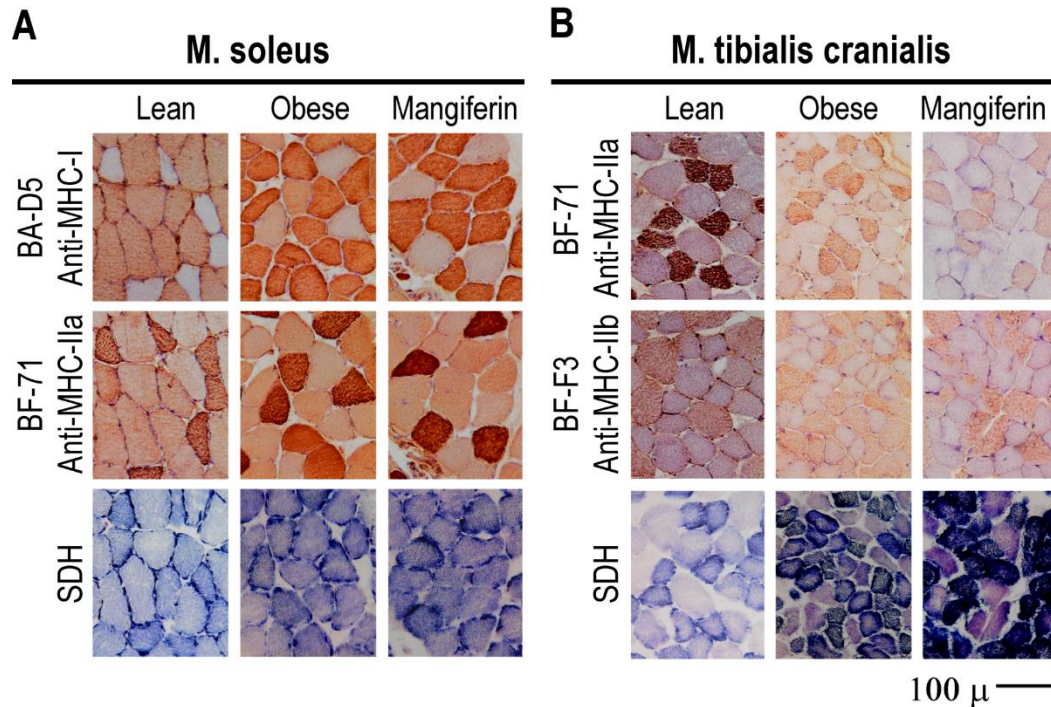
21%, respectively) in the obese mangiferin group than in the obese control group, but in general (IIB fibers in the tibialis muscle was an exception) were similar ($P > 0.05$) in obese mangiferin vs lean control rats.

Mangiferin counteracted obesity-induced switch toward a faster phenotype in white muscle

Soleus and tibialis cranialis muscle fibers were typed based on their immunoreactions to antibodies against specific myosin heavy chain isoforms, and the proportions of seven fiber types (I, I+IIA, IIA, IIAX, IIX, IIXB, and IIB) were compared in the three experimental groups (**Table 7.4**; **Fig. 7.3**). All these seven fiber types were identified in the tibialis cranialis muscle, but only three fiber types (I, I+IIA, and IIA) were found in the soleus muscle.

The three experimental groups were not comparable regarding their soleus and tibialis cranialis muscle fiber-type compositions (**Table 7.4**). In the soleus muscle of the two obese groups, slow-twitch type I fiber fractions were

reduced by 7%, whereas fast-twitch type IIA fiber percentages were increased by 72% and 49%, respectively, compared with the lean control group (**Fig. 7.3A**). Type I and IIA fiber percentages in the soleus muscle did not differ in mangiferin vs placebo obese rats. However, in obese rats treated with mangiferin, the percentage of hybrid fibers I+IIA in this muscle was lower than in obese control rats ($P = 0.04$), but comparable to the lean control group ($P > 0.05$). In the tibialis cranialis muscle of obese control rats, there was a significant slow-to-fast fiber-type switching in the direction $I \rightarrow IIA \rightarrow IIX \rightarrow IIB$, compared with the lean rats (**Fig. 7.3B**). This was indicated by decreased proportions of type I (34%), I+IIA (47%), IIA (23%), IIAX (50%), and IIX (25%) fibers, and increased frequencies of type IIXB (78%), and IIB (32%) fibers in obese vs lean control rats. The total relative number of hybrid fibers in this muscle was higher in obese than in lean control rats, but this difference did not reach statistical significance ($P = 0.16$). In general, fiber-type



▲ **Fig. 7.3 Mangiferin preserves fiber size and fiber-type composition, and enhances fiber oxidative capacity in skeletal muscle of obese rats.** Serial transverse sections of the soleus (A) and tibialis cranialis (B) muscles of representative lean (left columns), obese (middle columns), and obese treated with mangiferin (right columns) Zucker rats stained for immunohistochemistry against specific anti-myosin heavy chain (MHC) monoclonal antibodies and succinic dehydrogenase (SDH) histochemistry. Note in the muscles from the Zucker obese rats treated with mangiferin, the greater size of muscle fibers in both muscles, the abundance of fibers expressing MHC-IIa (M. tibialis), and the lower number of fibers expressing MHC-IIb (M. tibialis cranialis), compared with the muscles from the obese Zucker rats. Note also in muscles from both obese control and obese treated with mangiferin Zucker rats, the higher SDH staining in both muscles, compared with the muscles from the lean Zucker rats.

composition of the tibialis cranialis muscle did not differ significantly between the obese mangiferin group and the lean control group, but the percentage of type IIA fibers

was higher (37%, $P < 0.01$), and the proportion of type IIB fibers was lower (34%, $P < 0.01$) in mangiferin vs placebo obese rats. Total hybrid fibers in the tibialis

Table 7.4 Mangiferin effects on muscle fiber-type composition (%) of genetic-obese rats

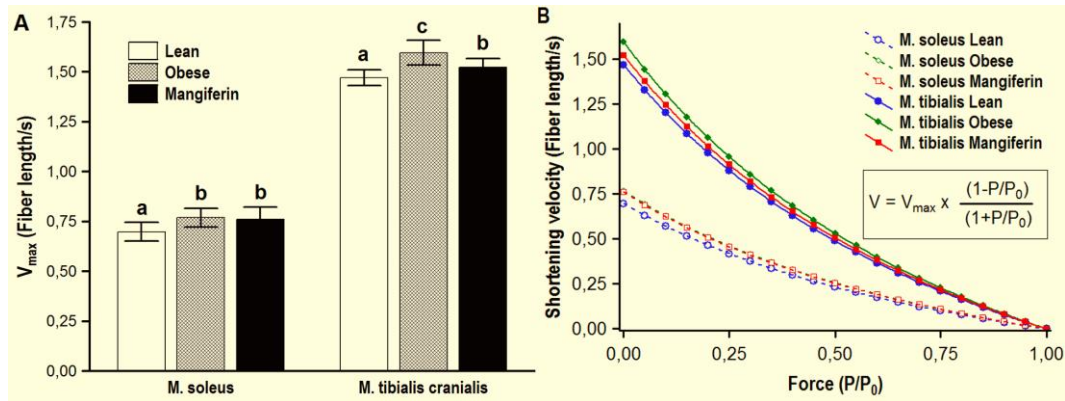
Fiber-Type	Lean	Obese Control	Obese Mangiferin	P value
M. soleus				
I	89.6 ± 7.6 b	83.1 ± 7.2 a	82.9 ± 8.9 a	0.01
I+IIA	1.5 ± 2.9 a	3.6 ± 3.3 b	1.8 ± 2.1 a	0.04
IIA	8.9 ± 5.9 a	13.3 ± 6.2 b	15.3 ± 7.9 b	0.01
M. tibialis cranialis				
I	4.7 ± 1.5 b	3.1 ± 2.8 a	3.7 ± 2.0 ab	0.06
I+IIA	1.7 ± 0.4 b	0.9 ± 1.1 a	0.7 ± 0.6 a	<0.001
IIA	27.9 ± 8.9 b	21.6 ± 8.1 a	29.5 ± 6.7 b	<0.01
IIAX	4.0 ± 1.7 b	2.1 ± 2.3 a	1.9 ± 1.4 a	<0.001
IIX	24.7 ± 8.5 b	18.6 ± 7.4 a	21.0 ± 6.5 ab	0.04
IIXB	10.4 ± 12.0 a	18.4 ± 7.6 b	20.0 ± 7.8 b	<0.01
IIB	26.6 ± 11.9 a	35.3 ± 14.0 b	23.3 ± 10.5 a	<0.01
Hybrid fibers	16.1 ± 11.7 a	20.3 ± 8.6 ab	22.3 ± 8.0 b	0.1

Values are means ± SD, n = 20 rats/group. One-way ANOVA (*P* values denote significance of differences between groups) and Fisher least significant difference post hoc were used to test for differences between pairwise groups; within a row, means with different letters differ significantly (*P*<0.05, at least)

cranialis muscle were comparable in the two obese groups (*P* > 0.05), but they were more frequent in the obese mangiferin group than in the lean control group. Together, these data indicated that mangiferin treatment prevented obesity-induced slow-to-fast fiber type transition in the white tibialis cranialis muscle, but not in the red soleus muscle.

The effects of mangiferin on the force-velocity relationship of soleus and tibialis cranialis muscles were estimated according to Hill's characteristic equation using relative frequencies of myosin-based muscle fiber types in each muscle, and compared in the three experimental groups (Fig. 7.4). As expected, predicted maximal shortening velocities (V_{\max}) were slower in the red soleus muscle than in the white tibialis cranialis muscle. In the soleus muscle, predicted maximal shortening velocities were faster in the obese control group (0.77 ± 0.05 fiber

length/s) and the obese mangiferin group (0.76 ± 0.06 fiber length/s) than in the lean control group (0.70 ± 0.05 fiber length/s; *P* < 0.001 in both), but they were comparable in the two obese groups (*P* > 0.05). In the tibialis cranialis muscle, however, predicted maximal shortening velocities were not comparable in the three groups. V_{\max} of this muscle was 9% faster in the obese control group (1.60 ± 0.07 fiber length/s) than in the lean control group (1.47 ± 0.04 fiber length/s; *P* = 0.00). As shown in Fig. 7.4, V_{\max} of tibialis cranialis muscle was intermediate in the obese mangiferin group (1.52 ± 0.05 fiber length/s), but significantly different compared with both lean control (*P* < 0.01) and obese control groups (*P* < 0.001). Again, these data demonstrate that mangiferin treatment counterbalanced obesity effects on muscle contractile profile, preserving a slower phenotype in white, not red, muscles.



▲ **Fig. 7.4 Prediction of the effects of mangiferin treatment on maximal shortening velocity (V_{max}) and the force-velocity relationship of soleus and tibialis cranialis muscles in lean, obese, and obese treated with mangiferin Zucker rats.** A: Predicted maximal shortening velocity (V_{max}) of both muscles. Values are means \pm SD ($n = 20$ rats/group); means with different letters differ significantly ($P < 0.05$, at least, Fisher least significant difference post hoc test). B: Force-velocity curves in soleus (dashed lines) and tibialis cranialis (solid lines) muscles were determined according to the Hill-type mathematical model (*inset*) [42], and compared between lean (blue lines), obese (green lines), and obese treated with mangiferin (red lines) Zucker rats. The proportion of each myosin-based muscle fiber type contributes to the whole muscle force-velocity relationship [43]. Data are expressed as means of 20 rats/group. V , shortening velocity; V_{max} , maximal shortening velocity; P , isometric tension; P_0 , maximal isometric tension.

Mangiferin increased mitochondrial oxidative enzyme activity in specific muscle fiber types

To determine the direct effect of mangiferin on muscle oxidative metabolism, we assessed the rate of histochemical SDH enzyme activity within individual muscle fiber types of soleus and tibialis cranialis muscles in the three experimental groups (Table 7.5; Fig. 7.3). The overall mean SDH activity of all muscle fiber types was significantly higher in the two groups of obese rats than in lean animals (soleus, 17%; tibialis, 19%; $P < 0.001$ in both). This obesity-related improvement of

muscle mitochondrial oxidative capacity involved (without exceptions) all soleus and tibialis cranialis muscle fiber types, with soleus muscle fibers being more oxidative than tibialis muscle fibers. In general, mean SDH activities of muscle fiber types in the two muscles were comparable in mangiferin vs placebo obese groups ($P > 0.05$). However, specific muscle fiber types, such as type IIA in soleus muscle, and types IIX and IIXB in tibialis muscle, exhibited higher mean SDH activities in the obese mangiferin group than in the obese control group (~9%, $P < 0.05$). This indicates that mangiferin had a direct effect on muscle metabolic profiles, by increasing

Table 7.5 Mangiferin effects on muscle fiber-type succinic dehydrogenase activity (OD/min) of genetic-obese rats

Fiber-Type	Lean	Obese Control	Obese Mangiferin	P value
M. soleus				
I	0.38 ± 0.04 a	0.44 ± 0.04 b	0.45 ± 0.04 b	0.00
IIA	0.45 ± 0.04 a	0.49 ± 0.06 b	0.53 ± 0.05 c	<0.001
All fiber-types	0.39 ± 0.04 a	0.45 ± 0.04 b	0.46 ± 0.04 b	0.00
M. tibialis cranialis				
IIA	0.58 ± 0.06 a	0.62 ± 0.05 b	0.62 ± 0.05 b	0.04
IIX	0.48 ± 0.10 a	0.57 ± 0.04 b	0.62 ± 0.08 c	<0.001
IIXB	0.43 ± 0.03 a	0.46 ± 0.02 b	0.50 ± 0.04 c	<0.001
IIB	0.31 ± 0.03 a	0.36 ± 0.02 b	0.37 ± 0.06 b	<0.001
All fiber types	0.44 ± 0.06 a	0.52 ± 0.05 b	0.53 ± 0.05 b	<0.001

Values are means ± SD, n = 20 rats/group. One-way ANOVA (*P* values denote significance of differences between groups) and Fisher least significant difference post hoc were used to test for differences between pairwise groups; within a row, means with different letters differ significantly (*P*<0.05, at least). For clarity, muscle fiber-types with a percentage below 5% (see **Table 7.4**) are excluded from this analysis

mitochondrial oxidative capacity of these type II fibers in genetic-obese rats.

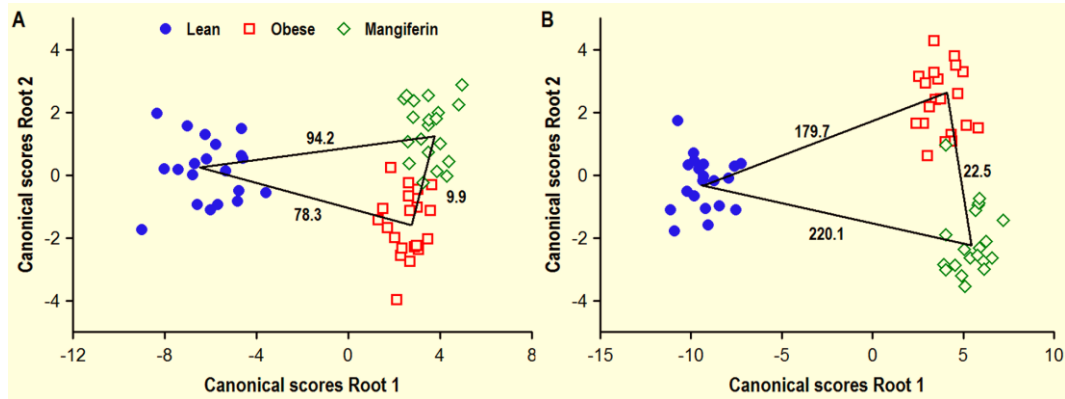
Mangiferin had a beneficial overall effect on skeletal muscle phenotypes of obese rats

To summarize quantitatively the degree of similarity or discrepancy of skeletal muscle phenotypes between the three experimental groups, a discriminant canonical analysis was conducted with data available for each muscle (**Fig. 7.5**). Near all observations (samples) analyzed in soleus and tibialis cranialis muscles (59/60 in both; 98%) were correctly discriminated in their respective experimental groups. Mahalanobis distances between group pairs confirmed significant differences of overall skeletal muscle phenotypes. Ample differences were noted between each group of obese rats (treated or not with mangiferin) and lean rats in the two muscles. Shorter, but significant, distances were also observed

between obese rats treated with mangiferin and obese control rats (9.9 in soleus and 22.5 in tibialis; *P* < 0.001 in both), indicating that mangiferin administration to obese Zucker rats, evoked a significant overall effect on size, contractile, and metabolic features of skeletal muscle fiber types.

DISCUSSION

Considerable interest in the beneficial biological activities of mangiferin, including anti-oxidant, anti-inflammatory, and anti-diabetic effects, has emerged in recent years [19-22]. However, few studies have addressed the potential ameliorative effects of this compound on obesity-related deleterious consequences in skeletal muscle [27,40]. The present investigation is to our knowledge the first study addressing the impact of mangiferin administration on skeletal muscle structure and function in animals with genetic obesity. The main



▲ **Fig. 7.5 Phenotypic classification of individual hind limb muscles of obese Zucker rats treated with mangiferin in relation to lean and obese controls by means of multivariate discriminant analysis.** Individual soleus (A) and tibialis cranialis (B) muscles of all experimental rats were classified into different groups as a function of a cohort of phenotypic muscle characteristics by means of discriminant canonical analysis. The discriminant model for the soleus muscle included the following muscle variables: wet weight, muscle-somatic index, predicted maximal shortening velocity, and percentage, lesser diameter and SDH histochemical activity of type I fibres. The same parameters were included in the statistical model for the tibialis cranialis muscles, but fiber-types IIA, IIX, IIXB and IIB were considered instead of type I fibres. The squares of the Mahalanobis distances between pairs of groups indicative of the overall phenotypic divergences are indicated; P values for the statistical significance of these comparisons between pairs of groups were always significant ($P < 0.001$).

finding was that chronic intake (8 weeks) of low-dose mangiferin (15 mg/kg BW/day) by obese Zucker rats resulted in muscle phenotypes that were significantly different compared with both obese and lean Zucker rats fed a placebo diet. This overall effect included preservation (or reversion) of obesity-induced sarcopenia in red and white muscles, and slow-to-fast fiber-type transition in white, not red, muscles, in addition of increased mitochondrial oxidative capacity in specific type II fibers in both muscle types. Thus, the authors' initial hypothesis was borne out.

The experiments were designed to administer

mangiferin not mixed with the food. This protocol has several advantages: first, the dosing is more exact and daily intake of the dose of mangiferin could be verified; second, and more important, by giving it apart we eliminated any potential effect due to decreased palatability of a mangiferin supplemented diet that could reduce food intake and thus contribute to ameliorate metabolic syndrome. In this study, mangiferin treatment resulted in a small decrease in food intake, which may be related to a potential modulatory effect of mangiferin on appetite. The dietary mangiferin dosage used in the present study (15 mg/kg BW/day) was slightly lower

compared with other studies in which dosages of up to 400 mg/kg were used [25]. In experimental trials of any pharmacophore, the use of low dosages is recommended to ensure safety against any potential toxicity. The low dosage of mangiferin used in the present study was effective in obese rats when daily administered over 8 weeks. Beneficial effects of mangiferin were also demonstrated in diabetic rats after intraperitoneal administration of 10 and 20 mg/kg for 14 days [32].

The obese Zucker rat is a well-established model of genetic obesity and Type 2 diabetes, characterized by hyperinsulinemia, hyperglycemia, and hyperlipemia, in addition to insulin resistance, as confirmed in this and other studies [4,44]. Mangiferin administration significantly improved oral glucose tolerance in glucose-loaded obese Zucker rats. In addition, it reduced plasma total cholesterol and LDL cholesterol, and increased HDL cholesterol levels in these obese animals. Moreover, mangiferin treatment also decreased circulating levels of FGF21, a potent metabolic regulator that is increased in conditions of obesity and insulin resistance [45]. These results substantiate and expand previous studies demonstrating effective anti-hyperglycemic (without inducing hypoglycemic state), anti-hyperlipidemic, and anti-atherogenic activities of mangiferin in diabetic animals [32,46]. Recent studies revealed that these beneficial actions of mangiferin are mediated by activation of AMPK signaling pathway, a metabolic sensor that regulates multiple intracellular systems including the cellular uptake of glucose and lipid utilization [35,37,39].

Ample evidence supports that inflammation plays a crucial role in muscle atrophy in patients with obesity and related metabolic dysfunctions [3,12]. It has been estimated that a 10% increase in the ratio of skeletal muscle mass to total body weight is associated with 11% reduction in the risk of insulin resistance [14]. Hence, the prevention of skeletal muscle sarcopenia has been

predicted to improve obesity-induced metabolic dysregulation [47]. Studies have shown that mangiferin decreases circulating markers of inflammation [23,25], and attenuates insulin resistance in obese mice [40]. The present study demonstrates for the first time that mangiferin can protect against obesity-induced skeletal muscle mass loss through preservation of myofiber cross-sectional size. Given that mangiferin is a potent anti-inflammatory agent that reduces inflammatory cytokines such TNF- α and IL-6 [23,25], and obesity-related inflammation promotes muscle atrophy via decreased muscle protein synthesis and increased muscle protein degradation [3], it is not unlikely that the protective effect of mangiferin against obesity-induced muscle sarcopenia could be mediated by inhibition of muscle inflammation signaling. Other natural antioxidants, such as quercetin and resveratrol, are useful for preventing skeletal muscle atrophy by suppressing inflammatory responses in obese mice [48], and promoting myogenesis and hypertrophy in murine myoblasts *in vitro* [49].

It is well known that obesity is associated with a decreased number of type I muscle fibers, and an increased proportion of type II fibers, as confirmed in this and other studies [5,9,16]. Our results further indicate that this obesity-induced slow-to-fast fiber-type transformation encompassed the full spectrum of myosin heavy chains according with the general scheme of sequential transitions of muscle fiber types: I \rightarrow I+IIA \rightarrow IIA \rightarrow IIAX \rightarrow IIX \rightarrow IIX \rightarrow IIXB \rightarrow IIB [50]. As a result, the overall predicted maximal shortening velocity of both soleus and tibialis muscles increased by ~10% in obese versus lean rats. Like for skeletal muscle mass, human studies have shown that a decreased type I-to-type II skeletal muscle fiber ratio correlates inversely with insulin resistance [10,11], suggesting that the prevention of slow-to-fast fiber-type transformation might also be useful to improve obesity-induced metabolic dysregulation. Previous *in vitro* and *in vivo* studies have

shown that mangiferin favors the activation of critical regulators of muscle fiber-type composition such as PPAR δ and PGC1 α [23,34], providing a potential mechanism for improvement the slow-to-fast muscle fiber ratio in diabetes and obesity. However, it is unknown whether mangiferin protects against obesity-related slow-to-fast muscle fiber transformation. A central finding of the present study was that mangiferin administration to obese rats resulted in an increased number of type IIA fibers and a decreased number of type IIB fibers in tibialis cranialis muscle when compared to non-supplemented obese rats. This indicates that mangiferin counteracts slow-to-fast fiber transformation in tibialis cranialis muscle of obese rats, which is confirmed by the finding that the predicted maximal shortening velocity of this muscle significantly slowed by ~5% in the obese mangiferin group compared with the obese control group. With the sole exception of the hybrid type IIXB fibers, the fiber type distribution of tibialis cranialis muscle was similar between the obese mangiferin and the lean control group. However, the predicted V_{\max} of this muscle was significantly faster by ~3.5% in the obese mangiferin than in the lean control group, indicating that mangiferin treatment preserved only partially obesity effects on muscle contractile profile.

Present design is limited to offer mechanistic links underlying variations of muscle fiber types observed in skeletal muscle of obese rats treated with mangiferin. Nevertheless, it is likely that upregulation of PPAR δ and PGC1 α receptors in tibialis cranialis muscle by mangiferin administration could be responsible for the observed difference in muscle fiber types and contractile phenotype of this muscle in obese Zucker rats. This is because mangiferin is a well-known activator of the PPAR δ -PGC1 α axis in diabetic obese rats [34], and downregulation of these receptors is one of the main reasons for the obesity-induced type I-to-type II muscle fiber transition [5,16]. Recent studies have shown that

supplementing obese Zucker rats with niacin and carnitine, two commonly prescribed drugs for the treatment of hyperlipidemia, induces the transition of fast to slow skeletal muscle fiber types through activation of PPAR δ and PGC1 α receptors [5,16].

The significance of the lack of effect of mangiferin administration to obese rats on fiber type composition and contractile profile of soleus muscle is uncertain. Given that transitions of muscle fiber types are influenced by the muscle basal status [50], these results can be related with the prominent slow-twitch phenotype of rat soleus muscle [51]. Accordingly, a more pronounced change toward a slower phenotype in the white tibialis cranialis muscle (composed primarily of fast fibers) than in the red soleus muscle (composed primarily of slow fibers) could be expected after mangiferin administration to obese rats.

The link between mitochondrial dysfunction and insulin resistance is still a matter of debate, especially in skeletal muscle, the main tissue involved in glucose homeostasis [13]. There are reports demonstrating impaired [5], unaltered [16], or increased [7,8] mitochondrial oxidative capacity in muscle from obese individuals. Possible reasons explaining this discrepancy include the different levels of physical activity between obese and lean subjects, and the choice of the parameters to be studied in evaluating mitochondrial function. A key finding of the present study was that the histochemical oxidative activity of individual muscle fibers was increased in all fiber types of red and white muscles in obese versus lean Zucker rats. This finding suggests that insulin resistance can be present without reductions in muscle mitochondrial content, and confirms that obesity per se provokes insulin resistance increasing muscle mitochondrial content and fatty acid oxidation [7]. However, intramuscular lipid accumulation occurs at much greater rate than the compensatory increase in both mitochondrial density and the rate of mitochondrial fatty acid β -oxidation [7].

The present study revealed that mangiferin improves skeletal muscle oxidative capacity in genetic-obese rats through increased SDH activity, a key enzyme of the Krebs's cycle, in specific muscle fiber types. An unbiased proteomics study also reported that mangiferin upregulates protein participating in mitochondrial bioenergetics, including the enzyme SDH [41]. Interestingly, mangiferin is a potent activator of the AMPK-PGC1 α pathway [23,34,37,38], and there is ample evidence that PPAR δ -PGC1 α receptors, together with AMPK, are critical regulators of mitochondrial biogenesis [see Ref. 15 for recent review]. Rasbach et al. reported that overexpression of PGC1 α caused a shift toward increased oxidative types of skeletal muscle fibers [17]. Consequently, it is coherent that positive effects of mangiferin on skeletal muscle cell oxidative capacity are mediated by the activation of the AMPK-PGC1 α pathway. Studies shown that other dietary antioxidants such as sudachitin and proanthocyanidins improve skeletal muscle mitochondrial biogenesis in obese rats through increased expression of PGC1 α and AMPK [52,53].

In conclusion, our study is the first to demonstrate that mangiferin significantly attenuated adverse skeletal muscle changes in obese rats. This action included preservation of both skeletal muscle mass and muscle fiber-type composition, and enhanced oxidative capacity in muscle fibers. Although mechanistic links could not be established, it is hypothesized that these protective effects of mangiferin on skeletal muscle structure and function can be associated with inhibition of inflammatory signaling pathways and activation of the AMPK-PGC1 α axis. Thus, mangiferin may be an useful dietary component for preventing obesity-associated deleterious skeletal muscle changes, hence improving obesity-induced metabolic dysregulation.

MATERIALS AND METHODS

Ethics

All experimental protocols were reviewed and approved by the Ethics Committee for Animal Research of the University of Cordoba (Cordoba, Spain). They followed the guidelines laid down by the Higher Council of Scientific Research of Spain following the normal procedures directing animal welfare (Real Decreto 223/88, BOE of 18 of March) and adhered to the recommendations included in the Guide for Care and Use of Laboratory Animals (US Department of Health and Human Services, NIH) and European laws and regulations on protection of animals, under the advice of specialized personnel.

Animals and design

Two strains of rats were used in this study: Zucker rats with the obese (*fa/fa*) phenotype ($n=40$) and Zucker rats with the lean (*Fa/Fa* or *Fa/fa*) phenotype ($n=20$). All rats were females and aged 8-10 weeks at the beginning of the experiment. Animals (Harlan Laboratories Models, Barcelona, Spain) were individually housed in standard vivarium cages in a temperature- and humidity-controlled environment, with a 12:12-h light-dark cycle and given *ad libitum* access to standard rat diet (Altromin Spezialfutter GmbH, Germany; values per 100 g: energy 351.8 kcal 1100 kJ⁻¹, protein content 18%, lysine 1.74%, methionine 1.0%, cysteine 0.31%, tryptophan 0.20%, fat 5%, ash 4.5%, sodium 0.24%, calcium 0.6%, phosphorus 0.6%) and tap water.

Before the experiment began, all rats were maintained for 2 weeks on the standard diet. Afterwards, obese Zucker rats were randomly divided in two groups of 20 rats each. In addition, 20 lean Zucker rats were used for the lean control group. Rats were trained to eat gelatin pellets, which they perceived as a treat. Gelatin pellets were prepared from cooking gelatin (McCormick España

SA, Sabadell, Spain) and distilled water using gelatin molds. Each gelatin pellet was made of 160 mg of powdered gelatin and 2 ml water. Two types of pellets which were externally undistinguishable were prepared: pellets containing mangiferin (Neuron Bio S.A, Granada, Spain) and pellets without mangiferin (placebo). The amount of mangiferin within each pellet was adjusted for each rat to provide a dose of 15 mg/kg BW. Rats in the lean control and the obese control groups were maintained for 8 weeks on the standard diet and received the placebo pellets daily. Obese rats in the treatment group received the standard diet and the pellets with mangiferin daily for 8 weeks. Rats were fed ad libitum and the pellets (mangiferin or placebo) were administered once daily in the morning. Food intake was recorded daily and the animals were weighed every two weeks.

Blood biochemistry

At the beginning of the experiment, a blood sample was obtained from the jugular sinus with the rat under anesthesia (inhaled sevoflurane), and served to compare blood biochemical variables before and after the 8-weeks experimental period. One week before the end of the experiment (week 7) glucose tolerance tests were performed in a subset of rats ($n = 10$ rats/group) in the two groups of obese rats. Briefly, rats were fasted, a baseline blood sample was obtained and an oral dose (2 g/kg) of glucose (Acofarma, Tarrasa, Spain) was administered in the form of gelatin pellets. Pellets were prepared as above described and were supplemented with glucose instead of mangiferin. Again, the amount of glucose added to the gelatin pellet was adjusted individually to provide a dose of 2g/kg. Subsequently 4 blood samples were drawn at 30, 60, 90 and 150 minutes after eating the glucose pellet. Blood samples were obtained by puncture of a tail vein and glucose was measured in whole blood using a glucometer (Arkray Factory Inc, Japan).

At 8 weeks, all rats were sacrificed by aortic puncture and exsanguination under deep general anaesthesia (sodium thiopental 50 mg kg⁻¹, Pentotal®, Abbot, Illinois, USA; ip). Blood samples were obtained from the abdominal aorta in heparinized syringes at the time of the euthanasia. Plasma separated by centrifugation was used for measurements of glucose, cholesterol and triglyceride levels by spectrophotometry (Biosystems, Barcelona, Spain), insulin and leptin concentrations by radioimmunoassay (Millipore, St. Charles, MO, USA), and fibroblastic growth factor 21 (FGF21) by ELISA (Millipore, St. Charles, MO, USA).

Muscle sampling and tissue preparation

Muscle samples were obtained at the time of sacrifice. Soleus and tibialis cranialis muscles were dissected and individual muscles were wet weighted. These muscles were selected as two representative muscles of a typical red, slow-twitch muscle (soleus, composed primarily of slow-twitch muscle fibers) and a characteristic white, fast-twitch muscle (tibialis cranialis, composed primarily of fast-twitch muscle fibers in its white region), respectively [51]. Also because these two hind limb muscles are opposite regarding their resting functional activities, and have a different energetic dependence on blood borne substrates [see Ref. 51].

Upon collection, tissue blocks from the muscle belly were mounted on cork blocks with the use of OCT embedding medium (Tissue-Tek II, Miles Laboratories, Naperville, IL, USA) and oriented so that myofibers could be cut transversely. Specimens were systematically frozen by immersion in isopentane (30 s), kept at the freezing point in liquid nitrogen, and stored at -80 °C until analyzed. Muscle samples were routinely frozen between 2 and 4 min after removal, because it has been demonstrated that the interval between removal and freezing has a significant (negative) effect on skeletal muscle fiber size [54]. All muscle sampling and muscle

preparation procedures were always carried out by the same investigator, experienced in skeletal muscle biopsy studies, taking care to standardize both the location and the freezing of the sample.

Myosin heavy chain (MHC) immunohistochemistry

Muscle samples were serially sectioned (10- μ m-thick) in a cryostat (Frigocut, Reichert Jung, Nubloch, Germany) at -20°C and used for immunohistochemistry. Immunohistochemistry was performed with five monoclonal antibodies specific against MHC isoforms: BA-D5 (DMS, Braunschweig, Germany; anti-MHC-I), SC-71 (DMS; anti-MHC-IIa), BF-35 (DMS; anti-MHCs-I plus -IIa and -IIb), S5-8H2 (Biocytex Biotechnology, Marseille, France; anti-MHCs-I plus -IIx and -IIb), and BF-F3 (DMS; anti-MHC-IIb). The specificity of these monoclonal antibodies for MHCs in rat skeletal muscle has previously been reported [55-57]. The immunoperoxidase staining protocol with avidin-biotin complex (ABC) protocol was used as previously described [58].

Quantitative enzyme histochemistry

Additional serial sections were used for quantitative enzyme histochemistry. The activity of the enzyme succinate dehydrogenase (SDH, EC 1.3.4.1), used as an oxidative marker, was determined on 10- μ m-thick sections, by using quantitative histochemical methods previously adjusted and validated in rat skeletal muscle [58].

Image analysis and morphometry

Sections were examined in a blind fashion by the same investigator (L.M.A.), who had experience of the normal appearance of mammalian skeletal muscle fibers. All serial sections for immunohistochemistry and enzyme histochemistry were visualized and digitized as previously described [59]. A region containing between

450 and 650 fibers was selected for further analyses. In the tibialis cranialis muscle, this area was selected from the core of the white (superficial) portion of the muscle, since it contains a higher number of fast-twitch muscle fibers (98%) than the red (deep) portion (93%) of the muscle [51]. Images were saved as digitized frames at 256 gray levels. The gray levels were converted to optical density (OD) units by using a calibrated set of OD filters. The digitized images of the fibers in the histochemical reaction (SDH) within the selected region were traced manually and analyzed for the lesser fiber diameter and the average OD for each individual muscle fiber. The average fiber OD for each histochemical reaction was determined as the average OD for all pixels within the traced fiber from three sections incubated with substrate minus the average OD for all pixels of the same fiber from other two sections incubated without substrate [58]. Because a number of factors can influence the reliability of histochemical enzyme activity determinations, we checked the variability on three consecutive sections for the SDH histochemical reaction by repeated measurements of the same individual fibers. Only coefficients of variation for triplicate measurements of ODs below 5% were accepted in the present study; this demonstrated the high analytical precision that can be achieved for the measurement of fiber OD on enzyme histochemical sections.

The fibers in the selected area were classified according to their MHC content by means of visual examination of immunostainings of the five serial sections stained with the battery of anti-MHC monoclonal antibodies as previously described [55,56]. The reactivity of each individual muscle fiber in these five consecutive sections was judged as positive or negative by comparing the intensity of the reaction of neighbouring fibers. Seven fiber types were categorized, four of them as pure fibers expressing a unique MHC isoform (i.e., type I, IIA, IIX and IIB), and other three as

hybrid phenotypes co-expressing two different MHC isoforms (type I+IIA, IIAX and IIXB).

The relative frequency of different muscle fiber types in the selected region was used to numerically express the fiber type composition of each muscle sample. The lesser fiber diameter of the same fibers was averaged according to fiber type. Individual SDH ODs of muscle fibers were averaged according to the MHC muscle fiber-type and used for statistical analyses. For minor fiber types (I+IIA and IIA in the soleus muscle, and I, I+IIA and IIAX in the tibialis cranialis muscle), there were so few fibres in most muscle samples that a statistically reliable determination of their lesser diameter and SDH activities was impossible. In consequence, muscle fibre-types showing, on average, a fibre percentage below 5% were excluded from these analyses. A polymorphism index for obese and lean animals was calculated in each muscle by dividing the number of hybrid fibers expressing more than one MHC isoform by the total number of fibers in the muscle sample [43].

Prediction of muscle shortening velocity

In an attempt to provide a functional assessment of the variation of myosin-based muscle fiber distribution on muscle's shortening speed, we used the following equation to predict the maximal shortening velocity (V_{\max} Muscle) of soleus and tibialis cranialis muscles [43], according to the mathematical model proposed by A. V. Hill [60]:

$$V_{\max} \text{ Muscle} = \sum [\%_{fi} \times V_{\max ft}] / 100$$

where $\%_{fi}$ is the proportion of each fiber type in Muscle, and $V_{\max ft}$ is the maximal shortening velocity for a given fiber type (fiber length s^{-1}). Values from Botinelli et al. [61] were used for $V_{\max ft}$, and $V_{\max ft}$ of hybrid fibers were averaged between V_{\max} of their respective pure fiber-types. In this model, soleus and extensor digitorum longus

muscles were used as representative slow-twitch and fast-twitch muscles, respectively [42]. Fiber-type composition are comparable in rat extensor digitorum longus and tibialis cranialis muscles [51].

Statistical analyses

All statistics and charts were run on Statistica 7.0 for Windows (StatSoft I, Statistica, Data software System, www.statsoft.com). Muscle sample was the unit of analysis for the present dataset. A total of 120 muscle samples (60 animals x two muscles –soleus and tibialis cranialis) were available for statistical analysis. Sample size and the power of a contrast of hypothesis were estimated by power analysis and interval estimation of the statistical software employed. Accepting an α -risk of 0.05 and a β -risk of 0.2 in a two-sided test, 20 subjects/group were considered necessary to recognize as statistically significant a difference greater than or equal to 0.05 OD units for SDH histochemical activity between any pair of groups assuming that 3 groups exists. The common standard deviation (SD) was assumed to be 0.06 and it was anticipated a drop-out rate of 0%. Normality of muscle variables was tested using a Kolmogorov-Smirnov test and data were expressed as means \pm SD. Unpaired t-test were used to test for differences of plasma variables between groups and before and after treatment with either mangiferin or placebo. One-way ANOVA was used to test for differences of muscle variables between groups at the end of the experimental period. When either a significant ($P < 0.05$) or a marginal ($0.05 < P < 0.1$) effect was observed, the Fisher least significant difference post hoc test was used to locate specific significant differences between pairwise groups.

Overall differences among experimental groups were estimated by squared Mahalanobis coefficients provided by multivariate discriminant analyses of the two hind limb muscles. This distance take into account all muscle fiber-type variables summarizing the overall phenotype of

each individual muscle sample, allowing its classification into one of the three groups. These coefficients served to compare overall muscle characteristics of group pairs to establish their homologies and differences regarding the control skeletal muscle phenotype.

ACKNOWLEDGMENTS

The authors thank Neuron Bio S.A. for kindly providing the mangiferin used in the present study.

FUNDING

The work reported here was supported by a Spanish Government Grant from the Instituto de Salud Carlos III (PI14/00467) with co-financing from European Funds. L.M.A., and J.L.L.R. were supported by grants of the PAI Group CTS-179 and Project P10-AGR-5963, Junta de

Andalucia, Spain.

DISCLOSURES

None of the authors has a financial or personal relationship with other people or organisation that could inappropriately influence or bias the content of the paper.

AUTHOR CONTRIBUTIONS

Conception and design of research: LMA EA-T J-LLR. Revised the literature: LMA J-LLR. Performed experiments LMA AR. Performed laboratory analyses: LMA AR J-LLR. Analysed data and interpreted results: LMA EA-T J-LLR. Prepared tables and figures: LMA AR J-LLR. Drafted manuscript: LMA EA-T J-LLR. All authors edited and revised critically the manuscript and approved its final version.

REFERENCES

1. Couturier A, Ringseis R, Mooren FC, Kruger K, Most E, et al. (2013) Carnitine supplementation to obese Zucker rats prevents obesity-induced type I to type II muscle fiber transition and favors an oxidative phenotype of skeletal muscle. *Nutr Metab (Lond)* 10: 48.
2. Denies MS, Johnson J, Maliphol AB, Bruno M, Kim A, et al. (2014) Diet-induced obesity alters skeletal muscle fiber types of male but not female mice. *Physiol Rep* 2: e00204.
3. Perry BD, Caldow MK, Brennan-Speranza TC, Sbraglia M, Jerums G, et al. (2016) Muscle atrophy in patients with Type 2 Diabetes Mellitus: roles of inflammatory pathways, physical activity and exercise. *Exerc Immunol Rev* 22: 94-109.
4. Pompeani N, Rybalka E, Latchman H, Murphy RM, Croft K, et al. (2014) Skeletal muscle atrophy in sedentary Zucker obese rats is not caused by calpain-mediated muscle damage or lipid peroxidation induced by oxidative stress. *J Negat Results Biomed* 13: 19.
5. Ringseis R, Rosenbaum S, Gessner DK, Herges L, Kubens JF, et al. (2013) Supplementing obese Zucker rats with niacin induces the transition of glycolytic to oxidative skeletal muscle fibers. *J Nutr* 143: 125-131.
6. Wessels B, Ciapaitė J, van den Broek NM, Houten SM, Nicolay K, et al. (2015) Pioglitazone treatment restores in vivo muscle oxidative capacity in a rat model of diabetes. *Diabetes Obes Metab* 17: 52-60.
7. Holloway GP, Bonen A, Spriet LL (2009) Regulation of skeletal muscle mitochondrial fatty acid metabolism in lean and obese individuals. *Am J Clin Nutr* 89: 455S-462S.
8. Lally JS, Snook LA, Han XX, Chabowski A, Bonen A, et al. (2012) Subcellular lipid droplet distribution in red and white muscles in the obese Zucker rat. *Diabetologia* 55: 479-488.
9. Oberbach A, Bossenz Y, Lehmann S, Niebauer J, Adams V, et al. (2006) Altered fiber distribution and fiber-specific glycolytic and oxidative enzyme activity in skeletal muscle of patients with type 2 diabetes. *Diabetes Care* 29: 895-900.
10. Hickey MS, Carey JO, Azevedo JL, Houmard JA, Pories WJ, et al. (1995) Skeletal muscle fiber composition is related to adiposity and in vitro glucose transport rate in humans. *Am J Physiol* 268: E453-457.
11. Lillioja S, Young AA, Culter CL, Ivy JL, Abbott WG, et al. (1987) Skeletal muscle capillary density and fiber type are possible determinants of in vivo insulin resistance in man. *J Clin Invest* 80: 415-424.
12. Lumeng CN, Saltiel AR (2011) Inflammatory links between obesity and metabolic disease. *J Clin Invest* 121: 2111-2117.
13. Martins AR, Nachbar RT, Gorjao R, Vinolo MA, Festuccia WT, et al. (2012) Mechanisms underlying skeletal muscle insulin resistance induced by fatty acids: importance of the mitochondrial function. *Lipids Health Dis* 11: 30.
14. Atlantis E, Martin SA, Haren MT, Taylor AW, Wittert GA (2009) Inverse associations between muscle mass, strength, and the metabolic syndrome. *Metabolism* 58: 1013-1022.
15. Valero T (2014) Mitochondrial biogenesis: pharmacological approaches. *Curr Pharm Des* 20: 5507-5509.
16. Couturier A, Ringseis R, Mooren FC, Kruger K, Most E, et al. (2014) Correction: Carnitine supplementation to obese Zucker rats prevents obesity-induced type I to type II muscle fiber transition and favors an oxidative phenotype of skeletal muscle. *Nutr Metab (Lond)* 11: 16.
17. Rasbach KA, Gupta RK, Ruas JL, Wu J, Naseri E, et al. (2010) PGC-1 α regulates a HIF2 α -dependent switch in skeletal muscle fiber types. *Proc Natl Acad Sci U S A* 107: 21866-21871.
18. Evans RM, Barish GD, Wang YX (2004) PPARs and the complex journey to obesity. *Nat Med* 10: 355-361.
19. Shah KA, Patel MB, Patel RJ, Parmar PK (2010) *Mangifera indica*

Chapter 7

- (mango). *Pharmacogn Rev* 4: 42-48.
20. Stohs SJ, Ray S (2015) Anti-diabetic and Anti-hyperlipidemic Effects and Safety of *Salacia reticulata* and Related Species. *Phytother Res* 29: 986-995.
 21. Vyas A, Syeda K, Ahmad A, Padhye S, Sarkar FH (2012) Perspectives on medicinal properties of mangiferin. *Mini Rev Med Chem* 12: 412-425.
 22. Benard O, Chi Y (2015) Medicinal properties of mangiferin, structural features, derivative synthesis, pharmacokinetics and biological activities. *Mini Rev Med Chem* 15: 582-594.
 23. Mahali SK, Verma N, Manna SK (2014) Advanced glycation end products induce lipogenesis: regulation by natural xanthone through inhibition of ERK and NF-kappaB. *J Cell Physiol* 229: 1972-1980.
 24. Pal PB, Sinha K, Sil PC (2014) Mangiferin attenuates diabetic nephropathy by inhibiting oxidative stress mediated signaling cascade, TNFalpha related and mitochondrial dependent apoptotic pathways in streptozotocin-induced diabetic rats. *PLoS One* 9: e107220.
 25. Tsubaki M, Takeda T, Kino T, Itoh T, Imano M, et al. (2015) Mangiferin suppresses CIA by suppressing the expression of TNF-alpha, IL-6, IL-1beta, and RANKL through inhibiting the activation of NF-kappaB and ERK1/2. *Am J Transl Res* 7: 1371-1381.
 26. Sellamuthu PS, Arulselvan P, Kamalraj S, Fakurazi S, Kandasamy M (2013) Protective nature of mangiferin on oxidative stress and antioxidant status in tissues of streptozotocin-induced diabetic rats. *ISRN Pharmacol* 2013: 750109.
 27. Guo F, Huang C, Liao X, Wang Y, He Y, et al. (2011) Beneficial effects of mangiferin on hyperlipidemia in high-fat-fed hamsters. *Mol Nutr Food Res* 55: 1809-1818.
 28. Kumar BD, Krishnakumar K, Jaganathan SK, Mandal M (2013) Effect of Mangiferin and Mahanimbine on Glucose Utilization in 3T3-L1 cells. *Pharmacogn Mag* 9: 72-75.
 29. Miura T, Ichiki H, Hashimoto I, Iwamoto N, Kato M, et al. (2001) Antidiabetic activity of a xanthone compound, mangiferin. *Phytomedicine* 8: 85-87.
 30. Miura T, Ichiki H, Iwamoto N, Kato M, Kubo M, et al. (2001) Antidiabetic activity of the rhizoma of *Anemarrhena asphodeloides* and its glucoside. *Biol Pharm Bull* 24: 1009-1011.
 31. Miura T, Iwamoto N, Kato M, Ichiki H, Kubo M, et al. (2001) The suppressive effect of mangiferin with exercise on blood lipids in type 2 diabetes. *Biol Pharm Bull* 24: 1091-1092.
 32. Muruganandan S, Srinivasan K, Gupta S, Gupta PK, Lal J (2005) Effect of mangiferin on hyperglycemia and atherogenicity in streptozotocin diabetic rats. *J Ethnopharmacol* 97: 497-501.
 33. Sellamuthu PS, Arulselvan P, Fakurazi S, Kandasamy M (2014) Beneficial effects of mangiferin isolated from *Salacia chinensis* on biochemical and hematological parameters in rats with streptozotocin-induced diabetes. *Pak J Pharm Sci* 27: 161-167.
 34. Huang TH, Peng G, Li GQ, Yamahara J, Roufogalis BD, et al. (2006) *Salacia oblonga* root improves postprandial hyperlipidemia and hepatic steatosis in Zucker diabetic fatty rats: activation of PPAR-alpha. *Toxicol Appl Pharmacol* 210: 225-235.
 35. Han J, Yang N, Zhang F, Zhang C, Liang F, et al. (2015) Rhizoma *Anemarrhenae* extract ameliorates hyperglycemia and insulin resistance via activation of AMP-activated protein kinase in diabetic rodents. *J Ethnopharmacol* 172: 368-376.
 36. Han J, Yi J, Liang F, Jiang B, Xiao Y, et al. (2015) X-3, a mangiferin derivative, stimulates AMP-activated protein kinase and reduces hyperglycemia and obesity in db/db mice. *Mol Cell Endocrinol* 405: 63-73.
 37. Niu Y, Li S, Na L, Feng R, Liu L, et al. (2012) Mangiferin decreases plasma free fatty acids through

Protective effects of mangiferin on skeletal muscle of obese rats

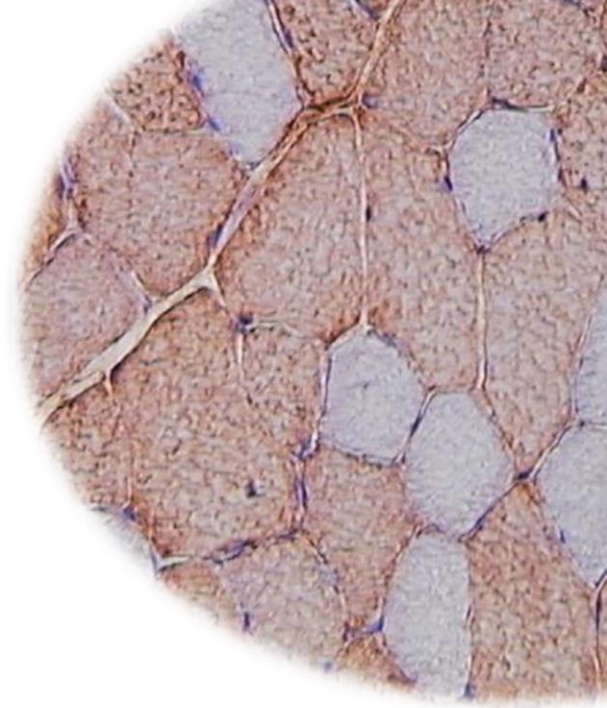
- promoting its catabolism in liver by activation of AMPK. *PLoS One* 7: e30782.
38. Wang F, Yan J, Niu Y, Li Y, Lin H, et al. (2014) Mangiferin and its aglycone, norathyriol, improve glucose metabolism by activation of AMP-activated protein kinase. *Pharm Biol* 52: 68-73.
39. Giron MD, Sevillano N, Salto R, Haidour A, Manzano M, et al. (2009) Salacia oblonga extract increases glucose transporter 4-mediated glucose uptake in L6 rat myotubes: role of mangiferin. *Clin Nutr* 28: 565-574.
40. Apontes P, Liu Z, Su K, Benard O, Youn DY, et al. (2014) Mangiferin stimulates carbohydrate oxidation and protects against metabolic disorders induced by high-fat diets. *Diabetes* 63: 3626-3636.
41. Lim J, Liu Z, Apontes P, Feng D, Pessin JE, et al. (2014) Dual mode action of mangiferin in mouse liver under high fat diet. *PLoS One* 9: e90137.
42. Jakubiec-Puka A, Ciechomska I, Mackiewicz U, Langford J, Chomontowska H (1999) Effect of thyroid hormone on the myosin heavy chain isoforms in slow and fast muscles of the rat. *Acta Biochim Pol* 46: 823-835.
43. Caiozzo VJ, Baker MJ, Huang K, Chou H, Wu YZ, et al. (2003) Single-fiber myosin heavy chain polymorphism: how many patterns and what proportions? *Am J Physiol Regul Integr Comp Physiol* 285: R570-580.
44. Durham HA, Truett GE (2006) Development of insulin resistance and hyperphagia in Zucker fatty rats. *Am J Physiol Regul Integr Comp Physiol* 290: R652-658.
45. Angelin B, Larsson TE, Rudling M (2012) Circulating fibroblast growth factors as metabolic regulators--a critical appraisal. *Cell Metab* 16: 693-705.
46. Aderibigbe AO, Emudianughe TS, Lawal BA (1999) Antihyperglycaemic effect of *Mangifera indica* in rat. *Phytother Res* 13: 504-507.
47. Sishi B, Loos B, Ellis B, Smith W, du Toit EF, et al. (2011) Diet-induced obesity alters signalling pathways and induces atrophy and apoptosis in skeletal muscle in a prediabetic rat model. *Exp Physiol* 96: 179-193.
48. Le NH, Kim CS, Park T, Park JH, Sung MK, et al. (2014) Quercetin protects against obesity-induced skeletal muscle inflammation and atrophy. *Mediators Inflamm* 2014: 834294.
49. Montesano A, Luzi L, Senesi P, Mazzocchi N, Terruzzi I (2013) Resveratrol promotes myogenesis and hypertrophy in murine myoblasts. *J Transl Med* 11: 310.
50. Pette D, Staron RS (2001) Transitions of muscle fiber phenotypic profiles. *Histochem Cell Biol* 115: 359-372.
51. Delp MD, Duan C (1996) Composition and size of type I, IIA, IID/X, and IIB fibers and citrate synthase activity of rat muscle. *J Appl Physiol* (1985) 80: 261-270.
52. Casanova E, Baselga-Escudero L, Ribas-Latre A, Cedo L, Arola-Arnal A, et al. (2014) Chronic intake of proanthocyanidins and docosahexaenoic acid improves skeletal muscle oxidative capacity in diet-obese rats. *J Nutr Biochem* 25: 1003-1010.
53. Tsutsumi R, Yoshida T, Nii Y, Okahisa N, Iwata S, et al. (2014) Sudachitin, a polymethoxylated flavone, improves glucose and lipid metabolism by increasing mitochondrial biogenesis in skeletal muscle. *Nutr Metab (Lond)* 11: 32.
54. Larsson L, Skogsberg C (1988) Effects of the interval between removal and freezing of muscle biopsies on muscle fibre size. *J Neurol Sci* 85: 27-38.
55. Acevedo LM, Lopez I, Peralta-Ramirez A, Pineda C, Chamizo VE, et al. (2016) High-phosphorus diet maximizes and low-dose calcitriol attenuates skeletal muscle changes in long-term uremic rats. *J Appl Physiol* (1985): jap 00957 02015.
56. Acevedo LM, Peralta-Ramirez A, Lopez I, Chamizo VE, Pineda C, et al. (2015) Slow- and fast-twitch hindlimb skeletal muscle phenotypes 12 wk after (5/6) nephrectomy in

Chapter 7

- Wistar rats of both sexes. *Am J Physiol Renal Physiol* 309: F638-647.
57. Schiaffino S, Gorza L, Sartore S, Saggin L, Ausoni S, et al. (1989) Three myosin heavy chain isoforms in type 2 skeletal muscle fibres. *J Muscle Res Cell Motil* 10: 197-205.
58. Rivero JL, Talmadge RJ, Edgerton VR (1999) Interrelationships of myofibrillar ATPase activity and metabolic properties of myosin heavy chain-based fibre types in rat skeletal muscle. *Histochem Cell Biol* 111: 277-287.
59. Acevedo LM, Rivero JL (2006) New insights into skeletal muscle fibre types in the dog with particular focus towards hybrid myosin phenotypes. *Cell Tissue Res* 323: 283-303.
60. Hill AV (1938) The heat of shortening and the dynamic constants of muscle. *Proc R Soc Lond B Biol Sci* 126: 136-195.
61. Bottinelli R, Schiaffino S, Reggiani C (1991) Force-velocity relations and myosin heavy chain isoform compositions of skinned fibres from rat skeletal muscle. *J Physiol* 437: 655-672.

CAPÍTULO 8

Conclusiones



Considerando los estudios complementarios que integran la presente tesis doctoral, se obtienen las siguientes conclusiones.

CONCLUSIONES ESTUDIO 1

1. La respuesta adaptativa a la uremia del músculo esquelético de rata durante la fase “estable” de la insuficiencia renal crónica (12 semanas post-cirugía) adquiere la modalidad de remodelación sin atrofia o con mínima hipertrofia, en la que las miofibras no cambian (o aumentan mínimamente) en tamaño, pero adquieren características contráctiles y metabólicas marcadamente distintas, acompañadas por una disminución de la capilaridad.
2. Esta remodelación es músculo-específica. Mientras en el músculo rápido resultó en una intensa transformación tipo-fibrilar lenta a rápida, en una conversión enzimática oxidativa a glucolítica y en una reducción de la densidad capilar, en el músculo lento el mismo estímulo urémico indujo una disminución del cociente metabólico oxidativo/glucolítico, acompañada de discreta transformación tipo-fibrilar rápida a lenta, hipertrofia fibrilar y proliferación mionuclear.
3. Los cambios observados en ambos músculos secundarios a la uremia fueron más pronunciados en machos que en hembras, mostrando clara evidencia que la reducción de los niveles de testosterona observada en ratas urémicas macho, pero no en hembras, desempeñó un papel importante en la plasticidad muscular inducida por uremia crónica.
4. Los niveles disminuidos del factor inducible de hipoxia 1α observados en el músculo rápido de ratas urémicas explican la limitación angiogénica de este músculo, pero no explican los cambios musculares observados en los tipos de fibras, enzimas metabólicas y tamaño fibrilar de estos animales, lo que sugiere una clara alteración en la respuesta celular a la hipoxia en músculos urémicos.

CONCLUSIONES ESTUDIO 2

1. La hiperfosfatemia intensifica los cambios en músculos esqueléticos de ratas con uremia mantenida durante 12 semanas, incluyendo una profunda transformación tipo-fibrilar lenta a rápida, atrofia fibrilar selectiva, disminución del tamaño del dominio mionuclear, del cociente metabólico oxidativo/glucolítico y de la capilarización de las fibras musculares.
2. Por su parte, la administración de dosis bajas de calcitriol (10 ng/kg, 3 días/semana, intraperitoneal) atenuó significativamente los cambios adversos en músculos esqueléticos de ratas urémicas alimentadas con una dieta alta en fósforo durante 12 semanas. Este efecto, que fue más evidente en el músculo rápido que en el músculo lento, incluyó la estabilización de las proporciones de los tipos de fibras musculares, hipertrofia fibrilar discreta, aumento del tamaño del dominio mionuclear, mejora del cociente metabólico oxidativo/glucolítico y neovascularización de las fibras musculares.

CONCLUSIONES ESTUDIO 3

1. La respuesta adaptativa del músculo esquelético de rata a la obesidad adquiere la forma de una inhibición generalizada del desarrollo de la fibra muscular y un cambio significativo hacia un fenotipo tipo-fibrilar de perfil más rápido. Estos cambios ocurrieron en paralelo con una modificación hacia un fenotipo metabólico más oxidativo, indicativo de un incremento del contenido mitocondrial en músculos esqueléticos.
2. Es destacable que las adaptaciones musculares secundarias a la obesidad fueron inespecíficas con respecto a la estructura y función del músculo.

CONCLUSIONES ESTUDIO 4

1. La suplementación de la dieta con dosis bajas de mangiferina (15 mg/kg de peso vivo/día, oral) durante 8 semanas atenúa significativamente los cambios

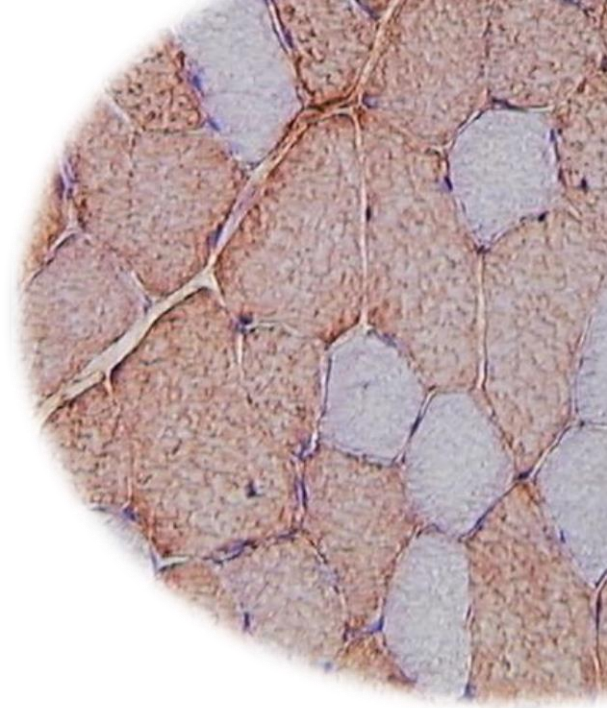
Capítulo 8

adversos observados en músculos esqueléticos rojo y blanco secundarios a la obesidad. Esta acción consistió en la conservación de la masa muscular esquelética y de la composición de los tipos de fibras musculares, así como en la mejora de la capacidad oxidativa de las fibras musculares.

2. En consecuencia, la mangiferina puede ser un suplemento dietético de utilidad para prevenir los cambios adversos que ocurren en músculos esqueléticos secundarios a la obesidad, mejorando así las alteraciones metabólicas asociadas a este problema de salud.

CHAPTER 9

Resumen - Summary



RESUMEN

Resumen Estudio 1

Acevedo LM, Peralta-Ramírez A, López I, Chamizo VE, Pineda C, Rodríguez-Ortiz ME, Rodríguez M, Aguilera-Tejero E, Rivero JL. Fenotipos de músculos esqueléticos del miembro pelviano de perfiles lento y rápido tras 12 semanas de nefrectomía 5/6 en ratas Wistar de ambos sexos. *Am J Physiol Renal Physiol* 309:F638-F647, 2015.

Este estudio describe las adaptaciones de los tipos de fibras en músculos del miembro pelviano, la interacción del sexo, y el posible papel que la hipoxia juega en esta respuesta en ratas con nefrectomía subtotal de 5/6 durante 12 semanas (Nx). Se valoraron los rasgos contráctiles, metabólicos y morfológicos de los tipos de fibras en los músculos sóleo (lento) y tibial craneal (rápido) de ratas Nx, y se compararon con animales controles con operación simulada. Ratas de ambos sexos fueron evaluadas en los dos grupos. En el músculo tibial de las ratas Nx se observó una transformación tipo-fibrilar lenta a rápida, la cual fue especialmente manifiesta en machos. Esta adaptación se acompañó de una disminución de la capacidad oxidativa y densidad capilar, un incremento de la capacidad glucolítica, y no se percibieron cambios en el tamaño y densidad nuclear de los distintos tipos de fibras musculares. También se observó una transformación metabólica oxidativa a glucolítica en las fibras del músculo sóleo de las ratas Nx macho, pero no en las hembras. Los niveles séricos de testosterona disminuyeron el 50% de su valor basal en las ratas Nx macho, pero no en las hembras. El nivel de proteínas del factor inducible de hipoxia 1α disminuyó un 42% en el músculo tibial de las ratas Nx machos. Los resultados demuestran que 12 semanas de Nx inducen una respuesta adaptativa músculo-específica en la que las miofibras no cambian (o aumentan mínimamente) en tamaño y densidad nuclear, pero adquieren características

contráctiles y metabólicas marcadamente diferentes, que se acompañan de una disminución del lecho capilar. Tanto la función muscular como el sexo desempeñan papeles importantes en estas adaptaciones.

Palabras claves: Insuficiencia renal crónica; cadena pesada de miosina; plasticidad muscular; hormonas gonadales; factor inducible de hipoxia 1α .

Resumen Estudio 2

Acevedo LM, López I, Peralta-Ramírez A, Pineda C, Chamizo VE, Rodríguez M, Aguilera-Tejero E, Rivero JL. Una dieta alta en fósforo potencia y bajas dosis de calcitriol atenúan los cambios en músculos esqueléticos de ratas con uremia prolongada. *J Appl Physiol* 120: 1059-1069, 2016.

Pese a que los trastornos del metabolismo mineral y del músculo esquelético son comunes en la enfermedad renal crónica (ERC), su posible relación no ha sido investigada. Las elevaciones plasmáticas de fosfato, hormona paratiroidea y factor de desarrollo fibroblástico 23, junto con unos niveles disminuidos de calcitriol en plasma, son rasgos habituales de la ERC. El elevado consumo de fósforo es un factor que favorece la progresión de esta enfermedad. Este estudio fue diseñado para determinar la influencia de un elevado consumo de fósforo sobre el músculo y para investigar también si la suplementación con calcitriol contrarresta los cambios negativos que acontecen en músculos esqueléticos asociados a la uremia prolongada. Para ello, se examinaron las proporciones y los rasgos metabólicos y contráctiles de los tipos de fibras en los músculos sóleo (lento) y tibial craneal (rápido) de ratas urémicas (sometidas a una nefrectomía subtotal de 5/6, Nx), y se compararon con ratas controles con operaciones simuladas (So). Tres grupos de ratas Nx recibieron una dieta estándar en fósforo (0.6%, Nx-Sd), o una dieta alta en fósforo (0.9%, Nx-Pho), o una dieta alta en fósforo más calcitriol (10 ng/kg 3 días/semana intraperitoneal,

Nx-Pho + Cal) durante 12 semanas. Dos grupos de ratas So recibieron una dieta estándar o una dieta alta en fósforo (So-Pho) durante el mismo periodo. Mediante un análisis estadístico multivariante en el que se consideraron todas las características de los tipos de fibras musculares se demostró que las ratas Nx-Pho + Cal mostraban fenotipos musculares con características intermedias entre el de las ratas Nx-Pho y So-Pho, y que los cambios musculares inducidos por la uremia fueron de mayor magnitud en las ratas Nx-Pho que en las ratas Nx-Sd. En ratas urémicas, el tratamiento con calcitriol preservó la composición de los tipos de fibras y la capilarización de las fibras musculares. Estos resultados demuestran que una dieta alta en fósforo potencia mientras que bajas dosis de calcitriol atenúan los cambios musculares adversos que ocurren en ratas con uremia prolongada.

Palabras claves: insuficiencia renal crónica; vitamina D activa; fósforo; hiperparatiroidismo secundario; tipo de fibra muscular.

Resumen Estudio 3

Acevedo LM, Raya AI, Ríos R, Aguilera-Tejero E, Rivero JL. La reducción de la masa muscular y un fenotipo rápido inducidas por obesidad ocurren con un incremento de la capacidad oxidativa en músculos esqueléticos rojo y blanco de ratas. *Histochem Cell Biol* (sometido en 2016).

Todavía está por establecerse una imagen nítida acerca de las adaptaciones de músculos esqueléticos a la obesidad y otras comorbilidades asociadas. Este estudio describe las adaptaciones de los tipos de fibras (tamaño, proporciones y capacidad oxidativa) en músculos del miembro pelviano en un modelo animal de obesidad genética. El diámetro menor, la composición fibrilar y la actividad histoquímica succínico deshidrogenasa (marcador oxidativo) fueron evaluados en músculos rojo (sóleo) y blanco (tibial craneal) de ratas Zucker obesas

(*fa/fa*), y se compararon con ratas Zucker delgadas (*Fa/Fa* o *Fa/fa*) de la misma edad (16 semanas) y sexo (hembras) (n=20 ratas/grupo). La masa muscular y el diámetro fibrilar menor de ambos músculos fueron menores en los animales obesos que en los delgados, incluso cuando el peso corporal incrementó en las ratas obesas. También se observó un fenotipo tipo-fibrilar más rápido en los músculos rojo y blanco de los individuos obesos, en comparación con los delgados. Estas adaptaciones estuvieron acompañadas por un incremento generalizado de la capacidad oxidativa de todos los tipos de fibras en ambos músculos. Estos resultados demuestran que la obesidad induce una respuesta adaptativa no específica a nivel muscular, en la que las fibras musculares experimentan atrofia significativa y cambian sus perfiles contráctil y metabólico hacia un fenotipo muscular más rápido y oxidativo. Es destacable que estas adaptaciones fueron comparables en cuanto a su naturaleza y magnitud en músculos rojo y blanco, lo que indica que el efecto de la obesidad sobre la plasticidad muscular es inespecífico con relación a la estructura y función de los músculos esqueléticos.

Palabras claves: tipo de fibra muscular; masa muscular; capacidad oxidativa muscular; obesidad; síndrome metabólico.

Resumen Estudio 4

Acevedo LM, Raya AI, Aguilera-Tejero E, Rivero JL. La mangiferina protege contra los cambios adversos del músculo esquelético y mejora la capacidad oxidativa muscular en ratas obesas. *PLoS One* (Sometido en 2016).

Los cambios en músculos esqueléticos secundarios a la obesidad incluyen atrofia muscular, transformación tipo-fibrilar lenta a rápida, y alteración de la capacidad oxidativa mitocondrial. Estos cambios han sido relacionados con incremento en el riesgo de padecer resistencia a la insulina. La mangiferina, el principal componente de la planta del mango *Mangifera indica L.*,

es un agente natural con propiedades anti-inflamatorias, anti-diabéticas y anti-hiperlipidémicas bien conocidas. Este estudio probó la hipótesis de que el tratamiento con mangiferina contrarresta la atrofia fibrilar y la transformación tipo-fibrilar lenta a rápida inducidas por la obesidad, favoreciendo un fenotipo oxidativo en músculos esqueléticos de ratas obesas. Un grupo de ratas Zucker obesas (*fa/fa*) fueron alimentadas con cápsulas de gelatina con (15 mg/kg peso vivo/día) o sin (grupo placebo) mangiferina durante 8 semanas. Otro grupo de ratas Zucker con el fenotipo delgado (*Fa/Fa* o *Fa/fa*) recibieron las mismas cápsulas de gelatina sin mangiferina, sirviendo como controles no obesos y no diabéticos. El diámetro menor, la composición fibrilar y la actividad histoquímica succínico deshidrogenasa (marcador oxidativo) de los distintos tipos de fibras fueron evaluados en los músculos sóleo y tibial craneal de ambos grupos de ratas. Un análisis multivariante con todos los rasgos de los tipos de fibras musculares indicó que las ratas obesas tratadas con mangiferina mostraron fenotipos musculares esqueléticos significativamente distintos al de las ratas obesas del grupo placebo y al de las ratas delgadas. El tratamiento con mangiferina preservó significativamente la masa muscular esquelética, el tamaño fibrilar transversal, y la composición tipo-fibrilar, y mejoró la capacidad oxidativa de las fibras musculares. Estos resultados demuestran que la mangiferina atenúa los efectos adversos de la obesidad sobre los músculos esqueléticos, abriendo una nueva aplicación de esta sustancia para mejorar los disturbios metabólicos asociados con la obesidad.

Palabras claves: músculo esquelético; fibra muscular; tipo de fibra muscular; obesidad; síndrome metabólico, diabetes tipo 2.

SUMMARY

Abstract Study 1

Acevedo LM, Peralta-Ramírez A, López I, Chamizo VE, Pineda C, Rodríguez-Ortiz ME, Rodríguez M, Aguilera-Tejero E, Rivero JL. Slow- and fast-twitch hindlimb skeletal muscle phenotypes 12 wk after 5/6 nephrectomy in Wistar rats of both sexes. *Am J Physiol Renal Physiol* 309:F638-F647, 2015.

This study describes fiber-type adaptations in hind-limb muscles, the interaction of the sex and the role of hypoxia on this response in 12 wk 5/6 nephrectomized rats (Nx). Contractile, metabolic and morphological features of muscle fiber-types were assessed in the slow-twitch soleus and the fast-twitch tibialis cranialis muscles of Nx rats, and compared with sham-operated controls. Rats of both sexes were considered in both groups. A slow-to-fast fiber-type transformation occurred in the tibialis cranialis of Nx rats, particularly in males. This adaptation was accomplished by impaired oxidative capacity and capillarity, increased glycolytic capacity and no changes in size and nuclear density of muscle fiber-types. An oxidative-to-glycolytic metabolic transformation was also found in the soleus muscle of Nx rats. However, a modest fast-to-slow fiber-type transformation, fiber hypertrophy and nuclear proliferation were observed in soleus muscle fibers of male, but not of female, Nx rats. Serum testosterone levels decreased by 50% in male but not in female Nx rats. Hypoxia-inducible factor-1 α protein level decreased by 42% in the tibialis cranialis muscle of male Nx rats. These data demonstrate that 12 wk of Nx induces a muscle-specific adaptive response in which myofibers do not change (or enlarge minimally) in size and nuclear density, but acquire markedly different contractile and metabolic characteristics, which are accompanied by capillary rarefaction. Muscle function and sex play relevant roles in these adaptations.

Key words: chronic renal failure, uremia, myosin heavy chain, muscle plasticity, gonadal hormones, hypoxia-inducible factor-1 α .

Abstract Study 2

Acevedo LM, López I, Peralta-Ramírez A, Pineda C, Chamizo VE, Rodríguez M, Aguilera-Tejero E, Rivero JL. High-phosphorus diet maximizes and low-dose calcitriol attenuates skeletal muscle changes in long-term uremic rats. *J Appl Physiol* 120: 1059-1069, 2016.

Although disorders of mineral metabolism and skeletal muscle are common in chronic kidney disease (CKD), their potential relationship remains unexplored. Elevations in plasma phosphate, parathyroid hormone and fibroblastic growth factor 23 together with decreased calcitriol levels are common features of CKD. High phosphate intake is a major contributor to progression of CKD. This study was primarily aimed to determine the influence of high phosphate intake on muscle and to investigate whether calcitriol supplementation counteracts negative skeletal muscle changes associated with long-term uremia. Proportions, and metabolic and morphological features of myosin-based muscle fiber-types were assessed in the slow-twitch soleus and the fast-twitch tibialis cranialis muscles of uremic rats (5/6 nephrectomy, Nx) and compared with sham-operated (So) controls. Three groups of Nx rats received either a standard diet (0.6% phosphorus, Nx-Sd), or a high-phosphorus diet (0.9% phosphorus, Nx-Pho), or a high-phosphorus diet plus calcitriol (10 ng/kg 3 d/wk ip, Nx-Pho+Cal) for 12 wk. Two groups of So rats received either a standard diet or a high-phosphorus diet (So-Pho) over the same period. A multivariate analysis encompassing all fiber-type characteristics indicated that Nx-Pho+Cal rats displayed skeletal muscle phenotypes intermediate between Nx-Pho and So-Pho rats, and that uremia-induced skeletal muscle changes were of greater magnitude in Nx-Pho than in Nx-Sd rats. In uremic rats,

treatment with calcitriol preserved fiber-type composition, cross-sectional size, myonuclear domain size, oxidative capacity and capillarity of muscle fibers. These data demonstrate that high phosphorus diet potentiates and low dose calcitriol attenuates adverse skeletal muscle changes in long-term uremic rats.

Key words: chronic renal failure, active vitamin D, phosphorus, secondary hyperparathyroidism, muscle fiber type

Abstract Study 3

Acevedo LM, Raya AI, Ríos R, Aguilera-Tejero E, Rivero JL. Obesity-induced muscle mass reduction and fast phenotype occur with increased oxidative capacity in red and white rat skeletal muscles. *Histochem Cell Biol* (submitted in 2016).

A clear picture of skeletal muscle adaptations to obesity and related comorbidities remains elusive. This study describes fibre-type adaptations (size, proportions and oxidative capacity) in hind limb muscles in an animal model of genetic obesity. Lesser diameter, fibre composition, and histochemical succinic dehydrogenase activity (an oxidative marker) of muscle fibre types were assessed in red (soleus) and white (tibialis cranialis) muscles of obese Zucker rats, and compared with age- (16 weeks) and sex-matched (females) lean Zucker rats (n=20/group). Muscle mass and lesser fibre diameter were lower in both muscles of obese compared with lean animals, even though body weights were increased in the obese cohort. A faster fibre-type phenotype also occurred in red and white muscles of obese subjects, compared with lean rats. These adaptations were accompanied by a generalized increment in oxidative capacity of all fibre-types in the two muscles. These data demonstrate that obesity induces a muscle-unspecific inhibition of muscle growth in which muscle fibres retain a reduced fibre size and show a faster and more oxidative phenotype. It was noteworthy that these adaptations were of comparable

nature and extent in red and white muscles, indicating that the influence of obesity on muscle phenotype is unspecific in regards to muscle structure and function.

Key words: muscle fiber type; muscle mass; muscle oxidative capacity; obesity; metabolic syndrome.

Abstract Study 4

Acevedo LM, Raya AI, Aguilera-Tejero E, Rivero JL. Mangiferin protects against adverse skeletal muscle changes and enhances muscle oxidative capacity in obese rats. *PLoS One* (Submitted in 2016).

Obesity-related skeletal muscle changes include muscle atrophy, slow-to-fast fiber-type transformation, and impaired mitochondrial oxidative capacity. These changes relate with increased risk of insulin resistance. Mangiferin, the major component of the plant *Mangifera indica*, is a well-known anti-inflammatory, anti-diabetic, and antihyperlipidemic agent. This study tested the hypothesis that mangiferin treatment counteracts obesity-induced fiber atrophy and slow-to-fast fiber transition, and favors an oxidative phenotype in skeletal muscle of obese rats. Obese Zucker rats were fed gelatin pellets with

(15 mg/kg BW/day) or without (placebo group) mangiferin for 8 weeks. Lean Zucker rats received the same gelatin pellets without mangiferin and served as non-obese and non-diabetic controls. Lesser diameter, fiber composition, and histochemical succinic dehydrogenase activity (an oxidative marker) of myosin-based fiber-types were assessed in soleus and tibialis cranialis muscles. A multivariate discriminant analysis encompassing all fiber-type features indicated that obese rats treated with mangiferin displayed skeletal muscle phenotypes significantly different compared with both lean and obese control rats. Mangiferin significantly preserved skeletal muscle mass, fiber cross-sectional size, and fiber-type composition, and enhanced muscle fiber oxidative capacity. These data demonstrate that mangiferin attenuated adverse skeletal muscle changes in obese rats, opening a novel application of mangiferin to improve obesity-induced metabolic dysregulation.

Key words: skeletal muscle; skeletal muscle fiber; muscle fiber type; obesity; metabolic syndrome; type II diabetes.

APÉNDICE

Abbreviations

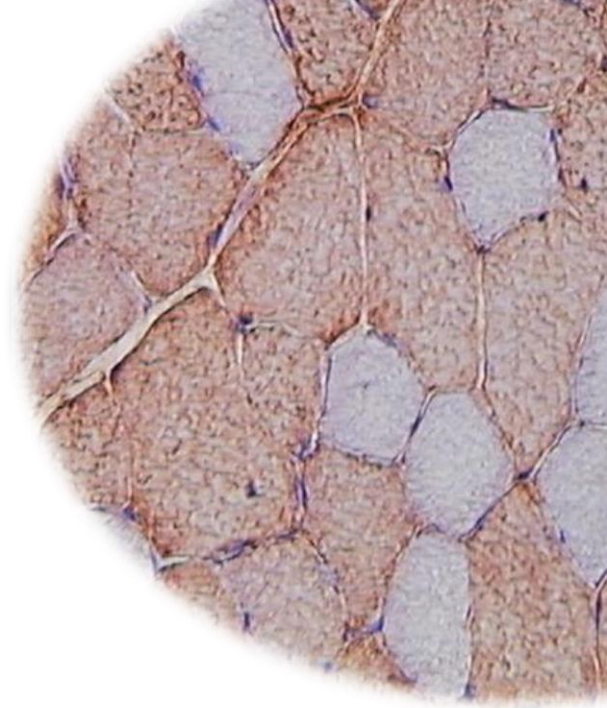
Curriculum vitae

Publicaciones

Actividades académicas

Agradecimientos

Financiación



Abbreviations

Consultar el cuadro anexo.

Curriculum vitae

Luz Marina Acevedo Betancourt nació el 6 de Enero de 1971 en Caracas, Venezuela. Curso estudios en la Universidad Central de Venezuela obteniendo el título de Médico Veterinario en Abril de 1996. Ingresó como Profesor Universitario en la Universidad Central de Venezuela en Abril de 1997. Realizó una estancia académica en el Laboratorio de Biopatología Muscular en la Universidad de Córdoba, en España en el 2002, recibiendo adiestramiento en técnicas de histoquímica convencional, histoquímica cuantitativa e inmunohistoquímica, aplicadas para la caracterización morfológica del músculo esquelético de los mamíferos. Realizo estudios de Postgrado en la Universidad Central de Venezuela obteniendo el título de *Maestría en Medicina Veterinaria* mención Patología en el 2004. Realizó un año sabático en la Universidad de Montreal, Montreal, Canadá entre 2006-2007 donde adquirió conocimientos en inmunocitoquímica con oro coloidal aplicadas a la microscopía electrónica de transmisión y morfometría en imágenes. Curso estudios de Postgrado en la Universidad de Córdoba, obteniendo el título de *Máster Universitario en Medicina, Sanidad y Mejora Animal* en 2011. En Octubre de 2011 inicio estudios de Doctorado en Biociencias y Ciencias Agroalimentarias en la Universidad de Córdoba, Córdoba, España.

Publicaciones

1- Artículos publicados

1.1 Guillermo H. Graziotti, Verónica E. Chamizo, Clara Ríos, Luz M. Acevedo, J. M. Rodríguez-Menéndez, C. Victorica and José Luis L. Rivero (2012) Adaptive functional specialisation of architectural design and fibre type characteristics in agonist shoulder flexor

muscles of the llama, *Lama glama*. *J Anat* **221**:151-163.

- 1.2 V. Chamizo, L. M. Acevedo, J.-L. L. Rivero (2015) Prevalence and clinical features of exertional rhabdomyolysis in Andalusian horses" *Veterinary Record* 177(2): 48
- 1.3 Luz M. Acevedo, Alan Peralta-Ramírez, Ignacio López, Verónica E. Chamizo, Carmen Pineda, María E. Rodríguez-Ortiz, Mariano Rodríguez, Escolástico Aguilera-Tejero, and José-Luis L. Rivero (2015) "Slow- and fast-twitch hind limb skeletal muscle phenotypes 12 weeks after 5/6 nephrectomy in Wistar rats of both sexes. *Am J Physiol Renal Physiol* **309** F638-47
- 1.4 Luz M. Acevedo, Ignacio López, Alan Peralta-Ramírez, Carmen Pineda, Verónica E. Chamizo, Mariano Rodríguez, Escolástico Aguilera-Tejero and José-Luis L. Rivero (2016) High-phosphorus diet maximizes and low dose calcitriol attenuates skeletal muscle changes in long-term uremic rats *J Appl Physiol* (1985) **120**:1059-69
- 1.5 Elisa Diez de Castro, Zafra Rafael, Luz M. Acevedo, José Pérez, Isabel Acosta, José-Luis L. Rivero, and Escolástico Aguilera-Tejero (2016) "Eosinophilic enteritis in horses with motor neuron disease". *J Vet Int Med* **30**:873-9

2- Artículos sometidos

2.1 Luz M. Acevedo, Ana Raya, Rafael Ríos, Escolástico Aguilera-Tejero, and José-Luis L. Rivero (2016) Obesity-induced mass reduction and fast phenotype occur with increased oxidative capacity in red and white muscle. Enviado con modificaciones respuesta al arbitraje el 21/09/2016 en la revista *Histochemistry and Cell Biology*.

AMPK	AMP-activated protein kinase
Ca	Calcium
CS	Citrate synthase
CKD	Chronic kidney disease
CRF	Chronic renal failure
CSA	Cross-sectional area
FFA	Free fatty acid
FGF-21	Fibroblastic growth factor 21
FGF-23	Fibroblastic growth factor 23
GPDH	Glycerol-3-phosphate dehydrogenase
H-E	Haematoxilin and eosin
HIF-1α	Hypoxia inducible factor 1 α
HPT	Secondary hyperparathyroidism
IL-6	Interleukin 6
MAbs	Monoclonal antibodies
MHC	Myosin heavy chain
MSI	Muscle–somatic index
Nx	Nephrectomy
Nx–Pho	5/6 nephrectomy and high–phosphorus diet
Nx–Pho+Cal	5/6 nephrectomy high–phosphorus diet plus calcitriol
Nx–Sd	5/6 nephrectomy standard diet
OD	Optical density
PPAR	Peroxisome proliferator activated receptors
PAS	Periodic acid-Schiff
PGC1α	PPAR γ coactivator
PTH	Parathyroid hormone
SDH	Succinate dehydrogenase
SOL	Soleus muscle
So	Sham–operated
So–Pho	Sham–operated high–phosphorus diet
So–Sd	Sham–operated standard diet
TC	Tibialis cranialis muscle
TNF α	Tumor necrosis factor α
VDR	Vitamin D receptor

2.2 Luz M. Acevedo, Ana Raya, Escolástico Aguilera–Tejero, and José Luis L. Rivero (2016) Mangiferin protects against adverse skeletal muscle changes and

enhances muscle oxidative capacity in obese rats. Para ser enviado con modificaciones en respuesta al arbitraje en la revista Plos One.

3- Abstracts

- 3.1 A. Peralta Ramírez, J.R. Muñoz-Castañeda, M.E. Rodríguez Ortiz, C. Herencia Bellido, C. Pineda Martos, J.M. Martínez Moreno, A. Montes de Oca González, F. Guerrero Pavón, S. Pérez Delgado, L.M. Acevedo, M.E. Peter, S. Steppan, J. Passlick-Deetjen, I. López Villalba, E. Aguilera-Tejero, y. Almadén Peña (2012) El Magnesio disminuye la Calcificación Vascular en Ratas Urémicas. Presentado en el XLII Congreso Nacional de la Sociedad Española de Nefrología, en Gran Canaria, España*.
- 3.2 Gómez-Laguna J, Cardoso-Toset F, Acevedo L.M, Fernández L., Chamizo V, García-Valverde R, López-Rivero J.L (2014) Myosin heavy chain fibre types and fibre sizes in intensive and free-range finishing Iberian pigs: Interaction with two alternative dietary protein concentration diets. Presentado en el 6th European Symposium of Porcine Health Management, en Sorrento, Italia.

Actividades académicas

1- Actividades docentes

Se participó en calidad de apoyo docente en la actividad práctica en el Laboratorio de Biopatología Muscular, en el dictado de la asignatura “Avances en Fisiología del Ejercicio y de la Locomoción Equina”, a los estudiantes del Máster Universitario en Medicina, Sanidad y Mejora Animal, de los cursos académicos 2011-2012, 2012-2013 y 2014-2015.

2- Asistencia a cursos, conferencias y seminarios

- 2.1 Asistencia al curso “XIII Curso Internacional sobre Medicina Deportiva Equina” Del 12 al 14 de mayo de 2011 en la Universidad de Córdoba.
- 2.2 Asistencia a la Conferencia “Aplicación de la Biotecnología en la Ciencia Veterinaria” El 28 Abril 2011 en la Universidad de Córdoba.

- 2.3 Asistencia al curso “La Investigación en Veterinaria y Ciencia y Tecnología de los Alimentos” del 7 al 11 de Noviembre de 2011 en la Universidad de Córdoba.
- 2.4 Asistencia al “III Encuentro Internacional en Sanidad Animal y Seguridad Alimentaria” del 14 al 15 de Marzo de 2012 en la Universidad de Córdoba.
- 2.5 Asistencia a las “V Jornadas de Divulgación de la Investigación en Biología Molecular, Celular, Genética y Biotecnología” del 27 al 28 de Marzo de 2012 en la Universidad de Córdoba.
- 2.6 Asistencia a la Conferencia “Estudios sobre la Leptina Gástrica: de la Biología Celular hacia la posible Aplicación Clínica”. 14 de Junio en la Universidad de Córdoba.
- 2.7 Asistencia a las I Jornadas de divulgación Científica” divulgA3”, el 15 de Marzo 2013 en el Rectorado de la Universidad de Córdoba.
- 2.8 Asistencia al Curso Práctico de “Microscopía Electrónica” del 04 al 07 de Marzo 2013, realizado en la Universidad de Córdoba.
- 2.9 Asistencia al Curso “Técnicas y aplicaciones de la Microscopía Electrónica e Inmunohistoquímica” del 25 al 27 de Junio de 2013 en la Universidad de Córdoba.
- 2.10 Asistencia al Curso “Introducción a las Técnicas de Microscopía Óptica y Electrónica” del 22 al 26 de Julio de 2013 en el Instituto Catalán de Paleontología Miguel Crusafont en Sabadell, Barcelona.
- 2.11 Asistencia al "Taller de Redacción de Documentos Investigadores y Divulgativos" del 1-4, 7-10 de Abril 2014, realizado en la Universidad de Córdoba.
- 2.12 Asistencia al curso "Técnicas Electroforéticas y su Aplicación en Agroalimentación" realizado 06 al 10 de Octubre 2014 en la Estación Experimental del Zaidín (CSIC) Granada, España.
- 2.13 Durante el período 2012-2014 Asistencia una vez al mes a Seminarios de Investigación, con la discusión de resultados de las investigaciones de los estudiantes

de Doctorado en conjunto con Investigadores del Instituto Maimónides de Investigación Biomédica de Córdoba (IMIBIC), de las líneas de investigación en Fisiopatología del Metabolismo Mineral, Metabolismo del Calcio y Biopatología Muscular.

- 2.14 Asistencia al curso "Introducción a la Microscopía Electrónica y Fotónica" realizado del 26 al 30 de Octubre 2015 en la Estación Experimental del Zaidín (CSIC) Granada, España.

Agradecimientos

A mis Tutores, los Profesores Doctores José Luis López Rivero y Escolástico Aguilera Tejero. Faltan palabras para agradecer al Profesor Dr. José Luis López Rivero por brindarme nuevamente la oportunidad de trabajar en el Laboratorio de Biopatología Muscular, bajo su extraordinaria orientación después de haber pasado tantos años desde mi estancia por unos meses en el 2002, donde tuve la excelente experiencia de continuar desarrollándome en la línea de investigación en Morfología del músculo esquelético en mamíferos que inicié en Venezuela gracias a los Profesores Dr. Luis Eduardo Sucre Párraga[†] y Dr. Héctor José Finol, quienes fueron los responsables de mi incursión en el fascinante mundo de la investigación. Al Profesor Escolástico Aguilera Tejero por brindarme la oportunidad de trabajar en el grupo de investigación que coordina en la línea de Fisiopatología en el metabolismo mineral, así como en el grupo de investigación del Metabolismo del calcio en el Instituto Maimónides de Investigación Biomédica de Córdoba (IMIBIC). Muy agradecida por sus invaluables orientaciones en los trabajos de investigación de la tesis doctoral.

A la Ilustre Universidad Central de Venezuela, "La casa que vence las sombras".

A la Excelentísima Universidad de Córdoba, mi segunda *alma mater*, que me abrió sus puertas brindándome un espacio para continuar en mi desarrollo

profesional en el área de la investigación.

Al Departamento de Anatomía y Anatomía Patológica Comparadas, a los Profesores y Personal de administración y servicio, inmensamente agradecida por su receptividad y valiosa colaboración.

Al Profesor Ignacio López por sus útiles consejos en las investigaciones realizadas.

Al Instituto Maimónides de Investigación Biomédica de Córdoba (IMIBIC), a través del grupo de investigación del Metabolismo del calcio, por toda la colaboración prestada y las orientaciones correspondientes en el desarrollo de las fases experimentales, así como en las determinaciones bioquímicas y demás técnicas desarrolladas para los trabajos de investigación de la presente tesis doctoral.

A mis compañeros Doctorandos: José Miguel, Raúl, Luis Miguel y Gabriela; y a los Doctores: Jaouad, Teresa, Sebastián, Denisse, Humberto, Gesabel, Alan, Latifa, Paola, María Denis, Gloria, Meelad, Elsa, y Joao, quienes en el transcurso de estos años han culminado con muchos éxitos sus estudios de doctorado, les agradezco sus palabras de aliento, así como sus acertadas orientaciones y ayudas, y en especial a mi compañera de laboratorio Verónica por su inestimable y valiosa colaboración en el desarrollo de la tesis doctoral.

A mis amigos y compañeros de trabajo de la Universidad Central de Venezuela Adelina, Gloria, Yamilet, Dayscarlid, Jelly, Bibiana, Herakles, José Gregorio, Héctor, Sonia y Luis Alberto, por su valioso apoyo y estímulo a pesar de las distancias.

Financiación

Un especial agradecimiento y mención a los entes o Instituciones que han hecho posible el desarrollo de los trabajos de investigación, mi estancia y el traslado entre Venezuela y España.

La financiación para la manutención, matrícula, traslado y otros gastos fueron posibles por una Beca

Financiación

Sueldo Exterior otorgada por el Consejo de Desarrollo Científico y Humanístico de la Universidad Central de Venezuela durante el periodo entre Enero de 2011 y Diciembre de 2015.

En el caso de los trabajos de investigación, éstos fueron financiados por subvenciones desde el Instituto Carlos III (PI14/00467 y PI00386) con cofinanciamiento de Fondos Europeos. Además por subvenciones de

Grupos PAI CTS-179 y el Proyecto P10-AGR-5963 a través de la Junta de Andalucía, España.

El financiamiento para traslado Venezuela-España (ida y vuelta) en el último trimestre de 2016 fue otorgado por la Asociación Universitaria Iberoamericana de Postgrado-AUIP a través del Programa de Movilidad Académica entre Universidades Andaluzas e Iberoamericanas en su convocatoria 2016.